THE UNIVERSITY *of* EDINBURGH

Microplastic degradation and interaction with organic micro-pollutants within wastewater treatment systems

Thomas Easton

THE UNIVERSITY *of* EDINBURGH

Submitted for the degree of Doctor of Philosophy
The University of Edinburgh
2024

Declaration

The work presented in this thesis is my own. Work produced by collaboration is identified and my contribution is stated. This work has not been submitted for any other degree or professional qualification.

This work was supported by a NERC Doctoral Training Partnership grant NE/S007407/1.

Abstract

Microplastic (MP) pollution is released to the aquatic environment within wastewater effluent due to its ineffective removal by traditional wastewater treatment plants (WWTPs). Once dispersed in riverine and marine ecosystems, MP pollution presents a health risk to animals and humans. Developing effective and sustainable treatment systems capable of removing and destroying MPs before they exit WWTPs is essential in preventing this flow of pollution to the environment. Advanced oxidation processes (AOPs) have gained recent attention as a potential sustainable treatment solution, capable of complete mineralisation of MPs in water. As an emerging area of study, information on the effectiveness, mechanism of action and real-world applicability of these treatment methods is greatly needed. This research fills gaps in the knowledge of the effectiveness of several AOPs for removal of MPs from wastewater.

Microplastic fibres originating from laundry washing are often found in high numbers in WWTP effluent due to their tendency to pass through filter membranes. In Chapter 4, the effect of UV irradiation and hydrogen peroxide AOP treatment (UVC/H_2O_2) on the removal of polyester MP fibres was studied. Physical and chemical degradation of the fibres was followed with a range on analytical characterisation techniques. A dose of 500 mg L^{-1} H_2O_2 under 4.0 mW cm^{-2} UVC irradiation caused mass loss of 52.7% after 48 h. The degradation of polyester resulted in the formation of shallow holes, pits and cracks across the fibre surface as well as changes to the abundance of oxygen containing functional groups. In real hospital laundry water, the rate of degradation was impeded by the chemical oxygen demand (COD) of the wastewater.

Incomplete degradation of MPs can result in the formation of smaller fragments with altered surface chemistry. In Chapter 5, the impact of sulfate based oxidation on this transformation of polyester fibre MPs was investigated. Persulfate activation by light, heat and ultrasound were compared for their effect on the chemical and physical characteristics of the MPs. Ultrasound significantly increased the fragmentation with smaller microplastic fibrils forming during treatment. The most aggressive treatment in terms of mass loss, UVC/PDS treatment (31.8 mW cm^{-2}, 500 mg L^{-1}), reduced the mass by 18.5% in 9 h with clear surface pitting and

cracking. Based on the rate at which MPs are degraded, incomplete mineralisation is likely to occur in wastewater treatment systems. The physical and chemical transformation observed at lab scale carries implications for the interaction of partially degraded MPs with organic contaminants in wastewater and aid in our understanding of MP fate.

MPs in the aquatic environment interact with organic micropollutants including antibiotics and can substantially increase their environmental mobility. Chapter 6 takes the antibiotic ceftazidime as an example to study this type of adsorption interaction. The effect of MP weathering degree, polymer type, size and shape of MPs are investigated using lab-scale batch adsorption experiments. As already shown in aforementioned chapters, the weathering of MPs drastically alters the chemical and physical characteristics of MPs and therefore impacts their environmental behaviour. Ten different MPs were weathered under simulated environmental conditions in order to investigate this effect further. Among the MPs studied, weathered PET fibers exhibited the highest adsorption reaching 1.432 mg g^{-1} after 48 h of contact time. The formation of holes, cracks and fragmentation of the MPs increased the surface area and therefore the number of adsorption sites.

Alongside these lab-scale investigations, Chapter 3 considers how proposed solutions to MP pollution exist within a complex landscape of policy and environmental regulation. The environmental and waste legislation in Scotland and the UK is complex and is currently in the process of change. As a case study to exemplify this, the MP and chemical pollution of sewage sludge and its use as a fertiliser material for land application is reviewed. This chapter shows that a sustainable solution to microplastic pollution from WWTPs must be considered as part of a much larger waste management system.

Lay summary

Microplastics (MPs) are released in wastewater treatment effluent to the environment where they pose a threat to the aquatic ecosystems and carry a risk to human health. By destroying MPs before they leave our treatment systems, we can prevent this harm. Rapid degradation using aggressive oxidising conditions has the potential to break down MPs into their component molecules (predominantly CO_2 and H_2O) which do not pose direct harm to the aquatic environment.

This work investigates the potential of oxidative degradation to destroy MPs within wastewater treatment systems. This was explored by using lab-scale experiments to test various oxidation systems for their effect on a range on MPs and studying the physical and chemical changes that resulted. This work also explores how partial degradation can change the properties of the MPs and make them more susceptible to interact with other pollutants within the wastewater, such as antibiotics. This was explored by performing experiments to determine the interaction of partially degraded MPs with an antibiotic in water. To put the work in context, the policy surrounding MP contamination within the products of wastewater treatment was also reviewed.

Acknowledgments

This thesis was only possible with the help and advice of many friends and colleagues. Firstly, I feel very lucky to have been supervised by Thalia Chatzisymeon whose guidance and support was essential in completing my work. I am also extremely grateful for valuable discussions and help from my second supervisor Vasileios Koutsos. Thank you both for making these 4 years so productive and rewarding.

My collaborators and co-authors have provided amazing feedback and help over the years in many aspects of my work and I am grateful to everyone involved. I am lucky to have met many fantastic scientists from across the field of microplastic research over the years and I would like to thank them all for inspiring and motivating me.

I would also like to thank every student, staff member and visitor to the University of Edinburgh water research group who helped and kept me company in and out of the lab over the years. Particular thanks have to go to Stuart Martin and the entire technical support team across the School of Engineering for always being happy to help with problems, big or small. Thanks also to the students I had the opportunity to supervise for their enthusiasm and hard work in the lab.

I am extremely grateful to have had a cohort of E4 DTP students alongside me throughout the process and I thank Stephanie Robin and the School of Geosciences team for organising so many great opportunities and trips together.

Thanks to Joanna Cloy and Kate Basley from Fidra and Phoebe Cochrane from Scottish Environment LINK for the opportunity to take a break from the lab and work with them on environmental policy.

Finally, a huge thanks to my family and friends. To mum and dad for always supporting me over my (almost 9...!) years at university and to Antonia for her love and support throughout this PhD.

Table of contents

Declaration 2
Abstract 3
Lay summary 5
Acknowledgments 6
Table of contents 7
List of tables 11
List of figures 12
List of abbreviations 18
Publication statement 20
1. Introduction 21
1.1 Motivation and research aims 21
1.2 Thesis structure 22
1.3 Background 24
1.3.1 The problem with plastics 24
1.3.2 Microplastics 26
1.3.3 Effect of microplastics on human health and environment 27
1.3.4 Sources of microplastic pollution to the aquatic environment 28
1.3.5 Prevalence of microplastics in wastewater 30
Polyester fibres 31
Polyethylene microbeads 32
Expanded foam particles 32
Tyre wear particles 32
1.3.6 Removal and treatment technologies 32
1.3.6.1 Physical processes 33
Screening and settling 34
Filtration and adsorption 35
1.3.6.2 Chemical processes 36
Photocatalytic treatment 36
Fenton and Fenton-like treatment 38
Ozone and peroxide based treatment 41
1.3.6.3 Biological processes 41
1.3.6.4 Summary of current removal technology performance 43
1.4 Photodegradation and advanced oxidation processes 45

1.4.1 Photolysis 45
1.4.2 UVC/H_2O_2 based AOPs 47
1.4.3 Sulfate based AOPs 47
1.5 Legislation and alternative solutions 49
2. Materials and methods 51
2.1 Materials 51
2.2 Preparation of microplastics 52
2.2.1 PET Fibres 53
2.2.2 PE beads 54
2.2.3 PS and PU foams 54
2.2.4 Rubber TWPs 54
2.3 AOP treatment of microplastics 55
2.3.1 UVC/H_2O_2 AOP reactor setup 55
2.3.2 Sulfate AOP reactor setup 56
2.3.3 Irradiation source 57
2.3.4 UV dose 57
2.3.5 Separation of microplastics from water 58
2.4 Analytical methods 58
2.4.1 Chemical characterisation 59
2.4.1.1 Fourier transform infrared spectroscopy 59
2.4.1.2 Chemical oxygen demand 63
2.4.1.3 Biological oxygen demand 64
2.4.1.4 Alkalinity 64
2.4.1.5 Turbidity 65
2.4.1.6 UV-visible spectrophotometry 65
2.4.1.7 High-performance liquid chromatography 67
2.4.2 Physical characterisation of MPs 69
2.4.2.1 Gravimetric analysis 69
2.4.2.2 Optical microscopy 70
2.4.2.3 Scanning electron microscopy 70
2.4.2.4 Atomic force microscopy 70
2.4.3 Adsorption of antibiotics 71
3. Policy and regulation of microplastics in wastewater treatment plants case study 73
3.1 Introduction 73
3.2 Background 74

3.2.1 Sludge production and application to agricultural land 75
3.2.2 Beyond agricultural application 77
3.3 Current policy context 78
3.3.1 Regulation in Scotland covering sludge application to agricultural land 78
3.3.2 Broader UK activity 80
3.3.3 European Union activity 81
3.4 Stakeholder overview 82
3.5 Contaminants of concern in sewage sludge applied to land 85
3.5.1 Heavy metals 85
3.5.2 Pathogens 87
3.5.3 Organic emerging contaminants, personal care products and pharmaceuticals 88
3.5.4 Microplastics 89
3.6 Treatment of sewage sludge 91
3.7 Impact to soil quality 94
3.8 Circular economy considerations 95
3.9 Key recommendations 96
3.10 Conclusions 97
4. Advanced oxidation treatment methods for removal of microplastics in laundry waste water 99
4.1 Experimental protocol for tracking microplastic degradation 99
4.1.1 Literature methods for MP testing material preparation 99
4.1.2 Polyester fibre microplastic preparation 101
4.1.3 Fibre length distribution as a measure of degradation 102
4.2 Initial screening and selection of oxidation treatment 105
4.3 Removal of polyester fibre microplastics from wastewater using a UVC/H_2O_2 oxidation process 106
4.3.1 Background 106
4.3.2 Materials and methods 108
4.3.3 Results and discussion 110
4.3.3.1 Feasibility of UV/H_2O_2 treatment for MP fibre degradation 110
4.3.3.2 Effect of UV dose and intensity 113
4.3.3.3 Effect of initial fibre concentration 121
4.3.3.4 Effect of H_2O_2 concentration 122
4.3.3.5 MPs degradation in real laundry wastewater 125
4.4 Conclusions 127

5. Transformation of polyester fibre microplastics by sulfate based advanced oxidation processes....129
5.1 Background and literature review....129
5.2 Materials and methods....131
5.3 Screening of sulfate activation methods....132
5.3.1 Photoactivation....132
5.3.2 Ultrasound assisted activation....137
5.3.3 Thermal activation....140
5.4 UVC/sulfate operating parameters and water properties....144
5.4.1 Consumption rate of oxidant....144
5.4.2 Effect of oxidant initial concentration....146
5.4.3 Effect of water pH....148
5.5 Polyester fibre transformation in real laundry wastewater....151
5.6 Conclusions....156
6. Antibiotic adsorption by microplastics in water....158
6.1 Background and literature review....159
6.2 Materials and methods....161
6.2.1 UV/visible spectrophotometry....162
6.2.2 Derivitisation of ceftazidime for visible range spectrophotometry....164
6.3 Artificial weathering of MPs for adsorption testing....168
6.4 Adsorption of ceftazidime by microplastics....170
6.5 The effect of weathering on microplastic surface structure....176
6.5.1 The effect of weathering on microplastic physical characteristics....176
6.5.2 The effect of weathering on polymer surface chemistry....181
6.6 PET fibre microplastic adsorption isotherms....182
6.7 Conclusions....184
7. Summary and conclusions....185
Future work and recommendations....190
Final thoughts....192
References....193
Appendix A: Supplementary data....226
Appendix B: Contaminants of concern present in sewage sludge....235
Appendix C: Statistical t-test outputs....236
Appendix D: Conference participation & Invited talks....237

List of tables

Table 1.1 Advanced oxidation treatment methods for microplastic removal from wastewater 39
Table 2.1 Irradiation sources and their measured UV output 57
Table 3.1 Thresholds relevant to sludge application to land 86
Table 3.2 Methods for sewage sludge treatment applied in Scotland 92
Table 3.3 Literature evidence of removal of chemical contaminants by sludge treatment ...93
Table 4.1 Average polyester fibre length measured by optical microscopy (n=550) 103
Table 4.2 Chemical characterisation of MP fibres and calculated kinetic parameters 124
Table 5.1 Calculated carbonyl index and reaction rates of treated polyester fibre samples 136
Table 5.2 Polyester fibre mass loss treated with US/PDS and US/PMS 139
Table 5.3 Polyester fibre mass loss treated with heat/PDS 142
Table 5.4 Polyester fibre mass loss at varied rates of sulfate addition 144
Table 5.5 Conditions and polyester mass loss results from varied starting pH experiments 149
Table 6.1 Microplastic samples studied for CAZ adsorption 170
Table 6.2 Calculated carbonyl index of PET, PE, PS and PU MP samples 181
Table 6.3 Linear and Langmuir isotherm fitting parameters for CAZ adsorption by pristine and weathered PET fibers 183
Table A.1 Spiked recovery of MP fibres from ultrapure water 226
Table A.2 Spiked recovery of MP fibres from real laundry wastewater 227
Table A.3 Spiked recovery of uncut polyester fibres from ultrapure water 227
Table A.4 Isotherm fitting data for ceftazidime adsorption by PET fibres 232
Table A.5 Chemical Oxygen Demand (COD) of treated polyester fibres by UVC/H_2O_2 AOP 232
Table A.6 Kinetic fitting parameters used to calculate rate of polyester removal by UVC/H2O2 under varied H2O2 concentrations 233
Table A.7 Outputs of statistical t-test of fibre length distribution assuming equal variance 236

List of figures

Figure 1.1 Global plastic production through time (produced using data from (2, 3)).....24

Figure 1.2 "Microplastic" by Oregon State University.....26

Figure 1.3 Major microplastic sources and transport routes to the aquatic environment 29

Figure 1.4 Reported microplastic removal performance of water treatment technologies 33

Figure 1.5 a) Publications reviewed considering water treatment for the removal of microplastics broken down by plastic shape. **b)** Publications reviewed considering water treatment for the removal of microplastics broken down by polymer type 44

Figure 1.6 Chemical structure of PDS and the ative salt of PMS.....48

Figure 2.1 Photos of MPs types studied for ceftazidime adsorption. Polyurethane (PU); Polystyrene (PS); Polyethylene (PE); polyester (PET) and tyre wear particles (TWP) 52

Figure 2.2 Schematic illustration of (a) the immersion photo-reactor setup and (b) top down photo-reactor setup.....55

Figure 2.3 Schematic illustration of (a) the immersion ultrasound activated reactor setup and (b) thermal activated reactor setup.....56

Figure 2.4 FTIR spectra of raw and weathered PET fibres.....60

Figure 2.5 FTIR spectra of PE beads as extracted from facewash, weathered by UVC/H_2O_2 and a reference PE film.....61

Figure 2.6 FTIR spectra of hard and soft PS foams before and after weathering 62

Figure 2.7 FTIR spectra of hard and soft PU foams before and after weathering 62

Figure 2.8 Calibration curve of CAZ in water measured by UV absorbance at 256 nm 66

Figure 2.9 Calibration curve of PDS in water measured by UV absorbance at 450 nm 66

Figure 2.10 Calibration curve of PDS in water measured by UV absorbance at 395 nm 67

Figure 2.11 HPLC chromatograph overlay of CAZ standard solutions 68

Figure 2.12 Calibration curve for Ceftazidime in water as measured by HPLC.....68

Figure 3.1 Fate of biosolids produced in Scottish treatment sites in the 2021/22 reporting year operated by Scottish Water (top) and contracted private finance initiative (PFI) sites (bottom) (data provided by Scottish Water) 76

Figure 3.2 Key stakeholder groups arranged by **a)** power to drive or promote change in how sludge to land is regulated and **b)** incentive to change current regulations.....83

Figure 3.3 Microplastic sources to wastewater treatment systems and subsequent release pathways 89
Figure 4.1 Polyester fibres **(a,b)** as supplied and **(c,d)** cut into short lengths with length distribution outlined in Section 4.1.3 101
Figure 4.2 Representative optical micrographs showing polyester fibres at 4x magnification **a)** untreated polyester fibres **b)** UVC 6 h **c)** UVC/H_2O_2 (100 mg L^{-1}) 6 h **d)** UVC/H_2O_2 (200 mgL^{-1}) 6 h (31.8 mW cm^{-2} UVC irradiation, 16.7 mg L^{-1} initial fibre concentration) 103
Figure 4.3 Distribution of MP fibre length after various treatment processes as measured by microscopy. The mean and median values are marked on the plot with outliers indicated by individual points on the graph (31.8 mW cm^{-2} UVC irradiation, 16.7 mg L^{-1} initial fibre concentration, n=550) 104
Figure 4.4 Concentration change of H_2O_2 in DI water exposed to 31.8 mW cm^{-2} UVC irradiation with starting concentration **a)** 100 mg L^{-1}, **b)** 200 mg L^{-1} and **c)** 500 mg L^{-1} (working volume 300 mL) 109
Figure 4.5 Mass loss performance after 9 h of treatment in DI water. Initial concentration of polyester fibres is 16.7 mg L^{-1}, H_2O_2 concentration was 500 mg L^{-1} and UVC dose was 129.6 J cm^{-2} 110
Figure 4.6 1000x magnification SEM images of polyester fibres treated for 9 h with **(a)** Control experiment **(b)** H_2O_2/dark **(c)** UVC **(d)** UVC/H_2O_2. 112
Figure 4.7 a) The effect of UV irradiance as a function of time against mass loss of MPs with UVC and UVC/H_2O_2 treatments **b)** Degradation of polyester fibres with increasing total applied UV dose. In each case, H_2O_2 concentration is 500 mg L^{-1} in DI water, starting fibre concentration of 16.7 mg L^{-1}.....114
Figure 4.8 1000x magnification SEM images of polyester fibres at varying times of treatment with **(a)** control experiment **(b)** UVC/H_2O_2 24 h **(c)** UVC/H_2O_2 48 h (**d)** UVC 24 h **(e)** UVC 48 h (where applicable H_2O_2 concentration of 500 mg L^{-1}, starting fibre concentration of 16.7 mg L^{-1}, UVC irradiance: 4.0 mW cm^{-2}).....116
Figure 4.9 (a)-(d) AFM height images of polyester fibre surface treated with UVC/H_2O_2 for 48 h and displaying typical degradation features (H_2O_2 concentration of 500 mg L^{-1}, starting fibre concentration of 16.7 mg L^{-1}, UVC irradiance: 4.0 mW cm^{-2}) 118

Figure 4.10 Surface map of polyester fibre surface treated with UVC/H_2O_2 for 48 h (H_2O_2 concentration of 500 mg L^{-1}, starting fibre concentration of 16.7 mg L^{-1}, UVC irradiance: 4.0 mW cm^{-2}).....119
Figure 4.11 Height profile along lines 1 and 2 as shown in Figure 4.9 d (measured from left to right) of UVC/H_2O_2 treated polyester fibre surface confirming the presence of shallow surface holes 120
Figure 4.12 Comparison of polyester fibre concentration decrease over time with varied starting concentrations (UVC/H_2O_2 treatment parameters: 31.8 mW cm^{-2} UVC, 500 mg L^{-1} H_2O_2 treatment over 9 h).....122
Figure 4.13 (a) Effect of varied H_2O_2 concentration on polyester fibre mass loss **(b)** Polyester fibre mass loss recorded at 9 h UVC/H_2O_2 and the effect of peroxide concentration. In all cases, the starting fibre concentration is 16.7 mg L^{-1}, UVC irradiance 31.8 mW cm^{-2}.....123
Figure 4.14 Mass loss and COD during UVC/H_2O_2 treatment of polyester fibres in DI water and laundry wastewater matrices. Starting fibre concentration of 16.7 mg L^{-1}, H_2O_2 concentration 1800 mg L^{-1}, UVC irradiance 31.8 mW cm^{-2}. 126
Figure 5.1 Mass loss of polyester fibres in a 6 h treatment period (MP initial concentration 8.3 mg L^{-1}, PMS and PDS initial concentration 500 mg L^{-1} in Di water, UV irradiation 31.8 mW cm^{-2}).....133
Figure 5.2 Effect of irradiation source on polyester fibre degradation (MP concentration 8.3 mg L^{-1} in DI water, PDS concentration 500 mg L^{-1}; LI UVC irradiation 4 mW cm^{-2}; HI UVC irradiation 31.8 mW cm^{-2}; UVA 12.45 mW cm-^{2}; solar 8.02 mW cm^{-2} UVA component) 134
Figure 5.3 SEM image of 24 h treated polyester fibres under **(a,c)** LI UVC/PDS (100 mg L^{-1}), **(b)** HI UVC/PDS (500 mg L^{-1}), **(d)** solar/PDS (500 mgL^{-1}) and **(e)** UVA/PDS (500 mgL^{-1}) 135
Figure 5.4 SEM images of polyester fibre surface exposed to UVC/PDS AOP treatment (a) raw fibres, (b) after 6 h treatment and (c) after 24 h treatment. (MP initial concentration 8.3 mg L^{-1}, PMS and PDS initial concentration 500 mg L^{-1}, UV irradiation 31.8 mW cm^{-2}) 39 ...135
Figure 5.5 PMS concentration change over time on application of ultrasound at various power (Starting PMS concentration 500 mg L^{-1}) 138
Figure 5.6 PDS concentration change over time on application of ultrasound at various power (Starting PDS concentration 500 mg L^{-1} in DI water).....138
Figure 5.7 SEM image of polyester fibre surface **(a)** raw PET fibre **(b)** treated with 500 W US for 6 h, 500 mg L^{-1} PMS **(c)** treated with 500 W US for 6 h,500 mg L^{-1} PDS.....139

Figure 5.8 Concentration change of PDS/PMS during heat treatment at varied temperature (initial persulfate concentration 500 mg L^{-1}, working volume 300 mL DI water).....141
Figure 5.9 Concentration change of PDS during heat treatment at varied initial PDS concentrations (temperature 75 ˚C, working volume 300 mL DI water) 142
Figure 5.10 SEM images of heat/PDS treated polyester fibres (initial PDS concentration 500 mg L^{-1}, temperature 21 (left), 60 (middle), 90 (right) ˚C.....143
Figure 5.11 Change in polyester fibre concentration during heat/PDS treatment (initial MP concentration 8.3 mg L^{-1}, PDS concentration 100 mg L^{-1} DI water).....143
Figure 5.12 Concentration change of PMS and PDS exposed to UVC irradiation (Starting oxidant concentration 500 mg L^{-1}, UVC irradiation 31.8 mW cm^{-2}, working volume 300 mL DI water).....145
Figure 5.13 Concentration of oxidant during PMS/UVC and PDS/UVC treatment with replenishment every 20 minutes (UV irradiation 31.8 mW cm^{-2}) 146
Figure 5.14 Mass loss from polyester fibres after 6 h of treatment with varied oxidant (PMS or PDS) concentration (MP initial concentration 8.3 mg L^{-1} in DI water, UVC irradiation 31.8 mW cm^{-2}).....147
Figure 5.15 Solution pH change over time during UVC activated treatment. 500 mg L^{-1} starting concentration of PMS (red traces) or PDS (black traces) 148
Figure 5.16 Mass loss and COD change during UVC/PDS treatment of polyester fibres in laundry water and DI water (MP concentration 8.3 mg L^{-1}, PDS initial concentration 500 mg L^{-1}, UV irradiation 31.8 mW cm^{-2}).....151
Figure 5.17 SEM images of polyester fibre surface treated in real wastewater for 9 h with PDS initial concentration 500 mg L^{-1}, UV irradiation 31.8 mW cm^{-2}.....152
Figure 5.18 AFM height images (5 x 5 μm^2) and 3D surface maps of polyester fibre surface (a) raw fibres, (b) treated in real wastewater for 9 h with PDS initial concentration 500 mg L^{-1}, UV irradiation 31.8 mW cm^{-2}.....153
Figure 5.19 Profile of height along the horizontal (x) and vertical axis (y) from pristine (top) and weathered (bottom) polyester fibres, as measured using AFM.....154
Figure 5.20 Root mean square of roughness (R_{RMS}) for pristine and weathered polyester fibres as calculated from AFM height images. Mean values are highlighted and 25, 75th percentile are marked on the box plot.....155
Figure 6.1 Chemical structure of ceftazidime (CAZ).....160

Figure 6.2 Ceftazidime in water upon exposure to UVC irradiation for (left to right) 0, 30, 60 and 90 minutes 162
Figure 6.3 Ceftazidime UV-visible absorbance spectrum change over time with UVC irradiation (Initial CAZ concentration 0.5 g L^{-1}, UVC irradiation 31.8 mW cm^{-2}) 163
Figure 6.4 Reaction scheme for diazotisation of ceftazidime and coupling with 3-aminophenol 165
Figure 6.5 Ceftazidime standard solutions after derivitisation (concentrations from left to right: 1000, 500, 200, 100, 50, 0 mg L^{-1}) 166
Figure 6.6 Calibration curve of derivatised ceftazidime in water measured at 500 nm 166
Figure 6.7 Azo-coupled ceftazidime UV-visible absorbance spectrum change over time with UVC irradiation (Initial CAZ concentration 0.5 g L^{-1}, UVC irradiation 31.8 mW cm^{-2}) 167
Figure 6.8 SEM images of polyester fibre surface at varying stages of degradation as result of hydrolysis accelerated degradation (0, 1, 2 h treatment) 168
Figure 6.9 Mass loss of polyester fibres after hydrolysis accelerated weathering. 169
Figure 6.10 Representative SEM images of **a)** PET, **b)** PE, **c)** PU, **d)** PS and **e)** TWP MPs (left) and their magnified surface structure (right) 171
Figure 6.11 Size distribution of PE beads as extracted from facewash and weathered by advanced oxidation process (UVC/H_2O_2, 500 mg L^{-1}, 9 h) 172
Figure 6.12 Adsorption capacity of CAZ over time by **(a)** PET fibers, **(b)** PE beads, **(c)** PS foams, **(d)** PU foams, and **(e)** TWP rubbers. (MPs concentration 2 g L^{-1}, CAZ concentration 10 mg L^{-1}) 173
Figure 6.13 a, b) Representative SEM images of weathered PET fibres (NaOH alkaline hydrolysis, 3 h) 176
Figure 6.14 AFM height images and surface maps of **a)** pristine PET fibre, **b)** weathered PET fibre and **c)** Roughness (R_{RMS}) of pristine and weathered polyester fibres 178
Figure 6.15 SEM images of PE beads extracted from facewash before (top) and after (bottom) weathering 179
Figure 6.16 SEM images of a) Hard PS b) soft PS c) hard PU and d) soft PU before (left) and after (right) weathering 180
Figure 6.17 SEM images of a) Bridgestone, b) Kumho, c) Michelin, d) Goodyear TWPs 181
Figure 6.18 CAZ adsorption by PET fibre MPs (working volume 10 mL, MPs 2 g L^{-1}) 183
Figure A.1 Spiked mass recovery of cut polyester fibres in ultrapure wastewater 226

Figure A.2 FTIR spectra of polyester fibres - Control Experiment 228
Figure A.3 FTIR spectra of polyester fibres – treated with H_2O_2/dark (500 mg L^{-1} H_2O_2) 228
Figure A.4 FTIR spectra of polyester fibres - treated with UVC 229
Figure A.5 FTIR spectra of polyester fibres - treated with UVC/ H_2O_2 (500 mg L^{-1} H_2O_2) 229
Figure A.6 FTIR spectra of polyester fibres - treated with UVC/ H_2O_2 (800 mg L^{-1} H_2O_2) 230
Figure A.7 FTIR spectra of polyester fibres - treated with UVC/ H_2O_2 (1200 mg L^{-1} H_2O_2) ...230
Figure A.8 FTIR spectra of polyester fibres - treated with UVC/ H_2O_2 (2000 mg L^{-1} H_2O_2) ..231
Figure A.9 Isotherm fitting plots for linear (left) and Langmuir (right) models 231
Figure A.10 Kinetic fitting of polyester fibre concentration decrease over time with varied starting concentrations (UVC/H_2O_2 treatment parameters: 31.8 mW cm^{-2} UVC, 500 mg L^{-1} H_2O_2 treatment over 9 h) 233
Figure A.11 Kinetic fitting of polyester fibre concentration decrease over time with varied starting concentrations of H_2O_2 (UVC/H_2O_2 treatment parameters: 31.8 mW cm^{-2} UVC, H_2O_2 treatment over 9 h).....234

List of abbreviations

Polymers

HDPE	high density polyethylene
LDPE	low density polyethylene
PA	polyamide
PAM	polyacrylamide
PC	polycarbonate
PES	polyester
PE	polyethylene
PET	polyethylene terephthalate
PI	polyimide
PLA	polylactic acid
PMMA	poly(methyl methacrylate)
POM	polyacetal
PP	polypropylene
PS	polystyrene
PTFE	polytetrafluoroethylene
PU	Polyurethane
PVA	Polyvinyl acetate
PVC	polyvinylchloride
TWP	tyre wear particle

Methods

AFM	atomic force microscopy
BOD	biological oxygen demand
CI	carbonyl index
COD	chemical oxygen demand
DRIFTS	Diffuse reflectance infrared Fourier transform spectroscopy
DSC	Differential Scanning Calorimetry
FTIR	Fourier transform infrared spectroscopy
GC-MS	gas chromatography - mass spectrometry
HPLC	high performance liquid chromatography
OM	optical microscopy
QI	quantitative imaging
RMS	root mean square
SEM	scanning electron microscopy
TOC	total organic carbon

UV-vis	UV-visible range spectrophotometry
XPS	X-ray photoelectron spectroscopy

Chemicals

CAZ	ceftazidime
NP2EO	nonylphenol diethoxylate
PAH	polyaromatic hydrocarbon
PBDE	polybrominated diphenyl ethers
PCB	polychlorinatedbiphenol
PDS	peroxydisulfate
PMS	peroxymonosulfate

General

AAD	advanced anaerobic digestion
AD	anaerobic digestion
AOP	advanced oxidation process
BAS	Biosolids Assurance scheme
BRC	British Retail Consortium
CIP	Chemical Investigation Program
DEFRA	Department for Environment, Food and Rural Affairs
DI	deionised
EA	Environment Agency
ESS	Environmental Standards Scotland
IAF	integrated authorisation framework
LED	light emitting diode
MOF	metal organic framework
MP	microplastic
NFU	National Farmers Union
PCP	personal care product
PFI	private finance initiative
PPE	personal protective equipment
SEPA	Scottish Environmental Protection Agency
SRUC	Scotland's Rural College
SS	sewage sludge
UK	United Kingdom
US	ultrasound
USA	United States of America
UV	ultraviolet
WWTP	wastewater treatment plant

Publication statement

This thesis includes re-prints (in part or in full) of the following papers that have been published in peer-reviewed journals or online:

I. A. Tursi, M. Baratta, **T. Easton,** E. Chatzisymeon, F. Chidichimo, M. De Biase, G. De Filpoa, Microplastics in aquatic systems, a comprehensive review: origination, accumulation, impact, and removal technologies. RSC Adv. **2022**, 12, 44, 28318-40 *http://dx.doi.org/10.1039/D2RA04713F*

II. **T. Easton**, The application of sewage sludge to agricultural land in Scotland: risks and regulations. Scottish Environment LINK, **2023**, policy paper *available online*

III. **T. Easton**, V. Koutsos, E. Chatzisymeon, Removal of polyester fibre microplastics from wastewater using a UV/H2O2 oxidation process, J. Environ. Chem. Eng. **2023**, 11, 1, 109057 *https://doi.org/10.1016/j.jece.2022.109057*

IV. **T. Easton**, K. Maksymiuk, L. Charlton, V. Koutsos, E. Chatzisymeon, Transformation of polyester fibre microplastics by sulfate based advanced oxidation processes, J. Environ. Chem. Eng. **2024**, 12, 3, 112988 *https://doi.org/10.1016/j.jece.2024.112988*

V. **T. Easton**, V. Budhiraja, Y. He, Q. Zhang, V. Koutsos, E. Chatzisymeon**,** Antibiotic adsorption by microplastics: Effect of weathering, polymer type, size and shape, **2024**, *under review.*

T. Easton is first author for three primary research article publications and one policy report and is third author for a review article. The co-authors listed in the papers are T. Easton's supervisors, project students and collaborators.

1. Introduction

1.1 Motivation and research aims

This thesis aims to explore the effect of oxidative wastewater treatment systems on microplastics present in domestic wastewater, in order to understand their transformation and risk to the aquatic environment. The potential for advanced oxidation methods as a treatment option is explored.

To this end, the overarching research objectives were:

1) To determine the potential for sustainable advanced oxidation methods as a treatment option for MP polluted water.
2) Understand the transformation and degradation of MPs within these systems
3) Understand the implications of this transformation on MP interaction with organic micro-pollutants present in domestic wastewater
4) Consider this work in the context of broader environmental and waste policy in Scotland

These objectives were explored in a number of novel investigations. The novelty of each chapter is noted throughout this thesis, the main ground-breaking aspects of this work are:

- The development of an in-house MP preparation and degradation protocol which allows batch treatment and reliable quantification and characterisation of MP fibres.
- The first investigation of UV/H_2O_2 treatment for removal of polyester from water and the first study of any AOP for removal of polyester MP fibres.
- The first investigation of a number of sulfate driven AOPs for the removal of polyester MPs from water and comparison of the degradation caused by varied persulfate initiation methods.
- The first study of the effect of ultrasound-assisted AOP treatment methods on the transformation of polyester MP fibres in water.

- Detailed characterisation of the effect various AOP treatment have on this class of MP in terms of physical and chemical changes as weathering progresses, advancing understanding of the mechanism of degradation.
- The use of atomic force microscopy to map MP surface changes at the atomic scale, a technique not previously applied to polyester MP fibres within the context of AOP weathering.
- The first study to consider the adsorption of the antibiotic ceftazidime by MPs and a detailed investigation into the effect of MP characteristics and type on this interaction.

1.2 Thesis structure

Chapter 1 includes a review of relevant literature, offering an introduction to the theoretical background as well as the current state of the art systems employed for MP remediation within wastewater treatment systems. This chapter then introduces advanced oxidation processes and their potential for the degradation of MPs. The subsequent experimental work builds upon this theoretical basis.

Chapter 2 gives an overview of the materials and methods utilised in the experimental work presented within the thesis.

Chapter 3 considers sewage sludge pollution as a case study to explore the waste policy landscape in Scotland. The contamination of sewage sludge by MPs and organic contaminants is reviewed from academic literature and relevant regulation is discussed. This work was undertaken as part of a placement within the organisation Scottish Environment LINK and offers insight into the problems microplastics can cause within wastewater systems and beyond.

Chapter 4 focuses on degradation of MPs under controlled lab conditions. An experimental method was developed and AOPs were screened for removal of polyester fibres from water. An effective UVC/H_2O_2 treatment was optimised and real laundry wastewater was treated. The degradation of fibres was investigated to better understand the mechanism of removal.

Chapter 5 investigates sulfate driven AOPs with a focus on the transformative effects they have on MPs. This chapter seeks to explore how partial degradation can change the chemical and physical properties of MPs, leading to altered environmental behaviour. The impact of various initiation methods for sulfate driven AOPs on MPs are considered, namely irradiation, heat and ultrasound.

Chapter 6 explores the interaction of MPs with antibiotics. Specifically, various MP types were screened for adsorption of ceftazidime. The effect of polymer type, MP shape, MP size and weathering degree were explored in order to shed light on the behaviour expected within real water systems. Building on the insights gained from previous chapters, this study exemplifies the complex interactions which occur within WWTPs.

Chapter 7 concludes the thesis, summarising the main findings of the research based on the original aims as well as highlighting lessons learned during the experimental investigation. Suggestions for future work are offered.

1.3 Background

1.3.1 The problem with plastics

Plastic is utilised in nearly all aspects of modern life. It is extremely versatile and has the benefits of being low-cost, robust and lightweight which make it an attractive material choice for a huge number of applications. Plastic production has grown at a staggering rate since the 1950s. Global demand for plastic reached 368 million tonnes (Mt) in 2019. (1) Baseline predictions presented in a report by the Organisation for Economic Co-operation and Development estimate that economic growth will drive global plastic production to 1321 Mt by 2060. (2) This predicted increase in use applies to all of the polymers considered in the report with plastic fibres used in textiles notably set to triple and certain packaging polymers doubling in production. Unfortunately, the features that make plastic a tremendously useful material also create a serious problem if plastic waste is mismanaged. As plastic demand grows, the amount of environmentally persistent waste the industry generates grows with it.

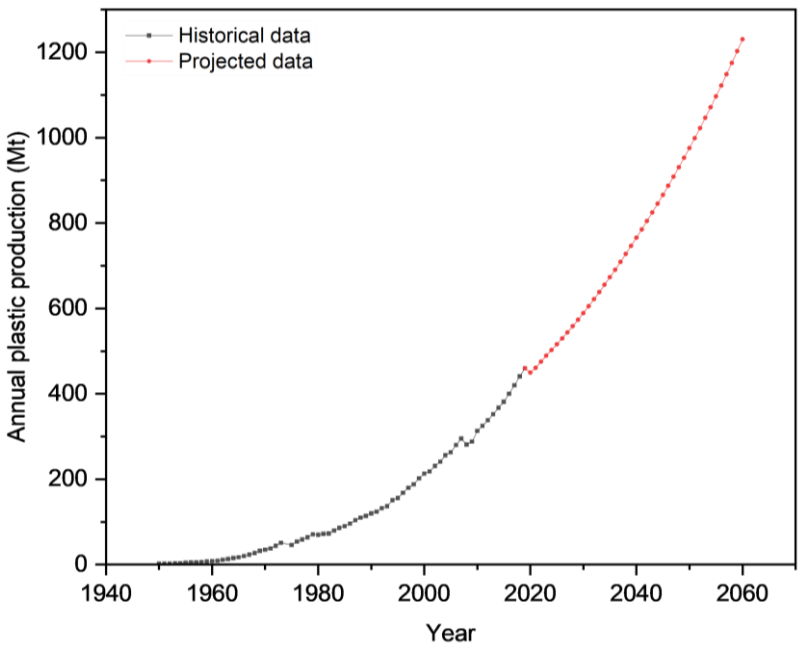

Figure 1.1 Global plastic production through time (produced using data from (2, 3))

The ocean is often the final sink for anthropogenic pollution. (4) By design, plastic degrades very slowly under natural conditions meaning it is accumulating in our rivers and oceans

where it may remain for hundreds or thousands of years. (5) Figures vary, but an estimated 1-2 million tonnes of plastic enter the marine ecosystem each year, largely due to the mismanagement of waste. (6, 7) As the global demand for plastic increases, so too does the amount of plastic entering this environmental compartment. Based on a modelling approach of growth in plastic demand against current commitments to waste reduction, the potential plastic release to the oceans under a 'business as usual' scenario estimates that 30 million tonnes of plastic pollution will enter aquatic ecosystems per year by 2040. In a best case scenario involving an entire global waste management system overhaul, annual releases of plastic pollution could be reduced to 5 million tonnes in the same timeframe. (8) Clearly, any meaningful intervention in this issue requires a massive global effort.

Once in the aquatic environment, plastic pollution has a number of consequences. Ocean ecosystems are impacted and disrupted by organisms ingesting plastic or becoming entangled in larger plastic debris. Ghost fishing describes the impact of derelict fishing gear on marine wildlife but smaller items such as plastic bags or drinking straws often make media headlines for the evident impact on wildlife. Less obvious but equally harmful effects include transport and leaching of harmful chemicals or additives contained within plastics. (9) These chemicals can be biomagnified within the food chain if ingested. The direct health effects of plastic in humans remain relatively unknown but several studies report endocrine, reproductive or toxic effects of plastic or the chemical additives carried on their surface. (10)

In addition to the clear environmental effect of plastic waste, long term economic harm can be done by allowing the issue to remain unaddressed. Fisheries experience decreased productivity resulting from contamination and harm to fish populations by ghost fishing. (11) Plastic is a resource that could find value in a circular economy by implementation of proper waste management strategies. Instead, plastic polluted coastlines lead to reduced tourism. The United Nations estimated a lower bound economic impact of $13 billion annually to worldwide fishing, tourism and shipping industries. (12)

The silver lining for a pollutant that is so widespread and visible on shorelines around the world, is a global awareness of the problem and desire for action. With the aid of high profile media attention and strong public will, there is currently an opportunity to tackle this

pervasive and persistent pollutant. As recently outlined by the high level panel for a sustainable ocean economy; (13) funding, policymaker attention and an ambition to drive change currently exist. This awareness presents a great opportunity to turn off the tap on plastic waste.

1.3.2 Microplastics

In the early 1970s, the first reports of small synthetic polymer fragments in the marine environment were published. (14, 15) It was not until 2004 that Thompson et al. (16) would coin the term microplastic (MP) to describe the ever increasingly abundant polymer fragments present in marine litter. In the last decade, scientific interest in the subject has surged, driven in large part by public awareness of plastic pollution in general. MPs are estimated to constitute 90% of the total plastic load in our environment. (17)

Figure 1.2 "Microplastic" by Oregon State University [1]

MPs are most commonly defined as particles smaller than 5 mm in size and can be classed into primary and secondary types. (18) Primary MPs are intentionally produced on the micrometre scale and sources include personal care products (PCPs) such as exfoliating face washes or toothpaste which can contain small beads of plastic. Industrial abrasion additives used in sandblasting often use small plastic pellets or fragments and industrial plastic precursor pellets (termed nurdles) are the raw form of plastic for industrial use, both of which can be directly released into the environment. Secondary MPs encompass any microscale

[1] Image reproduced under a CC BY-SA 2.0 DEED open access licence

fragment that is created by the weathering or fragmentation of larger polymer pieces. For example, the slow photodegradation of marine litter under UV exposure leads to smaller pieces of MP breaking off. The shedding of synthetic clothing fibres during washing cycles releases thousands of secondary MP fibre fragments in wastewater. A single fragment of plastic can break up to form thousands of micro and nano sized pieces in the natural environment.

Tiny fragments of plastic can present unique monitoring challenges due to their small size. One of the most important factors when considering an environmental pollutant is having a reliable method of determining its concentration and confirming its identity. There does not currently exist a standard sampling method for environmental MPs, although a call for standardised testing criteria is emerging within the research community. (19-21) Underestimation and misidentification of fragments is common in historical datasets, which presents a challenge for decision makers and researchers seeking to quantify the scale of the problem.

1.3.3 Effect of microplastics on human health and environment

MPs are classed as contaminants of emerging concern. (22) Once in the aquatic environment, MPs may be mistaken for food particles and ingested by marine organisms, leading to food dilution, choking and death in some cases. (23-25) Uptake by small marine organisms introduces MPs to the food web where bio accumulation can result. The potential toxic effect of microplastics is an area of intense research and it has not been determined what lasting damage these pollutants could inflict on marine organisms and the humans who eventually consume them. (26) In addition to physically obstructing feeding or digestive tracts in larger organisms, enhanced inflammatory responses and potential cytotoxic effects are reported in human cells exposed to MPs. (27-29) Polyester fibre toxicity has been tested on Xenopuslaevis larva using non homogeneous fibres from clothing waste. (30) Although no mortality was observed, adverse effects on larvae development were observed.

As potentially buoyant and highly mobile particles, MPs can also act as carriers of a number of toxic additives. The adsorption of co-contaminants such as antibiotics, pharmaceuticals and persistent organic pollutants to the MP surface amplifies the risk. Re-release of these chemicals into water or the gut of an organism can deliver a toxic pollutant. For a more detailed discussion, the direct and indirect toxicity of MPs to the aquatic environment are both reviewed in great detail elsewhere. (4, 10, 31-33) Plasticisers such as BPA and phthalates, flame-retardants and heavy metals can all be transported great distances by association to MPs. If ingested, these additives have known health impacts on organisms, which can be magnified by the bioaccumulation of the plastic.

Human exposure to MPs is mainly via ingestion, although inhalation and dermal contact also present a route of exposure. Evidence pointing to disruption of immune function (34), inflammatory response (10), oxidative stress (35), neurotoxicity (35) among others, highlight MPs as a cause for concern. Co-contaminants such as organic contaminants and heavy metals adsorbed by MPs pose an additional risk when they are ingested together. (36) MP toxicity in humans is extensively reviewed elsewhere. (24, 25, 32, 37) In general, evidence showing harm is limited but MP have been found in samples of almost every human tissue. The overriding message from many toxicity studies is that a precautionary principle should be applied to this pollutant class while further understanding of the direct and indirect toxic effects is developed.

1.3.4 Sources of microplastic pollution to the aquatic environment

A combination of vast amounts of plastic in circulation, a “throw away” consumer attitude and poor waste management results in a great number of routes for microplastic pollution to reach the aquatic environment.

Figure 1.3 shows sources of MPs to water via agriculture, urban, industry and wastewater. Agricultural runoff often contains MPs intentionally added to fertiliser mix, designed for controlled nutrient release as well as particles introduced unintentionally. (38) Urban storm water can collect plastic waste littering our terrestrial environment such as fragments of rubber released from car tyre abrasion, plastic masks/ PPE and even resin based road marking

paint. (39) Drainage systems then deposit these directly into rivers and estuaries in coastal regions. Industry sources are numerous and highly dependent on the type and scale of industry present. Primary microplastic beads called nurdles destined for the plastic production industry are regularly lost during shipping by spillage. (40) Landfill leachate was reported to contain a high proportion of very small microplastics which can make their way to rivers and oceans depending on the landfill location. (41)

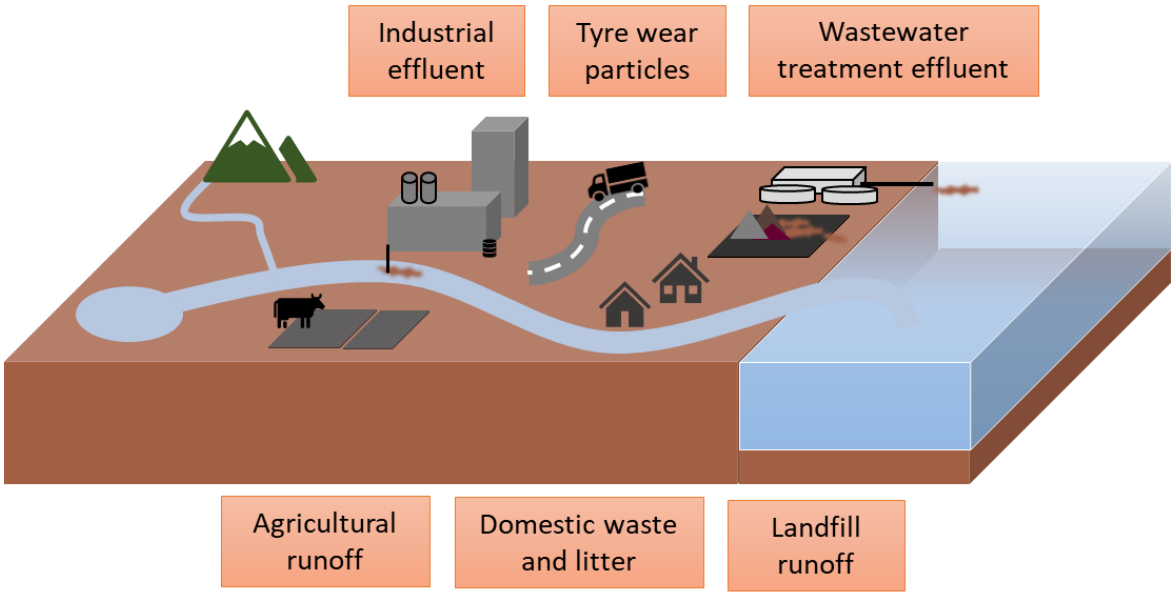

Figure 1.3 Major microplastic sources and transport routes to the aquatic environment

Wastewater and sewage treatment plants are a key source of plastic release to the marine environment. (42) In domestic wastewater, synthetic fibres originating from textile fabric are reported as a major contributor and usually consist of polyester or nylon. (43, 44) Personal care products containing polyethylene or polypropylene such as exfoliating face scrub or toothpastes recently attracted significant media attention. Commercial and industrial wastewater can contain huge numbers of MPs originating from acrylic paint or plastic dust from processing. The composition of wastewater plastic pollution varies greatly depending on the nature of the influent source and is discussed in detail in Section 1.3.5. (45)

1.3.5 Prevalence of microplastics in wastewater

Wastewater treatment plants (WWTPs) were not designed with MP pollution in mind. 15 million MPs have been estimated to be released in effluent each day from a single WWTP. (46, 47) The type and quantity of plastic varies greatly depending on the source of the wastewater with clear differences between domestic waste and industrial or commercial waste. (50) To engineer a solution suitable for treatment of these varied and complex waters is a challenge.

A growing body of literature has worked to identify trends in the plastic observed at various stages of treatment and it paints a complex and sometimes conflicting picture. The polymer type and particle shape observed depends on the wastewater influent and significant differences have been observed between samples from around the world. (51) The most common polymers found in influent at a treatment site in Scotland after coarse screening were alkyds (modified polyester (PES) commonly used in paints) (28.7%), polystyrene (PS)-acrylic (19.1%), PES (10.8%), polyurethane (PU) (8.9%), and acrylic (8.3%). The most common polymer found in the final effluent was PES (28%), polyamide (PA) (20%), polypropylene (PP) (12%), acrylic (12%), alkyd (8%), polyethylene (PE) (4%), PS (4%), and polyethylene terephthalate (PET) (4%). (52) The liquid fraction contained mainly flakes (67.3%), fibres (18.5%), film (9.9%), beads (3.0%), and foam (1.3%). At three WWTPs in Australia, the concentrations of different polymer species (PET, PE, polyvinylchloride (PVC), PP, PS and Nylon) varied widely with PET and PE as the most common polymers. (53) Fibres were the dominant type of microplastic detected in all wastewater effluent samples and were not completely removed even after advanced treatment processes. According to Mintenig et al. in a German study, the most common polymers were PE, polyvinyl acetate (PVA), PS, PES, and PA in a WWTP. (54) Whereas, the order of PET > PE > polyacrylamide (PAM) > PVC > PS > PP was reported at a WWTP in Finland. *(55)* In Eastern China, Huang et al showed effluent MP content comprised of PET (47%), PS (20%), PE (18%) and PP (15%). (56)

Variety in reporting methods as well as differences in the analytical techniques used across studies, makes it challenging to identify and prioritise specific sources of MPs which lead to high levels of pollution. One common trend in literature is that the majority of larger plastic

fragments such as microbeads are retained in solid phase during treatment while fibres and small particles are typically present in the effluent, indicating their poor removal. (57) A study of a Canadian WWTP found that fibres accounted for 82% of the MPs and had a total daily discharge of 141 million particles per day. (58) To narrow the focus of this thesis from all MP types and shapes, polyester MP fibres are selected for screening experiments as a particularly problematic MP, capable of passing through traditional WWTP systems. PE microbeads, PU/PS foam and TWPs are also considered within Chapter 6.

Polyester fibres

The contribution of wastewater on the number of polyester and acrylic fibres found in the marine environment has been linked to the generation of domestic laundry wastewater. (59, 60) Polyester is the most common MP fibre polymer type in effluent from commercial washing machines. (61, 62) Domestic washing machines are capable of producing more than 1900 fibres from the washing of a single garment and polyester has been identified as the leading fibre-shedding polymer. (59, 63) These fibres pass through screens and treatment systems more easily than other MP shapes due to their very small size in two dimensions. (62) The number of MP fibres in treated effluent varies depending on the treatment steps and the characteristics of the influent. (64) Between 0 - 54 polyester particles per litre was estimated within the effluent from 21 real treatment sites by Iyare et al. (65) Scaled up, this presents a large flow to the environment as one estimated total global flow of fibres from laundry to aquatic environments is 0.28 million tonnes every year. (66)

The occurrence of polyester fibres in sewage treatment works, river and estuarine sediments and along shorelines are disproportionately high, relative to the overall commercial demand for these polymers. (61) This can be taken as an indication that these MPs in particular are poorly removed in treatment processes. High prevalence in effluent is coupled with a greater accumulation of polyester in natural water. PET has a high density (1.38 g cm^{-3}) and tends to settle in environmental freshwater samples which affects its subsequent removal in natural environments. A relationship between plastic demand and use to the prevalence as a MP in the aquatic environment also showed dense PET was particularly prevalent within sewage sludge and deep water relative to its use for the same reason. (61)

Polyethylene microbeads

Microbeads found in WWTPs typically originate from personal care products (PCPs) such as facewash and toothpaste. (67) The beads are added as an exfoliant typically with a rough surface texture. Various polymer types have been used for these products with the most common being PP and PE. In Scotland, the number of microbeads in domestic wastewater is expected to be low due to the implementation of the Environmental Protection (Microbeads) (Scotland) Regulations 2018. This legislation bans the manufacture and sale of rinse-off personal care products containing plastic microbeads. (68) Specifically, solid microplastic ingredients, less than 5 mm in size are banned for use as personal care product additives, in line with REACH chemical legislation in the EU. (69)

Expanded foam particles

Foams used in the food industry and construction are prone to fragmentation and form MPs. From this use, PS and PU can enter water systems from domestic waste, rain runoff and landfill. (70) Limited information exists on the fate of this class of MP within WWTPs and warrants further study.

Tyre wear particles

Rubber tyre wear particles (TWP) are a major sources of MP runoff to water systems in built-up urban areas. Estimates place the contribution from TWPs at around 5-10 % of the global total amount of MP to ocean pollution. (71) TWPs are generated by the friction between tyres and roads and can be transported into wastewater during rainfall. (72) The diversity of tyre materials used around the world means this class of MP is also diverse and often associated with co-contaminants such as heavy metals and organic micro-pollutants found in urban areas. (73)

1.3.6 Removal and treatment technologies

The removal of MPs from water is a key challenge in the struggle to mitigate environmental pollution. Traditional water treatment plants are not designed to remove MP and they have

been globally identified as a major source of MP to the environment. (53, 55, 74, 75) It is important to understand our current ability to remove these pollutants *via* engineered treatment methods and identify key opportunities to reduce their concentration within receiving water bodies. For this purpose, physical, chemical and biological processes for the treatment of MP contaminated water (whose performance is shown graphically in Figure 1.4) are reviewed in this section.

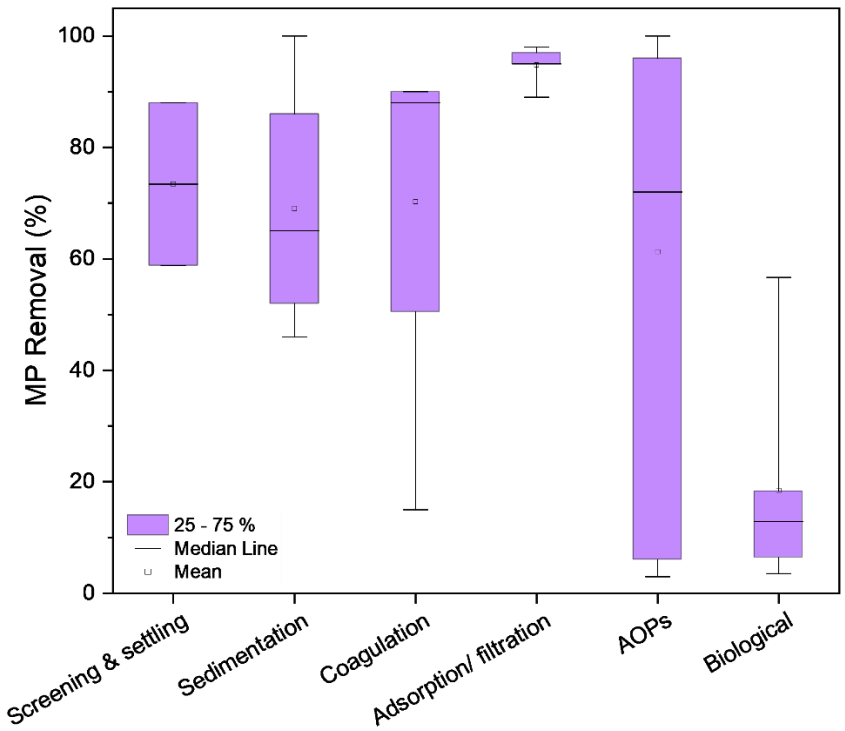

Figure 1.4 Reported microplastic removal performance of water treatment technologies

1.3.6.1 Physical processes

Physical separation processes for primary wastewater treatment include screening, skimming and sedimentation. Using these methods, fast and low-cost filtering of large contaminants is possible. The ability to remove MP depends on the wastewater characteristics as well as the type of treatment process applied.

Screening and settling

Traditional screening and settling methods may remove significant portions of suspended solids in water. For example, Liu *et al.* (76) observed that the average size and number of MP fragments present in the water in a Chinese WWTP decreased by 58.8 % and 40.7 %, respectively, after initial screening and sedimentation. The particles removed were mainly large but the authors also observed the adherence of MP to suspended solids in the water, allowing physical removal of smaller fragments and fibres that might not be expected otherwise. Moreover, screening and sedimentation have reportedly removed up to 88 % of anthropogenic solids in a treatment facility in the United States (although this classification includes more than just MP). (77) The importance of plastic density as related to settling velocity during the sedimentation step is highlighted by Iyare *et al*. (65) The huge variety of polymers in terms of density, shape and type that are found in wastewater can substantially influence their physical separation from water. Settling alone removes an average of 72 % of MP particles present in sewage influent but the smallest particles (<27 µm in diameter) are likely to pass unimpeded. As well as failing to capture the smallest particles, reliance on traditional separation processes to remove MP in this way presents another problem of transferring the pollutants from liquid to a concentrated solid waste. (78, 79) This can become a serious environmental problem when sludge is recycled for land treatment or disposed of inappropriately; thus potentially allowing MP to find their way back into the water system. (80)

The difference in density between MP and the natural organic matter of water presents an opportunity for physical removal. Several lab-scale studies have applied enhanced density separation in salt solution as an isolation method for MP samples in complex matrices such as wastewater or natural water. (81-83) Scaling up this method is challenging due to the large volumes of high-cost salt solutions required. (84) Alternatively, settling *via* coagulation seems promising for large-scale application. Using traditional Fe salt coagulation conditions, the removal of polyethylene (PE) MP was found to be poor with less than 15 % removal. (85) However, in the same experimental setup, using a high dose anionic PAM coagulant, removal was increased to over 90 %. This can be attributed to the low density of PE that inhibits settling of the produced flocs and reduces the efficiency of the coagulation treatment.

An impact of this effect was also observed by Ma *et al.* (86) where the highest efficiency removal of approximately 60% was achieved for the smallest sized MP. In addition to density, the shape of MP is likely to affect greatly the settling behaviour. Skaf *et al.* investigated the removal of both fibres and microspheres of PE using an alum coagulation method and they found that both could be adequately removed by sweep flocculation. (87) Less traditional coagulation-like methods such as the bioinspired agglomeration process developed by Herbort *et al.* (88, 89) suggest targeting specific MP in water. Electrocoagulation methods have also been explored and over 90% removal of PE beads was reported. (90) Despite the progress in the area, the main problem with coagulation based methods is the highly variable nature of MP surfaces. The surface charge is not easily predicted meaning that coagulants specifically designed for MP removal are less efficient than for the removal of organic material.

Filtration and adsorption

Some developed materials for adsorption and activated filtration aim to target MP in water. Biochar offers a low-cost option for removal of many pollutant classes, including MP. (91, 92) Sun *et al.* (93) engineered an adsorption separation process relying on a biodegradable chitin and graphene oxide sponge which is capable of removing up to 89% polystyrene from water. Batch filtration was proposed using a Zr-MOF system with over 95% efficiency for removal of PVDF microplastics. (94) While promising in performance, adsorption and batch filtration treatment pose a challenge in scaling up to meet the needs of a full scale WWTP.

Membrane separation of MP is an option already employed at scale. Malankowska *et al.* review in detail the advances made in microfiltration, ultrafiltration and nano-filtration methods in the removal of MP. (95) Michielssen *et al.* suggest retrofitting WWTPs with granular sand filtration and membrane filtration has the highest potential for MP removal in a meta-analysis of available technology. (77) This finding was backed up for large scale studies in a comparison of municipal WWTPs where rapid sand filtration removed 97% of MP. (55) However, the high potential removal efficiency comes at the cost of membrane pore blockage and resulting flux reduction when applying high-pressure filtration techniques. Such issues arose within just 48 h of ultrafiltration when 38% flux reduction occurred due to MP blockage of pores during treatment of MP contaminated water. (96) MP interaction with

organic matter in the water may also enhance the rate of membrane fouling. The size of MP in the raw water were found to be the major factor influencing fouling during freshwater ultrafiltration treatment with the most severe effects at a MP size of 1 µm. (97) However, continuous filter module rotation could significantly reduce the fouling and the treatment became more attractive for large scale application. MP in landfill leachate were successfully removed using membrane separation. Interestingly, the researchers identified the re-release of captured MP from the filter back into the effluent suggesting that the particles are not permanently immobilised onto the membrane and may still be released into the environment. Similar removal and re-release behaviour occurred in ultrafiltration membrane treatment of drinking water as well as some MP penetrating the membrane itself. (98) Despite a 98% removal by reverse osmosis treatment, fibers of plastic under 200 µm passed unimpeded indicating that membrane processes alone cannot completely remove MP.

1.3.6.2 Chemical processes

Effective chemical degradation of polymers could mineralise MP during water treatment and avoid transferring any waste to a new solid phase. Advanced oxidation processes (AOPs) are an effective means to remove biologically recalcitrant contaminants by the generation of non-selective, highly reactive radicals. AOPs are effective in the removal of emerging organic pollutants, such as antibiotics, personal care products, trace organics. (99-101) Recently, their potential application in the rapid degradation of MP is drawing attention. (102) During chemical degradation, the surface of the polymer undergoes chemical change and the MP subsequently fragment.

Photocatalytic treatment

The majority of research published in AOP treatment of MP focuses on photocatalytic methods and is summarised in Table 1.1. Titania (TiO_2) based photocatalysis is the most common treatment due to its low cost and relatively high radical generating ability. (103) Due to the need for a surface contact during heterogeneous photocatalysis, the morphology of the catalyst is an important area of focus with researchers exploring the use of nanotubes and nanoparticles.

Using TiO_2 doped with C and N, a significant loss of mass of 72% was lost from high density PE beads after an extended treatment time of 50 h. (104) The authors enhanced performance by lowering the water temperature and pH which was attributed to the enhanced radical forming ability of the optimised process as well as changes to plastic properties at low temperature. Nitrogen doped TiO_2 was also utilised in a study focusing on the effect of plastic shape on removal rate. (105) By considering the surface area difference between samples (beads *vs.* flakes) as well as the MP particle size, it was concluded that light illumination was the main factor affecting removal. Furthermore, it was observed that the low density PE flakes, an insoluble water pollutant, were floating on the water surface blocking light and oxygen from reaching the submerged catalyst. This probably resulted in generating fewer radicals thus yielding a removal efficiency less than 5%. Similarly, a low removal in water was also observed during treatment of PS with TiO_2, which was attributed to low transmittance of UV light. (106) Removal of the MP from water by physical means prior to AOP treatment allowed effective oxidation but this can limit the practical applicability of the method at large scale.

Other catalyst doping strategies have been explored such as the use of Pt doped ZnO based AOP. (107) It was found that the proportion of carbonyl and vinyl surface groups on a low density PE film was increased when treated, which indicates surface oxidation. As well as doping, the effect of synthesis conditions on MP removal has been explored. The synthesis method employed for catalyst preparation was investigated by comparing traditional sol–gel and bio derived N-doped TiO_2, with an improvement in MP removal observed for the latter green-synthesised material. (108) Synthesis of ZnO catalysts was tuned to produce a variety of nanorod lengths and the effect of their morphology on plastic removal was studied. (109) High surface area ZnO supported on a glass fibre substrate enabled trapping of low density MP in place in contact with the catalyst for continuous flow treatment. (110) In the first AOP treatment specifically reported for fibre degradation, a combination of UVC irradiation and TiO_2 photocatalysis achieved 97% mass reduction of polyamide in 48 hours. (111) Less common materials have also been investigated such as a PMS carbon nanospring based catalyst and hydroxy-rich ultrathin sheets (112, 113) and TiO_2 supported on β-SiC alveolar foams. (114)

Fenton and Fenton-like treatment

Fenton based AOPs combine hydrogen peroxide and Fe(ii) ions to produce oxidizing hydroxyl radicals, activated by light or heat. (115) A few of these treatment methods have recently been applied for MP removal and are summarised in Table 1.1.

Many of the Fenton based treatment processes reported in the literature were developed with the aim of accelerating the ageing of MP in order to study the change in adsorption or transport behaviour. (116-118) Although not aimed at removing MP completely, these studies provide important insight into how plastic degradation is initiated by Fenton processes and could be harnessed for water treatment applications. For example, during Fenton treatment of PS and HDPE over long timescales, issues with the deposition of ferric hydroxide were observed thus leading to poor removal from water, despite steps taken to mitigate this. (117) Thermal methods of activating the Fenton reaction can offer an alternative mechanism of action, as explored by Hu *et al.* (119) A high mass loss of plastic was observed for a range of polymers but the treatment required the use of high temperatures in order to break down the crystallinity of the plastics, which limits its applicability at large scale. Furthermore, combining heterogeneous systems (*i.e.* solid iron on a supporting matrix) with photocatalysis resulted in significant reduction in size of PVC and PP particles after 7 days. (120)

Table 1.1 Advanced oxidation treatment methods for microplastic removal from wastewater

AOP	MP targeted	Monitoring methods	AOP performance	Other parameters	Ref.
C,N–TiO_2 photocatalysis	PE beads	Mass loss, FTIR measured carbonyl index (CI), microscopy	50 h, mass loss 72% and large increase in CI	Visible light LED (400–800 nm), temperature 0–40 °C, pH 3–11, lamp distance 25 cm, 4 L^{-1} MPs, 4 g L^{-1} catalyst (optimum removal at pH 3, 0 °C)	(104)
N–TiO_2 photocatalysis	PE beads and flakes	Mass loss, CI	50 h, mass loss < 5% for all (4.6% HDPE and 1.8% LDPE)	Visible light LED (400–800 nm), pH 3, room temperature, 4 g L^{-1} MPs, lamp distance 21.5 cm	(105)
ZnO nanorod photocatalysis	PE film	Microscopy (SEM), mechanical change, CI	175 h, CI increase of 30%	Visible light 50 W dichroic halogen ambient air. Deionised water	(109)
N–TiO_2 photocatalysis	PE beads	Mass loss, SEM, CI	8 h, mass loss < 3% in aqueous solution	27 W visible fluorescent lamp (400–800 nm), room temperature, lamp distance 12 cm, 2 g L^{-1} MPs	(108)
PMS/carbon nanospring photocatalysis	PE	Mass loss, CI, SEM	8 h, 40% mass loss	pH 3–11, MPs 5–12 g L^{-1}, temperature 25–160 °C (>150 °C optimum)	(112)
ZnO photocatalyst supported on glass fibre	PP	Size change, CI, SEM	456 h, 65% reduction in volume	Visible light 60 mW cm^2, 300 mL min^{-1} continuous flow treatment of 10^4 particles per L	(110)
TiO_2 nanoparticle photocatalyst film	PS	Diameter change, DRIFTS, GC-MS	24 h required for removal of 400 nm starting diameter particles	254 nm UV irradiation	(106)
ZnO nanorod photocatalysis with Pt modification	PE film	CI, SEM	175 h	Visible light 50 W, room temperature, lamp distance 10 cm	(107)
TiO_2	PA fibre	Mass loss, CI, total organic carbon (TOC), SEM	48 h, 94% mass loss	UVA irradiation, room temperature, 5 lamp photo reactor	(111)

Modified TiO_2 photocatalysis	PMMA, PS	TOC	7 h, flow reactor	UVA irradiation 112 W m^2	(114)
Hydroxy-rich ultrathin BiOCl photocatalysis	PE	Mass loss	5 h, 6% mass loss	250 W of 420 nm irradiation; MP and catalyst 1 g L^{-1}	(113)
Photo-Fenton	PS	SEM, CI, HPLC/MS, contact angle, C : O atomic ratio (XPS)	108 h, CI increase	500 W mercury lamp, 12 g L^{-1} MPs	(116)
Fenton	PS and HDPE	Size distribution, CI, C : O ratio by XPS	1–30 days	pH 4, 3 mM Fe, 4.5 mg mL^{-1} H_2O_2	(117)
Fenton	PE, PP, PVC, nylon	Microscopy	10 min, minor surface area decrease	Room temperature, pH 5, 7 g L^{-1} MPs, 3–10 mg mL^{-1} Fe	(118)
Thermal Fenton	PE, PS, PP and PET	Mass loss, CI, DSC to determine crystallinity, XRD, SEM, Raman spectroscopy, particle sizing by zetasizer	16 h, 96% mass loss	4 mM Fe^{2+}, 300 mM H_2O_2	(119)
Heterogeneous photo Fenton/photocatalysis	PP, PVC	FTIR, particle diameter by microscopy	7 days, 94–96% size reduction	Nano zero valent iron and combined with ZnO/SnO_x photocatalysis, 60 mW cm^2 visible light	(120)
Ozonation	PE	FTIR, XPS	60–180 min, increase in CI	Ozone 4–7 mg L^{-1}	(121)
Ozonation	Mixed MPs obtained from real wastewater	Particle counting	99.2% removal after tertiary treatment (incl. removal *via* other methods during the treatment process)	Ozone 12.6 mg L^{-1} for 1 min during tertiary treatment	(122)
Ozonation, H_2O_2/ozone	PE, PP, PS	Adsorption, XRD, SEM, FTIR	10 min, ozone dose of 88 mg L^{-1}	O_3 : H_2O_2 molar ratio of 0.5	(123)

Ozone and peroxide based treatment

Ozone has been applied either on its own, (121) or in combination with radical generating hydrogen peroxide (123) to degrade MP. In the latter case, a 10 minutes treatment affected the surface chemistry and associated adsorption behaviour of several types of plastic. Although the treatment is not directly designed for removal, the resulting change in adsorbance properties is relevant to understanding how MP treated with AOPs may carry additional micro pollutants through the water treatment process and therefore extending the treatment duration may be an option for investigation. Similarly, Zafar *et al.* considered the effect of ozone treatment on the surface of PE particles and found that reaction time was more effective in increasing the oxygen prevalence on the surface compared to ozone dose. (121) Hidayaturrahman *et al.* reported that ozonation combined with primary, secondary and coagulation steps removed 99.2% of MP in a full-scale treatment plant. (122) While reasonably high removal performance is possible, slow reaction rates currently limit the applicability of AOPs in water treatment. Long contact times of several hours are not feasible in a high throughput system. In order to bring AOPs into the focus for water treatment, improvements to the rate of degradation are essential.

1.3.6.3 Biological processes

Biodegradation of plastic is an intensive area of research and has potential for application in wastewater treatment. (124-126) Traditional water treatment systems typically involve an element of biodegradation for the removal of organic matter. In most cases, these systems fail to adequately remove MP, leading researchers to explore alternatives.

In a systematic review for MP removal, Iyare *et al.* (65) identified that 19 out of 21 traditional wastewater treatment systems included activated sludge treatment as a secondary step. On average, activated sludge could reportedly remove 16% of MP from the water (across a broad range of 0.2 – 52 %). Alongside limited effectiveness, relying only on traditional water treatment methods like this can create further challenges. Physical transfer of MP out of the wastewater moves the plastic pollution into another part of the water treatment process – the sludge. Also, MP can affect the activity of bacteria used for organic matter decomposition

as well as cause issues downstream in sludge treatment. (76, 127, 128) Wei *et al.* showed that PET MPs inhibited aerobic digestion of waste activated sludge (WAS) by approximately 10%, which was attributed to its influence on microbial communities. (128) In another study, anaerobic digestion of WAS was found to be impeded by the presence of PVC MP. Moreover, bisphenol A leaching out of the plastics was linked to a decrease in methane production and inhibition of the treatment in this case. (129)

Biofiltration of wastewater was identified as a more effective biological secondary step for MP removal than activated sludge with an average of 19% from the treatment systems surveyed. (65) However, the presence of MP in these systems drastically impedes the effectiveness of treatment for other contaminants. Membrane bioreactors (MBR) reportedly experience immediate decline in removal of organic matter from 80% to below 50% upon addition of PVC MP. (130) This was attributed to an increase in membrane fouling as a result of MP build up. In order to avoid these knock-on effects to treatment system performance, the presence of MP needs to be taken into account when (re)designing water and wastewater treatment processes. Developing biological treatments specifically aimed at combatting plastics is a challenging area of research but is clearly required to overcome the shortcomings of traditional WWTPs. Outwith the context of wastewater treatment, bacteria, bacterial consortia (131-134) and fungi (135, 136) have been investigated for their ability to degrade plastics. Microbial digestion is an extremely attractive option to solve the problem of plastic waste in a potentially sustainable way. One of the main hurdles in each case is the lengthy treatment times required (many reported biodegradation options take weeks or months) for it to be effective for large scale application. In 60 days, PE was biodegraded by a specifically isolated microbial consortium to reduce its mass by just 14.7%. (134) PET increased crystallinity and reduced in particle diameter as a result of bacterial degradation in a high pH process over 48 h but complete removal was not achieved. (137) Using a surfactant to improve interfacial activity, bacterial degradation of PET reached 11% mass loss in 5 days. (138)

As well as the lengthy digestion times required, biological systems are likely to struggle to cope with the diverse nature of our plastic waste. Enzymatic digestion relies on specific target groups in the polymer chain being broken. To tackle the huge range of polymers present in

our waste, a great many different plastic digesting microorganisms will be required. (139) As it stands, these engineered systems are not currently capable of treating the high flow of microplastics in our water treatment systems due to the long timescales required but are under constant development as reviewed comprehensively elsewhere. (140)

1.3.6.4 Summary of current removal technology performance

As previously discussed, a broad range of polymer types and MP shapes are present in the environment. Lab scale treatment studies have focused on a number of different MP subtypes. It is important to consider the effect of this when evaluating the efficacy of a reported treatment system. Figure 1.5 a and b show the papers discussed in this section, broken down by which MP types and shapes are focused on. Furthermore, Figure 1.4 highlights the performance of treatment technologies reviewed here in terms of MP removal from water. It can be observed that primary treatment (screening, settling, sedimentation) can remove about 50–90% of MP from wastewater, while adsorption and filtration are able to remove more than 95%. The percentages for advanced oxidation processes can span from very low to almost complete removal of MP. For biological engineered technologies the removal can be up to 20%. Physical treatment methods offer reasonably consistent high removal rates but are hampered by the production of solid waste and process problems such as membrane blockage. Chemical and biological treatment methods are an area of intense research and have the potential to effectively destroy MP if the rate of degradation can be significantly improved. Further research into these important water treatment systems is required to further understand their potential in tackling MP pollution.

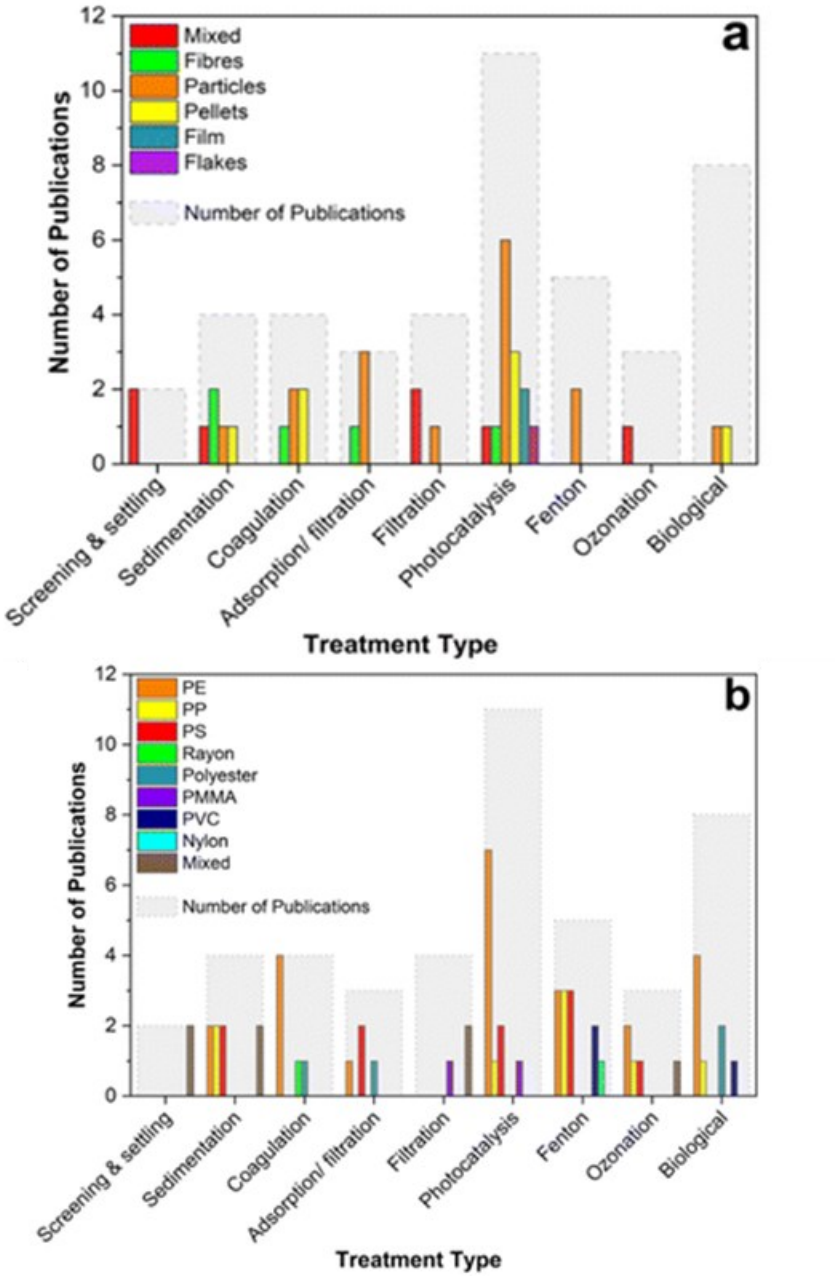

Figure 1.5 a) Publications reviewed considering water treatment for the removal of microplastics broken down by plastic shape. **b)** Publications reviewed considering water treatment for the removal of microplastics broken down by polymer type.

In preparation of Figure 1.4 and 1.5, a systematic literature review was performed using the DiscoverEd and Web of Science database search function to extract all relevant manuscripts up to the date of search (1st September 2022) The following search strategy was used: (Microplastic OR micro-plastic OR nanoplastic OR MP) AND (wastewater OR WWTP OR waste water)

1.4 Photodegradation and advanced oxidation processes

AOPs are an effective means to remove biologically recalcitrant contaminants. The introduction of powerful oxidants has been shown to be effective in the removal of antibiotics, personal care products and more recently, MPs. AOPs generate non-selective, highly oxidising free radicals in solution and offer the potential to rapidly initiate oxidation reactions in polymer chains, driving their degradation towards complete mineralisation within a timescale relevant for remediation and water treatment. Oxidative degradation of polymers is complex and dependent on a number of conditions. Generally, the visible physical impacts are shown similarly across polymer types. Oxidative degradation occurs at the polymer surface, forming a brittle layer susceptible to shrinkage and stress fracturing. Cracking and fragmenting can then occur due to the weakened physical state of the material, exposing new surfaces to oxidation. (141) The MP surface microlayer has also been identified as a key compartment for degradation in the natural marine environment. (142) Because of this, the shape of microplastic will affect the rate of degradation due to the surface area exposed. (143) Additionally, plastic additives such as UV stabilisers or dyes will affect the rate of degradation. (144) The mechanism of AOP action is not the focus of this thesis, however, photodegradation of polymers and relevant AOPs used in experimental studies are introduced and outlined here as these are important to consider when comparing the efficacy of AOP treatments.

1.4.1 Photolysis

Polymers containing light absorbing chromophores can be directly degraded by photo irradiation. High energy UV irradiation is capable of breaking polymer chains and generating free radicals. As these radical driven reactions propagate, the polymer molecular weight is reduced, leading to changes to the plastic properties and fragmentation into smaller particles. (145)

The specific mechanism of photodegradation is polymer dependent. Polymers like Teflon (PTFE), Plexiglas (PMMA), polyimides (PEI, PI), and silicones have high stability to photo oxidation, whereas polycarbonate (PC) and PES/PET have moderate UV resistance. Natural rubber, PS, polyacetal (POM), Nylon (PA), Cellulose, PVC, and many polyolefins are considered

highly sensitive. (31) Photostability varies with bond strength, presence of chromophores and availability of reactive H atoms on secondary/tertiary carbon sites (H atoms on tertiary sites are more photolabile). Notable examples of polymer types relevant to this thesis are discussed here.

PE is a non-absorbing polymer as its structure contains no chromophores capable of absorbing in the UV-vis range. Oxidation progresses via absorption by chromophoric polymer defects. (146) In one study the abundance of PE unsaturation had no effect on the rate of photooxidation, perhaps indicating that the initiation stage of photodegradation of PE does not occur at these sites. (147) However, the extent of branching influenced the rate due to the change in number of exposed tertiary H atoms. (148) HDPE, LDPE and also 'biodegradable' versions have been compared to examine the differing rate of photooxidation over long term exposure to UVB radiation. (149) Degradation tracked by vinyl or carbonyl group abundance and crystallinity suggested that the greater extent of branching is responsible for faster photodegradation of LDPE compared to HDPE. Polymer crystallinity is also relevant. Crystalline HDPE has a lower chain mobility which promotes radical recombination at the expense of radical propagation reactions, therefore slowing the rate of degradation. (143)

PET absorbs light below 360 nm, with very high adsorption in the UV range below 300 nm. However, due to poor quantum yields, PET resists rapid degradation by this absorbed radiation. (150) Aromatic and aliphatic sections of the polymer chain both undergo oxidising reactions leading to chain scission and chain branching. The mechanism is then thought to proceed via radical Norrish type I and II reactions, detailed elsewhere. (146, 151-153) Photolysis initiated photo-oxidation of PET yields carbon monoxide, carbon dioxide and carboxylic acid products, although the potential incomplete mineralization products are numerous and complex. Radical intermediate recombination forms a cross-linked structure and new chromophores. (154) In terms of the physical changes to MPs, discoloration and plastic embrittlement are commonly observed for partially photo-degraded PET.

1.4.2 UVC/H_2O_2 based AOPs

The UVC/ H_2O_2 process is the most commonly commercially implemented AOP and is therefore of particular relevance to consider for its potential for MP treatment. (103) Hydrogen peroxide decomposes under UV radiation to produce two hydroxyl radicals as per Reaction 1.1.

$$H_2O_2 + hv \rightarrow 2HO^{\cdot} \qquad (1.1)$$

Hydroxyl radicals are a neutral free radical with powerful oxidising capability (E_0 = +2.7 V). They are short lived and present in very low concentrations in solution (less than 10^{-12} mol L^{-1}) due to their very high reactivity. Hydroxyl radicals initiate oxidising reactions non-selectively via hydrogen atom abstraction, electrophilic addition and electron transfer reactions, making them attractive option for treating complex mixtures of contaminants such as in wastewater.

Radicals are capable of initiating the degradation of polymers by introducing new functional groups to the polymer chain. (155) Typically, this begins with the introduction of hydroxyl and carbonyl functional groups which are then capable of subsequent oxidation as described in Section 1.4.1. Subsequent chain oxidation, crosslinking, or scission can occur as well as specific reaction with aromatic and side chain groups depending on the polymer type. (156) In the case of UVC/ H_2O_2, photodegradation by UVC and attack by hydroxyl radicals occur together.

1.4.3 Sulfate based AOPs

Sulfate based AOPs depend on the cleavage of a peroxide bond in a persulfate precursor, generating reactive sulfate radicals *in situ*. Persulfate can also directly oxidise organic contaminants, an attractive benefit over using H_2O_2. (157) Two sulfate generating precursors were considered in this thesis; potassium peroxydisulfate (PDS) and potassium peroxymonosulfate (PMS).

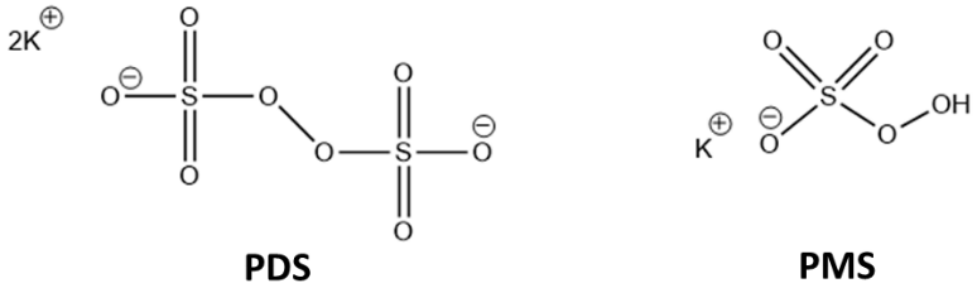

Figure 1.6 Chemical structure of PDS and the ative salt of PMS

The triple salt form of PMS ($2KHSO_5 \cdot KHSO_4 \cdot K_2SO_4$), a persulfate generating precursor, is a slightly more powerful oxidant than H_2O_2 (E_0 = 1.82 V). (158) The active salt in PMS (HSO_5^-) is photolysed by 254 nm ultraviolet (UV) irradiation (although it is possible to use longer wavelength UVA (159)) to form a combination of radicals according to Reaction 1.2.

$$HSO_5^- + h\nu \rightarrow SO_4^{\cdot -} + HO^{\cdot} \quad (1.2)$$

$$SO_4^{\cdot -} + H_2O \rightarrow SO_4^{2-} + HO^{\cdot} + H^+ \quad (1.3)$$

$$HSO_5^- + HO^{\cdot} \rightarrow SO_5^{\cdot -} + H_2O \quad (1.4)$$

$$HSO_5^- + SO_4^{\cdot -} \rightarrow SO_4^{2-} + H^+ \quad (1.5)$$

In water, a subsequent pH dependant reaction converts the sulfate radicals to hydroxyl according to Reaction 1.3. (103) High initial concentrations of PMS or poorly optimised oxidant dosing have been shown to hinder the rate of degradation of organics via radical scavenging Reactions 1.4 and 1.5. (160)

PDS has oxidising potential of 2.1 V and is activated by UV photolysis to produce sulfate radicals according to Reaction 1.6. (158, 161)

$$S_2O_8^{2-} + h\nu \rightarrow 2SO_4^{\cdot -} \quad (1.6)$$

The sulfate radicals then undergo reactions similar to those generated in the PMS system with the potential for radical recombination and scavenging. Photolysis is the most common activation method for sulfate based AOPs but cleavage of the peroxide bond is possible using

heat, ultrasound or catalytic means. The mechanism of activation in ultrasound system yields hydroxyl radicals as both a direct oxidising agent and as radical initiators within cavitation bubbles. Reactions 1.7 - 1.12 show the reactions which occur in solution for PDS and PMS in this case where))) represents the application of ultrasound.

$$H_2O +))) \rightarrow HO^{\cdot} + H^+ \quad (1.7)$$

$$S_2O_8^{2-} +))) \rightarrow 2SO_4^{\cdot -} \quad (1.8)$$

$$HSO_5^- +))) \rightarrow SO_4^{\cdot -} + HO^{\cdot} \quad (1.9)$$

$$SO_4^{\cdot -} + e^- \rightarrow SO_4^{2-} \quad (1.10)$$

$$S_2O_8^{2-} + 2H_2O \rightarrow HO_2^{\cdot} + 2SO_4^{\cdot -} + 3H^+ \quad (1.11)$$

$$S_2O_8^{2-} + HO_2^{\cdot} \rightarrow 2SO_4^{\cdot -} + H^+ + O_2^{\cdot -} \quad (1.12)$$

The mechanism of activation in thermo-initiation system is initiated by Reactions 1.13 and 1.14.

$$S_2O_8^{2-} + heat \rightarrow 2SO_4^{\cdot -} \quad (1.13)$$

$$HSO_5^- + heat \rightarrow SO_4^{\cdot -} + HO^{\cdot} \quad (1.14)$$

1.5 Legislation and alternative solutions

This thesis focuses on the role wastewater treatment systems have in microplastic pollution in aquatic environments. Developing removal technology and understanding the transformation and fate of MPs within these systems is essential in developing a strategy to combat the pollution problem. However, environmental and waste policy and regulation is complex and must be considered to fully understand the possible solutions.

In Scotland, the UK and Europe, limited legislation specifically covers microplastic pollution with some clearly defined product bans coming into force in the last few years. For example, the Environmental Protection (Microbeads) (Scotland) Regulations 2018 bans the

manufacture and sale of rinse-off personal care products containing plastic microbeads. (68) Consultations on a similar ban covering plastic containing wet wipes is underway in Scotland. (162) A bill proposing all washing machines to include a microplastic filter has been introduced recently in the Scottish Parliament. (163) In the case of wastewater treatment systems, control of the MP at source offered by these regulations certainly offer a more sustainable solution to the waste produced and should be embraced where they can be easily implemented. However, as already summarised in Section 1.3.4, the sources and flows of MPs to water are numerous and diverse making an attempt to completely stop their release impossible. In reality a combined approach is needed. Understanding MP sources, transformation and fate within WWTPs will allow policy makers to target specific products for legislative intervention. For MPs not captured by these controls, a water treatment solution capable of their mineralisation offers a barrier to environmental release.

Chapter 3 explores the relationship between scientific understanding and policy making in more detail by considering one specific consequence of MP and chemical pollution within the wastewater treatment system. Sewage sludge applied to land for fertiliser in Scotland contains MPs and chemical contamination, showing how incomplete removal of these pollutants during treatment can have far reaching environmental consequences.

2. Materials and methods

This chapter presents the materials, analytical techniques and experimental methods used throughout this thesis. Each experimental chapter also presents a summary of the key materials and methods relevant to the results presented within it, where further detail is required.

2.1 Materials

Experiments presented in this thesis were performed using either Deionised (DI) water or real laundry wastewater. DI water (ultra pure, 18.2 MΩ cm) was produced with an ELGA LabWater purification system. Laundry wastewater, pre-treated by sock filtration and thermal disinfection, from a UK hospital's laundry store was provided by Dryden Aqua Ltd. The wastewater was collected from a site handling predominantly polyester clothing and bedding items, with associated unknown organic and biological contaminants. At the end of the washing cycle, the waste water was drained from the machine, sealed and stored at 4 ^{o}C. It was allowed to settle and only the supernatant liquid then used in order to avoid transfer of settled solids. The collected wastewater samples were fully characterised in Section 4.3.2.

A number of radical generating oxidising agents were utilised within this thesis. These are; hydrogen peroxide solution 35 wt. % (Sigma Aldrich), sodium peroxydisulfate (PDS) (98% Thermo Scientific Chemicals) and potassium monopersulfate (PMS) triple salt (Oxone® Fisher Scientific). Raw solutions and powders were diluted in appropriate volumes of water as per the concentration requirements of each experiment. During treatment, H_2O_2 concentration was estimated using peroxide testing strips (Quantofix with ranges 1-150 mg L^{-1} and 50-1000 mg L^{-1}) while the concentrations of PDS and PMS were determined using UV-visible spectrophotometry as described in Section 2.4.1.6.

Ammonium iron(II) sulfate hexahydrate (99%, Fisher Scientific), ammonium thiocyanate (99%, Thermo scientific), potassium iodide (99 %, Acros organics), and sodium bicarbonate (99.5% Thermo Scientific) were used as received. Ceftazidime (98%) was obtained from Cambridge Bioscience. Sodium hydroxide pellets and acetic acid (99.7%) were purchased from Fischer

Scientific. Acetonitrile and Ultrapure water of HPLC grade were used in HPLC analysis. Sodium nitrite (98%), 3-Aminophenol (98%) and sulfamic acid (99%) were obtained from Fischer Scientific UK Ltd.

2.2 Preparation of microplastics

No standard method exists to prepare microplastic standards for lab scale testing. (164) The materials prepared for experiments in this thesis are presented in this section alongside methods to prepare them ie. extraction, weathering, cutting, grinding. Figure 2.1 shows photographs of the prepared MPs for testing.

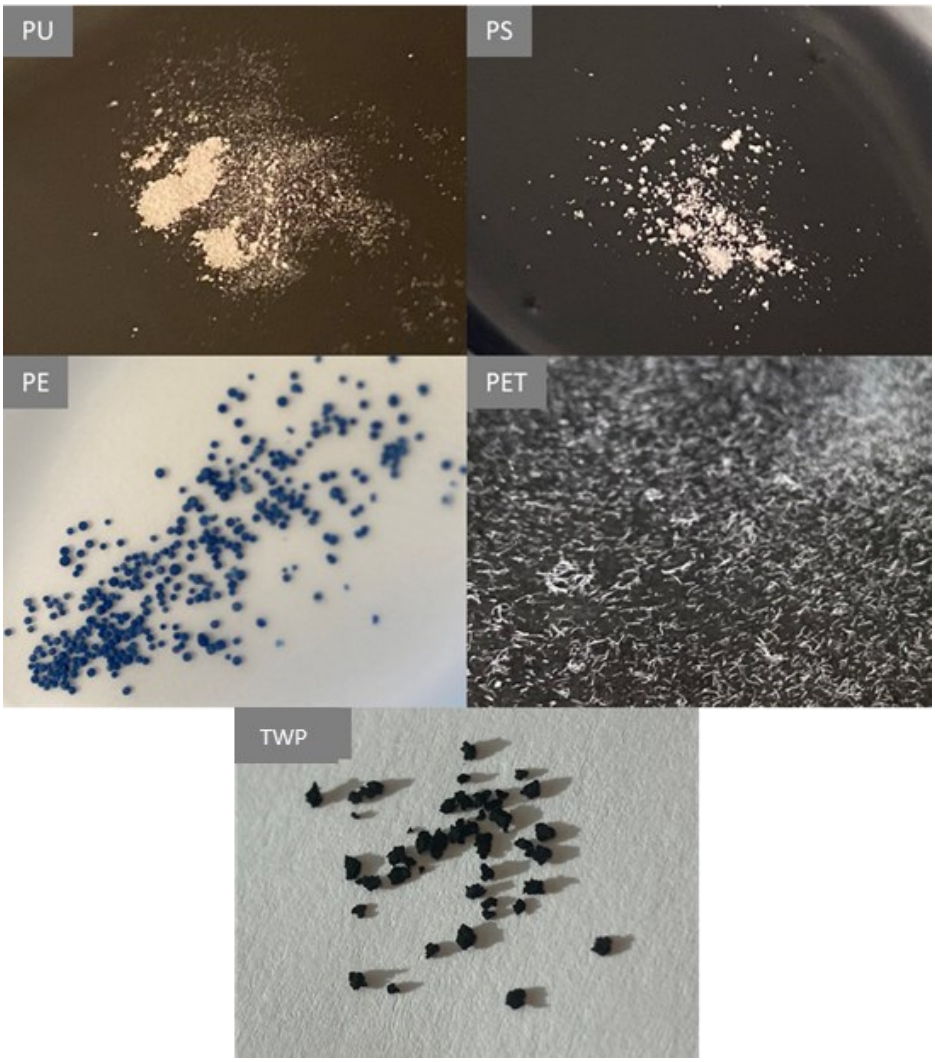

Figure 2.1 Photos of MPs types studied for ceftazidime adsorption. Polyurethane (PU); Polystyrene (PS); Polyethylene (PE); polyester (PET) and tyre wear particles (TWP)

2.2.1 PET Fibres

Polyethylene terephthalate fibres (PET) with a diameter of approximately 40 µm and length of 3 cm were purchased from Phoenix Fibres UK. For experiments requiring measurement of mass loss, these fibres were used as received. In this way, material loss during weighing and transfer of samples is minimised. For experiments which do not rely on fibre mass measurement, such as characterising physical and chemical transformation of fibres or adsorption of organics, the fibres were manually cut into environmentally relevant lengths, using grade 420 stainless steel pointed scissors. The length distribution was then confirmed by optical microscopy (median length 733 µm, mean length 849 µm), as shown in Section 4.1.3.

For use in adsorption experiments presented in Chapter 6, large numbers of uniformly weathered MPs were required. For this purpose, UV and AOP weathering was rejected due to it being time consuming and the potential of producing variation in the weathering degree, thus affecting the comparability of adsorption results. To prepare PET fibres with a controlled degree of degradation, a hydrolysis treatment was applied which has been shown to reproducibly produce environmentally relevant reference materials. (165) PET fibres were immersed for 1, 2 or 3 h in a 10% sodium hydroxide solution at a temperature of 90 ˚C prior to rinsing with DI water and drying to constant mass (50 ˚C). When developing this method, Sarno et al. observed similar physical changes to fibres weathered under UV. The mechanism of degradation in this hydrolysis system is distinct from UV photolysis with degradation proceeding by hydrolysis of the polymer chain to form ethylene glycol and terephthalic acid monomer units as compared to the Norrish type photolysis degradation induced by UV irradiation discussed in Section 2.3.(165, 166) Despite this variation in mechanism, the amount of terephthalic acid and ethylene glycol generated during hydrolysis from degradation of the polymer chain was also shown to be similar to UV photolysis of fibres and importantly showed a similar physical degradation, showing relevance of the prepared material to real environmental systems. It is expected that fewer surface groups containing high degree of oxygen will be formed as a result of the hydrolysis method as compared to an AOP driven mechanism and this must be considered when interpreting chemical interaction

of these fibres. For these reasons, hydrolysed fibres were used in Chapter 6 to consider adsorption of CAZ by polyester MPs.

2.2.2 PE beads

PE beads were extracted from commercial facewash using a method modified from Cheung et al. (167) Facewash was rinsed in de-ionised water pre-heated to 90 ˚C and stirred to dissolve the non-plastic solids. The solution was then filtered (2.4 µm glass fibre filter) and the MP beads rinsed with hexane to remove the final traces of soap and wax solids. The MPs were then rinsed a final time with DI water and dried to constant mass (50 ˚C).

2.2.3 PS and PU foams

PS and PU foam MPs were prepared and provided by the National Institute of Chemistry, Ljubljana, Slovenia. Hard PS was procured from Styrodur 2800C, Bauhaus. Soft PS is procured from FRAGMAT EPS F. Terms hard and soft are used here to describe the difference in density of the two samples as indicated by the manufacturer. This difference is thought to be caused by variation in the manufacturing conditions of the polymer materials. Hard PU was procured from BACHL PIR MV, PIR/PUR 026, Bachl Kft., Hungary. Soft PU was procured from Repsol, Spain. PS and PU foams were cryogenically ball milled in a Domel Tehtnica MillMix 20 and were then weathered for 600 h in a Xenon test chamber, Q-SUN Xe-3 chamber, according to the ISO 4892-2:2013 standard to replicate environmental degradation. (168) During weathering, samples were exposed to 60 W m^{-2} of irradiation at 38 °C in the chamber with 50% relative humidity at a fan speed of 2000 rpm.

2.2.4 Rubber TWPs

TWPs were prepared and provided by the National Institute of Chemistry, Ljubljana, Slovenia. TWPs were produced via cryogenically ball milled in a Domel Tehtnica MillMix 20 from end-of-life commercial tyres and not subject to further artificial weathering. Four tyre brands were used to prepare MPs: Bridgestone 225/45 R 17 91W (December 2016), Kumho 10.00 R 20 16PR (February 2002), Michelin 245/45 R 18 100V (April 2018) and Goodyear 205/55 R 16 91T (November 2014).

2.3 AOP treatment of microplastics

2.3.1 UVC/H_2O_2 AOP reactor setup

During initial screening experiments, a number of lab scale batch UV reactors were tested. Figure 2.2 a shows an immersion reactor and Figure 2.2 b shows a top-down reactor for application of light to a sample. The immersion reactor comprises a jacketed glass beaker with cold water flow to maintain constant temperature within the reactor housing a quartz glass tube and lamp. This setup allows full 360 degree irradiation of the water sample and minimises the distance from the light source. The reactor was covered with aluminium foil to reflect light inwards and prevent ambient light from entering the reactor. This reactor has a 300 mL working volume and mixing of the solution is achieved using a magnetic stirring bar and plate. In the top-down conformation, dual lamps housed within protective quartz tubes are arranged above the samples. Four samples may be treated in a single batch and the working volume of each is 50 mL. As there is no water flow, the temperature increase in the reactor must be carefully monitored. In a typical experiment, the ambient temperature within the top-down reactor increased to 31 ± 4 ˚C during irradiation. In each case, the entire reactor was enclosed within a blacked-out fume hood to prevent intrusion of any external light and to prevent harmful UVC radiation leaking to the room.

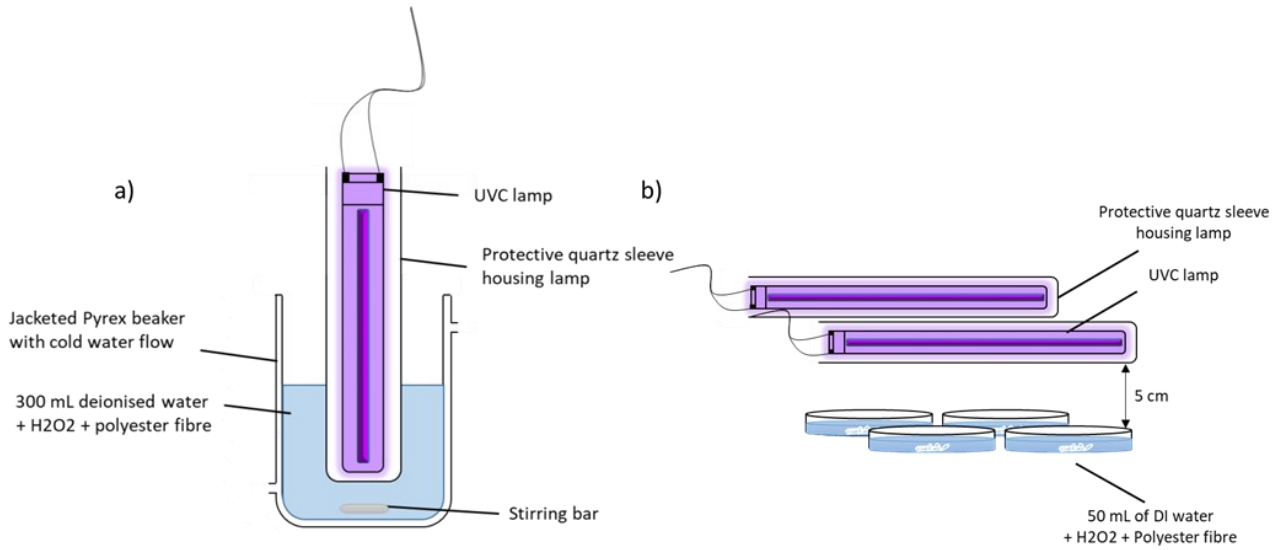

Figure 2.2 Schematic illustration of (a) the immersion photo-reactor setup and (b) top down photo-reactor setup.

2.3.2 Sulfate AOP reactor setup

Chapter 5 presents results from sulfate driven AOP treatment, activated by various means (light, heat and ultrasound). Prior to AOP treatment, the MP fibres were rinsed in deionized (DI) water and dried (105 ^{o}C, 30 min) in order to remove the effect of static interference on the mass as measured by analytical balance. After this, the accurate starting mass was recorded and the fibres immersed in the appropriate water matrix within the reactor with a working volume of 300 mL. The solution was continuously stirred (200 rpm) to ensure complete mixing of the solution as well as gentle agitation of the fibres, avoiding aggregation on the side of the reactor wall.

For experiments requiring ultrasonic activation of sulfates, a Branson Sonifer SFX550 capable of delivering up to 550 W of power at 20 kHz via an immersed horn was used as shown in Figure 2.3 a. For experiments under varied temperature, a non-jacketed beaker resting atop an electronically controlled heating plate with stirring ensured stable temperature over the course of the treatment analogous to the setup in Figure 2.3 b. For UV activation, a UV lamp was immersed in the water within a protective quartz sleeve in order to provide the maximum radiation dose to the sample (Figure 2.2 a). The reactor was enclosed within a blacked out fume hood to prevent intrusion of any external light and to prevent harmful UVC radiation leaking to the room.

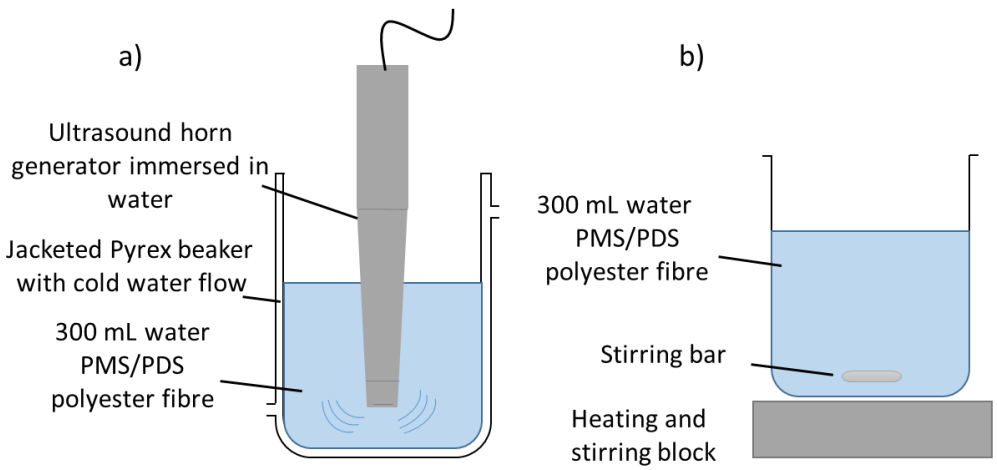

Figure 2.3 Schematic illustration of (a) the immersion ultrasound activated reactor setup and (b) thermal activated reactor setup.

2.3.3 Irradiation source

UV irradiation was varied by changing the lamp used in the reactor. A UVC fluorescent lamp with 55 W power (TUV PL-L 55W, Phillips) connected to a control ballast (HF-Performer III, Phillips) was used to provide 254 nm irradiation (31.8 mW cm^{-2}) to the solution. For experiments requiring a lower UVC irradiance (4.0 mW cm^{-2}), an 11 W lamp was used (PLS112P-TUV, PLS). For experiments under UVA irradiation, an 11 W 365 nm fluorescent lamp (DUL S BL, Osram) was used (12.45 mW cm^{-2}). To assess the feasibility of activating sulfates by natural solar light, an LCS-100 small area solar simulator fitted with an AM1.5G filter was used (8.02 mW cm^{-2} UVA component). In this case, a top-down irradiation of the sample was carried out in a modified set up of Figure 2.2 b.

The lamps used in this thesis are detailed in Table 2.1, including the UV output as measured using a digital UVP UVX Radiometer (Analytik Jena) equipped with a 254 or 365 nm sensor and a 10:1 signal attenuator.

Table 2.1 Irradiation sources and their measured UV output

Light source	Power (W)	UVC output 265 nm (mW cm^{-2})	UVA output 365 nm (mW cm^{-2})
PLS112P-TUV UVC lamp, PLS	11 W	4.0	-
TUV PL-L 55W UVC lamp, Phillips	55 W	31.8	-
DUL S BL UVA lamp, Osram	11 W	-	12.5
LCS-100 solar simulator		-	8.0

2.3.4 UV dose

The UV dose applied during the experiments was calculated from the irradiation values according to Equation 2.1:

$$D = I_{avg} \times t \qquad (2.1)$$

Where D is the UV dose in mJ cm^{-2}, I_{avg} is the UV irradiation in mW cm^{-2} as measured by digital radiometry and t is exposure time in seconds.

2.3.5 Separation of microplastics from water

After treatment, weathering or mixing with co-contaminants, the MPs were separated from the solution. Methods for MP isolation vary in the literature depending on the complexity of the sample. Environmental water samples are generally highly complex mixtures of analyte and can be contained within an undesired, interfering matrix. Samples collected from plastic polluted waters are also unlikely to contain a single type of MP pollutant. Robust methods for separation of plastics prior to analysis aid in the accurate identification and characterisation steps. A number of reviews discuss these extraction methods (81, 169-171). The extraction method selected for all weathering and AOP experiments presented within this thesis is vacuum filtration. Each solution was filtered over 1.6 µm glass fibre filter and dried to constant mass (105 ^{o}C). The extraction method selected for adsorption experiments presented within Chapter 6 is syringe filtration. In this case, the solution was filtered using 0.22 µm syringe filters and the captured solid MPs discarded.

2.4 Analytical methods

The analytical study of microplastics in aquatic systems is an area of intense active research. The development of reliable tools and protocols for measurement and identification of suspected plastics presents a major challenge in the field of environmental science. (172) Misidentification leading to false positive and negative results is a common issue when analytical characterisation methods are not robust. (172, 173) Several high quality reviews outline the current analytical ability within a variety of environmental compartments including sediment, soils (81), ocean, freshwater (174) and wastewater. In general, any microplastic analysis is advised to contain an element of visual counting, chemical polymer identification and surface characterisation. (175)

As previously mentioned, a key challenge in the field of microplastic research is the lack of widely applied analytical methods for their detection and characterisation. A number of techniques were applied over the course of this investigation to determine both physical and chemical properties of MPs and are introduced here.

2.4.1 Chemical characterisation

2.4.1.1 Fourier transform infrared spectroscopy

Fourier transform infrared (FTIR) spectroscopy is one of the most commonly used methods to identify polymer type in microplastic analysis and to follow degradation. During analysis, information on the vibration modes in the target molecules are collected as an interferogram. Application of a Fourier transform yields an absorbance spectra as it relates to wavenumber. This powerful technique also has an added benefit of showing the oxidation degree of a polymer. As the surface of the oxidised plastic develops oxygen containing functional groups, their characteristic absorbance peak on the FTIR spectra can be followed.

FTIR has four main modes by which it can be conducted: transmission, diffuse reflectance, reflection-absorption and attenuated total reflectance (ATR). The simplest and most common is ATR-FTIR where large solid samples can be placed onto a crystal surface and irradiated. Focal plane array (FPA) based micro-FTIR imaging in transmission mode allows individual particles down to 20 µm to be captured. (176, 177) For even smaller fragments, alternative methods such as Raman spectroscopy may be employed. (178, 179) Raman spectroscopy offers similar benefits in analysis as FTIR but has been reported to detect particles sizing down to 10 µm and micro-Raman techniques may push this limit even lower for sample sizes below 1 µm. (175) When considering a sample of many MPs, of mixed oxidation degree, an average signal can simply be gathered using ATR-FTIR, as applied in this thesis.

Chemical composition change on the surface of MPs during oxidation is an indicator of the extent of degradation. (180) The formation of oxygen containing surface groups as the polymer chains are oxidised gives a qualitative indication of the extent of degradation. FTIR is used to obtain an IR spectrum of the polymer surface, yielding information on the presence

of functional groups. FTIR spectra of the polyester fibres were collected using a PerkinElmer Spectrum Two ATR-FTIR spectrometer. Representative spectra for MPs before and after weathering (according to various weathering processes as outlined in Section 2.2) are included in Figures 2.4 – 2.7.

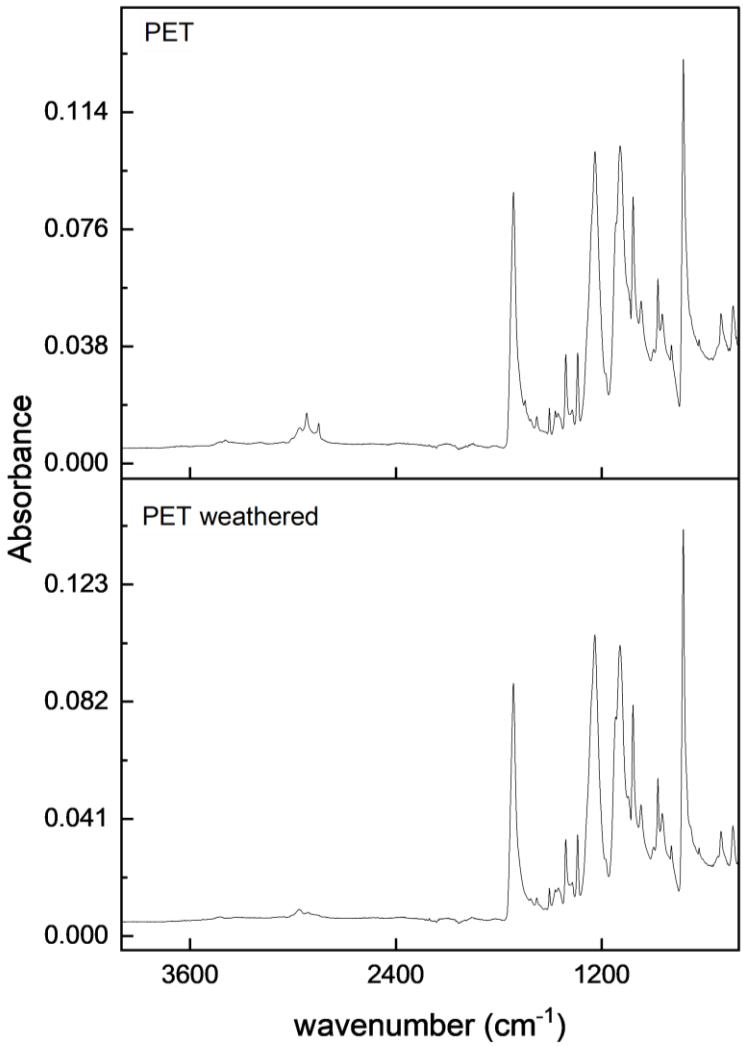

Figure 2.4 FTIR spectra of raw and weathered PET fibres (3 h NaOH hydrolysis as described in Section 2.2.1)

Characteristic peaks for polyester (PET) were assigned as: 2968 cm^{-1} (C-H ethyl stretch), 1711 cm^{-1} (C=O carbonyl stretch), 1578 cm^{-1}, 1504 cm^{-1} and 1409 cm^{-1} (aromatic C-C stretch and ring CH in-pane bending), 1367 cm^{-1} and 1338 cm^{-1} (CH_2 wagging), 1239 cm^{-1}, 1117 cm^{-1}, 1092 cm^{-1} and 969 cm^{-1} (C-O ester stretch), 1016 cm^{-1}, 872 cm^{-1}, 792 cm^{-1} and 718 cm^{-1} (aromatic ring vibration, bending and torsion). (181-183). Additional complexity in the signal band between 2800-3000 cm^{-1} is attributed to traces of water remaining in the sample due to

incomplete drying while unidentified additives or contaminants may contribute to the presence of the peaks at 2087 and 1645 cm^{-1}.

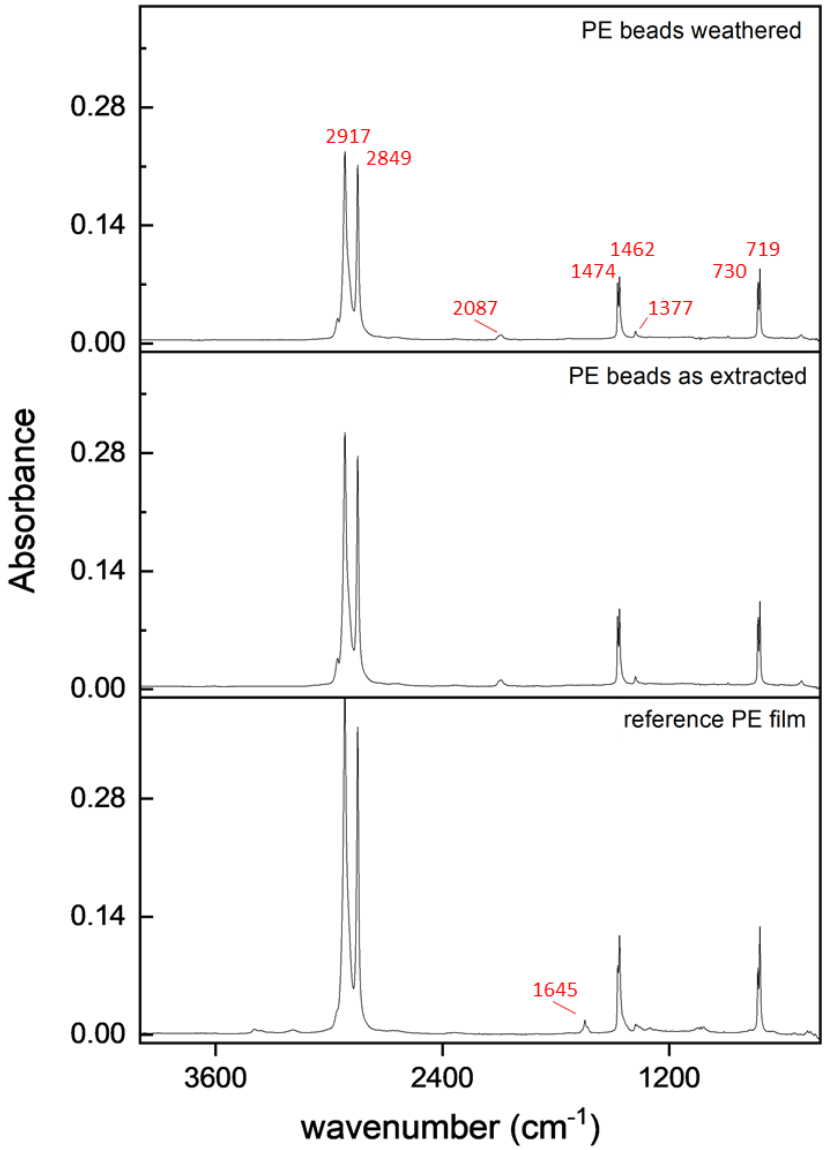

Figure 2.5 FTIR spectra of PE beads as extracted from facewash, weathered by UVC/H_2O_2 and a reference PE film

Characteristic peaks for PE were assigned as: 2917 cm^{-1} (CH_2 Asymmetric C-H stretch), 2849 cm^{-1} (CH_2 Symmetric C-H stretch), 1474 cm^{-1}, 1462 cm^{-1} (CH_2 bending), 1377 cm^{-1} (CH_3 umbrella mode), 719 cm^{-1}, 730 cm^{-1} (CH_2 rocking). (184) The spectra of PE beads show typical identifying peaks for linear low-density polyethylene confirmed by comparison to a sample of PE film. (184)

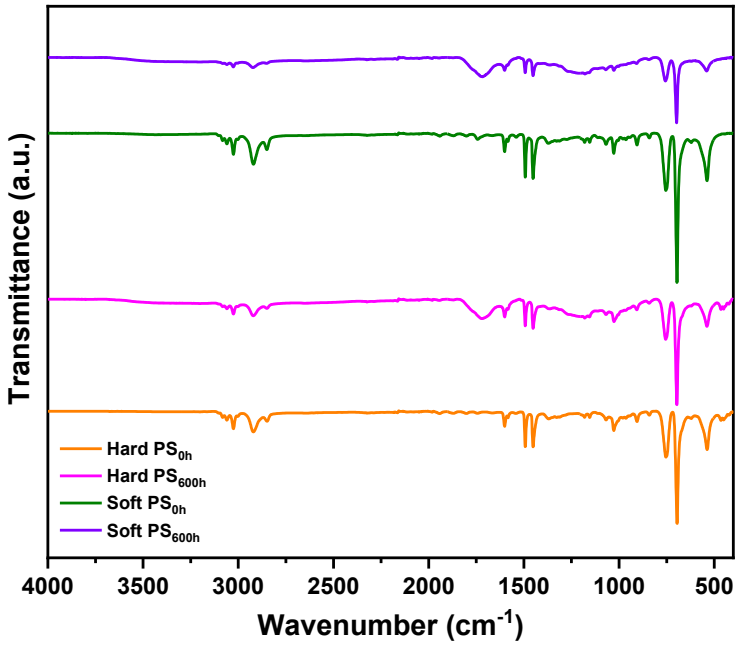

Figure 2.6 FTIR spectra of hard and soft PS foams before and after weathering

Characteristic PS peak assignment is: 3025 cm^{-1} (aromatic C-H stretching) 2940 cm^{-1} (C-H stretch), 1735 cm^{-1} (C=O carbonyl stretch), 1600 cm^{-1} (C=C stretching), 1490 cm^{-1} (C-H aromatic stretching), 1028 cm^{-1} (C=C aromatic), 699, 755 cm^{-1} (aromatic ring deformation). (185)

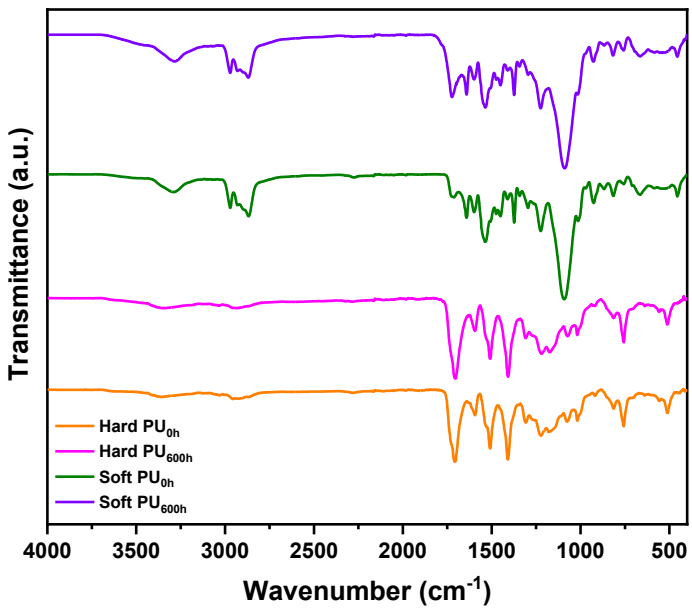

Figure 2.7 FTIR spectra of hard and soft PU foams before and after weathering

PU peak assignment is as follows: 3370-3170 cm^{-1} (N-H stretching), 1650 cm^{-1} (C=O carbonyl stretch), 1570-1515 cm^{-1} (N-H bending), 1310-1230 cm^{-1} (C-N stretching), 750-680 cm^{-1} (N-H bending). (186)

The carbonyl index (CI) is defined by the ratio of signal associated to the carbonyl stretching to a reference signal, which is unaffected by oxidation treatment and is calculated accoding to Equation 2.2. (180)

$$Carbonyl\ Index\ (CI) = \frac{Area\ of\ carbonyl\ peak}{Area\ of\ reference\ peak} \qquad (2.2)$$

2.4.1.2 Chemical oxygen demand

Chemical oxygen demand (COD) allows accurate analysis of the digestible organic material present in water. Within this thesis, COD is used to characterise real wastewater before and after treatment with AOPs. Triplicate 2 mL samples of water were collected and added to COD digestion tubes (Palintest PL450 (0-150 mg L^{-1}) or PL484 (0-1500 mg L^{-1})) After careful inversion several times to mix with the contents, the digestion tubes were transferred to a block heater (Hach 16500-10) for 2 h at 150 ^{o}C before cooling to room temperature overnight. The COD of each water sample was then recorded by colorimetry (YSI 910 COD Colorimeter).

Residual hydrogen peroxide present in water can interfere with COD measurements and can present a problem when monitoring water treated using a peroxide based AOP. In the presence of H_2O_2, a dominant reaction proceeds during the digestion according to Reaction 2.3: (187, 188)

$$K_2Cr_2O_7 + 3H_2O_2 + 4H_2SO_4 \rightarrow K_2SO_4 + Cr_2(SO_4)_3 + 7H_2O + 3O_2 \qquad (2.3)$$

As the colorimetric measurement of COD relies on accurate determination of chromium reduction, this reaction results in an artificially elevated COD result when H_2O_2 is present. According to Reaction 2.3, the theoretical value for COD attributable to H_2O_2 in solution is 470.6 mg L^{-1} per 1000 mg L^{-1} H_2O_2. An experimentally validated correlation equation (Equation 2.4) proposed by Kang *et al.* (189) presents a correction factor allowing the calculation of the

COD due to organic material of interest other than residual peroxide if the concentration of H_2O_2 is known.

$$COD_{actual} = COD_{measured} - f[H_2O_2] \quad (2.4)$$

Where $f = 0.4706$

This correction factor has been applied to the COD results for all samples with a residual peroxide confirmed with peroxide testing strips (Quantofix with ranges 1-150 mg L^{-1} and 50-1000 mg L^{-1}). Based on experimental validation in synthetic wastewater, the correction factor may be applied to solutions with residual H_2O_2 concentration is below 200 mgL^{-1} and the background COD does not exceed 435 mgL^{-1}.(189)

2.4.1.3 Biological oxygen demand

Biological oxygen demand (BOD) represents the amount of dissolved oxygen consumed by aerobic organisms within water. BOD of real wastewater samples was measured by respirometry using OxiTop (IS-6 – WTW) pressure measuring heads. The wastewater samples were homogenised by stirring and the appropriate volume for testing transferred to BOD sample bottles. N allylthiourea inhibitor solution (NTH 600) was added based on the sample COD and the bottles sealed and incubated in a thermally controlled water bath at 20 ˚C for 5 days. BOD values were recorded by the measurement heads.

2.4.1.4 Alkalinity

The alkalinity of water is its capacity to act as a base. Carbonate, bicarbonate and hydroxide ions contribute to total alkalinity. Conversion of these ions by addition of acid occurs in a stepwise manner (ie. carbonate to bicarbonate and then bicarbonate to carbonic acid). Total alkalinity of real wastewater was measured by pH titration. HCl (0.1 M) was added dropwise by burette to a stirred beaker containing 25 mL of wastewater. The pH of the solution was monitored by pH probe (Hannah Instrument 9025) to record the equivalence point and to calculate the alkalinity.

2.4.1.5 Turbidity

Turbidity is a measure of the optical clarity of a solution as affected by sediment, organic material and suspended solids. Turbidity of real wastewater samples was measured using a HACH Model 2100N Turbidimeter.

2.4.1.6 UV-visible spectrophotometry

Spectrophotometry measures light absorbance across the UV and visible (Vis) ranges. By comparing the absorbance at a given wavelength to a calibration curve, the concentration of an analyte in solution can be calculated. Within this thesis, the concentrations of various analytes in solution were followed using UV-visible absorption spectrophotometry.

Measurements were taken using a Shimadzu UV-Pro 1800 instrument and data analysis performed using UV-Pro software. The concentration of analyte in solution was determined according to the Beer-Lambert law (Equation 2.5) which describes the linear relationship between the concentration and the absorbance of the solution.

$$A = \varepsilon\, c\, l \qquad (2.5)$$

A is the absorbance, ε is the molar extinction coefficient, c is the analyte concentration and l is the path length through the solution in cm. In a typical experiment, an appropriate wavelength range was selected, encompassing the maximum absorbance peak for that particular analyte (at wavelength λ_{max}). Absorbance at λ_{max} for each sample was recorded and compared to a calibration curve to determine the concentration. Calibration curves were prepared by serial dilution of a known concentration of analyte, within the linear region of the absorbance-concentration relationship. All solutions tested for experiments in this thesis were diluted to within the appropriate linear range, as determined from their calibration curves. The concentration of ceftazidime (CAZ) was measured by UV absorbance at 256 nm as described in Chapter 6, with Figure 2.8 showing the calibration curve.

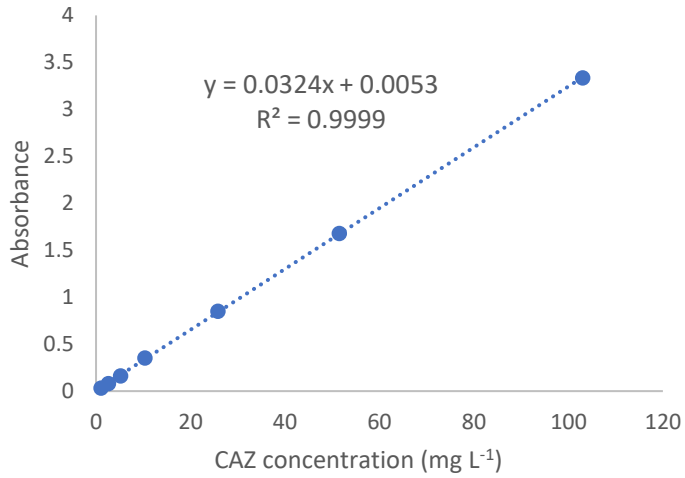

Figure 2.8 Calibration curve of CAZ in water measured by UV absorbance at 256 nm

The concentration of PDS and PMS was determined from the UV absorbance, as compared to a calibration curve (shown in Figures 2.9 and 2.10). PDS samples were first prepared according to the method described by Huang et al. (291) Briefly, sample aliquots (0.25 mL) were added to the solution of deionised water (0.75 mL), H_2SO_4 (1.25 M, 10 mL), and ammonium iron(II) sulfate hexahydrate (0.4 M, 0.1 mL). After mixing and allowing to react for 40 minutes, ammonium thiocyanate (0.6 M, 0.2 mL) was added to produce a coloured product (λ 450 nm). PMS samples were prepared using the modified iodometric titration method presented by Wacławek et al. (292) Sample aliquots were added to a solution (5 mL) comprised of potassium iodide (100 g L^{-1}) and sodium bicarbonate (5 g L^{-1}) and mixed prior to analysis of the peak at 395 nm.

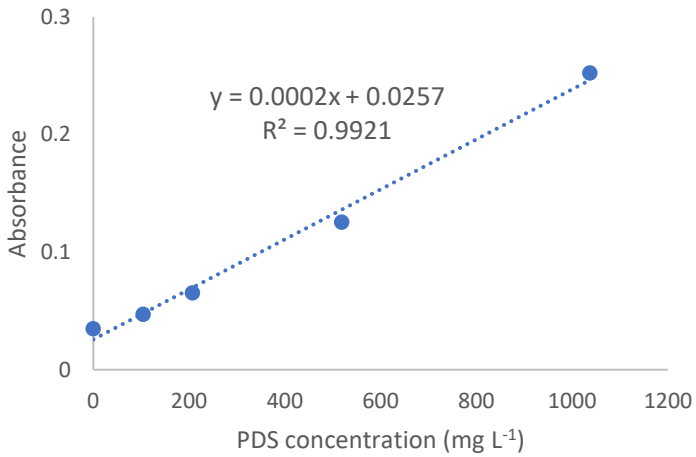

Figure 2.9 Calibration curve of PDS in water measured by UV absorbance at 450 nm

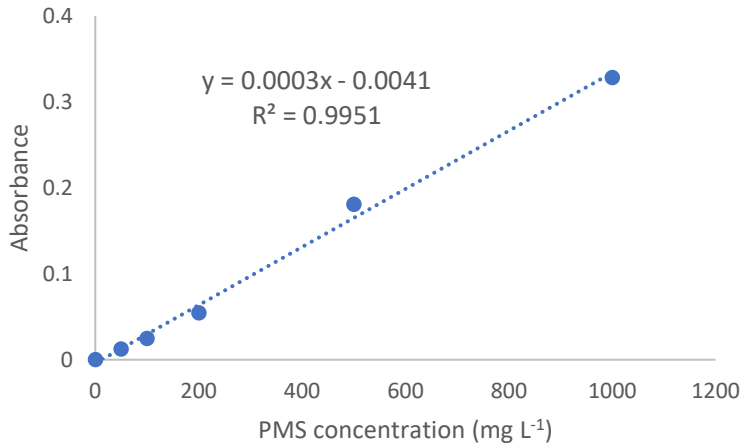

Figure 2.10 Calibration curve of PDS in water measured by UV absorbance at 395 nm

2.4.1.7 High-performance liquid chromatography

For batch adsorption experiments presented in Chapter 6, CAZ was reliably quantified by HPLC. Standard solutions of CAZ in ultrapure water were prepared by serial dilution. The concentration of CAZ was determined using a Shimadzu HPLC with SIL-20A HT auto sampler, LC-20AD Liquid chromatograph, CTO-20A column oven and SPD-20A UV-Vis detector on a C18 column (250x4.6 mm, 5mm) from Phenomenex, USA. The method was adapted from Raniot Kaur et al. (190) Mobile phase acetonitrile (65%) and 0.1% acetic acid (45%), flow rate 1 ml min^{-1}, injection volume 10 µL. The Instrument parameters included detection wavelength of 256 nm, injection volume 5 µL and column temperature of 30 ˚C. Peak area was compared to a standard curve to determine the concentration in samples after adsorption. Samples and standards were prepared in ultrapure water and filtered through 0.45 µm syringe filters prior to analysis. Standard solution signals show high degree of linearity in the range tested (1- 100 mg L^{-1}) as shown in Figures 2.11 and 2.12.

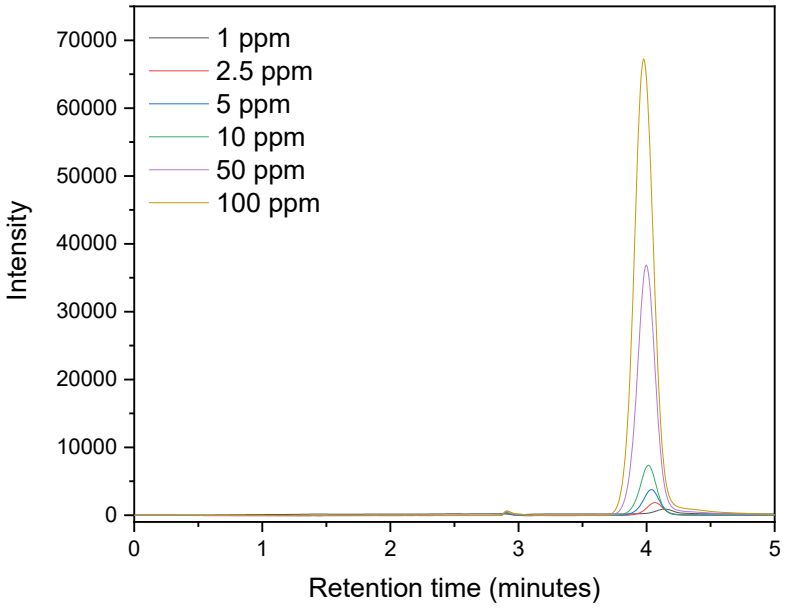

Figure 2.11 HPLC chromatograph overlay of CAZ standard solutions

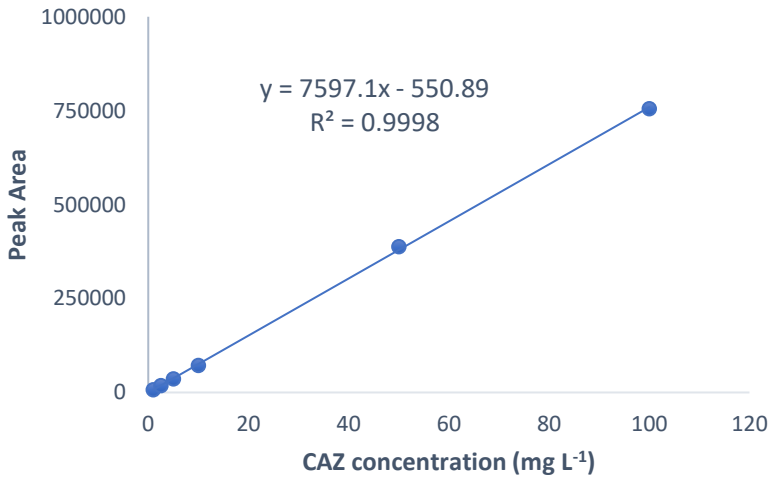

Figure 2.12 Calibration curve for Ceftazidime in water as measured by HPLC

2.4.2 Physical characterisation of MPs

2.4.2.1 Gravimetric analysis

One of the main indicators currently used to assess the efficacy of MP degradation lab based experiments from the literature is the change in the mass of plastic over time. (109, 111, 117, 191). At designated time points, fibres were physically removed from the reactor vessel for mass testing. This was achieved by filtration of the entire reactor volume through a pre-weighed glass fibre filter (Whatman, 1.6 µm pore) paper, ensuring all secondary fragments larger than this pore size are accounted for in the mass calculation. It is important to note that smaller fragments lost through the filter are not counted towards this mass measurement. Therefore, the results presented in this thesis consider the degradation of the bulk MPs, and not the mineralisation of plastic. After rinsing with deionised water, the fibres and paper were dried at 105 degrees ^{o}C for 30 minutes, prior to weighing. Using Equation 2.6, the percentage mass lost is calculated where m_0 is the dry mass of fibres prior to treatment and m is final mass of the dry fibres recovered after treatment.

$$Mass\ loss\ (\%) = \frac{(m_0 - m)}{m_0}\ x\ 100 \qquad (2.6)$$

Total solids and total suspended solids were measured by gravimetric analysis. Wastewater samples were filtered with pre-weighed 1.6 µm glass fibre filter paper by vacuum filtration and dried to constant mass (50 ˚C) prior to recording their final mass.

To determine the standard error of this mass loss measurement, triplicate experiments were conducted and the standard deviation of mass loss reported alongside the average result. Additionally, spike recovery experiments were conducted in triplicate from ultrapure water and real laundry wastewater samples to investigate the effect of experimental error. As presented in the appendix (Table A.1, A.2 and Figure A.1), a variety of initial concentrations of MP fibre were stirred in the water (300 mL) for 5 minutes without irradiation. The samples were then recovered according to the experimental procedure outlined in Section 2.4.2.1 and the fibre mass measured. Spike recovery for samples above 5 mg were > 98% and > 93 % for ultrapure and laundry water respectively. For experiments requiring a lower concentration of

MP, uncut fibres result in a reduced relative amount of mass loss due to experimental loss with a starting mass of just 0.5 mg yielding a recovery of 93 %.

2.4.2.2 Optical microscopy

Optical microscopy is widely applied in literature across the fields of environmental monitoring and wastewater treatment to observe MP number, surface changes or particle fragmentation. It has been used to image MPs in wastewater (46) as well as complex biological samples. (192, 193) Within this thesis, MPs were imaged using a 4x – 100x (Wang biomedical) optical microscope, and photographed using a 12 MP Standard wide-angle Apple iPhone camera. Particle counting and sizing was performed in ImageJ image processing software with reference to a micrometre scale.

2.4.2.3 Scanning electron microscopy

Scanning electron microscopy (SEM) allows detailed imaging of solid surfaces at the nano-micro scale and is particularly useful for particle counting, sizing and surface characterisation. The benefits of this characterisation method for MP analysis are widely reported and make it an essential tool in this thesis. (194) SEM was used to image the surface of all MPs studied. Samples were fixed to an aluminium stub using conductive carbon tape and coated with gold (5 nm thickness) by sputter coating. Images were collected using a JSM-IT800 Field Emission scanning electron microscope in secondary electron imaging mode using an accelerating voltage of 15 kV, 30 micron aperture and a working distance of approximately 7 mm.

2.4.2.4 Atomic force microscopy

Atomic force microscopy (AFM) is a surface characterisation technique capable of mapping topography at the atomic scale. It has been widely used for polymer analysis and in recent years for MP characterisation. (195, 196) In this thesis, AFM was employed to investigate the small-scale changes in surface roughness of MPs, including visualising the evolution of holes and micro-cracks as a result of AOP treatment and calculating an averaged roughness value for the surface. For AFM analysis, individual fibres were fixed to a glass slide using double sided adhesive. Analysis was performed on a JPK NanoWizard AFM, equipped with an

Inverted Optical Microscope and was carried out in quantitative imaging (QI) mode using NTESPA cantilever probes (Bruker AFM Probes, Camarillo, CA, USA) with a nominal spring constant and tip radius of 40 N/m and 8 nm, respectively. Data analysis was performed using Gwyddion software. (197) Images were sharpened and a second order polynomial background subtraction was applied, removing the effect of curvature of the fibre surface.

The root mean square (RMS) of surface roughness (R) is a measure of the average height (h) deviation from the mean value and can be expressed as shown below. In Chapters 5 and 6, R_{RMS} was calculated according to Equation 2.7 from triplicate 5 × 5 µm AFM scans in order to provide a quantitative measure of the changing roughness of MPs due to weathering. This analysis was performed within JPK Nanowizard software.

$$R_{RMS} = \sqrt{\frac{h_1^2+h_2^2+h_3^2+\cdots+h_n^2}{n}} \qquad (2.7)$$

2.4.3 Adsorption of antibiotics

In Chapter 6, the adsorption of CAZ by various MPs is investigated. All adsorption experiments were conducted in batch and at room temperature and ambient pH. MPs were weighed into glass vials and 10 mL of a stock solution of antibiotic in water was added. The vials were capped and shaken on an orbital shaker (Denley orbital mixer platform) at a speed of 200 rpm. At the end point, the solution was filtered using 0.22 µm syringe filters. Control experiments were conducted to measure the adsorption of antibiotic onto the interior glass surface of the vial and to consider the leaching of degradation products from the MPs into the water which may interfere with quantification of CAZ.

Adsorption Q (mg g^{-1}) was calculated according to Equation 2.8 where C_0 is the initial concentration of CAZ (mg g^{-1}), C_e is the equilibrium concentration (mg L^{-1}) of CAZ, m is the mass of adsorbent (g) and V is the total volume of the reaction mixture (L).

$$Q = \frac{C_0-C_e}{m} \times V \qquad (2.8)$$

A linear model and the Langmuir model were applied to calculate the adsorption isotherms of CAZ on PET microplastic fibres. The linear model is described as:

$$Q = K_d C_e \quad (2.9)$$

The Langmuir isotherm model introduced a finite limit on the number of adsorption sites in a planar surface and is described as:

$$Q = Q_{max} \frac{K_L C_e}{1+K_L C_e} \quad (2.10)$$

Where K_d (L g^{-1}) is the linear partition coefficient, Q_{max} is the maximum monolayer adsorption capacity (mg g^{-1}) and K_L (L mg^{-1}) is a coefficient describing the adsorption interaction between plastic surface and CAZ.

3. Policy and regulation of microplastics in wastewater treatment plants case study

The application of sewage sludge to agricultural land in Scotland

3.1 Introduction

This chapter is comprised of work undertaken for Scottish Environment LINK (ScotLINK) while working on a 3-month placement as an environmental policy researcher in 2022-23. The project was a collaboration and its aims were developed with the needs of the organisation in mind as well as my own expertise in chemistry and microplastic pollution. The subject of contamination of sewage sludge applied to land as an agricultural fertiliser was explored. This report provides a detailed summary of current policy and recommendations for changes to regulation based on the scientific literature and insights of key stakeholders.

This case study holds much value for understanding the context of my research. Microplastics are a contaminant of concern in our wastewater systems and warrant detailed research in the lab. However, they exist alongside a complex mixture of chemical and biological contaminants which must be considered when deciding on an effective course of action. Furthermore, the environmental and waste legislation in Scotland and the UK is complex and in the process of constant change. These factors should all be forefront in the mind of environmental researchers who wish for their work to have measurable impact in the field beyond furthering scientific understanding. Therefore, this chapter should be considered as a case study on how microplastic pollution in WWTPs must be treated as part of a larger system.

This chapter is published online and has been disseminated among Scottish Environment LINK's membership of over 40 organisations as well as key representatives within Scottish Environment Protection Agency (SEPA) and Scottish Water. Conclusions and recommendations were developed through interviews with representatives from SEPA, Scottish Water, Environmental Rights Centre for Scotland (ERCS), Marine Conservation Society and National Farmers Union Scotland (NFUS). The report was revised according to

comments received from ScotLINK, Fidra, SEPA and Scottish Water representatives. Published content authored by T. Easton is reproduced with permission.

3.2 Background

The proposal for an Integrated Authorisation Framework (IAF) in Scotland intends to overhaul outdated waste handling regulations including those covering the application of sewage sludge to agricultural land. Consultation on the proposed framework was open for comment in 2023. This offered the opportunity to call for tighter regulation on contaminants present in the material which may harm Scotland's soils and present a risk to health. This report provides a brief overview of this complex issue and provides evidence to aid in a response to the IAF consultation for ScotLINK members.

The application of sewage sludge (SS) to land is a seemingly sustainable solution to solid waste produced in Scottish wastewater treatment plants. The practice provides a low-cost supply of nutrients and organic matter to farms and reduces Scotland's reliance on environmentally damaging mined chemical fertilisers. Contamination of sewage sludge with pathogens, organic chemicals and microplastics is not covered by the current regulations meaning these pollutants are applied to land unchecked. The sustainability benefits of nutrient recycling and waste reduction should not come at the price of contaminated soil and potential accumulation of pollutants in Scottish farmland, crops and food sources.

This chapter seeks to summarise the key considerations that new regulation of sludge application to land should take into account and act as a general overview document for members of Scottish Environment LINK.

The complex regulatory system for SS application to agricultural land is a result of the range of definitions for this material. Sludge may be classified as a waste material, fertiliser or energy generating resource. The large range of stakeholders across industries matches this complexity. Changes to regulation will have knock on effects in the water, waste handling, farming industries as well as the natural environment, which must be considered.

During treatment of wastewater, pollutants partition into a solid phase termed SS. This is a nutrient rich waste material with value as a fertiliser due to high nutrient and organic matter concentrations. Its application to land is encouraged in the UK to reduce waste and promote a circular economy. (198) Captured in the sludge alongside beneficial components are microplastics and organic pollutants. When SS is applied to land, these contaminants enter the soil, potentially affecting aquatic and terrestrial life, food and grazing crops (and therefore human health) as well as affecting long-term soil health. (199)

The benefits of SS application to land are clear from a circular economy point of view with valuable material otherwise going to waste or even requiring significant energy inputs to incinerate and dispose of safely. However, this should not come at a cost of land pollution, which undermines the sustainability of its use. Many stakeholders call for tighter regulation on the content of SS applied to land until the risk of land contamination can be proven safe. (199) The waste handling policy landscape in Scotland is set to change in the near future under the IAF, giving a potential opportunity to update regulations on sewage sludge use in agriculture.

3.2.1 Sludge production and application to agricultural land

SS is the semi-solid waste produced during wastewater treatment and is generated by a number of processes. Physical bar screens remove large solid debris in the wastewater, which go to landfill. Smaller solids such as organic matter, food waste, textiles and paper settle in sedimentation tanks where they form the primary sludge. (200) The clarified wastewater is treated biologically (aerobic or anaerobic digestion). These bacterial processes form a secondary sludge comprising of remaining solids, microorganisms and their waste. (201)

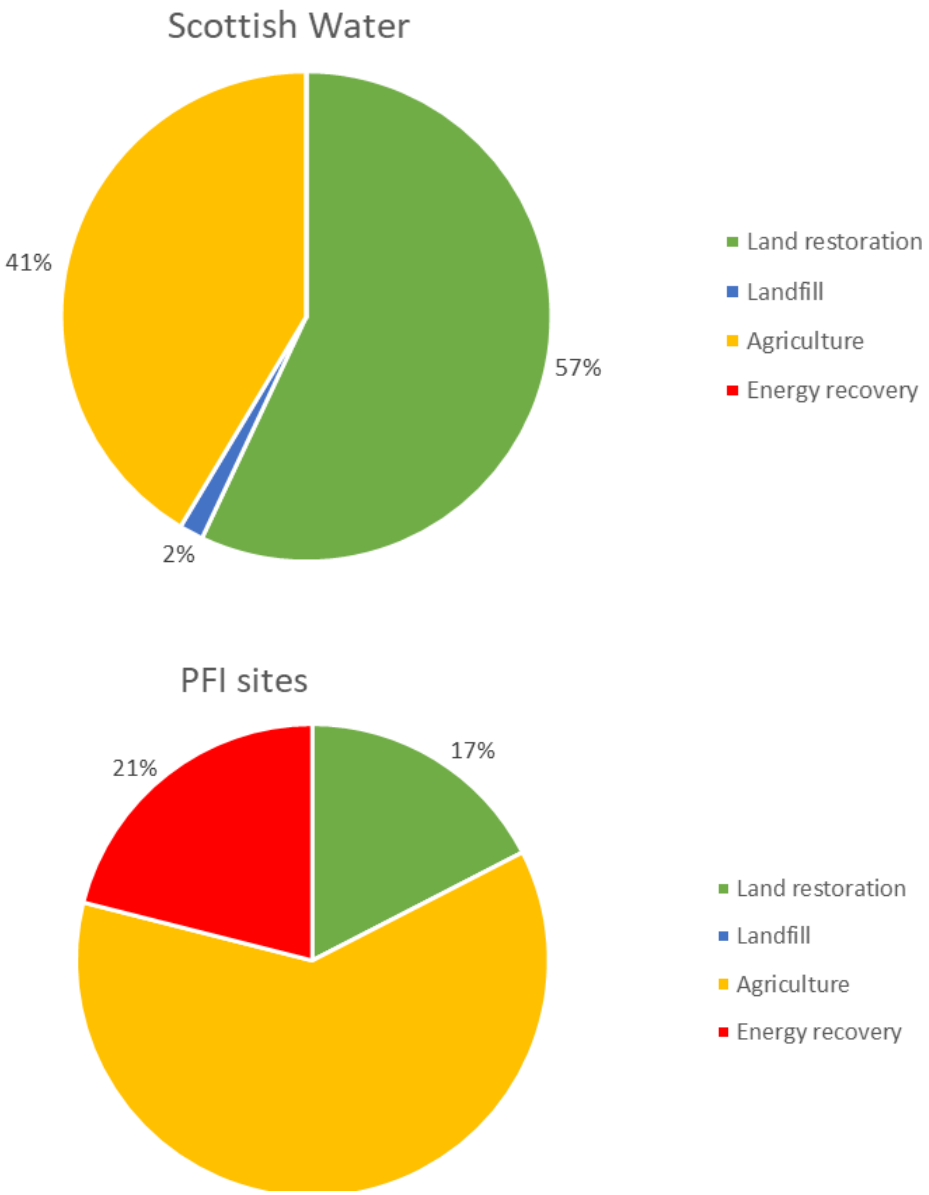

Figure 3.1 Fate of biosolids produced in Scottish treatment sites in the 2021/22 reporting year operated by Scottish Water (top) and contracted private finance initiative (PFI) sites (bottom) (data provided by Scottish Water)

Figure 3.1 presents the total amount of sludge applied to land for Scottish Water sites and for private finance initiative (PFI) sites (which are more numerous).[2] 245000 wet tonnes of

[2] A Private Finance Initiative (PFI) is defined as a long-term contract between a private party and a government entity. The private sector partner designs, builds, finances and operates a public asset and related services. The private party bears the risks associated with construction and maintenance and management responsibility, and remuneration is linked to performance.

wastewater bio-resource was produced in Scotland in the 2021/22 annual period (a combined total of 63% of dry bio-resource was applied to agricultural land in Scotland). (202) The majority totalling 142297 wet tonnes originates from PFI treatment sites, with 103281 wet tonnes produced by Scottish Water. Wet sludge can be treated by a number of different processes and the regulation and guidance available does not stipulate what processes must be followed.

3.2.2 Beyond agricultural application

Disposal of sewage sludge at sea was the preferred end of life solution until the banning of the process in the late 90s. In 1990, just 19.8% of Scotland's sewage sludge was applied to agricultural land with 70.1% being dumped at sea. (201) As awareness of potential problems with this solution grow, attention is being paid to sludge treatment methods offering the potential for energy recovery. To this day, sludge can be sent to landfill for disposal or incinerated.(203) Due to a lack of infrastructure at these sites, energy recovery is not applied at SW sites.[3]

Incineration is carried out at temperatures over 800 ˚C and requires a pre-dewatered sludge. Energy recovery is possible from the flue gas but simultaneously, harmful gasses are generated and require treatment prior to release. (204) Incineration can be considered a viable end of pipe solution which destroys chemical contaminants and pathogens if a high temperature is used although this would need to be tailored for the identity and quantity of contaminants present in the sludge. High process cost and energy requirements are not balanced by the generation of a low-value ash meaning that this is an economically intensive option. (204)

Pyrolysis and gasification of sludge takes pre-dried material and maximise the conversion to energy. Pyrolysis is carried out up to temperatures of 600 ˚C in the absence of oxygen and produces a biochar as well as bio-oil and gaseous products such as hydrogen and methane. The quality and quantity of useful products depend on the content of the sludge itself and

[3] From conversations with SW representatives November 2022

careful optimisation of the pyrolysing conditions. Heavy metal contamination can impact the quality of the biochar produced and the complex nature of the pyrolysis process may limit the application in some cases but this treatment brings advantages in reducing the production of harmful gaseous pollutants and a potential useful product. Gasification is a similar process carried out at a higher temperature up to 1000 ˚C in a partially oxygenated environment and carries similar advantages and disadvantages to pyrolysis.

An option to recover valuable nutrients from the sewage sludge without simply applying it to land is an area of intense research. As a key example, Germany has embraced phosphorus recovery from sludge. (205) In amended sludge ordinance introduced in 2017, medium and large sized WWTPs were banned from passing sludge directly to agricultural land and must apply a recovery process to it. Phosphorus recovery is generally achieved via precipitation, metallurgical and thermal chemical processes or the older and more established wet chemical recovery from sewage sludge ash after incineration.(205) Driven by the need for careful control of fertiliser application, public perception of sludge to land and circular economy benefits, from 2029, phosphorus recovery will be required for all German sewage sludge. (205)

Land reclamation projects utilise sludge with it providing organic matter and nutrients to areas of very poor soil quality. Regulation for this type of land application is distinct from sludge use in agriculture and is not discussed in this chapter.

3.3 Current policy context

3.3.1 Regulation in Scotland covering sludge application to agricultural land

The UK regulatory environment is complex with SS falling under a number of definitions both as a fertiliser and as a waste product.

As an organic matter fertiliser, SS is subject to the spreading controls of the Water Environment (Controlled Activities) (Scotland) Regulations 2011. Furthermore, EU Nitrate

Directive requirements are presented in the UK Code of Practice for the Agricultural Use of Sewage Sludge to which farmers voluntarily adhere. Together, these requirements include limits on the amount of nutrients added to soil, stipulations on where fertiliser can be spread to avoid runoff to water bodies and specific weather conditions under which spreading is authorised. These regulations do not include mention of pollutants, emerging contaminants or microplastics.

Pollution of sludge is covered to some extent by legislation in the *1989 Sludge Use in Agriculture regulations* (SUiAR). (203) Controls are present to account for pH and heavy metal contamination including Cr, Cd, Cu, Pb, Hg, Ni, Zn. The SUiAR stipulates that soil is tested before first application and any biosolids are tested at 6-month intervals to ensure levels are below a safe level. Records of testing results are retained and may be audited by the Scottish Environmental Protection Agency (SEPA). The *Safe Sludge Matrix* (aka ADAS Matrix) was a 1999 addition to SUiAR and prevents the spreading of untreated sludge to land unless it is injected or mixed with soil. (206) Sludge applied to land in Scotland must undergo advanced treatment in order to meet the requirements of the Safe Sludge Matrix. Mainly this involves advanced anaerobic digestion, thermal drying or lime pasteurisation. Pathogen loads are reduced with an aim to lower indicator bacterial E. Coli by 6 log (ie. 99.9999% removal) and Salmonella to zero. Although the matrix does not mention any other pollutants, the treatment may reduce the levels of many contaminants as discussed in Section 3.5.

The Biosoliods Assurance Scheme (BAS) is a voluntary scheme set up in 2015 by Assured Biosolids (A not-for-profit run and owned by UK water companies) and is intended to compliment the regulation by introducing pathogen limits for sludge spread to land. (207) Although not law, Scottish Water is certified by this scheme meaning all SS produced by its sites is treated to reduce pathogen loads. This is achieved by treating sludge to the standards presented in the Safe Sludge Matrix. Under the requirements of the BAS, limitations on spreading are put in place for areas vulnerable to nitrate pollution (termed Nitrate vulnerable zones NVZs). Handlers are required to test field soil and SS prior to first application and maintain records of all applications.

Biosolids (including SS) are transported as a waste material and hauliers must register as professional transporters of waste with SEPA. Waste Management Licensing (Scotland) covers processes that see sludge imported (such as large sludge treatment sites used to treat quantities of sludge from smaller sewage treatment works). The requirements of these licenses cover odour management and stipulates that no risk to water, air, soil, plants or animals occurs by their handling. Storage of sludge falls under the Paragraph 8 waste exemption whereby handlers are required to notify SEPA of storage locations and intended use.

Sludge application to land in Scotland was reviewed in a Scottish Government commissioned report by the Hutton Institute in 2016. (198) The report gives an overview of sludge production in Scotland, reviews of the regulatory environment under which it is handled and initially assesses of the risk to human health by a number of common pollutants present within it (see Section 3.5)The report included recommending the incorporation of the Safe Sludge Matrix into law in Scotland as well as significant changes to the way SEPA regulates and permits sludge storage and handling. The report concluded that complete assessment of the risk to health could not be carried out due to insufficient data but most of the chemical contaminants considered did not pose a high risk to receptors at the levels expected in soil. Despite this, accumulation and uptake into food crops was highlighted. Monitoring of chemical pollutants in sludge is key to ensuring levels remain at a safe minimum and the report recommends introduced robust testing and monitoring program in Scotland.

3.3.2 Broader UK activity

In England and Wales, a 2020 Environment Agency policy paper was published on a strategy for safe and sustainable sludge use. (208) The primary aim is addressing concerns around the outdated SUiAR being unfit for purpose and requiring updating. Covering England only, the strategy brings sludge use under Environmental Permitting Regulation, making SUiAR obsolete. It is not clear what action on emerging contaminants and microplastics will be taken but the paper acknowledges that emerging risks associated with organic and inorganic chemicals, anti-microbial resistance and plastics should be assessed. Within its aims, the

paper recognises the need to also work across the UK including via the Chemical Investigation Program.

The UK Water Industry Research (UKWIR) Chemical Investigation Program (CIP) and the Scottish CIP are actively working on understanding trace level chemical pollution in the water and wastewater environment. It has recently included significant work on sludge pollution levels. (209) The second CIP Scotland Sludge report carried out sampling at Galashiels anaerobic digestion sewage treatment centre over a 13 month period. Metals and pharmaceuticals were sampled and compared to the EU Sludge Directive 2011 working draft limits. The contaminants in question were found below these limits.

The third CIP Scotland has carried out sampling at the Seafield anaerobic digestion (AD) Cambi sewage treatment centre and Galashiels AD sewage treatment centre between September 2021 & September 2022 although data is not currently publicly available.

3.3.3 European Union activity

In the EU, a number of regulations currently cover sludge use on agricultural land. Namely, the Water Framework Directive 2000/60/EC on water protection, Directive 91/271/EEC on urban waste water treatment, Directive 96/61/EC concerning integrated pollution prevention and control, Directive 99/31/EC on the Landfill of Waste and Directive 86/278/EEC on the use of sludge in agriculture. Much like the policy landscape in the UK, this is a complex regulatory system reflecting the many activities SS handling is relevant to.

The Urban Waste Water Treatment Directive encourages sludge reuse wherever appropriate and puts specific requirements on sludge use in agriculture. (210) The European Commission held a recent public consultation and targeted stakeholder consultation on the Evaluation of the Sewage Sludge Directive (SSD 86/278/EEC) (the consultation closed Q3 2021), seeking to revise its content and update regulation. A working draft outlining some elements of the ongoing consultations is available including revised limits on heavy metals previously proposed in 2011. (211)

While the SSD places limits on heavy metals, care of Nitrogen and Phosphorus levels, it has some perceived shortcomings. The SSD was originally intended to promote the use of SS in agriculture and although prohibits the use of untreated sludge (unless directly injected untreated sludge), the SSD does not specify what treated sludge is defined as. The directive also neglects to control emerging contaminant and microplastic loads in applied sludge. The regulation was first introduced in 1986 and the European Commission (EC) consultation investigates if it is still fit for purpose.

In 2014, the SSD was reviewed under the "Ex-post evaluation of certain waste stream directives" which notably highlighted issues around pollutants of emerging concern and microplastics. (212) Since the directive was developed, scientific understanding of many of the potential problems associated with SS application to land has advanced and many call into question the relevance of some directive points. The EC evaluation aims to complement previous reviews and advise on the need to revise the SSD, much like the case in the UK with the Environment Agency strategy and SEPA consultations. (Section 3.3.1 - 3.3.2)

3.4 Stakeholder overview

Sewage sludge use in agriculture involves a large range of stakeholders across farming, energy and waste management industries as well as those concerned with the environmental implications of its application to land. Figure 3.2 summarises key stakeholder groups identified in Scotland during this project. Stakeholders are grouped by their perceived power to implement change in the way sludge to land is regulated as well as the perceived level of concern each group has for implementing this change.

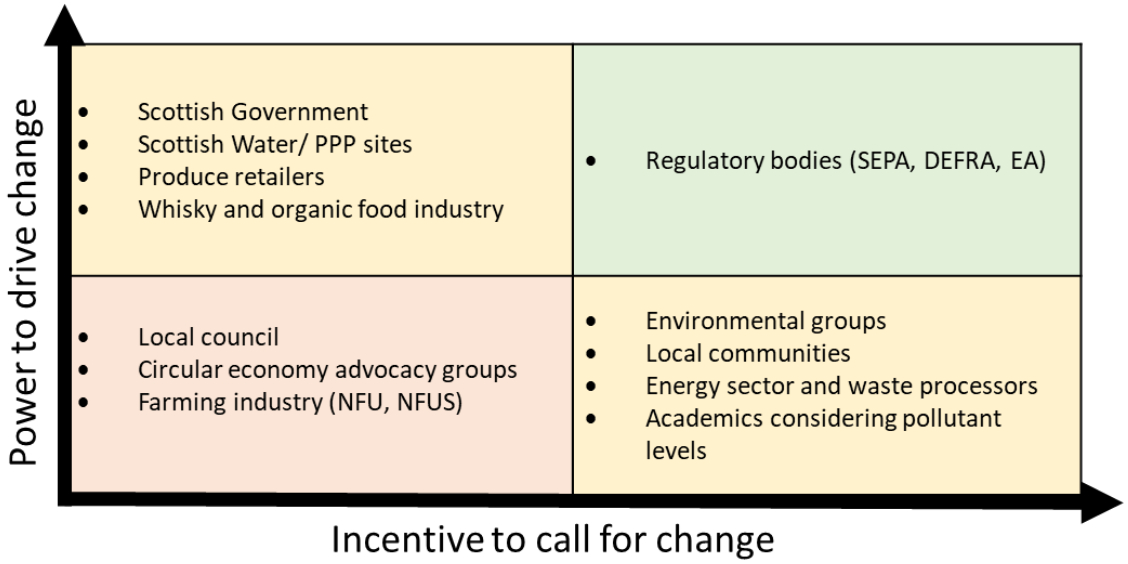

Figure 3.2 Key stakeholder groups arranged by **a)** power to drive or promote change in how sludge to land is regulated and **b)** incentive to change current regulations

The main concerns of government and associated funding bodies lie with risk to human health, economic impact, public perception and maintaining Scotland's reputation as a leader in human and environmental health. The Scottish government broadly supports actions promoting a circular economy and energy sustainability in line with their ongoing commitments and specifically the circular economy bill. (213) Re-use of SS is in line with the vision of zero waste in Scotland. However, as the EU and other UK governments are actively implementing changes to outdated sludge regulations, Scottish government must act on its own outdated sludge regulation to keep up. The high cost of an overhaul to treatment systems and the fact that the current system is perceived as the environmentally friendly option is a major barrier to government action as is the lack of clear evidence when it comes to levels of contaminants leading to increased public health risk.

Water companies produce, handle and oversee the disposal of waste SS. Scottish Water actively fund research on identifying contaminants present in sludge and treatment improvement with a long-term goal of bringing contracted PFI sites back under their control and updating processes at these sites. Economic drivers and a lack of strict regulation of the content of final sludge biosolids are barriers to change in current processes. Awareness of the

potential chemical contaminant levels in sludge is high and Scottish Water are involved in the Chemical Investigation Program. Benefits of sludge recycling to water companies and sludge processors mainly lie in energy recovery potential and a disposal route in line with their circular economy goals.

Regulators such as SEPA currently have limited power under the SUiAR as well as limited value gain from monitoring SS use (as sludge use is not permitted directly, they cannot regain money spent regulating it).(203) Updated regulation under the IAF offers a flexible permitting scheme and the potential for tighter control of compliance to regulation. In particular SEPA is committed to promoting safe levels of contaminants in soil and sludge as well as monitoring and auditing of application procedures. The independent body Environmental Standards Scotland (ESS) has identified soil health as a key area of focus and acts as a watchdog for SEPA in terms of regulation adherence and policy suitability. ESS will not take action unless there is clear evidence of systemic problem in Scotland. In general, barriers to any change in regulation of chemicals lies with the lack of a clear evidence of harm and associated legislation from Government. Furthermore, the lack of a current alternative use for sewage sludge which aligns with circular economy goals restricts any change to the current handling process.

Protection of soil is an important driver for many stakeholders. Environmental NGOs as well as farmers and farming bodies (NFU/NFUS) are concerned about long-term soil health as well as accumulation of environmentally persistent chemicals. The health of agricultural soils for future growing and grazing is most likely to be of concern to farm land owners and may be less of a concern for tenant farmers who are the users of biosolids fertilisers. The Scottish farming industry also relies on fertiliser availability and SS is an attractive low-cost option. As well as the soil, consideration of the crops grown in it and animals grazing on it brings in another group of stakeholders. The British Retail Consortium (BRC) are a trade association for all UK retailers and contributed to the development of the Safe Sludge Matrix. At the individual retailer level, many organic produce suppliers and many whisky producers will not use crops grown on SS treated land, as understood from discussions with NFUS representatives. The high soil quality requirements of the whisky industry are the driving force behind this preference. (214) In the future, pressure to meet high standards such as

these from produce retailers may reduce the available land for sludge application as farmers are restricted to keep their land SS-free.

3.5 Contaminants of concern in sewage sludge applied to land

3.5.1 Heavy metals

Heavy metals present in soil and sewage sludge have long been part of regulation in Scotland. This pollution originates from industrial activity, corrosion of sewerage systems or surface runoff from roads and urban areas. (215) Levels in sludge vary based on the nature of the influent wastewater being treated and the proportion of it that comes from industrial sources. As outlined in Section 3.3.1, maximum loads for key heavy metals are set within the SUiAR regulations in order to avoid risk to human health via metal uptake by plants. With scientific literature well established in this area of concern, regulators around the world generally implement similar controls and testing requirements. In the European Union, a precautionary principle is applied to limits with many member states setting their own limits well below the European Sludge Directive requirements. (216)

In the UK, as industry has moved away from producing highly polluting industrial wastewater thanks to effective source control measures, heavy metal limits appear to be met by sludge producing sites. In a 2012 European wide review, a large scale evaluation of contaminant levels in 63 sewage sludge samples from 15 different EU countries including the UK concluded that heavy metal levels were below the limits set by current regulation. (217) In the UK, Charlton et al. studied the long term effect of Zn, Cu and Cd in SS application on soil microbial biomass carbon. (218) When considering an immediate risk to humans, the limits on heavy metals were deemed sufficient to prevent a large accumulation in agricultural plants. The study did however conclude that the limits did not protect soil health in the same way. For two of the metals studied, disruption to the soil microbial community was observed at application of metal levels below the UK regulatory limits. Specifically, a decline in Rhizobium Most-probable number occurred due to the historical application of sewage sludge contaminated with Zn below the application concentration limits (Table 3.1). Where total Cu

ranged from 100-135 mg kg^{-1}, similar impacts to Rhizobium population was observed although to a lesser extent indicating that Zn limits in particular should be lowered to protect long term soil health. This raises questions on the suitability of the current limits for long-term environmental protection. The Chemical Investigation Program (Scotland) is also active in trying to understand the levels of heavy metals present in sludge. Sludge sampling conducted in 2019 at the Scottish Water Galashiels site found all regulated metal levels to be below the proposed limits in the revised European Commission 2011 Sludge Directive revision working document outlined in Table 3.1.

Table 3.1 Thresholds relevant to sludge application to land

	EU Sludge Directive (210) [mg/kg dry matter]	**Working draft 2011 - revision (211) [mg/kg dry matter]**
Cadmium	20-40	10
Chromium		1000
Copper	1000-1750	
Lead	750-1200	500
Mercury	16-25	10
Nickel	300-400	300
Zinc	2500-4000	2500

There remains concern in the scientific community over low levels of heavy metals applied to land leading to accumulation (219-221) and affecting long term soil health (222), despite the regulation and testing currently in place. Uptake of heavy metals by food crops presents a route to human exposure. In the sludge review, commissioned by the Scottish government, the lab based nature of many of these studies was highlighted. (198) The review noted that although accumulation of heavy metals in food crops was shown in a large number of research studies, the conditions of a laboratory-based exposure experiment were not realistic to determine the risk for real world soils, understood to be due to the lack of complexity in the soil systems considered. The report therefore did not conduct any formal risk assessment for heavy metals.

3.5.2 Pathogens

Domestic wastewater is a major source of pathogens to wastewater and therefore to SS. Bacteria (223), viruses (224, 225), protozoa (226) and prions (227) have been detected in SS and pose a potential health risks to humans. Despite this, UK legislation does not currently include acceptable limiting levels of pathogen load in SS applied to land. The voluntary Safe Sludge Matrix stipulates that sludge be treated to reduce pathogen loads before application to land (although it does not specify how this should be achieved). Based on the planted crop type, clear guidance is given to determine the minimum level of pathogen reduction that is acceptable in order to reduce the risk to an acceptable level. All water companies in the UK adhere to the Matrix and are certified under the Biosolids Assurance Scheme.

In order to determine the microbiological load of environmental samples, E. Coli is typically used as an indicator. The Safe Sludge Matrix uses E. Coli reduction as the indicator for quality assurance dictating that treatment of sludge destined for application to land falls below threshold limits. Some criticise this approach due to the potential to produce a false negative result for pathogen contamination if the microbiological species present (i.e. something other than E. Coli) is in a much higher concentration than the indicator organism. Furthermore, re-growth of bacterial after sludge treatment (during storage or within the soil) may also lead to levels above those expected from initial test results. Viruses, protozoa and prions are expected to be affected in varying degrees by different treatment methods but are not tested for. (228)

An important concern in SS application to land is the potential for promoting antimicrobial resistance. (229) Antibiotics and pharmaceuticals in wastewater and sludge applied to land can cause problems themselves (see section 3.5.3) but might additionally result in an increase in antibiotic resistance. Advanced sludge treatment such as anaerobic digestion or lime stabilisation reduces the viability of bacteria including those with antibiotic resistance. (229) Despite a reduction in live bacteria, SS spreading to land may be a significant source of antibiotic resistant genes to the environment. (230) Genetic elements encoding resistance to every major class of antibiotic were identified in samples of composted sludge. (231) A

discussion of the potential transfer of resistance within the soil environment enabled by the presence of this genetic material is available in the literature. (232-234) In a study by Chen et al. of the long-term impacts of sludge to land, the overall diversity of bacteria in soil increased significantly. (235) The researchers attributed this shift in bacterial community to a transfer of genetic material and genes in the environment, accelerated by the presence of SS.

3.5.3 Organic emerging contaminants, personal care products and pharmaceuticals

Chemical pollutants that are removed, but not destroyed by water treatment methods, are transferred into the sludge. The identity and quantity of chemical contaminants present in wastewater is hugely variable depending on the nature of activities producing it. Heavily industrialised, agricultural and domestic wastewater catchment areas all produce different chemical contaminants of concern.

The James Hutton Institute identified 35 organic contaminants of concern and 25 personal care products (PCPs) and pharmaceuticals present in sludge in their report prepared for the Scottish Government, as summarised in full in Appendix B. (198) They selected chemicals from literature based on their presence in sludge and the availability of environmental partitioning data (specifically the partition coefficients which allow calculation of the proportion of pollutant retained in water, soil, plant matter etc.). Combining the literature data with worst-case scenario pollution levels present in the biosolids enables an estimate of the concentration of organics which may enter into food crops, water and soil.

Of the chemicals considered, the report highlights several as contaminants of key concern. These are the detergents nonylphenol and nonylphenol diethoxylate (NP2EO), and the flame retardants PBDE-99 and PBDE-209. Of the PCPs and pharmaceutical contaminants investigated benzothiazole, triclocarban, cyclomethicone 5 & 6 and atenolol were deemed to carry a risk to human health via exposure in food crops. If the levels reach those modelled, deleterious effects would be experienced by those exposed. Risk to health via food crop exposure was also mentioned for metformin, sertraline and tamoxifen although this was

deemed to be minimal. The report advises that these risks may be mitigated from careful crop type management to reduce uptake into produce and source control of pollutants.

Globally, estimates of the chemical pollution risk of sludge to land highlight similar contaminants of concern. Mejias *et al.* (236) review the literature on pharmaceutical content of sludge and impacts when applied to land. A huge range of compounds and their metabolites are present in sludge. Concentrations are affected by anaerobic digestion and composting treatment with final concentrations diluted through mixing with soil. However, the authors highlight critical compounds triclocarban, triclosan, ciprofloxacin and 17α-ethinylestradiol carry risk even at the levels applied and call for an assessment of the distribution and risk of organics and their metabolites in soil and sludge. Verlicchi et al. discuss literature on pharmaceuticals and personal care products in treated and untreated sludge with a focus on chemicals retained in soil after application. (237) Estradiol, ciprofloxacin, ofloxacin, tetracycline, caffeine, triclosan and triclocarban are highlighted as critical compounds in the soil and the authors again call for improved environmental risk assessment on the issue.

3.5.4 Microplastics

Microplastics make their way into our wastewater system by many routes including domestic laundry, urban runoff and cosmetic products, as described in detail in Chapter 1. (24)

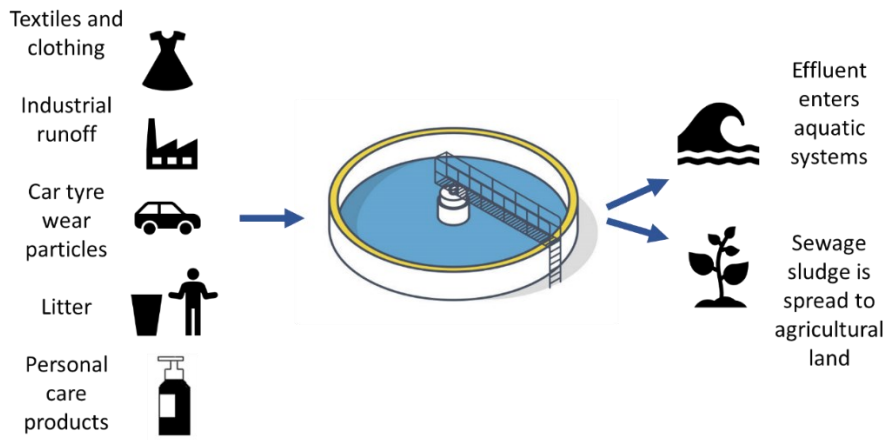

Figure 3.3 Microplastic sources to wastewater treatment systems and subsequent release pathways

Primary microplastics are produced on the micrometre scale. Personal care products (PCPs) such as exfoliating face washes or toothpaste can contain small beads of plastic, similarly industrial abrasion additives used in sandblasting often use small plastic pellets or fragments. Industrial plastic precursor pellets (termed nurdles) are the raw form of plastic for many industrial uses. Secondary microplastics are microscale fragments created by the weathering or fragmentation of larger polymer pieces. For example, shedding of synthetic clothing fibres during washing cycles releases thousands of secondary microplastic fibre fragments in wastewater. A single primary microplastic can break up to form thousands of micro and nano sized pieces in water. (238) Not only does the particle size draw concern for their distinct mechanism of toxicity in biological systems (34) but the generation of a larger number of small particles means plastic may pass through WWTPs more easily.

In a water treatment system, plastics are highly resistant to any destructive treatment processes and therefore generally are not destroyed but moved out of the water. Their removal results in their concentration into the solid sludge phase. Up to 99% removal rates from water have been recorded for a site in Scotland, with similarly high proportions at sites around the world. (52, 84, 239) A number of stages contribute to this high value with larger fragments separated during screening and filtration steps and smaller microplastics settling out during a sedimentation stage or being captured in the sludge produced during biological digestion reactors. The result is very high concentrations of microplastics in the sludge. (65, 77, 78, 80, 240)

The actual concentration of microplastics in wastewater effluent and sewage sludge is highly variable and any estimate therefore comes with significant uncertainty. Literature has estimated from 720 – 14900 particles per kg (wet weight) and 1000 – 170900 particles per kg (dry weight) in SS. (65) In part, this is due to fluctuations in the microplastic load of wastewater entering the treatment site but also due to challenges in measuring microplastic concentrations. (19, 172, 175) The type of wastewater treatment applied also affects the proportion of microplastics removed from water as reviewed by Iyare et al. (65). Their meta analysis indicated that the initial primary treatment steps of skimming and sedimentation removed the majority of plastics from the water (around 72%). The settling velocity of the

particles in water allowed them to conclude that during this stage, larger particles are preferentially removed meaning SS is likely to contain high proportions of the largest fraction. This is in agreement with a study that observed contents of sludge from a treatment works in Glasgow contained a high proportion of large microplastics when compared to the effluent water. (52) Of 15000 microplastics per cubic meter estimated to enter into a Swedish treatment plant (12000 population equivalent in size), more than 99% were captured in the sewage sludge. (75)

When scaled up, this level of pollution means that huge numbers of microplastics are present in the sludge applied to agricultural land. For the EU, assuming an approximate generation of 10 million tonnes of sludge annually, a range of $7.2 \times 10^{12} – 1.49 \times 10^{14}$ (7.2 - 149 trillion) plastic particles pervades it. (65) Sludge has been named a prime driver of soil plastic pollution by researchers. (241)

Despite the clear evidence of pollutant presence, identifying risk thresholds is a challenge when considering microplastic pollution. The body of literature on environmental risk, although continuously developing, is yet to define a safe level of exposure in soil. Without a broadly accepted defined safe level, it is impossible for regulators to set limits for microplastics in environmental media, including SS.

3.6 Treatment of sewage sludge

There is a large body of literature on chemical and biological contaminants present in SS. Determining whether these pollutants present a risk to human health if spread on land can be challenging as exposure to the levels present in the raw sludge is unlikely unless direct contact with raw SS is made. Risk describes the probability of adverse effects occurring and is a function of the inherent toxicity of the chemical or pathogen, how much is in the environmental medium and how much exposure the individual has. Sludge treatment systems are capable of reducing the concentration of some contaminants and the nature of treatment results in different levels of contaminant removal.

Raw sludge is treated in Scotland by a number of different processes. Most commonly applied is Anaerobic Digestion (AD). Biological breakdown of the organic matter in sludge is carried out at ~35 ˚C and have the benefit of producing biogas. (242) Advanced anaerobic digestion (AAD) adds a thermal hydrolysis pre-treatment step. High pressure heating up to 200 ˚C improves the bioavailability of the organic content in sludge and improves the efficiency of the subsequent biological treatment and biogas production. (223) Thermal drying reduces the wet volume of sludge significantly and is carried out at high (~450 ˚C) temperatures. Generally, the dried sludge is destined for incineration and energy recovery but may also be applied to land as discussed previously. Liming involves heating sludge over 55 ˚C under extremely alkaline conditions. Each treatment results in a different quality of biosolids material termed conventional or enhanced treated. In Scotland, most sludge is treated using one of the following methods presented in Table 3.2. The type of treatment applied has implications for the quality of the final sludge in terms of contaminant load. Enhanced and conventionally treated sludge can be applied in different circumstances under the requirements of the Safe Sludge Matrix.

Table 3.2 Methods for sewage sludge treatment applied in Scotland

Treatment method	Material produced, dry matter	Treatment requirements met [4]
AAD, followed by de-watering	biosolids cake, 30%	Enhanced
Drying (no AD or stabilisation)	biosolids pellets, 95%	Enhanced
Liming and de-watering	biosolids cake, 40%	Enhanced
AD, followed by de-watering	biosolids cake, 25%	Conventional
AD, followed by de-watering and drying	biosolids pellets, 95%	Enhanced
AD of liquid sludge	Liquid, 4%	Conventional

[4] Conventionally treated sludge is expected to have a $2\log_{10}$ (or 100-fold) reduction in *E. coli* while enhanced treated should reach $6\log_{10}$ (or 1,000,000-fold) removal of *E. coli* and 100% removal of *Salmonella*

A comparison of the removal of a selection of chemical contaminants (selection based on those identified in the James Hutton report (198)) of key sludge treatment methods used in Scotland is presented in Table 3.3.

A lack of comprehensive literature and contradictory results in lab experiments (eg. In the case of NP removal by AD) makes it difficult to determine the removal of contaminants prior to land application. In this case 'no evidence' is used to indicate that the removal efficiency of this chemical pollutant has not been reported in the literature reviewed while 'no impact' indicates that the removal process did not reduce the concentration of the chemical pollutant in the literature reviewed. Although treatment may be capable of attenuating the concentration of some organic contaminants, others may pass through unchecked and be applied to land in the same amounts they are present in the raw sludge. Regular testing of soil treated with SS would provide valuable data to understand the fate of these chemical contaminants and not only help develop an understanding of chemical fate but also a clear indicator of potential risk to health from chemical exposure.

Table 3.3 Literature evidence of removal of chemical contaminants by sludge treatment

	Removal efficiency of sludge treatment				
Chemical pollutant	**Anaerobic Digestion**	**Drying**	**Thermal hydrolysis**	**Liming**	**Reference**
Atenolol	41 - 63 %	No evidence	No evidence	No evidence	(243, 244)
Triclocarban	10 - 11 %	No evidence	99%	No impact	(243, 245, 246)
Benzothiazole	No evidence	No evidence	No evidence	No evidence	
PBDE 99 & PBDE 209	21 - 24 % & 31 - 64 %	No impact	No evidence	No evidence	(247, 248)
PCB 118 & PCB 138	18 – 20 %	No evidence	No evidence	No evidence	(249, 250)
Cyclomethicone 5 & 6	~59 % & No removal	No evidence	No evidence	No evidence	(251, 252)
Nonylphenol (NP) and NP2EO	2.6 - 100%	No evidence	No impact	No evidence	(253, 254)

3.7 Impact to soil quality

SS has a high content of organic matter and biogenic elements (C, N, P), which are essential for plant growth and development as well as soil microbiota health. SS application to land is a useful way of ensuring elements are recycled and provides a cheap source of fertiliser. The rate of application to agricultural land is important in preventing excessive nutrient loads entering the soil or causing runoff to waterways is controlled in Scotland the Biosolids Assurance Scheme as discussed in Section 3.3.1.

Dry sludge typically contains 50-70% organic matter and 30-50% mineral components, although this is highly variable depending on the nature of the wastewater and treatment system the sludge is derived from. (255) Soils amended with SS have shown improved soil structure, nutrient storage, improved porosity and water retention. (256, 257)

The nutrient content of biosolids depends largely on the treatment process with thermally dried sludge providing the largest proportion of N, P, K, S and Mg (in line with providing the highest dry matter content). (258) Comparing this with the discussion of treatment type on contaminant loads in Section 3.6 makes clear that the biosolids fertilisers with the highest nutrient levels have the higher contaminant loads. In Scotland, much of the sludge applied to land undergoes advanced anaerobic digestion producing solid material with a relatively low proportion of nutrients by mass. On a dry weight basis, biosolids contain between 1-11% N and 0.7-7.5% P while commercial chemical fertilisers can range 15-82% N and 8-76% P. (259, 260) Low nutrient concentrations may actually provide an advantage over chemical fertiliser in the slow release of nutrients to soil over time. The large range in availability of N and P is likely due to varying soil conditions, sludge or fertiliser origin and method of measurement. (261, 262) A full breakdown of the available nutrient loads of biosolids is available in a technical note prepared by Scotland's Rural College (SRUC). (263)

SS increases the microbial biomass and diversity in the soil. This can have implications beyond those for antibiotic resistance already discussed in Section 3.5.2. Increased microbial biomass competes with crops for P uptake. The P delivered within SS is provided in a higher chemical

form than commercially available fertilisers, meaning its delivery to plants is slower. (264) With increased competition from bacteria for nutrients, the actual benefit to plants is likely significantly lower than initially indicated by simple total nutrient loads delivered.

SS can provide a useful cheap fertiliser which despite having some drawbacks in terms of element delivery and availability, can improve the soils ability to promote plant growth. The main drawback in terms of soil quality is the long-term sink of persistent pollutants such as microplastics and organic chemicals. Limited information is available as to the fate and transfer of many of these chemicals but due to their longevity in natural systems, it can be expected that continued long-term application to land will result in an accumulation.

3.8 Circular economy considerations

Application of sludge to land was introduced as an alternative to disposal at sea or landfill with circular economy benefits in mind. Any proposal seeking to change this practice must consider carefully the sustainability implications of its replacement.

Many alternative SS treatments are energy intensive (incineration, nutrient recovery, pyrolysis) and require significant infrastructure overhaul to be viable options in Scotland. These are discussed in detail in Section 3.6 and all hold positives and negatives in terms of their circular economy potential. Direct disposal options generally are not in line with these goals. The final ash produced by incineration holds high levels of contaminants and flue gas produced during the process is environmentally harmful. Nutrient recovery, although process intensive, may offer a solution that recovers the valuable mineral content of sludge. After nutrient extraction, the remaining residual material is a heavily contaminated waste with no viable use and is usually incinerated or pyrolysed. Pyrolysis has the potential to produce a useful biochar by-product at a lower operating temperature than incineration.

Farmers using sludge fertiliser on agricultural land do so as a cheap source of nutrients. The most common alternative to sludge fertiliser is to use mined phosphorus based fertilisers which are damaging to the environment and come with a significant toll in terms of

greenhouse gas emission. (265) In a recent article from Food Manufacture, the importance of fertiliser availability to Scottish food security was laid clear. (266) A reported 200% increase in fertiliser costs presents as a key challenge for growers in 2023. Some farming communities call for the government to ensure farmers can make efficient use of nutrient sources and SS offers some benefit in this context. The number of farmers currently relying on sludge for fertiliser in Scotland is low. If the practice stopped, the alternative for fertilising these sites is highly priced and environmentally damaging.

3.9 Key recommendations

Application of sewage sludge to agricultural land introduces organic chemical and microplastic pollution to Scottish soils. There is no monitoring system in place for levels for these contaminants and a limited understanding of the potential risk to health from human exposure or bioaccumulation impact. Upcoming changes to the way SS regulation is managed under the Integrated Authorisation Framework offer improvement over the complex combination of regulatory schemes currently in place but does not seek to introduce any new limits on these emerging contaminant classes. Sewage sludge to land is a complex area with numerous stakeholders across the water, farming, waste and energy sectors. Policymakers should consider this alongside the benefits in terms of circular economy and nutrient recycling that the practice offers. While the benefits of sludge recycling over disposal are clear, it must be achieved in a safe and environmentally friendly way to align with the circular economy goals and the human right to a healthy environment as set out by the Scottish Government.

In response to the consultation on the implementation of the IAF, attention should be drawn to the numerous issues associated with application of SS to land in Scotland. An overhaul of the complex and outdated legislation on this issue is welcome but in order to protect soils and the health of our environment, the Scottish Government must take further action. Recommendations are:

I. Incorporation of existing voluntary schemes (Biosolids assurance scheme and Safe Sludge Matrix) into law to ensure all sludge produced in Scotland destined for agricultural land meets minimum quality levels.
II. Regulatory bodies to be given increased power to audit and enforce compliance with contaminant levels of sludge and soils, allowing confidence in the current safety of sludge use may be increased as well as providing a potential value recovery mechanism to regulators via permitting costs.
III. Based on the evidence provided in Scottish Government Commissioned reports, monitoring of key chemical contaminants should be carried out in soils and sludge to determine the level of long term risk posed by emerging contaminants.
IV. Based on this testing, maximum safe levels for emerging contaminants and microplastics may be defined, allowing regulations on maximum allowed levels to be created.
V. Alternatives to sludge spreading to agricultural land should be explored and prioritised if the level of risk cannot be defined based on current knowledge.

3.10 Conclusions

As a case study, this chapter presents MP pollution of wastewater within a much larger system of pollutants, regulation and environmental impact. This chapter is included within the thesis to show that any solution hoping to address microplastic pollution in WWTPs must consider a complex and diverse range of legislation and knock-on impacts. Treatment of wastewater using traditional methods such as filtration or flocculation moves many contaminants into the solid sludge phase. While the water effluent of such plants has been effectively treated, the pollutants of concern may simply have been moved to another phase where they can cause environmental harm in unforeseen ways.

The process of exploring policy and regulation of SS to this level of detail sheds light on the fact that MP pollution forms only one aspect of regulation and pollution concern. To drive change and have impact within this space, technology and information around MP pollution must be set within a larger context.

Regarding MPs specifically, of the recommendations made as a result of this analysis, short term improvements rely on accurate testing of MP content in wastewater and sludge. Long term goals are based around reducing the input sources of MPs to WWTPs in the first place. The focus of this thesis on removal and transformation of MPs within WWTP systems must also align with these goals. Complete removal of pollutants via mineralisation avoids the problem of MP transfer into a solid sludge phase. Until complete source control is possible, the application of AOPs for MP removal may offer a way to prevent this problem. In order to achieve this, a clear understanding of which AOP methods are feasible for MP removal is needed, alongside knowledge of MP degradation in these systems. Subsequent chapters in this thesis explore these ideas in detail, contributing directly towards this goal.

4. Advanced oxidation treatment methods for removal of microplastics in laundry waste water

The experimental work presented in this chapter explores the effects AOPs have on the chemical and physical properties of polyester fibres with the aim of optimising a treatment for effective MP removal. I chose to initially narrow my focus to microplastic fibres commonly found within domestic laundry wastewater to simplify the experimental design and MP characterisation during AOP screening. As previously discussed, this class of MP represents a major component of those resistant to removal by traditional WWTP systems and is therefore of particular importance.

Section 4.1 discusses the initial development of an experimental protocol for MP fibre analysis in the lab. Data presented in Section 4.2 uses this developed experimental protocol to investigate the effect of UVC activated AOPs on MP fibres in water. The work in this section is published in the paper titled: Removal of polyester fibre microplastics from wastewater using a UV/H_2O_2 oxidation process. (267) Published content is reproduced within this chapter as permitted under a CC BY 4.0 licence.

4.1 Experimental protocol for tracking microplastic degradation

To track MP degradation, weathering and removal from water, a reliable experimental procedure is essential. In the field of microplastics research, there are few standard methods for analytical techniques, degradation conditions and experimental protocol. (164) The aim of the work presented in this section was to develop methods which allow polyester fibre MP degradation to be followed. Specifically, a lab scale AOP treatment capable of producing reproducible results and a method to effectively measure MP degradation was developed.

4.1.1 Literature methods for MP testing material preparation

Washing of synthetic clothing is reported to release microplastic fibres in the length range of 100-1000 µm with a diameter 6-30 µm. (268-271) To study MP fibres in lab scale experiments requires a source of raw fibres within this size range. Despite their prevalence in our

environment, analytical standards of MP fibres are not currently commercially available and must be prepared.

A simple method to prepare MP fibres is cutting fibre lengths from a commercially produced material. This typically results in relatively long fibres (>500 µm in length) with a wide length distribution but uniform diameter. (67) Fragments of nylon have been prepared in this way by trimming nylon fishing line. (272) Polypropylene and polyacrylic wool fibres have been prepared simply by cutting with sharp scissors. (273, 274) Some novel techniques have emerged such as grinding supercooled polypropylene rope in a commercial coffee grinder which produced a broad distribution of MP fibre lengths. (275) The benefit of these cutting and grinding processes is a fast preparation of MP fibre with easily obtained materials and equipment. For applications where a precise length of fibre is required (such as biological uptake or toxicity studies), more precise methods have been developed. A cryogenic microtome (cryotome) protocol was reported by Cole et al. (276) This method involves freezing the fibres and precisely sectioning lengths. The authors engineered a customised cutting tool to produce a more uniform length of fibre. (270) In certain laundry wastewater specific studies, MP fibres have also been collected directly by washing polyester clothing and filtering the wash water. (53)

Other methods are available for non-fibrous MP preparation. Powdered plastic may be prepared by grinding supercooled plastic granules using a cryogrinding setup consisting of a stainless-steel ball-mill. This process can produce a uniform, fine powder, with particle size depending on the polymer type and grinding time. Polypropylene dispersions have been prepared by this method (277) and cryo-ground TWP, PS and PU MPs are utilised in experiments detailed in Chapter 6 of this thesis. An in situ sonication-based fragmentation method for PS, PET, and polylactic acid (PLA) has been reported to produce a sample of synthetic weathered fragments such as those found in the ocean. (278) To prepare isolated samples of microbeads, direct extraction from personal care products is possible. Facial scrubs can be used as a source for these beads (279) as in Chapter 6 of this thesis where PE is extracted for use in experiments.

4.1.2 Polyester fibre microplastic preparation

Commercial PET fibres with a length of 3 cm and diameter of 40 µm were purchased from Phoenix Fibres, UK. Fibres were then cut into short lengths using surgical stainless-steel scissors. The MP fibres were imaged by optical microscopy to determine their fibre length distribution (Section 4.1.3). Figure 4.1 shows the fibres as supplied (a, b) and after cutting (c, d). Using this simple method, MP fibres were prepared quickly and consistently offering a close representation of the microplastic fragments present in wastewater. (280)

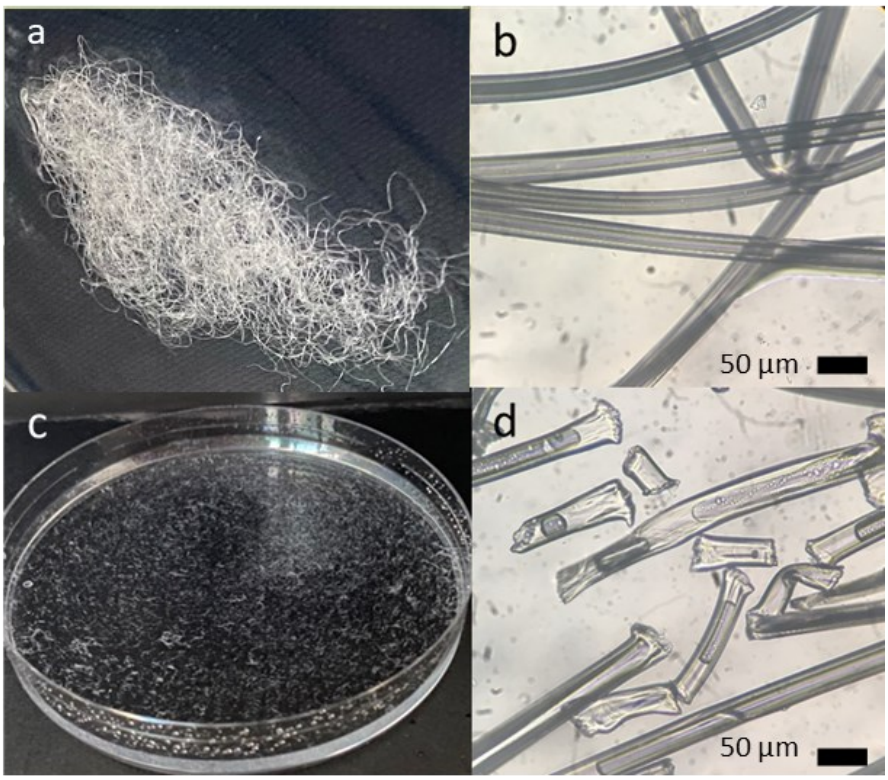

Figure 4.1 Polyester fibres **(a,b)** as supplied and **(c,d)** cut into short lengths with length distribution outlined in Section 4.1.3

One of the most commonly used methods to track MP degradation is mass loss. MPs are isolated from the water and their mass determined and compared to that before treatment as in Section 2.4.2.1. Mass loss measurement allows comparison of treatment efficacy to external data sets and is an important metric to measure degradation. The recovery of MP fibres from water is therefore important for the experiments presented in this thesis. In this way, material loss during the weighing procedure was minimised and controlled. Spike

recovery of pristine polyester fibres from ultrapure water and laundry wastewater was first considered. MP fibres were dispersed in water as shown in Figure 4.1 c. They were stirred for 5 minutes and then separated from the water by vacuum filtration through a pre-weighed 0.45 µm pore glass fibre filter and dried (105 ˚C, 30 min) prior to recording their mass and calculating the recovery. Various starting masses were considered to investigate the potential of the isolation method for different fibre concentrations in water (1.7 – 2280 mg L^{-1}). The data is presented in the appendix (Table A.1, Table A.2, Figure A.1) alongside standard deviation of each sample set. All samples were isolated from 300 mL working volume.

The spike recoveries for fibre masses of ~5 mg and above was >98%. However, the loss of material in experiments with a small starting mass represented a substantial relative mass loss of the sample with very large standard deviations. This method was therefore deemed unsuitable for testing small changes in mass of a fibre sample over time as required for long term degradation experiments. Instead, for these experiments, longer uncut fibres are used. Calibration of the recovery of 3 cm lengths of PET fibre from ultrapure water is presented in the appendix (Table A.3) and shows reduced experimental mass loss of material. The spike recovery of fibre masses of 1.5 mg was >96% as compared to 92.9% for cut fibres, indicating this method is better suited for reduced error in degradation experiments.

4.1.3 Fibre length distribution as a measure of degradation

Tracking the size and length of particles with optical microscopy can reveal decreases in the average size as a result of physical surface weathering or fragmentation. This may allow a measure of degradation during treatment without the reliance on complete material recovery as required for mass loss calculations. Sørensen et al. found that under UV degradation, polyester fibres did not show significant surface change but did fragment to a degree that was measurable with statistical significance. (166)

To explore MP fibre length distribution as an option for tracking polyester weathering, three weathering treatment conditions were applied for 6 h and optical micrographs of the resulting fibres compared to raw fibres as a control. Treatment was either photo-irradiation with UVC or UVC/H_2O_2 AOP using two levels of peroxide concentration (100 mg L^{-1} or 200 mg

L^{-1}) and the experimental setup shown in Figure 2.2 a. Representative micrographs from each sample are shown in Figure 4.2.

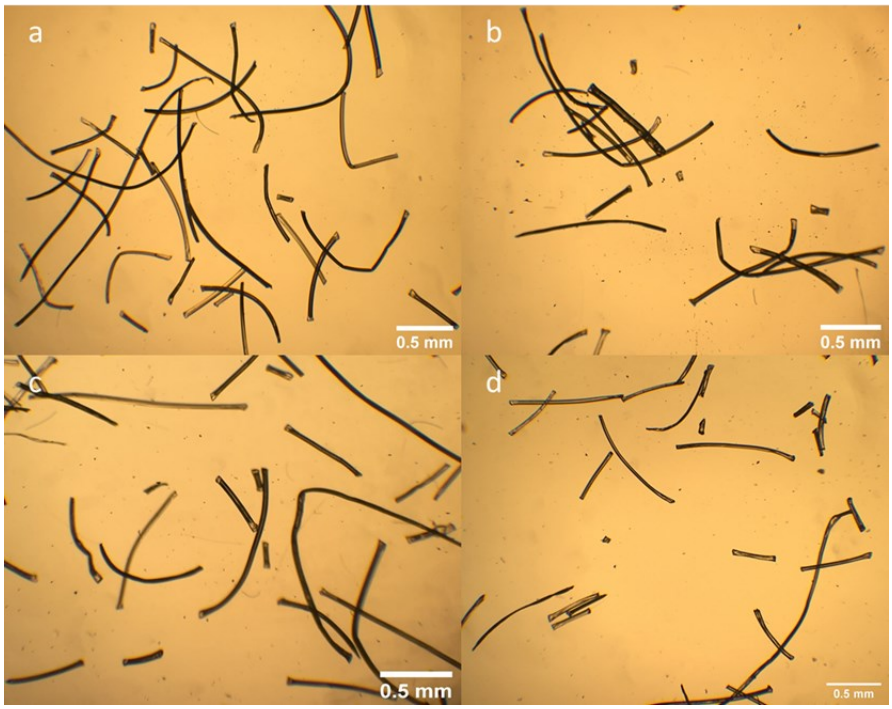

Figure 4.2 Representative optical micrographs showing polyester fibres at 4x magnification **a)** untreated polyester fibres **b)** UVC 6 h **c)** UVC/H_2O_2 (100 mg L^{-1}) 6 h **d)** UVC/H_2O_2 (200 mgL^{-1}) 6 h (31.8 mW cm^{-2} UVC irradiation, 16.7 mg L^{-1} initial fibre concentration)

A total of 550 fibres from each treatment type were measured with ImageJ analysis software, using the segmented line tool to measure arc length and fibre size determined by reference to a stage micrometer scale calibration. Figure 4.3 and Table 4.1 show the measured results.

Table 4.1 Average polyester fibre length measured by optical microscopy (n=550)

Treatment	Median fibre length	Mean fibre length
control	733	849
UVC	703	852
UVC/H_2O_2 100 mg L^{-1}	456	628
UVC/H_2O_2 200mg L^{-1}	556	695

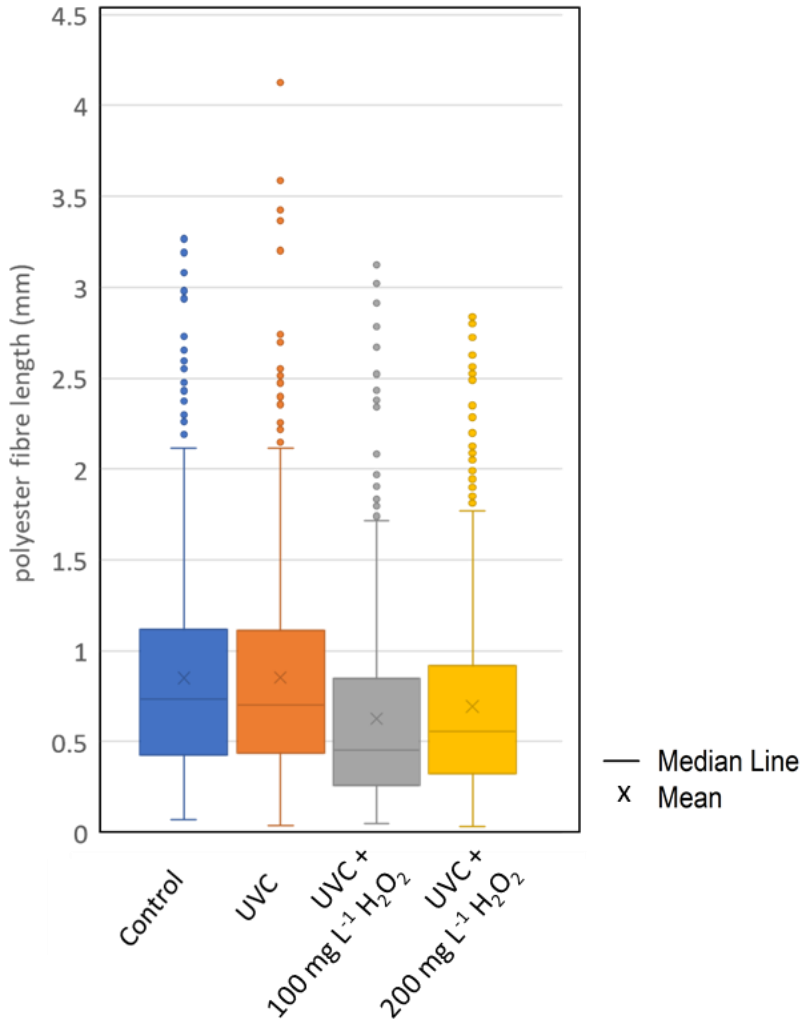

Figure 4.3 Distribution of MP fibre length after various treatment processes as measured by microscopy. The mean and median values are marked on the plot with outliers indicated by individual points on the graph (31.8 mW cm^{-2} UVC irradiation, 16.7 mg L^{-1} initial fibre concentration, n=550)

While the overall range of fibre lengths measured under each treatment remains largely unchanged, a trend in the average length towards shorter fibre lengths is evident for both UVC/H_2O_2 treatments. A t-test was performed to confirm the significance of decrease to length in the case of each UVC/H_2O_2 treatment (Appendix C). No statistically significant change was observed for the length of fibres treated with UVC only. The benefit of using average fibre length as a measure of degradation are a removal of reliance on experimental recovery of MP fibres from water after treatment. Material loss will still influence the result, but this is reduced by imaging a large number of fibres likely to provide a representative

measure of degradation. The limitations of this method are due to the magnification of the image and user measurement uncertainty. Fragments smaller than ~0.025 mm are not counted meaning a large number of very small fragments present in each sample are ignored by the measurement.

Due to the limitation at very short fibre lengths, the time-consuming nature of fibre length measurement. This option was not explored further for use within this chapter to track MP fibre degradation. MP sizing is revisited in Chapter 6, where the diameter of PE beads is used to show degradation.

4.2 Initial screening and selection of oxidation treatment

Selection of appropriate AOPs for initial investigation was based on literature review and preliminary experiments. As described in Section 1.3.6.2, a number of lab scale experiments reported in the literature have considered MP degradation by AOPs including both heterogeneous catalysis and homogeneous photo-chemical methods. AOPs selected for initial testing in this thesis were chosen based on a number of key criteria. Namely, appropriateness for wastewater treatment system application, simplicity and reproducibility of lab scale testing and novelty of their application to tackling MP pollution.

Heterogeneous photocatalysis was ruled out for initial testing. MP degradation was predominantly followed by mass loss in batch experiments at lab scale. Introduction of a solid catalyst complicates the experimental recovery of MPs by introducing an additional separation step and increasing the potential for experimental loss of material. This separation difficulty was not coupled with a clear increase in the efficiency of degradation as detailed in Section 1.3.6.2 , Table 1.1. AOPs involving solid catalysts were therefore avoided.

Photochemical AOPs offer a simple experimental procedure. Reagent concentrations can be easily monitored in solution and good mixing of MP with oxidising reagents is possible, increasing the potential for radicals to reach the MP surface. Treatment can be continuously carried out for extended time periods without the need for constant user monitoring as might be required for heterogeneous photocatalysis and, once complete, MPs can be readily

separated from the water by filtration. For these reasons, photochemical methods are the focus of the experimental work presented in this chapter.

The tested technologies should hold relevance for large scale application in WWTPs. Therefore, established oxidation systems with tried and tested technology typically used to target recalcitrant organic pollutants or pathogens in water were initially screened. Ozonation, UV photolysis, UV/H_2O_2, Fenton, photo-Fenton and electrochemical oxidation are commonly applied at scale and have been extensively studied for decades.(101, 281, 282) Novelty was a key consideration when selecting a treatment to study as the field of oxidation treatment of MP contaminated wastewater is relatively new and expanding rapidly. Based on the literature review, previously unexplored systems were considered for testing. UV photolysis and UV/H_2O_2 were selected for initial screening, the results of which are presented in this chapter. Emerging technologies such as ultrasound assisted, sulphate and peroxymonosulphate driven oxidation are explored in Chapter 5.

4.3 Removal of polyester fibre microplastics from wastewater using a UVC/H_2O_2 oxidation process

The aim of this study is to investigate the removal of MP fibres from laundry wastewater using a UVC/H_2O_2 treatment for the first time. The effect of the treatment with varied operational parameters like H_2O_2 concentration, UV dose and treatment time on the physical and chemical properties of PET fibres was studied. Analytical and microscopy methods were used to monitor water quality and changes on the MPs surface and of their chemical composition during treatment.

4.3.1 Background

The general challenge and scale of MP polyester fibre pollution is outlined in detail in Section 1 which sets out the reasons for selecting this target wastewater for experiments presented in this section. Laundry wastewater contains MPs released during the washing of synthetic fabrics and is a significant source of pollution into WWTPs. A number of studies have described the removal of organic matter and micro-pollutants from this target wastewater

using AOPs and these are reviewed in detail elsewhere. (283) Laundry water contains a high concentration of surfactants and soap additives, alongside organic contaminants. Specific to hospital laundry wastewater, pharmaceuticals, pathogens and other trace organic micro-pollutants are also present. Despite this complex composition, the chemical oxygen demand of hospital laundry wastewater treated with UV/H_2O_2 was completely removed in 2 h of treatment in a study by Zotesso et al., showing that this class of AOP can feasibly be applied. (284) Prior to this study, MP contamination present in laundry wastewater has not been targeted with AOPs in the same way.

Exposure to UV radiation and atmospheric oxygen slowly leads to fragmentation and eventual natural attenuation of plastic. This mechanism has been widely studied for plastic debris floating on water exposed to sunlight (143, 146, 285) as well as in the polymer industry where the aim is generally to avoid plastic ageing by a similar mechanism (147, 286). By artificially accelerating this weathering process, oxidation may become a feasible method to remove MPs from water during treatment. AOPs utilising ultraviolet (both UVA and UVC) radiation have been successfully applied in treatment of wastewater containing biologically recalcitrant pollutants (99, 100, 287, 288) and have the benefit of oxidising organic pollutants to their mineral components (commonly CO_2 and H_2O) rather than transferring or concentrating them into a new waste stream such as solid waste by filtration. (101) Many WWTPs are already or could be easily equipped with high intensity 254 nm wavelength UVC lamps, thus avoiding the need for complete process overhaul. It is important to note that despite fragmentation and loss of MP mass, the generation of smaller fragments and NPs must be considered within AOP systems. Consideration of these fragments is made in Section 4.3.3.2

Recently, the first report of an AOP method for degradation of MP fibres in water used TiO_2 photocatalysis and achieved 97% mass loss from polyamide after 48 h of treatment under UVC irradiation using a slurry of 100 mg L^{-1} solid catalyst. (111) The authors showed that polyamide degradation can be followed with microscopy and spectroscopic techniques. The use of UVC/H_2O_2 treatment on MPs in wastewater has not been reported. The removal of polyester MP fibres from water or real wastewater with any AOP has also not been studied prior to this work despite this polymer type and morphology representing a significant proportion of the MPs identified in real treatment effluent. The work presented within this

chapter fills this research gap and offers new insight into the potential for AOPs to remove MP pollution from wastewater.

4.3.2 Materials and methods

The experimental treatment setup is described fully in Section 2.3 and analytical methods are outlined in full in Section 2.4. Polyethylene terephthalate fibres (PET) with a diameter of approximately 40 µm (Phoenix Fibres, UK) were used as supplied in rough lengths of 3 cm. In a typical experiment, the fibre concentration in the water was 16.7 mg L^{-1}. Appropriate volumes of hydrogen peroxide solution 35 wt. % (Sigma Aldrich) were added to the solution by micro pipette and the final H_2O_2 concentration confirmed with peroxide test strips (Quantofix). Laundry wastewater was collected from a Scottish hospital's laundry store. This wastewater was pre-treated by sock filtration and thermal disinfection prior to collection. It was stored in sealed bottles at 4 ˚C. The wastewater was left to settle and the appropriate volumes of the supernatant liquid were used in order to avoid transfer of settled solids. The collected wastewater samples had a recorded pH of 7.78, COD of 514 ± 3 mg L^{-1}, BOD of 84 ± 3 mg L^{-1}, total suspended solids 45.6 ± 8.7 mg L^{-1} (supernatant) and 463.3 ± 15.2 mg L^{-1} (mixed bulk), turbidity 114 ± 15 NTU, total alkalinity of 700 mg $CaCO_3$ L^{-1} and a conductivity of 1230 µS cm^{-1}.

Unless otherwise stated, experiments were conducted using an immersed lamp reactor shown in Figure 2.2 a. The temperature was kept constant at 18 ± 1 ˚C during treatment. Long-term (48 h) experiments were conducted in a top-down reactor shown in Figure 2.2 b with a working volume of 50 mL and at a temperature of 31 ± 4˚C. Fresh aliquots of H_2O_2 solution were added by micropipette every 60 min when required due to oxidant consumption and the mass of fibres was tracked by filtration of the entire working volume of each sample at designated time points.

Scanning electron microscopy (SEM) was used to image the surface of the fibres and atomic force microscopy (AFM) was employed to investigate the small-scale changes in surface roughness of the fibres. Using FTIR spectra, the CI for polyester fibres was calculated. The carbonyl peak was defined as the area under the graph between 1560 - 1753 cm^{-1} and the

reference peak chosen was 1360-1420 cm^{-1} which is attributed to an aromatic C-C stretching and ring CH in-plane bending. (181) The intensity of this reference is not expected to be altered as a result of oxidation of the polymer surface (196) allowing the CI to be used as a measure of relative surface oxidation between fibre samples. The chemical oxygen demand (COD) was measured by means of the potassium dichromate standard method.

To determine the need for peroxide replenishment, the consumption of peroxide under UVC irradiation in the immersion reactor are provided in Figure 4.4. H_2O_2 concentration was measured using peroxide test strips (Quantofix with ranges 1-150 mg L^{-1} and 50-1000 mg L^{-1}). Based on the rate of consumption, replenishment of peroxide every 60 minutes was employed in experiments, unless stated otherwise.

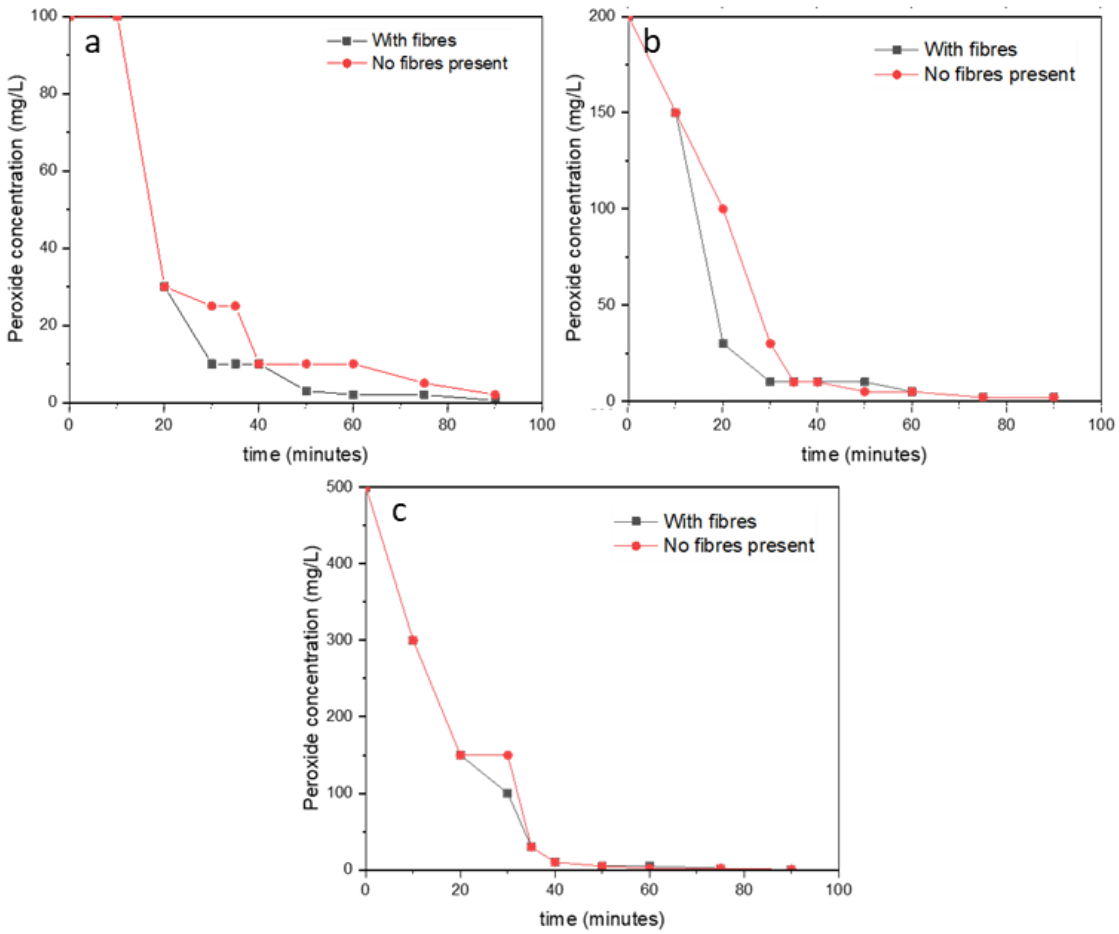

Figure 4.4 Concentration change of H_2O_2 in DI water exposed to 31.8 mW cm^{-2} UVC irradiation with starting concentration **a)** 100 mg L^{-1}, **b)** 200 mg L^{-1} and **c)** 500 mg L^{-1} (working volume 300 mL)

4.3.3 Results and discussion

4.3.3.1 Feasibility of UV/H_2O_2 treatment for MP fibre degradation

To determine the removal efficiency of polyester fibres from water, experiments were carried out in the presence or absence of irradiation and H_2O_2, and the results are shown in Figure 4.5. Initial polyester concentrations of 16.7 mg L^{-1} were selected to ensure reliable recovery during the mass measurement as outlined in Section 4.1.2. At this stage, mass loss is used as a measure of removal for triplicate samples and a control experiment (no treatment) was also performed. The standard deviation of each sample group is indicated by the error bars.

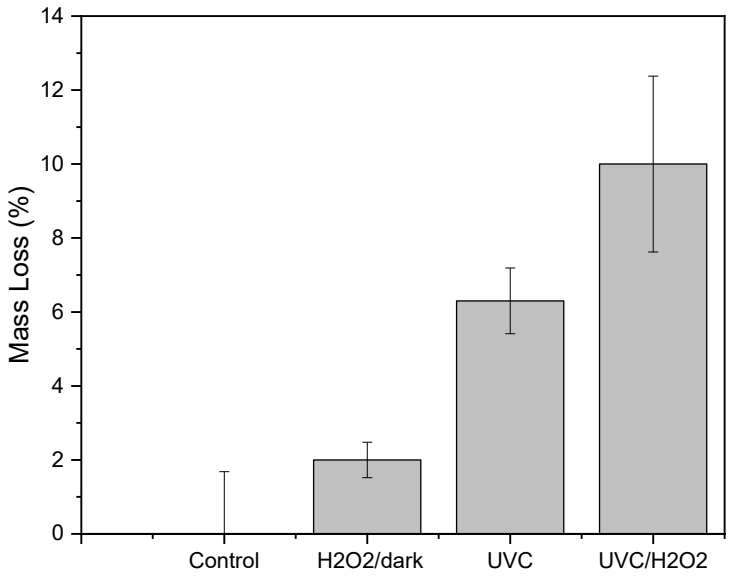

Figure 4.5 Mass loss performance after 9 h of treatment in DI water. Initial concentration of polyester fibres is 16.7 mg L^{-1}, H_2O_2 concentration was 500 mg L^{-1} and UVC dose was 129.6 J cm^{-2}.

The control experiment of fibres immersed in DI water with no light exposure showed no mass loss after 9 h. In comparison, UVC photo-degradation alone reduced the mass of fibres by 6.3%, chemical oxidation in a solution of H_2O_2 without UV irradiation reduced the mass by 2% and the combined photochemical advanced oxidation resulted in the largest mass loss of 10%. Small amounts of MP may be lost through the fibre pores might can account for the small mass loss observed in the H_2O_2/dark system. This enhanced removal efficiency of the

UVC/H_2O_2 process can be attributed to the synergetic effect of the combined processes. The photochemical degradation mechanism of UVC/H_2O_2 is expected to proceed by radical oxidation mainly. The treatment has a strong oxidising potential due to the creation of large number of hydroxyl radicals in solution which are formed by photolysis of the O-O bond in hydrogen peroxide. (44) The powerful oxidising capability of the hydroxyl radical (2.7 V and 1.8 V in acidic and alkaline media respectively) (34) and the formation of a large number of active hydroxyl radicals in solution during AOP treatment can degrade polyester fibres. In the absence of UV irradiation, H_2O_2 does not split into radicals and there is no initiation of the oxidative degradation mechanism. This indicates that the formed hydroxyl radicals contribute to the degradation of polyester rather than H_2O_2 directly. Direct UVC photolysis of polyester proceeds via an alternative initiation step of bond cleavage of the polymer backbone, leading to the formation of radicals via a Norrish type I or type II mechanism as detailed in Section 2.3. (45) Within a lab scale photo-reactor, a combination of hydroxyl initiated radical degradation and direct photo-degradation is expected to contribute to MP degradation.

The loss of mass as a result of each treatment was considered alongside the physical changes of the fibre surface. Figure 4.6 shows SEM images of representative fibres from each process after 9 h treatment.

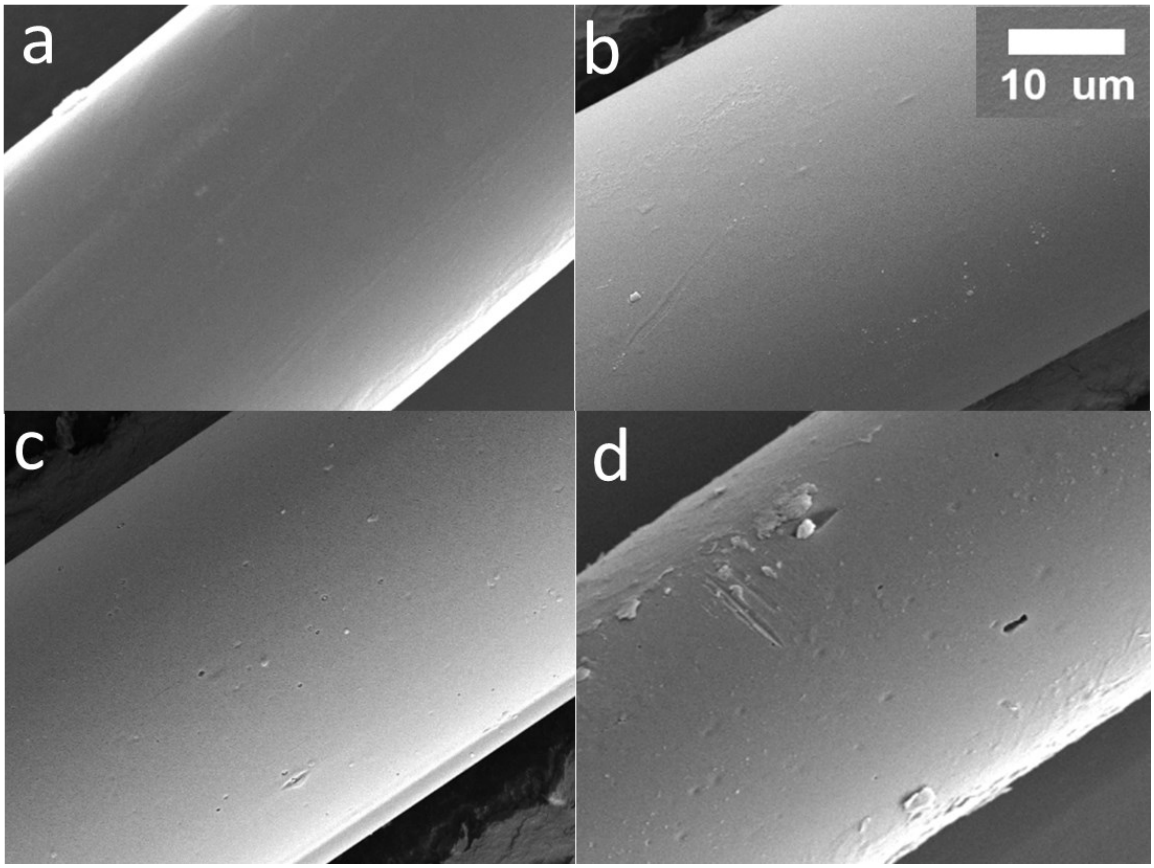

Figure 4.6 1000x magnification SEM images of polyester fibres treated for 9 h with **(a)** Control experiment **(b)** H_2O_2/dark **(c)** UVC **(d)** UVC/H_2O_2.

The control fibres (Figure 4.6 a) and the fibres exposed only to H_2O_2 in the dark (Figure 4.6 b) present a smooth and uniform surface with no clear evidence of physical change. The surface of fibres exposed to UVC (Figure 4.6 c) is pitted and rough in comparison and small holes and cracks are visible. These features are also evident in the image of fibres treated by UVC/H_2O_2 (Figure 4.6 d) with a clearly roughened surface, larger holes and increased amount of debris present on the fibre. The presence of pitting and hole formation indicates surface degradation of the polymer and has been observed in other AOP treatment methods for plastics. Tofa et al. (109) observed the formation of small holes and surface cracks on polyethylene films by optical microscopy and this was attributed to attack by hydroxyl radicals. Similar features have been observed in AOP degradation of polyamide fibres treated with TiO_2/UV (111) as well as a selection of polymers (polystyrene, polyethylene, polyvinyl chloride and PET) upon exposure to UV. (289) In addition, debris visible on the surface of the fibres in Figure 4.6 d may be small fragments of plastic released during the degradation process. Polyester fibres

have been shown to produce a large number of small fragments after extended exposure over 2 months to UV, primarily due to the fibres breaking down into shorter length segments (166). These initial degradation experiments show that a UVC/H_2O_2 based AOP can reduce the bulk mass of polyester fibres in water, more rapidly than the application of UVC photolysis or H_2O_2 alone. In order to apply such a method at scale, significant improvements to the rate of removal are needed. Therefore, a number of parameters were varied in consequent experiments to understand their impact on degradation efficiency of the UVC/H_2O_2 oxidation process.

4.3.3.2 Effect of UV dose and intensity

The effect of UV intensity, of 4.0 and 31.8 mW cm^{-2} (corresponding to a UV dose of 129.6 and 1030 J cm^{-2} over a 9 h treatment), was studied using two lamps of differing UV power outputs of 11 W and 55 W, respectively. Results are shown in Figure 4.7 a where mass loss is plotted against treatment time for each level of UV intensity applied.

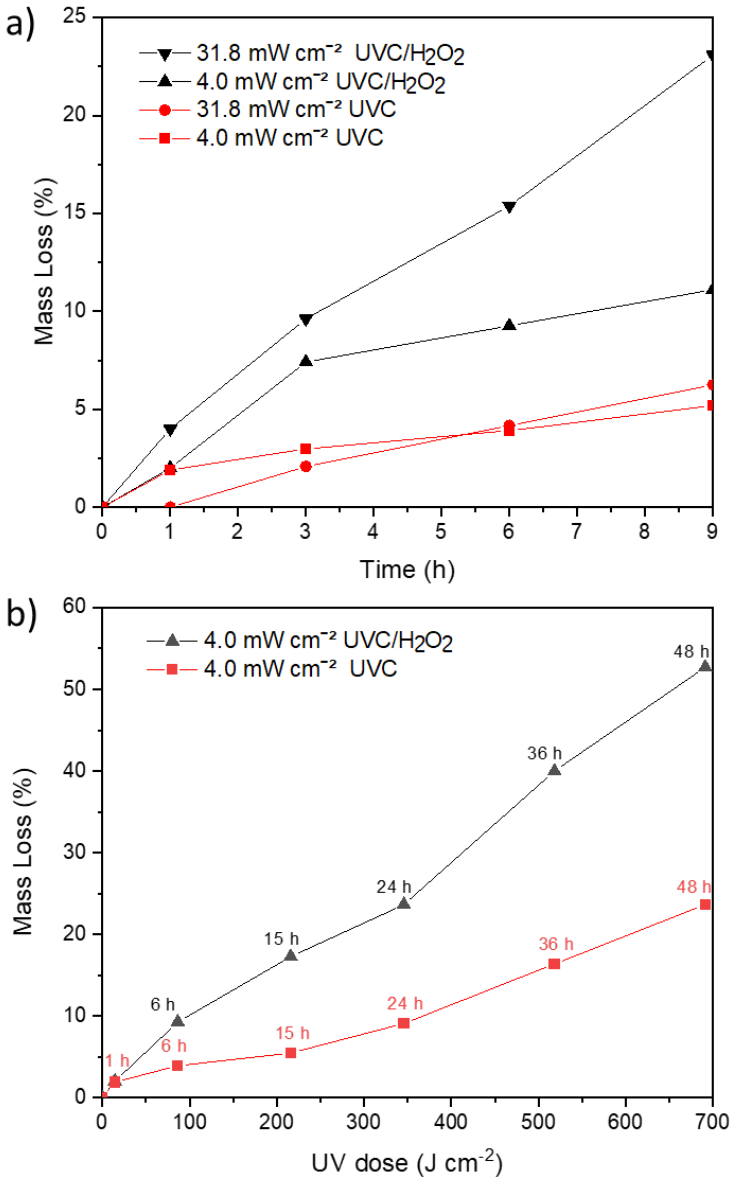

Figure 4.7 a) The effect of UV irradiance as a function of time against mass loss of MPs with UVC and UVC/H_2O_2 treatments **b)** Degradation of polyester fibres with increasing total applied UV dose. In each case, H_2O_2 concentration is 500 mg L^{-1} in DI water, starting fibre concentration of 16.7 mg L^{-1}.

For a UV/H_2O_2 treatment, a higher intensity of UV irradiation increases the rate of hydroxyl radical generation and therefore is expected to increase the rate of mass loss. Figure 4.7 a shows that after 9 h of UVC treatment, fibre mass loss was 5.2% and 6.3% for low and high intensity lamps respectively, indicating that an increase in radiation intensity alone does not significantly affect the rate of MP removal via direct UVC photo-degradation. A comparatively

high rate of mass loss is observed during UVC/H_2O_2 treatment where mass loss was 11.1% and 23.1% under 4 mW cm^{-2} and 31.8 mWcm^{-2} irradiation, respectively. A higher dose of UV does increase the rate of MP removal here, which can be attributed to the increased number of hydroxyl radicals being generated in the water.

For the low and high irradiation intensity systems, an energy demand of 0.12 kWh m^{-3} and 0.954 kWh m^{-3} for 9 h treatment respectively. Tertiary filtration demand ranges from $7.4 \cdot 10^{-3}$ to $2.7 \cdot 10^{-3}$ kWh m^{-3}, UV disinfection typically uses between 0.045 and 0.11 kWh m-^{3}, and mechanical utilisation for the dosage of chemicals (e.g., chlorinated reagents, aluminium or iron salts) expends $9.0 \cdot 10^{-3}$ - 0.015 kWh m^{-3}(290). Significant improvements in efficiency in terms of energy use are required for this method to be economic at scale.

Experiments over varying timescales allowed the total UV dose applied to be varied in a large range while keeping the UV intensity constant. By increasing the treatment time to 48 h, a total dose 691.2 J cm^{-2} UV could be delivered using a 4.0 mW cm^{-2} intensity UV lamp in the top-down reactor setup shown in Figure 2.2 b. In a real treatment facility, the same effect can be achieved by adjusting the residence time of wastewater in the photo-reactor without requiring an increase in the number or power of lamps. Figure 4.7 b shows the resulting mass loss as plotted against the total dose of UVC radiation received. Under each treatment condition, the mass loss of polyester fibres increases almost linearly over the 48 h treatment as total UV dose applied increases to 691.2 J cm^{-2} with the most effective combined UVC/H_2O_2 process achieving a final mass loss of 52.7% and the UVC treatment alone resulting in 23.6% mass loss. As degradation occurs at the surface of fibres, the rate may be limited by availability of the surface area of fibres to UV light and to hydroxyl radicals in solution rather than the direct effect of UV irradiation. The two sets of results in Figure 4.7 indicate that increasing residency time within the photocatalytic reactor is a more effective method for improving efficiency than increasing UV irradiance. Increased treatment time allows the surface to be progressively degraded and as a result, new polymer surface is exposed to the hydroxyl radicals, allowing the mass loss to progress.

The effect of treatment on the surface of the fibres was probed in detail using surface characterisation methods of SEM and FTIR. For fibres treated over long timescales, the

number of holes and pits evident on the fibre surface increased as shown in Figure 4.8 which presents SEM images of polyester fibres exposed to UVC only as well as those exposed to the UV/H_2O_2 at varying time intervals.

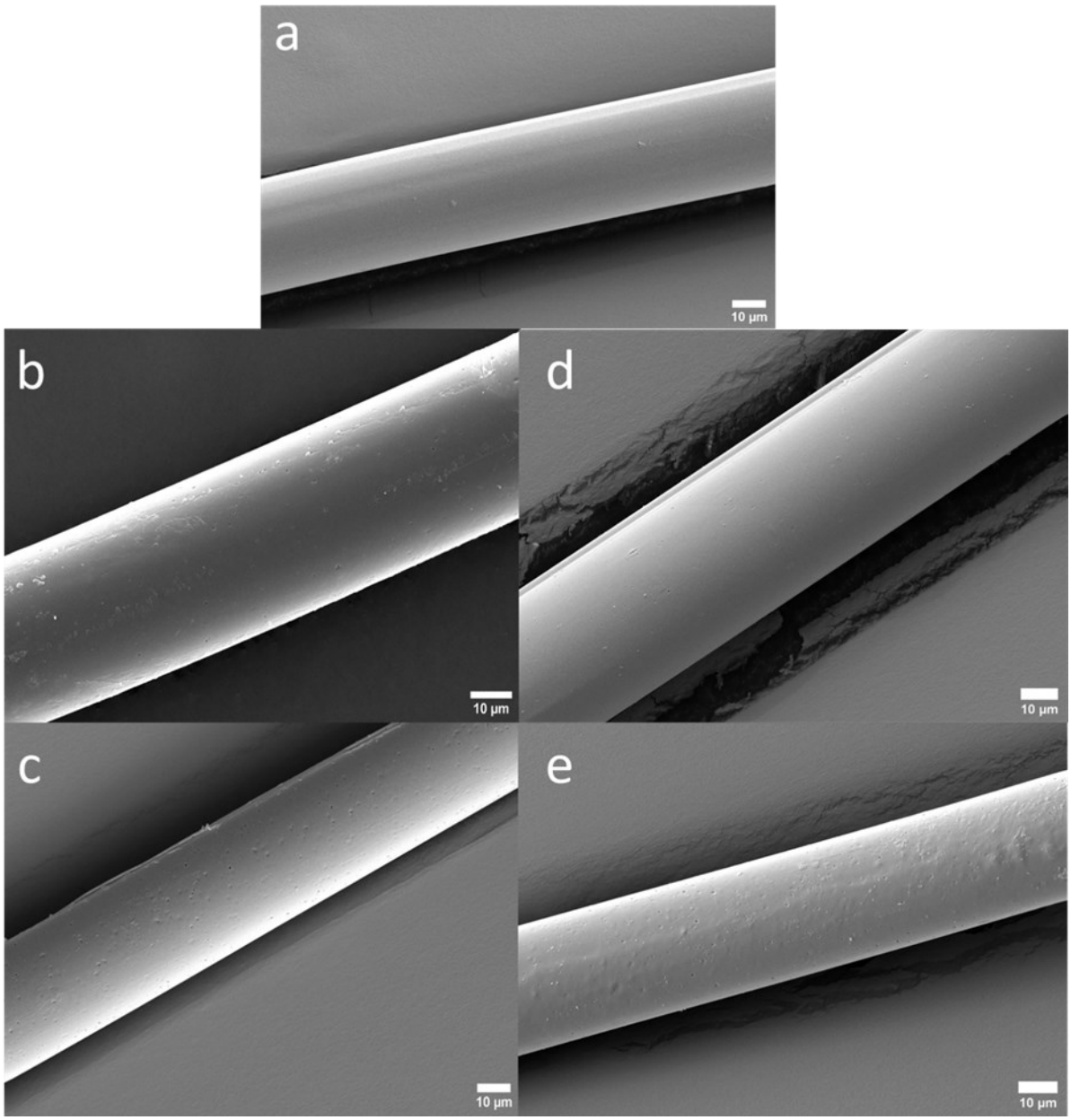

Figure 4.8 1000x magnification SEM images of polyester fibres at varying times of treatment with **(a)** control experiment **(b)** UVC/H_2O_2 24 h **(c)** UVC/H_2O_2 48 h (**d)** UVC 24 h **(e)** UVC 48 h (where applicable H_2O_2 concentration of 500 mg L^{-1}, starting fibre concentration of 16.7 mg L^{-1}, UVC irradiance: 4.0 mW cm^{-2}).

As compared to the virgin polyester fibres (Figure 4.8 a), all treated samples show surface changes with the development of pitting and micro crack formation. SEM images taken after 24 h of treatment with UVC/H_2O_2 (Figure 4.8 b) and UVC (Figure 4.8 d) methods both show evidence of surface degradation in the form of shallow holes and pitting. The number of these features then increases after 48 h treatment as more of the fibre surface is pitted (Figures 4.8 c and 4.8 e). One impact of the surface roughness changing is an increased surface area of exposed polymer. It is possible that as degradation proceeds further, the rate of mass loss may be increased due to increased availability of reaction sites.

Lateral cracking of the fibres was observed as well as delamination of fibre strands after 48 h of treatment. These features indicate the reduced physical strength of the fibre which can lead to fragmentation. It is by this fragmentation mechanism that the removal of MPs is expected to proceed with small nanoplastics and microplastics breaking away from the bulk fibre. This fragmentation behaviour has been directly observed in oxidative degradation of PET pellets exposed to UV radiation over 112 days. (291) In addition to fragmentation, Gewert et al. identified likely chain scission products in the reaction water of polyester pellets exposed to UV over 5 days by liquid chromatography.(285) The physical changes observed in fibre samples by SEM suggest that small fragments of plastic are released to the water during treatment by cracking and fragmentation of the bulk fibre. These observations can also be linked to the decrease in average fibre length for UVC/H_2O_2 treated PET compared to UVC and control samples presented in Section 4.1.3.

The features of plastic degradation observed in SEM images provide information on the visible features only. It is important to be able to examine in more detail the change in surface texture of polymers exposed to oxidative treatment to better understand the potential impact on materials properties and fragmentation behaviour. AFM imaging is an attractive option to provide new and detailed information to this end such as the depth of holes and cracks in the surface and changes to the mechanical properties of the polymer. Figure 4.9 a-d show sections of treated polyester fibre with lateral features resembling cracks (dotted red circle) and holes visible across the surface nd may be compared to the raw untreated fibre surface imaged in Figure 6.14. In the images, dark regions indicate indentations in the surface while bright white regions indicate raised sections of the surface or debris. The presence of

cracking in a direction perpendicular to the fibre length is observed in Figure 4.9 a and c where dark indented features cross the width of the fibres. These cracks are expected to drastically reduce tensile strength and enable easy fragmentation of the fibre into shorter lengths. Surface holes and pits are clearly visible as dark regions in Figure 4.9 b and 4.9 d. The surface shown in Figure 4.9 d is also mapped in 3D in Figure 4.10. The presence of such surface defects will likely also have a detrimental effect on the overall strength of the fibres in addition to contributing to the loss of mass. The presence of holes and lateral cracks has been observed directly in long term (10 month) exposure of polyester fibres to UV. (280)

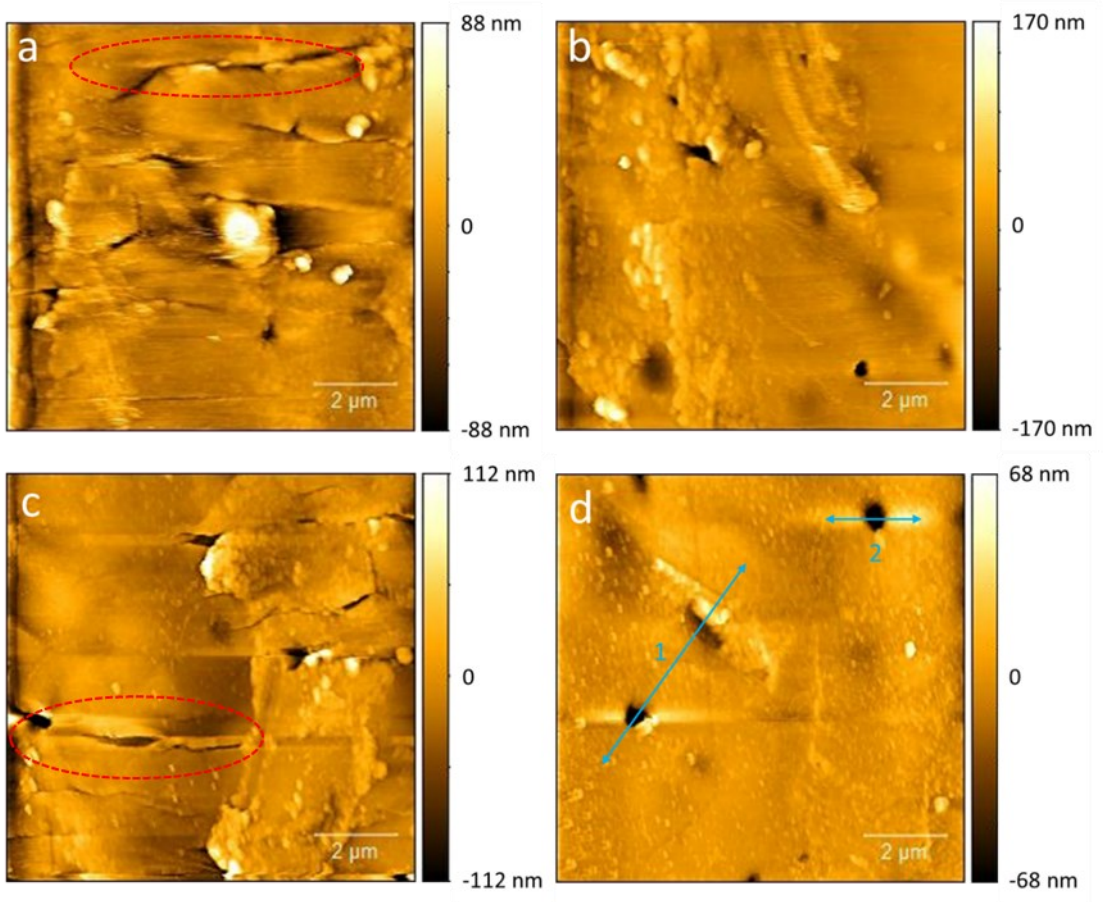

Figure 4.9 (a)-(d) AFM height images of polyester fibre surface treated with UVC/H_2O_2 for 48 h and displaying typical degradation features (H_2O_2 concentration of 500 mg L^{-1}, starting fibre concentration of 16.7 mg L^{-1}, UVC irradiance: 4.0 mW cm^{-2}).

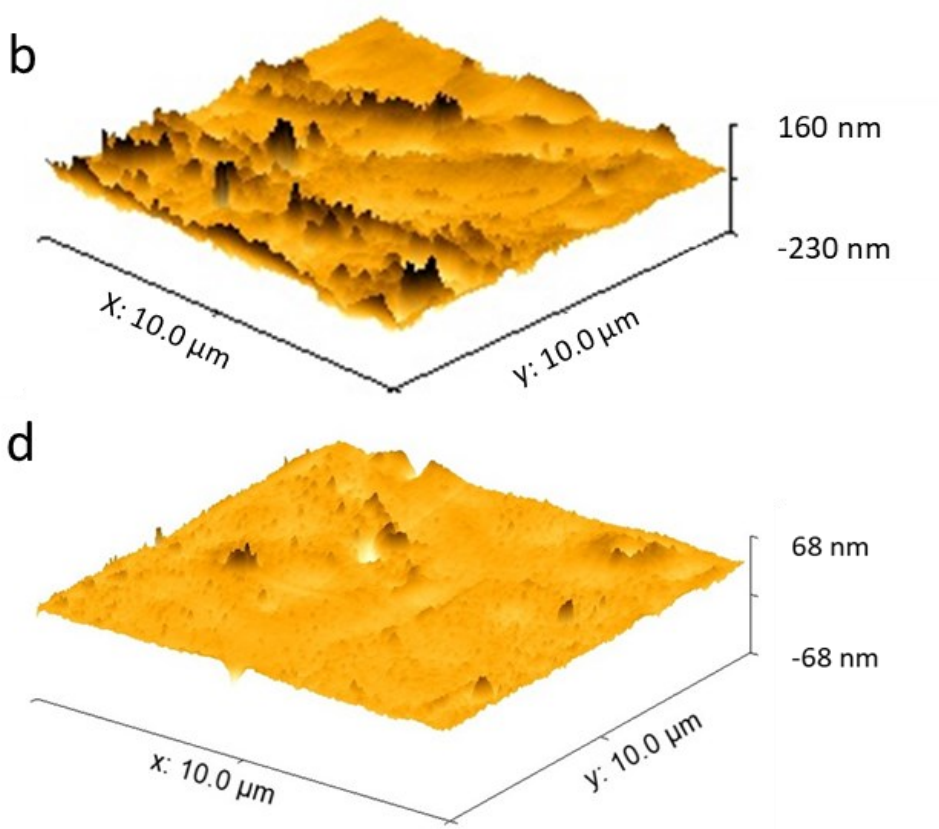

Figure 4.10 Surface map of polyester fibre surface treated with UVC/H_2O_2 for 48 h (H_2O_2 concentration of 500 mg L^{-1}, starting fibre concentration of 16.7 mg L^{-1}, UVC irradiance: 4.0 mW cm^{-2}).

The depth of the surface holes was estimated by recording height profiles; two such profiles taken along lines 1 and 2, marked on Figure 4.9 d, are plotted below in Figure 4.11. The holes were determined to have depths in the range of 10 to 100 nm. These number and depth of surface degradation features could be tracked accurately by this AFM technique, offering a new way to follow MP degradation in water. It is expected that as degradation progresses, the profile of the surface will continue to evolve with more holes, cracks and pits visible.

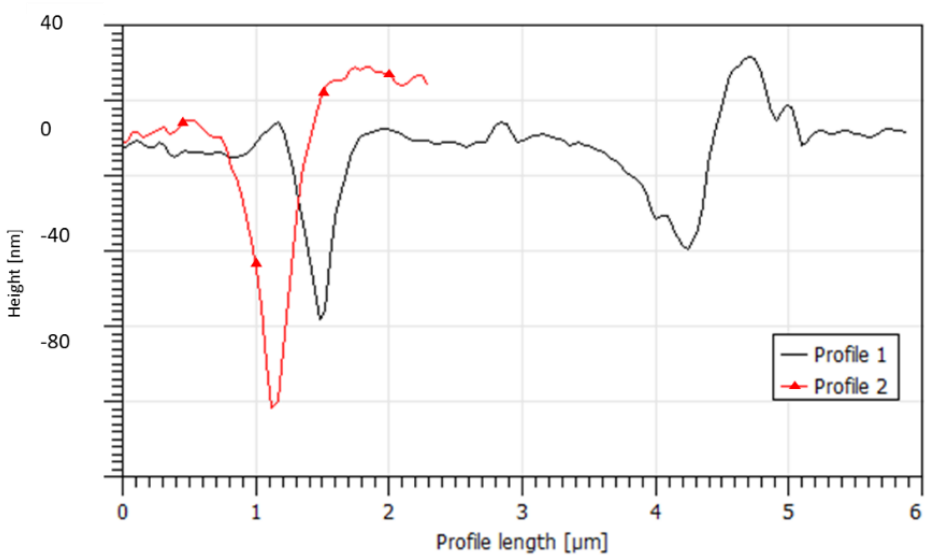

Figure 4.11 Height profile along lines 1 and 2 as shown in Figure 4.9 d (measured from left to right) of UVC/H_2O_2 treated polyester fibre surface confirming the presence of shallow surface holes.

By considering the change in chemical oxygen demand (COD) of the water during treatment, information on the release of small fragments or soluble components from the bulk fibre can be gained. (111) No measurable increase in COD was observed when photo-oxidation (UVC) alone was applied at 31.8 mW cm^{-2} irradiation intensity; whereas a COD of 7.0 ± 3.6 mg L^{-1} was recorded when MPs were treated under 4.0 mW cm^{-2} UV irradiance. After UVC/H_2O_2 treatment, the water had a residual COD of 11.3 ± 1.6 mg L^{-1} and 6.0 ± 1.4 mg L^{-1} after 9 h under 31.8 mW cm^{-2} and 4.0 mW cm^{-2} intensity irradiance, respectively. The COD of the water in control experiments (polyester fibres in DI water in the dark) was 1.4 ± 1.2 mg L^{-1} and the fibre loaded water samples at the start of treatment had a COD of 1.9 ± 1.8 mg L^{-1} for UVC/H_2O_2 treatment. The COD results are also presented in Table A. 5. The results indicate that as treatment progresses, soluble organics or plastic fragments are released to the water, and slightly increase the COD. This is possible as secondary nanoplastic fragments present in the water from the degradation of fibres may permeate the 1.6 µm pores of the filters. At high UV flux in the UVC only case, the rate of removal of these fragments and organics by direct degradation exceeds their production, therefore resulting in a lower measured COD. The formation of nanoplastics is supported by the changes in physical appearance of the fibre surface discussed in Section 4.3.3.1 with pitting and cracking extent progressing with

treatment time and evidence of increased debris on the fibre surface.. The observed trend in COD is in contrast to Lee et al. (111) who noted the lowest COD of the treated water for a TiO_2-UV based AOP treatment compared to UV photo oxidation of polyamide fibres. Degradation of polyester in water can release a range of fragments and free chemicals that can contribute to the COD of the water. (166, 285) In a study by Sørensen et al., high-resolution mass spectrometry analysis identified carboxylic acid monomer units and short chain oligomers after 5 days of UV degradation. (166) Further investigation of the presence of such degradation products is an interesting route and may yield useful information into the chemical degradation mechanism of fibres under harsh advanced oxidation treatment conditions. Analysis of nanoplastic degradation products via advanced analytical techniques such as dynamic light scattering and nano-gravimetric analysis may yield a detailed understanding of the fragmentation mechanism at the nano-scale. (21, 292)

4.3.3.3 Effect of initial fibre concentration

To determine whether the rate of mass loss at a given peroxide concentration and UV irradiance is dependent on the initial concentration of fibre present in the reactor, the starting polyester mass was varied (Figure 4.12). This series of experiments can also serve as a first indication of the scale effect on this treatment method which is an important consideration for real world applicability. MP degradation increases from 8.4% to 23.1% when the plastic load is 8.0 mg L^{-1} and 17.3 mg L^{-1}, respectively. This may be attributed to the limited availability of the lower (i.e. 8 mg L^{-1}) fibre surface to interact with the generated radicals in the solution. In the case of the highest plastic load (32.0 mg L^{-1}) essayed, the MPs degradation rate is reduced compared to that of 17.3 mg L^{-1}. In this case, the ratio of hydroxyl radicals to fibre mass may be reduced to a level which impedes degradation or the degradation rate may be limited by the penetration of UV light to the surface. It is known that water with a high level of suspended solids (in this case MP fibres) results in reduced efficiency of AOP methods which rely on radical formation in close proximity to the target pollutant. (293)

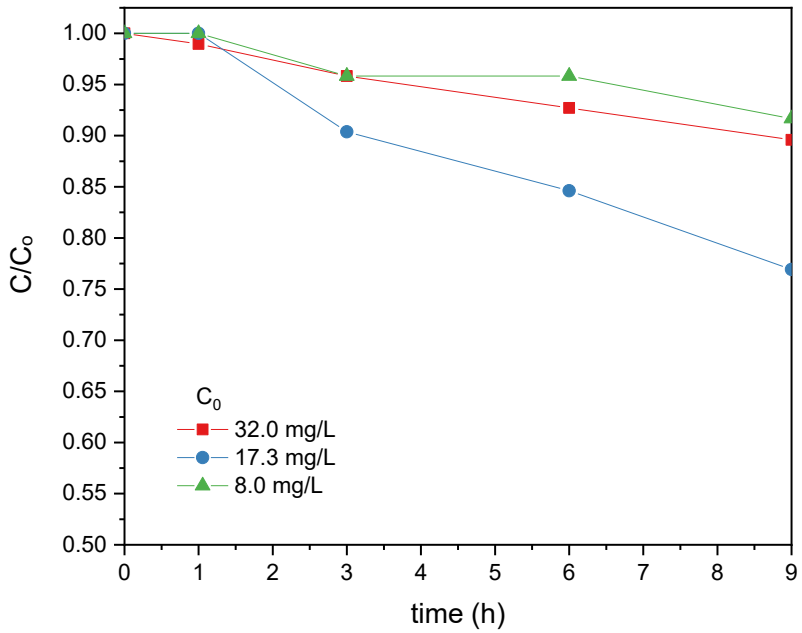

Figure 4.12 Comparison of polyester fibre concentration decrease over time with varied starting concentrations (UVC/H_2O_2 treatment parameters: 31.8 mW cm^{-2} UVC, 500 mg L^{-1} H_2O_2 treatment over 9 h).

The kinetics of the UVC/H_2O_2 process are complex due to the involvement of a large number of radical reactions and intermediates. A full kinetic model has been developed previously for the degradation of several organic pollutants by UVC/H_2O_2. (293, 294) In the case of polyester fibres, the rate of mass loss can be reasonably described by a pseudo first order kinetic process. The apparent kinetic rate constants are 0.0093, 0.0133 and 0.0073 h^{-1} for initial concentrations of 8.0, 17.3 and 32.0 mg L^{-1}, respectively and are presented graphically in the appendices. For consideration in real wastewater systems, the actual environmental concentration of MPs may differ significantly from the values selected in these experiments. A range of 1-7216 particles per litre in raw effluent was estimated (65) although limited information is available on the mass of MPs in these systems.

4.3.3.4 Effect of H_2O_2 concentration

The concentration of H_2O_2 in the reactor was varied within the range 0 - 2000 mg L^{-1} and the mass loss over 9 h of treatment was monitored as shown in Figure 4.13 a. Where 0 mg L^{-1}

H_2O_2 is added, degradation proceeds by direct photodegradation. Hydrogen peroxide concentration was maintained at the target value by regular addition of appropriate amounts of H_2O_2 solution every 60 min. The mass loss after 9 h of treatment is plotted as a function of H_2O_2 concentration in Figure 4.13 b. In all cases the UVC irradiance was kept constant at 31.8 mW cm^{-2}.

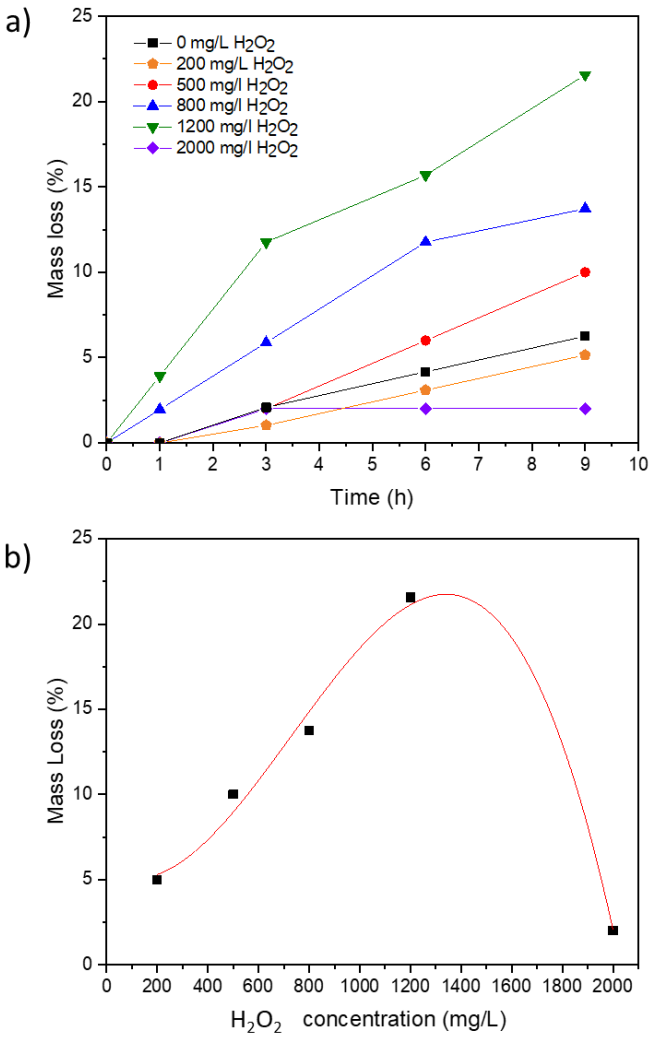

Figure 4.13 (a) Effect of varied H_2O_2 concentration on polyester fibre mass loss **(b)** Polyester fibre mass loss recorded at 9 h UVC/H_2O_2 and the effect of peroxide concentration. In all cases, the starting fibre concentration is 16.7 mg L^{-1}, UVC irradiance 31.8 mW cm^{-2}.

As the H_2O_2 concentration is increased from 200 to 1200 mg L^{-1}, the rate of mass loss at 9 h increases close to linearly to a maximum degradation of 21.6% observed at a dose of 1200 mg L^{-1}, as shown in Figure 4.13 b. A significantly lower mass loss of just 2.0% after 9 h is recorded at the highest 2000 mg L^{-1} H_2O_2 concentration and can be attributed to the

scavenging effect that removes active hydroxyl radicals from solution, thereby reducing the efficiency of H_2O_2-mediated AOPs. (295) For a given photocatalytic reactor geometry and UV dose, the concentration of H_2O_2 must be carefully optimised in order to maximise the availability of hydroxyl radicals.

To understand the chemical oxidation of the polyester fibre surface, FTIR spectra were gathered for pristine and treated fibres. The variation in mass loss as well as the physical appearance of the surface between different treatment methods is expected to be associated to a difference in the relative abundance of oxygen containing functional groups on the surface. The control experiment (no treatment applied) was used to define the baseline. Characteristic peaks are fully described in Section 2.4.1.1. The carbonyl index (CI) was calculated and the results for the polyester fibre samples are tabulated in Table 4.2. FTIR spectra of all samples used in the calculation are included in the appendices as Figures A.2-A.8.

Table 4.2 Chemical characterisation of MP fibres and calculated kinetic parameters (starting fibre concentration of 16.7 mg L^{-1}, UVC irradiance 31.8 mW cm^{-2}).

Treatment	CI of fibres	increase relative to control (%)	Mass loss of fibres at 9 h (%)	K_{app} (h^{-1})	$t_{1/2}$ (h)
Control Experiment	6.11	-	0.0	-	-
H_2O_2/dark (500 mg L^{-1} H_2O_2)	6.09	-0.3	2.0	0.0014	495.1
UVC	6.20	1.5	6.3	0.0075	92.4
UVC/H_2O_2 (500 mg L^{-1} H_2O_2)	6.19	1.3	10.0	0.0122	56.8
UVC/H_2O_2 (800 mg L^{-1} H_2O_2)	6.73	10.1	13.7	0.0171	40.5
UVC/H_2O_2 (1200 mg L^{-1} H_2O_2)	6.69	9.5	21.6	0.0260	26.7
UVC/H_2O_2 (2000 mg L^{-1} H_2O_2)	6.76	10.6	2.0	0.0024	288.8

All samples exposed to UVC radiation showed a modest increase (between 1.3% and 10.6%) in the relative signal for carbonyl stretching as compared to the control fibres. The fibres treated with H_2O_2 in the dark retained a very similar CI of 6.09 to the control experiment (CI = 6.11), which is consistent with the SEM observation that these conditions had no visible

effect on the surface of the fibres. As the concentration of H_2O_2 applied in treatment is increased from 0 to 2000 mg L^{-1}, the CI increases from 6.20 to values over 6.70 for all concentrations above 800 mg L^{-1}. An increase (between 11-40%) in carbonyl band intensity relative to the C-O stretching peak was observed elsewhere for long term (365 days) degradation of PET in simulated marine conditions. (296) In another study, the number of carbonyl surface groups was shown to increase on a PET film after 7 hours exposure to UV radiation in XPS data. (297) The mechanism of degradation depends on the evolution of functional groups on MP surface. This data suggests that the UVC/H_2O_2 treatment results in carbonyl formation within 9 h when a concentration of 800 mg L^{-1} H_2O_2 or higher is used.

The apparent rate constant (k_{app}) and half life ($t_{1/2}$) for each experiment were calculated according to a pseudo first order kinetic process in line with the rate dependence observed in Section 4.3.3.3 and in previous related work. (111) The kinetic parameters are presented in Table 4.2, as calculated in the appendices (Table A.6, Figure A.11). The best performing treatment of UVC with 1200 mg L^{-1} H_2O_2 solution had a rate constant of 0.260 h^{-1}, outperforming the other conditions studied and with a calculated half-life of polyester fibres of 26.7 h. For realistic application in water treatment, the rate of degradation requires further improvement in order to reduce the energy requirements and operation costs associated with long treatment times. Addition of about 1.6 times more H_2O_2 (2000 mg L^{-1}) resulted in a huge decrease in the rate constant to 0.0024 h^{-1}, once again highlighting the impact of radical scavenging within the system when excess concentrations of hydroxyl radicals are present. Despite the reduced rate of mass loss, the CI increase was similar to that observed for the optimised treatment indicating that surface oxidation alone is not sufficient to lead to fibre fragmentation and mass reduction.

4.3.3.5 MPs degradation in real laundry wastewater

To determine the effect of complex wastewater matrices on the UVC/H_2O_2 treatment, appropriate amounts of polyester fibres were spiked into real laundry wastewater. Typical commercial laundry wastewater has been reported to have particularly high COD and a large variety of organic components including detergents, fragrances, solvents etc. (298) The

sample used in this study is a hospital laundry wastewater and (characterised in Section 4.3.2) has a COD of 514 ± 3 mg L^{-1}. It is expected that the rate of mass loss from the plastic will be reduced due to other organic and inorganic components present in the wastewater competing with the MPs for hydroxyl radicals (299). Zotesso et al. (284) considered the treatment of hospital laundry wastewater by a coagulation, filtration and UV/H_2O_2 treatment, finding complete COD removal was possible using an optimised ratio of H_2O_2. However, the removal of MPs from the wastewater was not investigated. Figure 4.14 shows the results obtained during treatment of MPs by UVC/H_2O_2 in pure deionised water and in real hospital laundry wastewater matrices.

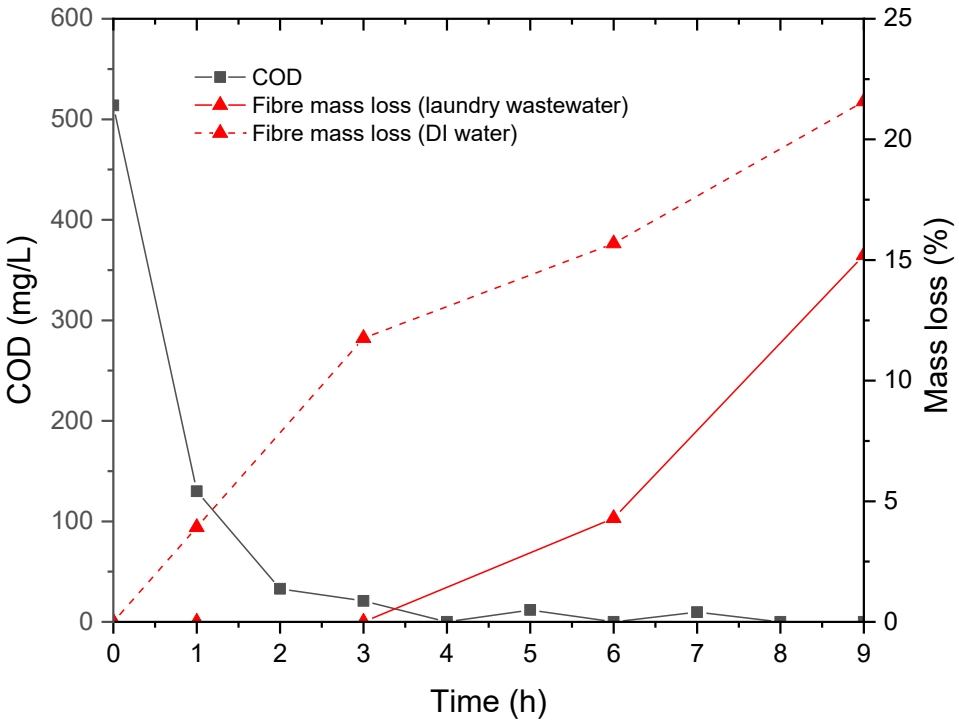

Figure 4.14 Mass loss and COD during UVC/H_2O_2 treatment of polyester fibres in DI water and laundry wastewater matrices. Starting fibre concentration of 16.7 mg L^{-1}, H_2O_2 concentration 1800 mg L^{-1}, UVC irradiance 31.8 mW cm^{-2}.

The onset of degradation of polyester fibres in the laundry wastewater matrix is delayed by roughly 3 h as compared to the treatment applied in DI water. This can be rationalised when considering the change in COD of the wastewater over time, shown by the black line. The COD

of the water decreases to 20.9 mg L^{-1} within the first 3 h of treatment. From 3 h, the fibre mass begins to decrease at a similar rate (k are 0.0104 h^{-1} and 0.0119 h^{-1} in DI and wastewater matrices, respectively) to the experiments performed in DI water reaching a final removal of 15.2% in wastewater compared to 21.6% in DI water. The delay in the onset of mass loss indicates that radicals from the UVC/H_2O_2 treatment are impeded from attacking the MPs by the competitive reaction with background organic content of the water, indicating that MPs are more recalcitrant to oxidation than soluble organic pollutants.

4.4 Conclusions

This study aimed to degrade polyester microfibers in laundry wastewater using photo-degradation induced by UVC radiation and an oxidation treatment consisting of UVC/H_2O_2. The development of an experimental procedure was essential to allow reliable collection of mass loss results. MP sizing and mass loss were initially considered as a metric to follow degradation with the latter selected for reproducibility based on spiked recovery results. With a reliable experimental protocol in place, the investigation of UVC photodegradation and UVC/H_2O_2 AOP treatment was possible. It was found that increasing the UV dose by extending treatment time and by increasing the intensity of UV irradiation both resulted in increased mass removal by means of UVC/H_2O_2. Pitting and crack formation observed by SEM and AFM indicate that the mass loss is mainly from surface degradation and fragmentation of the fibres. The effect of H_2O_2 reagent concentration was also explored and at the best operational conditions essayed (1200 mg L^{-1} H_2O_2 under UVC irradiance of 31.8 mW cm^{-2}) a polyester half life of 26.7 h could be achieved. An increase in the relative strength of the carbonyl signal in FTIR spectra was observed for a number of treated MP fibres relative to the raw polymer indicating that surface oxygen containing groups increased in abundance as a result of oxidative degradation of the polymer chains. The ability of the UVC/H_2O_2 process to remove polyester fibres from a complex real laundry wastewater with a high background COD was also studied. It was observed that the background organic content was oxidized first followed by MPs mass loss, which indicate that the proposed technology could be used as a final MPs treatment step when COD will have been removed by other biological and/or physicochemical processes.

The developed method is the first use of a UVC/H_2O_2 AOP for MP degradation in water and for removing polyester fibres from laundry wastewater matrix, an important source of MPs to the environment. This work could provide feedback on mechanisms of MPs' degradation in water and wastewater as well as their weathering process to relevant stakeholders and policy makers in order to further mitigate plastic pollution environmental problem.

With reference to the research aims previously outlined in Section 1.1, this chapter contributes towards:

1) Determine the potential for sustainable advanced oxidation methods as a treatment option for MP polluted water.
2) Understand the transformation and degradation of MPs within these systems

The optimised UVC/H_2O_2 treatment degrades polyester MP fibres in the timescale of hours to days. In terms of the potential of this method to large scale water treatment, slow degradation rate and the need for high concentration of oxidant and large UV dose limit the potential for direct scale up. Scale-up in real world systems with a lower concentration of MPs may be possible but requires further optimisation of the UV and peroxide dose to determine feasibility. As a proof of concept, the developed treatment sheds light on how MPs may degrade in such systems and offers a starting point for future development of AOPs which accelerate this degradation. The mechanism of fragmentation and oxidation was explored using chemical and physical characterisation methods. Understanding this process is not only essential in the development of effective removal methods but also in understanding how partial degradation may transform MPs.

5. Transformation of polyester fibre microplastics by sulfate based advanced oxidation processes

The rate of polyester degradation observed in experiments presented in Chapter 4 indicates a slow removal by the selected traditional AOP methods. However, the degradation of fibres resulted in clear physical and chemical changes as shown in the SEM and AFM imaging and FTIR spectra. These changes hold relevance to the environmental fate and therefore risk of MPs within the aquatic environment. In this chapter, the impact of sulfate based oxidation on polyester MP fibres was investigated. Light, heat and ultrasound activation of persulfate resulted in varied degrees of mass loss and surface degradation, as probed by SEM, AFM and FTIR. Ultrasound activation of persulfate resulted in significantly increased fragmentation and formation of smaller microplastic fibrils. Optimised UVC/PDS treatment (31.8 mW cm^{-2}, 500 mg L^{-1}) resulted in an 18.5% mass loss over 9 h with clear surface pitting and cracking. Extended treatment under these conditions for 24 h did not result in significantly increased mass loss but did cause an increased degree of surface degradation and increased roughness, indicating that incomplete mineralisation is likely in wastewater systems accompanied by MP transformation. The influence of a real laundry wastewater matrix was also studied and a decreased rate of mass loss was observed due to competing radical reactions with the organic content of the wastewater. The results of these investigations advance understanding of the mechanism of MP fragmentation and degradation and therefore contribute to mitigating MP water pollution. This physical and chemical transformation in real water treatment systems substantially affects the interaction with organic contaminants and changes the potential environmental risk of MPs.

This chapter is published in the paper titled: Transformation of polyester fibre microplastics by sulfate based advanced oxidation processes. (300) Published content is reproduced within this chapter as permitted under a CC BY 4.0 licence.

5.1 Background and literature review

While contained within wastewater treatment systems, MPs may undergo chemical and physical transformation. (49) This could be a result of the physical fragmentation, chemical

degradation of the polymer itself or interaction with other components of the wastewater such as adsorption of organics onto the MP surface. (301, 302) Attention has recently grown on the use of AOPs for the removal of MPs from water. A number of lab scale investigations including those presented in Chapter 4 have shown that these oxidative methods result in physical and chemical degradation of MPs in water, with varying rates of removal and extent of degradation reported.

AOP testing for MP degradation thus far mainly consists of lab-scale batch treatment, typically over the course of many hours with the aim of maximising mass loss to determine optimum conditions of treatment. Polyethylene beads and films reduced in mass by 72% after 50 h exposure to doped powder TiO_2 catalysts in a photocatalytic degradation reported by Ariza-Tarazona et al. (104, 108) In another study, ZnO photocatalysis resulted in physical and chemical transformation of polyethylene film surface after 175 h of treatment. (107, 109) Photo-Fenton treatment of polystyrene accelerated the ageing process (as measured by oxygen content and surface texture) during a 108 h treatment. (116) The authors also showed a difference in the adsorption behaviour of organics on the surface as a result of these changes, highlighting the need to consider how transformation of MPs can impact their fate in the environment. The first study investigating microplastic fibre degradation in AOP systems reported polyamide mass loss of 97% within 48 h using a TiO_2 photocatalyst. (111) Again the degradation of fibres was tracked by microscopy and spectroscopy to consider physical and chemical alteration. In Chapter 4, the removal of polyester fibres using a H_2O_2/UVC AOP showed that under optimised conditions, polyester mass loss reached 52.7% in 48 h. Significant physical surface changes as probed by SEM and AFM imaging were observed as well as chemical changes based on FTIR spectroscopy. (267) Sulfate based systems were shown to cause fragmentation and chemical surface alteration of polystyrene and polyethylene in a heat activated treatment. The major changes were observed after 30 days of treatment. (18, 21) Nylon-6 and polystyrene MP degradation via heat activated PMS was shown to proceed via successive oxidation and chain-scission products identified with surface-enhanced Raman scattering and mass spectrometry. (22) Persulfate activated by heat was shown to degrade polyethylene MPs faster than ozonation and Fenton treatments, as measured by atomic force microscopy infrared spectroscopy. (23) The theoretical background of sulfate driven AOPs is summarised in Section 1.4.3.

With the growing body of literature considering AOPs as a treatment option for MPs contaminated water, it is important to consider what transformative effect such oxidation can have on the polymers. Removal is often incomplete, particularly in a real wastewater treatment system where partial degradation occurs. (303) These transformed MPs are released to the environment after exposure to AOP treatment systems with altered physical and chemical properties. (301) This chapter aims to determine the effect of sulfate based AOPs on polyester microplastic fibres which are present in laundry wastewater to better understand the potential risk posed by the release to the environment. Two persulfate generating precursors, PMS and PDS, were tested for their effect on polyester fibres during treatment. Prior to this work, no study has considered the effect of sulfate based AOPs on polyester MPs, nor has compared the effect of initiation method of these systems (heat, ultrasound or light activation) on the transformation of MPs. These factors are important to consider how different treatment systems will affect the fate of plastic pollution entering the environment.

5.2 Materials and methods

The experimental treatment setup is described fully in Section 2.3 and analytical methods are outlined in full in Section 2.4. Polyethylene terephthalate fibres (PET) with a diameter of approximately 40 µm (Phoenix Fibres, UK) were used as supplied in rough lengths of 3 cm. In a typical experiment, the fibre concentration in the water was 16.7 mg L^{-1} and was tracked by mass determination as outlined in detail in Section 2.3. Laundry wastewater was collected from a Scottish hospital's laundry store and is fully characterised in Chapter 4. Experiments were conducted using an immersed lamp reactor, immersed ultrasound horn reactor or heated using a plate heater. Where temperature was not varied purposely, it was kept constant at 18 ± 1 ^{o}C during treatment. SEM and AFM were used to image the fibre surface and to calculate the roughness at the nano scale. FTIR spectroscopy was used to obtain an IR spectra of the polymer surface yielding information on the presence of functional groups and chemical oxidation. (180) Using FTIR spectra, the CI for polyester fibres was calculated using the carbonyl peak (1560 - 1753 cm^{-1}) and a reference peak (1360-1420 cm^{-1}) corresponding

to an aromatic C-C stretching and ring CH in-plane bending. (181) The concentration of PMS and PDS was measured using UV-Visible spectrophotometry.

5.3 Screening of sulfate activation methods

Persulfate generating precursors can be activated by a number of initiation methods. In order to understand the transformative potential of this AOP family on MPs, initiation by photo-irradiation, ultrasound, and thermal energy, was studied and compared.

5.3.1 Photoactivation

Two commonly used persulfate generating precursors (PDS and PMS) were compared in UVC photoactivated AOP experiments. Transformation of polyester fibres during PDS and PMS based UVC AOP treatment was compared to a series of blanks in order to determine if the AOP treatment enhances degradation rate as compared to each chemical or photo-oxidising condition independently. Blank experiments were carried out in the dark (control), in the presence of peroxymonosulfate (PMS/dark), peroxydisulfate (PDS/dark), and UVC only (UVC) and the results from a 6 h treatment are shown within Figure 5.1.

The mass loss rate observed in the control experiment, as well as each experiment conducted in the dark were low (< 3%). Irradiation with UVC resulted in a slightly higher rate with 4.3% mass loss. The radical generation during UVC/PMS and UVC/PDS treatment resulted in an increased rate of mass loss of polyester fibres with 14.2 and 15.1% respectively. This enhanced degradation rate is likely due to the formation of oxidising radicals during irradiation of PDS and PMS and highlights the potential application of these AOPs in treating microplastic contaminated wastewater. (304) The rate of mass loss is slow meaning that water treated in this manner in a real wastewater treatment system will not be free from microplastics. Indeed, partial degradation and transformation of the fibres is likely and the extent to which this occurs will be investigated.

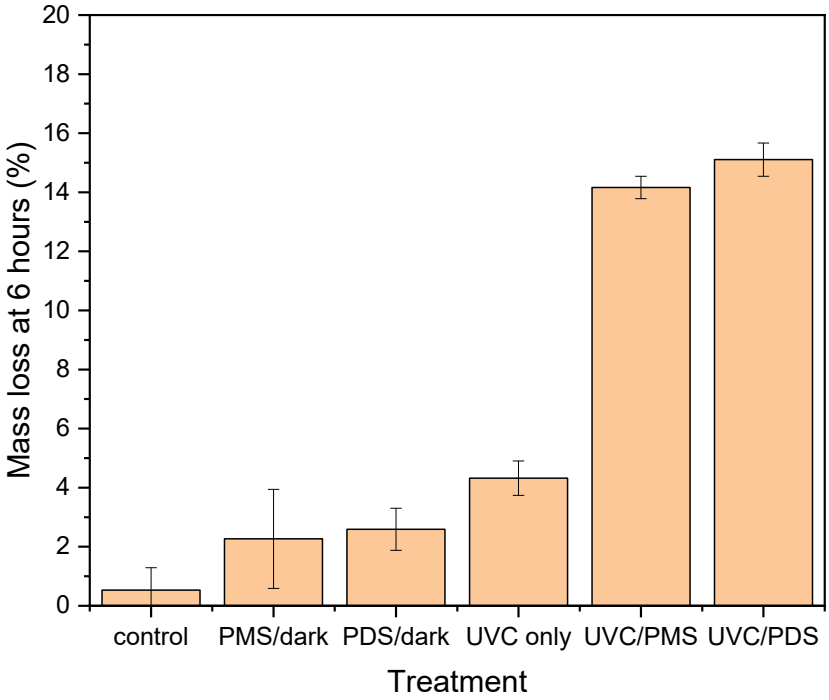

Figure 5.1 Mass loss of polyester fibres in a 6 h treatment period (MP initial concentration 8.3 mg L^{-1}, PMS/PDS initial concentration 500 mg L^{-1} in DI water, UV irradiation 31.8 mW cm^{-2})

The peroxide bond in PDS and PMS can also be photoactivated at wavelengths in the UVA and UVB ranges. (305) Hence, UVA, UVC and solar irradiation were compared for initiation of PDS and their effect on the transformation of polyester fibres. Additionally, the intensity of UVC irradiation was varied by switching lamps as outlined in Section 2.3.3, between low intensity (LI 4 mW cm^{-2}) and high intensity (HI 31.8 mW cm^{-2}). Figure 5.2 shows the effect of long-term treatment via these methods on polyester fibres in terms of mass loss.

Interestingly, after an initial decline in mass between 0-6 h treatment by UVC/PDS, treatment up to 24 h by UVC/PDS results in mass loss reaching a relatively stable level after 9 h. Under higher intensity UVC, mass loss plateaus at 27% and under low intensity irradiation, at 21%. UVA and solar initiated sulfate treatments resulted in very low mass loss over 24 h (< 5%). This is likely due to slow generation of radicals and limited surface degradation. UVC can directly photo degrade polyester (267) while UVA and solar irradiation require treatment times of weeks to months to observe significant MP change without the use of catalysts (166, 306). The combined effect of UVC photooxidation and AOP generation of oxidising radicals

results in degradation of polyester which is expected to be accompanied by more pronounced chemical and physical transformation of the surface properties.

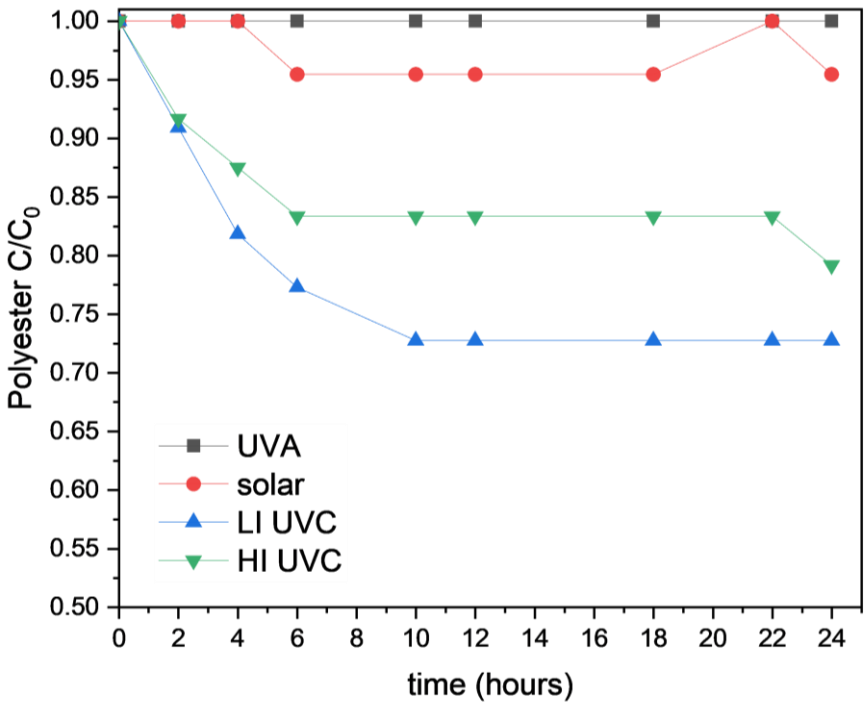

Figure 5.2 Effect of irradiation source on polyester fibre degradation (MP concentration 8.3 mg L^{-1} in DI water, PDS concentration 500 mg L^{-1}; LI UVC irradiation 4 mW cm^{-2}; HI UVC irradiation 31.8 mW cm^{-2}; UVA 12.45 mW cm^{-2}; solar 8.02 mW cm^{-2} UVA component)

SEM images of the surface after 24 h of each treatment are shown in Figure 5.3. UVA/PDS treated fibres have a smooth surface with a small number of debris, solar/PDS treated fibres exhibit a small number of pitted holes and LI UVC /PDS treated fibres have a noticeably rough surface with the appearance of micro-cracks and fissures. HI UVC /PDS SEM images display a noticeably degraded surface featuring surface pitting as well as cracking. At the timescales relevant to transformation within a wastewater treatment system, solar and UVA irradiation systems are likely to result in little to no alteration of the microplastic fibres while UVC based treatments lead to chemical and physical change.

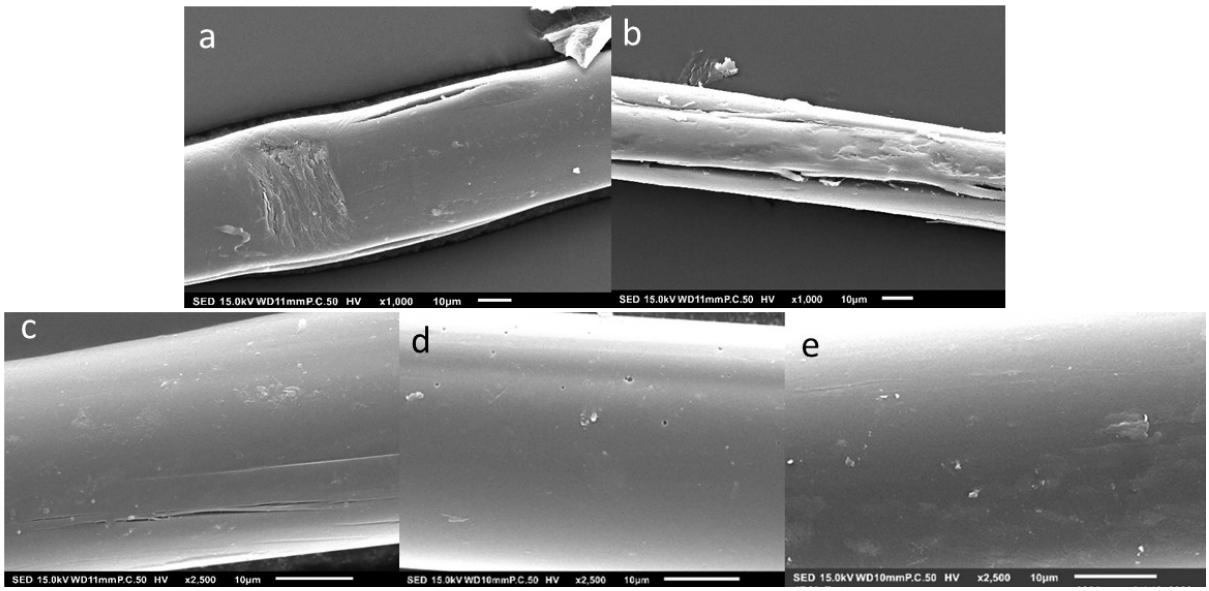

Figure 5.3 SEM image of 24 h treated polyester fibres under **(a,c)** LI UVC/PDS (100 mg L^{-1}), **(b)** HI UVC/PDS (500 mg L^{-1}), **(d)** solar/PDS (500 mgL^{-1}) and **(e)** UVA/PDS (500 mgL^{-1})

To show progression of surface weathering over time, Figure 5.4 shows fibres extracted at various time points during a UVC/PDS AOP treatment.

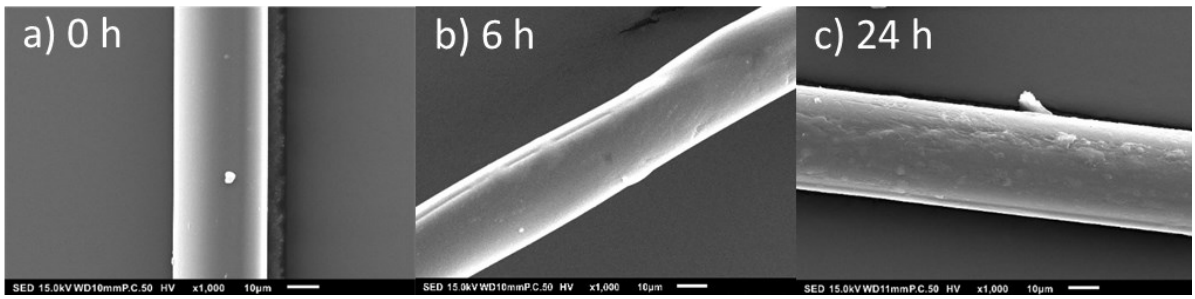

Figure 5.4 SEM images of polyester fibre surface exposed to UVC/PDS AOP treatment (a) raw fibres, (b) after 6 h treatment and (c) after 24 h treatment. (MP initial concentration 8.3 mg L^{-1}, PMS and PDS initial concentration 500 mg L^{-1}, UV irradiation 31.8 mW cm^{-2})

As the treatment time increased, the number of surface features increases with pitting and roughness evident in the partially degraded fibre samples. Increased pitting and surface roughness have been shown to drastically alter the environmental impact of microplastics. (307). The changes observed in UVC/PDS and UVC/PMS treated fibres may affect MP toxicity

after environmental release or their ability to adsorb organic contaminants within treatment systems. (301)

Alongside mass loss as an indicator of polyester degradation, the chemical composition of the surface was probed using FTIR spectroscopy and the carbonyl index was calculated as described in Section 2.4.1.1. A control experiment conducted with polyester stirred in darkness allowed assignment of the baseline and characteristic peaks for polyester (PET). These are: 2968 cm^{-1} (C-H ethyl stretch), 1711 cm^{-1} (C=O carbonyl stretch), 1578 cm^{-1}, 1504 cm^{-1} and 1409 cm^{-1} (aromatic C-C stretch), 1367 cm^{-1} and 1338 cm^{-1} (CH_2 wagging), 1239 cm^{-1}, 1117 cm^{-1}, 1092 cm^{-1} and 969 cm^{-1} (C-O ester stretch), 1016 cm^{-1}, 872 cm^{-1}, 792 cm^{-1} and 718 cm^{-1} (aromatic ring vibration, bending and torsion) (181-183, 267). The calculated carbonyl index of control experiments as well as PDS based AOP treated fibres are included in Table 5.1.

Table 5.1 Calculated carbonyl index and reaction rates of treated polyester fibre samples (MP initial concentration 8.3 mg L^{-1}, replenishment of PDS every 60 min)

Treatment type	PDS initial concentration, mg L^{-1}	Pseudo first order rate constant K_a, min^{-1}	CI after 6 h of treatment	CI after 24 h of treatment
control	0	-	5.82	5.79
UVC/PDS	200	-	5.91	-
	500	0.0174	5.89	6.03
	1000	0.0054	5.88	-
	2000	0.008	6.25	-
Solar/PDS	500	0.0059	5.81	5.62
UVA/PDS	500	0.0013	5.70	5.75
US/PDS	500	0.0116	6.57	6.92

UVC/PDS treatment of polyester results in a small increase in CI relative to the control experiment for oxidant concentrations 200 - 1000 mg L^{-1}. Solar and UVA activation methods did not lead to an increase in CI relative to the control. The data suggests that high concentrations of oxidant in the water under UVC irradiation leads to formation of carbonyl

groups on the polymer surface. The implications for environmental fate as well as the potential to adsorb co-contaminants are a change in hydrophobicity of the MP surface. (303, 308) Long treatment times of 24 h for UVC/PDS result in a further increase to CI while the control experiment, solar and UVA treated fibres did not display significant change with extended treatment time. Although the CI is calculated from an averaged signal from three FTIR spectra, the increase in CI is small and further experiments are required to determine the long-term effect of UVC irradiation on the surface chemistry of polyester.

5.3.2 Ultrasound assisted activation

Persulfate can be also activated by ultrasound (US) according to reactions outlined in Section 1.4.3. Potential environmental applications of this AOP have been reviewed in detail by Gujar et al. (309) Cavitation bubbles formed during the process increase the rate of PDS and PMS decomposition and therefore aid in the generation of sulfate radicals. Furthermore, sonication in water results in the formation of hydroxyl radicals. The combined action of radicals can lead to a complex range of potential degradation pathways. Mixing is also enhanced by the US which aids in mass transfer. The impact of this activation mechanism on the transformation of polyester fibres was investigated as the additional effects of US are expected to change the mechanism of degradation and potentially the final physical and chemical characteristics of fibres. The consumption of PDS and PMS was first investigated without any MPs present and was found to depend on the US power supplied to the reactor (ranging from 0 W to 500 W). Results are shown in Figures 5.5 and 5.6.

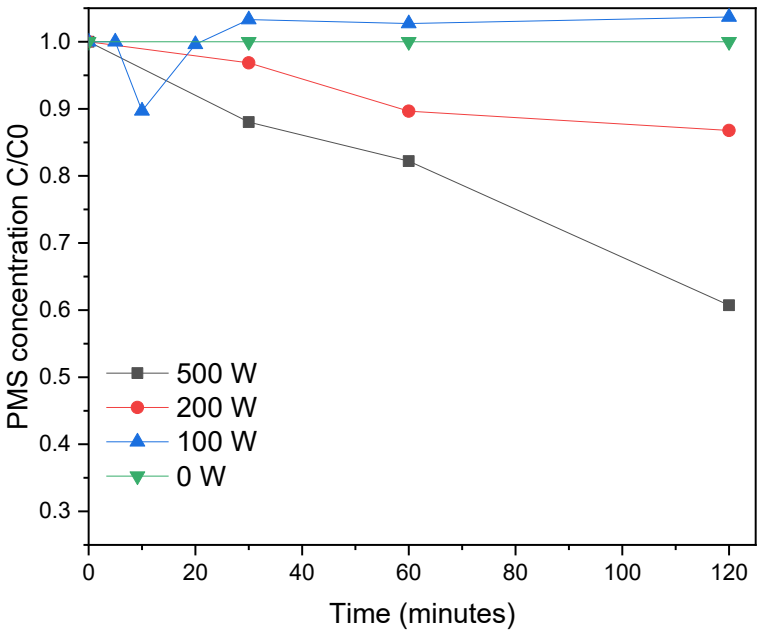

Figure 5.5 PMS concentration change over time on application of ultrasound at various power (Starting PMS concentration 500 mg L^{-1})

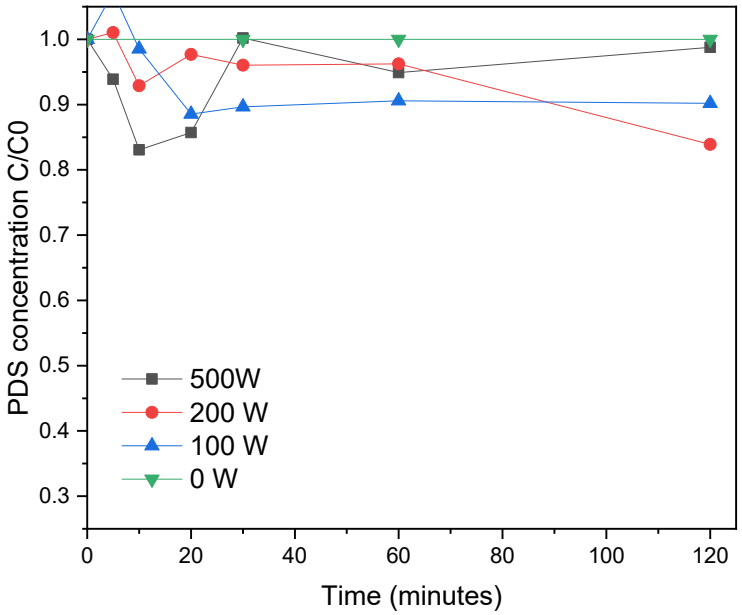

Figure 5.6 PDS concentration change over time on application of ultrasound at various power (Starting PDS concentration 500 mg L^{-1} in DI water)

Interestingly, even at the highest energy US, PDS concentration did not significantly decrease in 2 h of treatment, whereas PMS concentration was reduced by over 40% indicating that PMS is likely to be more effectively activated by this method and will produce a higher concentration of oxidising species in water. A low and high power setting (100 W and 500 W)

were selected for testing the effect of the initial concentrations (at 100 and 500 mg L^{-1}) of PDS and PMS on mass loss. Table 5.2 shows the resulting mass losses after 6 h of treatment while Figure 5.7 shows the physical surface degradation imaged by SEM.

Table 5.2 Polyester fibre mass loss treated with US/PDS and US/PMS (MP initial concentration 8.3 mg L^{-1})

Oxidant concentration (mg L^{-1})	**Mass loss % after 6 h**	
	100 W US power	500 W US power
none	0	3.8
100 PDS	-	7.4
500 PDS	1.8	8.3
100 PMS	-	11.5
500 PMS	7.4	16.0

The mass loss is higher for treatments using PMS as compared to PDS, likely due to the more effective activation of this reagent by US. High power (500 W) US results in a larger overall mass loss as compared to 100 W power in all cases. High power US is also expected to greatly increase the degree of fragmentation by mechanical agitation, thus increasing the number of nano/micro plastics formed from breakdown of the bulk fibres. Further investigation into this mechanism would provide valuable information on the fate of MPs in such systems.

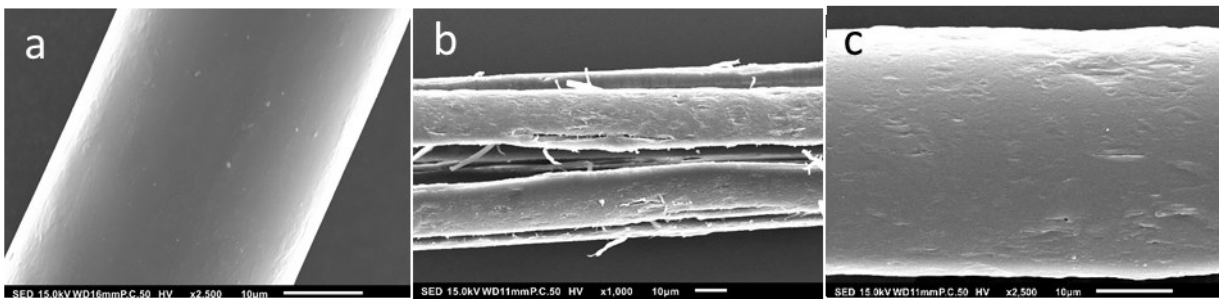

Figure 5.7 SEM image of polyester fibre surface **(a)** raw PET fibre **(b)** treated with 500 W US for 6 h, 500 mg L^{-1} PMS **(c)** treated with 500 W US for 6 h,500 mg L^{-1} PDS

Comparing the treated fibres with raw untreated polyester makes clear that the US/PMS and US/PDS AOPs have a degradation effect on the surface after 6 h. Pitting and surface roughness increases and fibres become fragmented with smaller sections appearing to separate from

the bulk plastic. Fragmentation features observed in the treated fibre samples where delamination and splintering of the fibre results in small sections breaking away from the bulk. High power US results in visibly increased degree fragmentation and larger mass loss. Weakened sections of the bulk fibre are split open and the fibre is delaminated. Extended US treatment up to 6 h leads to the formation of polyester fibrils at these weak points as shown in Figure 5.7 b. The fragmentation observed is not unlike the formation of fibrils reported by Cai et al. during abrasion of polyester, although these tests were not performed in water.(310) The authors showed that fibre ends became fibrillated with some textile surface damage. These fragments are prone to further degradation in the solution via radical processes. Fragments present at the end of 6 h UVC/PMS treatment were captured in the filtration step and are therefore included in the final mass measurement. Water treatment methods involving high mechanical mixing or US energy are more likely to lead to significant fragmentation and break up of microplastics. Additionally, treatment by this method presents a very high energy consumption in the lab scale experiments considered. For a 2 hour treatment at the highest intensity, the US/PMS treatment has an energy intensity of 3.33kWh m-3 while the lower intensity treatment for the same length of time consumes 0.667 kWh m-3. While potentially beneficial in leading to degradation in the long term, in a wastewater treatment setting, this transformation may result in the release of larger numbers of smaller fragments and potentially nanoplastics and is an important area for further study.

5.3.3 Thermal activation

Thermal activation of persulfate occurs via thermolysis (thermal bond breaking) and is generally seen as an attractive option due to the simplicity of the process, despite the high energy demand. (311) The reactions of activation are shown in Section 1.4.3. High temperatures also aid in mass transfer and may affect the polymer crystallinity depending on its composition. In PDS, the peroxide bond energy is 140 kJ mol^{-1} meaning a temperature greater than 30 $^{\circ}C$ is sufficient to generate radicals. (312) The peroxide bond energy of PMS is higher than PDS due to the presence of only one bond weakening SO_3 group, although an experimentally determined value was not available for comparison. (313, 314) Thermal activation of PMS is expected to occur at a higher temperature and few literature studies consider this method without the aid of additional activation methods. These factors were

explored in a series of polyester degradation experiments at varied temperatures. Initially, the rate of PDS or PMS consumption in pure water at varied temperature was investigated at a range of temperatures (60, 75 and 90 ˚C) (Figure 5.8). The energy intensity of the thermal process is 0.014, 0.019 and 0.025 kWh m-3 for activation at 60, 75 and 90˚C respectively.

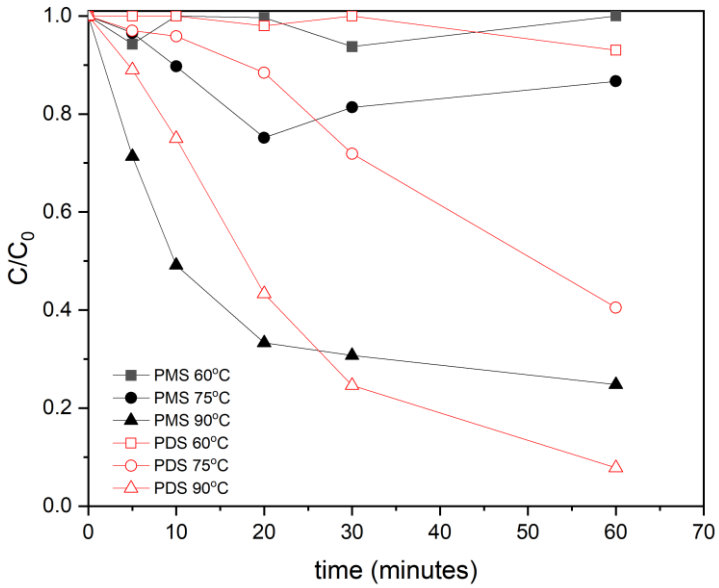

Figure 5.8 Concentration change of PDS/PMS during heat treatment at varied temperature (initial persulfate concentration 500 mg L^{-1}, working volume 300 mL DI water)

It was observed that insignificant (consumption was ≤20%) activation of PMS was observed at temperatures below 90 ˚C, while the relevant values for PDS were higher achieving about 58% consumption at 75 ˚C. This is in agreement with previous reports that heat alone is a poor activator for PMS. (311) Therefore, only PDS based treatment was carried forward for testing on MP transformation. A series of initial PDS concentrations at 75 ˚C thermal initiation temperature are shown in Figure 5.9. As the initial concentration of PDS is increased from 50 to 1000 mg L^{-1}, the rate of consumption at 75 ˚C declines.

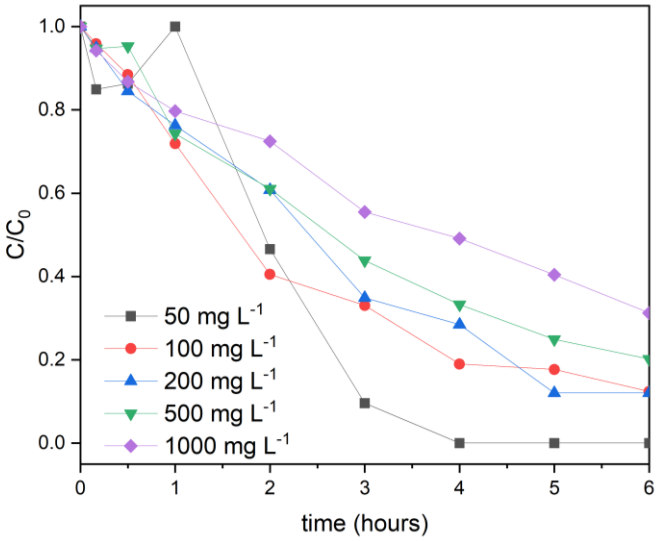

Figure 5.9 Concentration change of PDS during heat treatment at varied initial PDS concentrations (temperature 75 ˚C, working volume 300 mL DI water)

In order to investigate the effect of this difference on the polyester fibres, a low and high value of 100 and 500 mg L^{-1} were selected for subsequent experiments. Results of the effect on polyester fibre MPs and mass loss for the heat/PDS process are presented in Table 5.3.

Table 5.3 Polyester fibre mass loss treated with heat/PDS (MP concentration 8.3 mg L^{-1})

Temperature (˚C)	Mass loss % after 6 h	
	100 mg L^{-1} PDS	500 mg L^{-1} PDS
21	4.2	3.6
60	4.0	< 3
75	3.6	4.3
90	3.8	< 3

Mass loss after 6 h, remained unchanged (~4%), for both initial concentrations of PDS, relative to the room temperature control experiment by heat activated treatment. High temperature testing at 90 ºC brought experimental challenges of rapid evaporation as well as moving the conditions away from a feasible and sustainable large-scale treatment scenario. SEM images representative of the fibre surface for PDS/heat treatment are included in Figure 5.10, where no clear surface change was observed as the fibres appear to remain smooth and featureless in agreement with the mass loss results.

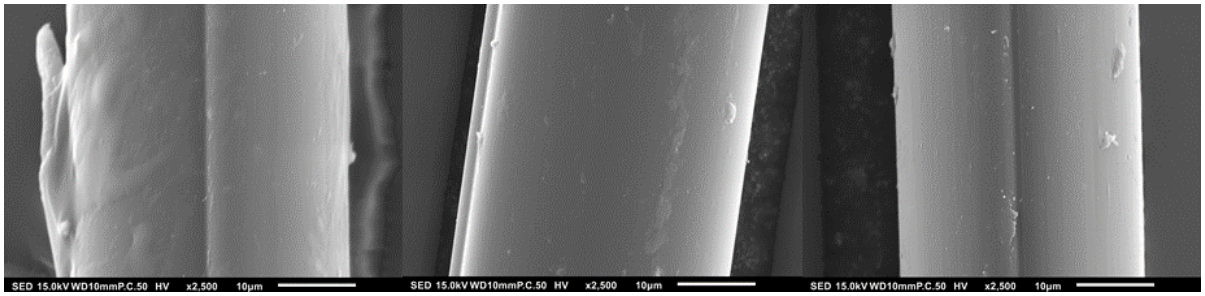

Figure 5.10 SEM images of heat/PDS treated polyester fibres (initial PDS concentration 500 mg L^{-1}, temperature 21 (left), 60 (middle), 90 (right) ˚C

A longer term treatment over 24 h was carried out for selected conditions and these results are shown in Figure 5.11. In this case, at regular intervals, the volume of water was topped up to account for evaporation.

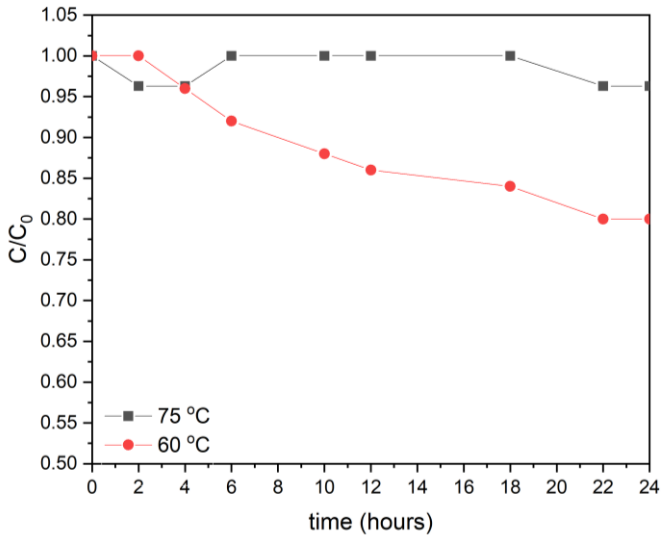

Figure 5.11 Change in polyester fibre concentration during heat/PDS treatment (initial MP concentration 8.3 mg L^{-1}, PDS concentration 100 mg L^{-1} DI water)

A slow rate of polyester mass loss (k_a 0.0099, R^2 0.97), that fits well the pseudo-first order reaction rate, occurs at a temperature of 60 ˚C in the presence of PDS, reaching a final mass loss of 20% in 24 h. At 75 ˚C, mass loss after 24 h was just 3.7%. This trend is expected based on the temperatures typical for heat activation of PDS. In a recent review of thermal PDS

activation (315), most successful reported AOPs used a temperature around 60 °C, with higher temperatures cited as energy inefficient despite the potential to produce radical species at a faster rate. (316-318) Raising the temperature negatively impacts treatment efficacy by promoting unwanted decomposition of PDS. (313)

5.4 UVC/sulfate operating parameters and water properties

Subsequent experiments considered the effect of water properties and process parameters on the performance of UVC initiated sulfate oxidation process as this is the technology most likely to be applied at scale in real WWTP systems.

5.4.1 Consumption rate of oxidant

During treatment, the rate of PMS or PDS consumption is related to the number of active radicals in the system. Oxidant is consumed during AOP treatment, according to the equations shown in Section 1.4.3. UVC irradiation for 60 and 120 m resulted in complete consumption of PMS and PDS, respectively as shown in Figure 5.12. PDS was reduced by more than 80% of the initial concentration (C_0 = 500 mg L^{-1}) within 60 m and PMS was reduced to the same level in less than 20 m. Varied rate of oxidant addition was tested based on this information with the concentration of PMS and PDS replenished to a target concentration of 500 mg L^{-1} every 20 m, 60 m and not at all after initial dosing. Table 5.4 shows that providing fresh oxidant impacts the rate of degradation of polyester.

Table 5.4 Polyester fibre mass loss at varied rates of sulfate addition (UVC irradiation 31.8 mW cm^{-2}, initial fibre concentration 8.3 mg L^{-1})

PDS or PMS replenishment rate	Mass loss after 6 h (%)	
	UVC/PDS	UVC/PMS
No replenishment	14.8	14.3
60 m	16.7	12.0
20 m	25.0	0

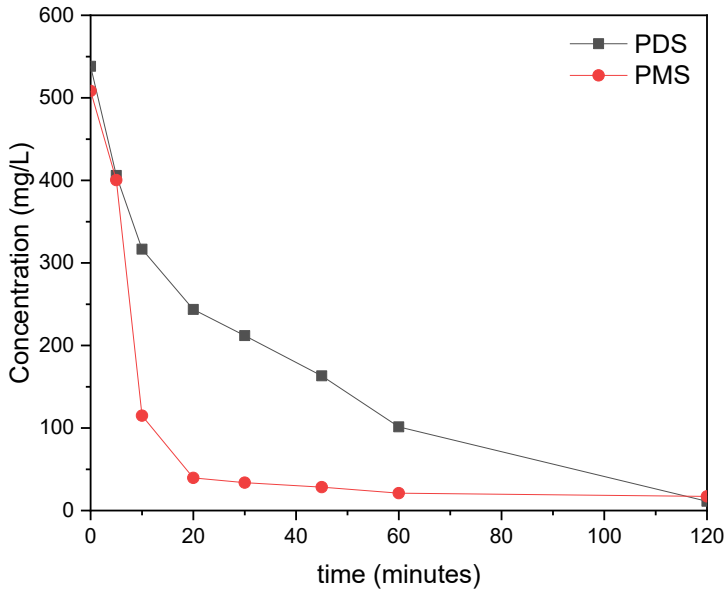

Figure 5.12 Concentration change of PMS and PDS exposed to UVC irradiation (Starting oxidant concentration 500 mg L^{-1}, UVC irradiation 31.8 mW cm^{-2}, working volume 300 mL DI water).

For PMS, increasing the rate of replenishment results in a drop in rate of polyester mass loss with no mass change observed for the most frequent 20 min replenishment UVC/PMS treatment. In contrast, increasing the rate of replenishment of PDS results resulted in an increase to the mass loss with a large mass loss of 25% in 6 h for the 20 min UVC/PDS treatment. This difference in trend was examined by considering the difference in activation for each oxidant as well as the potential for unwanted side reactions in solution Both reactors start with a PDS or PMS concentration of approximately 500 mg L^{-1} under constant UVC irradiation. For UVC/PDS, subsequent addition of PDS every 20 m results in an increase to the overall concentration. This build-up of oxidant exceeds the rate of removal via UV activation or side reaction. PMS, on the other hand, shows no accumulation of oxidant (Figure 5.13).

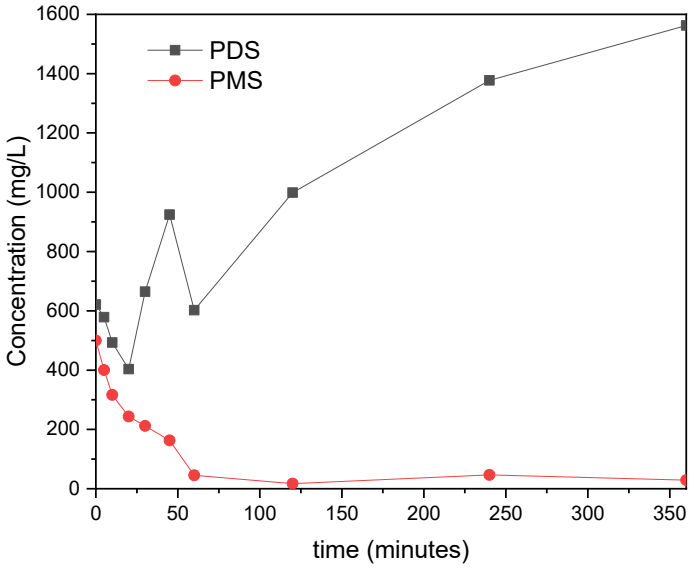

Figure 5.13 Concentration of oxidant during PMS/UVC and PDS/UVC treatment with replenishment every 20 minutes (UV irradiation 31.8 mW cm^{-2})

Frequent addition of PMS is therefore likely to lead to a very high concentration of radical species in solution. Unwanted side reaction and radical termination is more likely under these conditions and removes active oxidising species from solution more rapidly than they are able to attack the polyester fibre surface, therefore reducing the rate of mass loss. (160) As PDS photolysis occurs more slowly, radicals enter the solution at a steady rate, reducing the impact of unwanted side reactions and radical termination. These results hold relevance for large-scale systems where dosing may be carried out at regular intervals. Build-up of PDS within the system must be monitored in this case.

5.4.2 Effect of oxidant initial concentration

The initial concentration of oxidant (C_0) in the system was varied and treatment carried out for 6 h without replenishment of PDS or PMS. The results are shown in Figure 5.14.

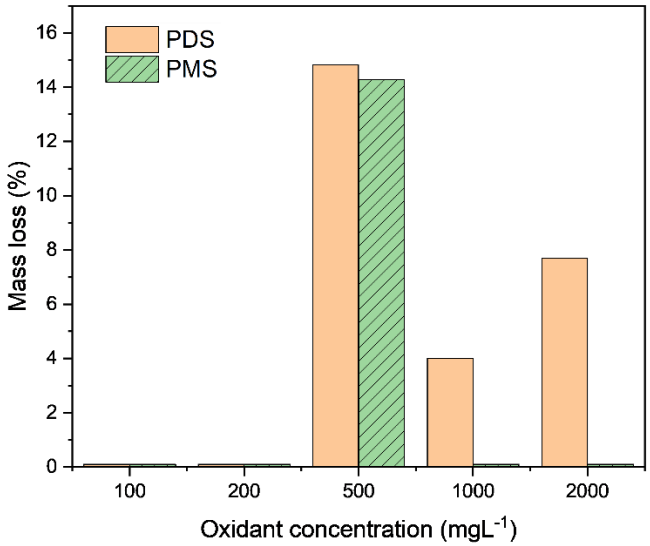

Figure 5.14 Mass loss from polyester fibres after 6 h of treatment with varied oxidant (PMS or PDS) concentration (MP initial concentration 8.3 mg L^{-1} in DI water, UVC irradiation 31.8 mW cm^{-2})

In the case of UVC/PMS treatment, the only initial concentration yielding significant mass loss in 6 h is a dose of 500 mg L^{-1} PMS which resulted in mass loss of 14.3%. UVC/PDS treatment resulted in mass loss for 500, 1000 and 2000 mg L^{-1} initial PDS dosing with mass loss 14.8, 4.0 and 7.7% respectively. At very low oxidant concentrations (i.e. 100 and 200 mg L^{-1}), radical generation is slow while at high oxidant concentration, the potential for competing side reaction and radical scavenging increases and reduces the active radical concentration in the water. At room temperature, this has been shown to occur at PDS concentrations of 0.6 mM during the UV activated degradation of amoxicillin. (319) At very high initial concentration of oxidant (e.g. 1000 and 2000 mg L^{-1}), efficiency is reduced by the competing side reactions discussed in Section 1.4.3.

The rate of mass loss is reasonably described by a pseudo first order kinetic process. The apparent kinetic rate constants (k_a) for each condition of UVC/PDS treatment are presented in Table 5.1, alongside the CI change observed for each oxidant concentration. For a PDS concentration of 2000 mg L^{-1} a larger increase in the CI of 7.4% relative to the control was observed. This trend is in line with previous findings on the effect of oxidant concentration on polyester fibre CI change in an H_2O_2/UVC treatment in Chapter 4, (267) and suggests that

surface oxidation is promoted by a high concentration of PDS in the system despite this condition not leading to the greatest rate of mass loss.

5.4.3 Effect of water pH

Controlling the pH is an important factor in optimising sulfate based AOP treatment. (304, 320, 321) In this study, the initial solution pH during UVC irradiation is altered, in order to determine if the transformation of polyester fibres is affected. The pH was then allowed to change without interference as the treatment was applied. The pH of tested solutions adjusted to 8.5 generally decreased over the course of treatment as shown in Figure 5.15 due to the formation of acidic degradation products as well as the protons released in Reaction 1.11 (Section 1.4.3). (322) For solutions adjusted to pH 11 or retained at pH 3, the UVC irradiation had no effect. The pH of an aqueous solution of Oxone without adjustment is < 3.5 due to the presence of $KHSO_4$.

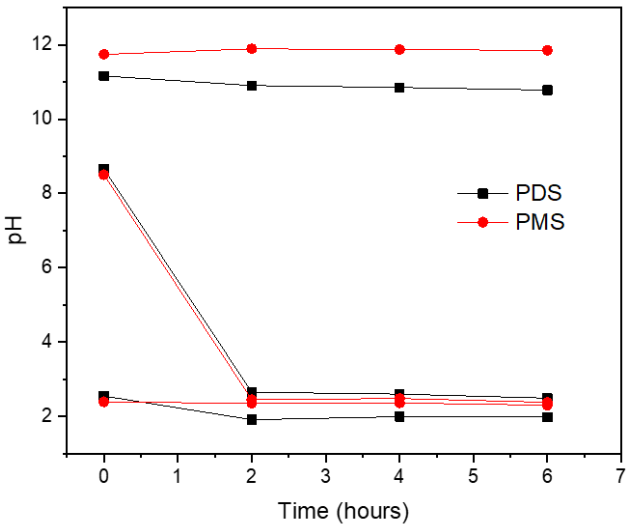

Figure 5.15 Solution pH change over time during UVC activated treatment. 500 mg L^{-1} starting concentration of PMS (red traces) or PDS (black traces)

Higher PMS concentrations were linked to a more distinct drop in pH as treatment progressed due to its decomposition to form acidic products. In this investigation, the initial solution pH was controlled by dropwise addition of NaOH or H_2SO_4 for both PDS and PMS treatment systems. Mass loss after 6 h of UVC/PDS treatment reached 14.8, 7.7 and 16% for a starting

pH of 2.5 and 8.5 and 11 respectively. Mass loss after 6 h of UVC/PMS treatment reached 14.3, 3.6 and 12.5% for a starting pH of 2.5 and 8.5 and 11 respectively. Full conditions, results and the pseudo first order rate constants for each condition are provided in Table 5.5.

Table 5.5 Conditions and polyester mass loss results from varied starting pH experiments

Treatment conditions	Initial pH	PMS or PDS concentration (mg L^{-1})	Temperature (˚C)	Mass loss after 6 h of treatment (%)	K_a
Dark control	2.56	0	21	0	-
	8.48	0	20	0	-
	11.41	0	21	0	-
UVC/PMS	2.39	500	15	14.3	0.0193
	8.5	500	15	3.6	0.0036
	11.74	500	15	12.5	0.0163
UVC/PDS	2.55	500	19	14.8	0.0174
	8.66	500	19	7.7	0.0080
	11.16	500	19	16.0	0.0219

Initial pH is clearly a key factor in the efficiency of the sulfate radical systems with the highest rate of mass loss observed under low pH (in the case of UVC/PMS) and high pH (in the case of UVC/PDS). In both the PDS and PMS systems, the rate of polyester mass loss decreases as the pH is increased from 2.5 to 8 and then increases as the initial pH is increased to 11.

This trend agrees well with results from UV/PMS degradation of sulfamethoxazole investigated by Mouamfon et al. (323) and also benzoic acid as shown by Guan et al. (320) High pH is favourable to faster rates of removal of organics due to the added impact of alkali activation of persulfate. PDS and PMS both undergo (via distinct mechanisms) alkaline hydrolysis. PDS produces hydrogen peroxide anions and subsequently, superoxide radicals while PMS yields singlet oxygen, hydroxyl radicals and superoxide anions. (324-326) Specific detail of these reactions are reviewed in detail elsewhere. (327) The rate of alkali activated sulfate systems for pollutant removal alone is generally very slow. In treatment of BPA

polluted water, initial pH (adjusted with 0.1 M NaOH) of over 7 was found to enhance the rate of pollutant removal over 6 h. (160) Zhao et al. showed that PDS activated by alkaline conditions alone did not influence the removal of PAH in soil (328). PH adjustment may therefore be better utilised alongside another method of persulfate activation for efficient pollutant removal. At low pH, hydrolysis activation of the system does not occur. Instead, the treatment is purely driven by UVC activation of the PMS or PDS. The poor rate of removal in the intermediate case of pH 8.5 is likely due to quenching of radical generating intermediates. Activation of PMS and PMS in water results in the formation of acidic intermediates, as shown in reactions 1.2-1.5. By increasing the pH without providing conditions suitable for alkaline hydrolysis to occur, these intermediates can be quenched. This reduces the availability of radicals in the system and therefore results in a lower rate of degradation. (329)

Variation in the reactor temperature was monitored. UVC/PMS treatment was carried out at 15˚C, UVC/PDS treatment at 19 ˚C and dark control at 20.5±0.5 ˚C. Variation was due to changes in the ambient room temperature but was deemed to have no significant impact on the rate of degradation based on the temperature dependence results discussed in section 5.3.3 which indicate a temperature in excess of 60 ˚C to begin causing thermal degradation in these systems.

5.5 Polyester fibre transformation in real laundry wastewater

The transformation of pollutants in wastewater by AOPs can be influenced by the presence of additional co-contaminants or water characteristics. (330, 331) To determine the effect of a complex matrix, real samples of laundry wastewater were spiked with known concentration of MPs and treated with UVC/PDS, which yielded the highest mass loss in the screening of operating conditions essayed above. Hospital wastewater has a particularly high chemical oxygen demand and contains a complex mixture of persistent organic contaminants. (298) Polyester mass loss and wastewater COD change results are shown in Figure 5.16.

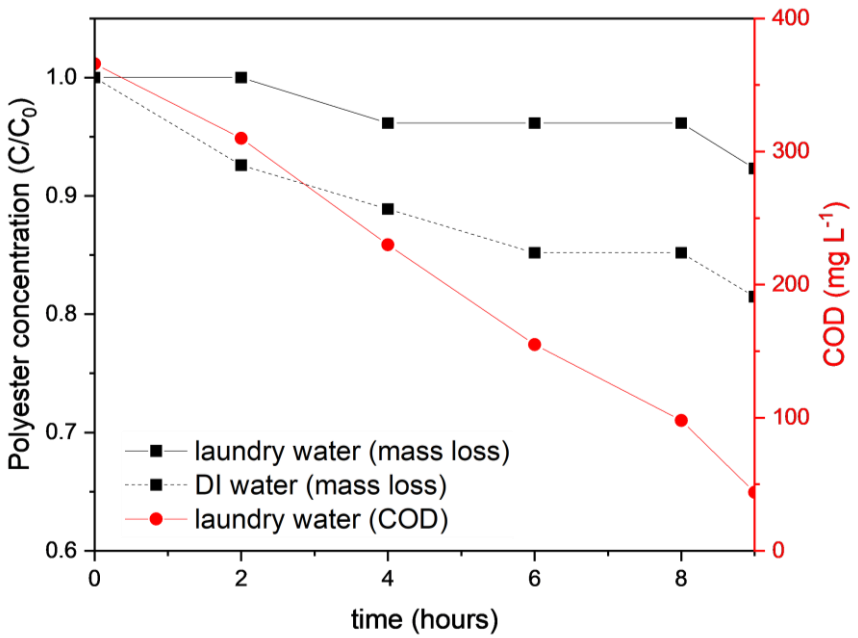

Figure 5.16 Mass loss and COD change during UVC/PDS treatment of polyester fibres in laundry water and DI water (MP concentration 8.3 mg L^{-1}, PDS initial concentration 500 mg L^{-1}, UV irradiation 31.8 mW cm^{-2})

Polyester degradation in real wastewater (solid black line) proceeds at a slower rate than in DI water (dashed black line), reaching 7.7% (k_a = 0.0077) and 18.5% (k_a = 0.0234) respectively in 9 h. This is due to the presence of additional contaminants and organic matter within the water which compete with the polymer surface for reaction with oxidising radicals. (267) The total COD in the real wastewater (solid red line) drops from 366 mg L^{-1} to 44 mg L^{-1} as background matrix contaminants are oxidised. Under realistic conditions, fibre transformation progresses at a slower rate leading to a lower mass loss (solid black line)

compared to deionised water matrix (dash black line) during the oxidation process. The physical and chemical changes of polyester fibres in real wastewater samples were investigated. SEM and AFM images shown in Figure 5.17 indicate that weathering of the fibre surface does occur during AOP treatment, despite slower mass loss.

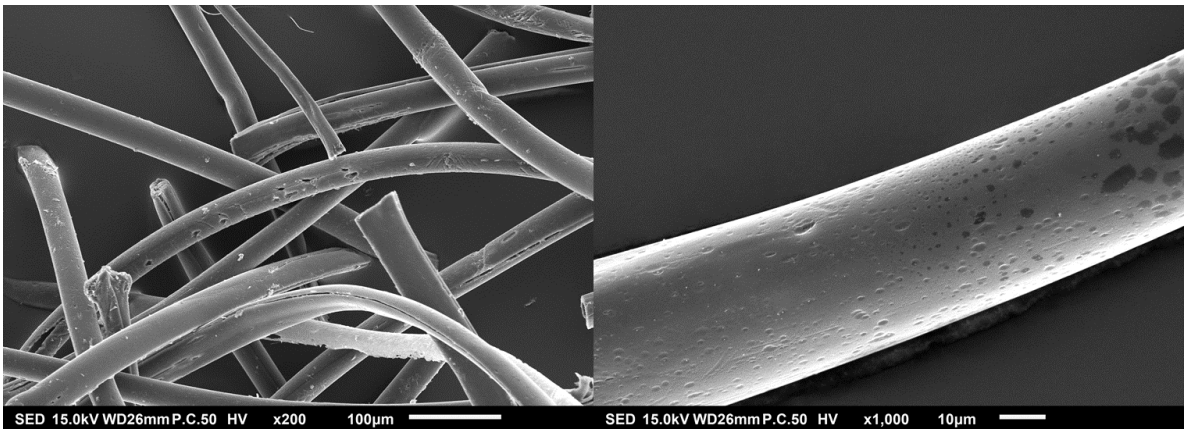

Figure 5.17 SEM images of polyester fibre surface treated in real wastewater for 9 h with PDS initial concentration 500 mg L^{-1}, UV irradiation 31.8 mW cm^{-2}

Surface roughness is increased in the treated sample as compared to raw polyester with evidence of surface debris and fragmentation in the SEM images. In the AFM images, this roughness can be quantified. Figure 5.18 shows a comparison of representative surfaces (5x5 μm^2) from pristine fibres (a) and treated for 9 h in real wastewater (b).

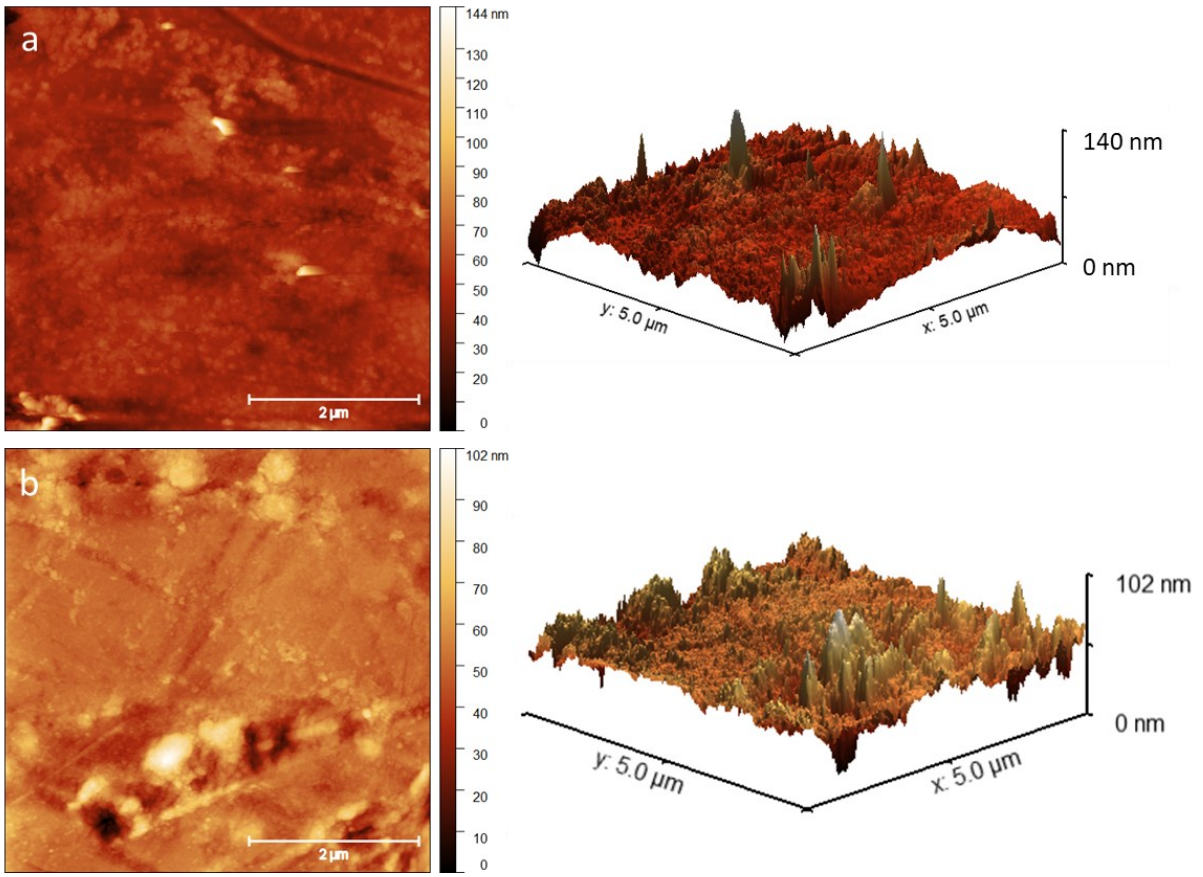

Figure 5.18 AFM height images (5 x 5 µm^2) and 3D surface maps of polyester fibre surface (a) raw fibres, (b) treated in real wastewater for 9 h with PDS initial concentration 500 mg L^{-1}, UV irradiation 31.8 mW cm^{-2}

White areas on the images represent raised sections of the surface while dark areas represent indentation, holes or cracks. The raw fibre shows a relatively smooth surface with debris showing up as bright white spots. This corresponds well with the SEM image of the raw fibre (Figure 5.4 a & 5.7 a). After treatment the surface of the fibres becomes rough, with additional debris and holes evident as light and dark spots respectively. The features are more clearly visualised in the 3D surface maps of each surface with pitting and ridges evident in both of the weathered samples. This is additionally visualised in Figure 5.19 where height profiles along the vertical (y) and horizontal (x) axes are shown for each image. The AFM measurement of height allows the surface roughness to be calculated which represents a measure of vertical deviation from an average height value.

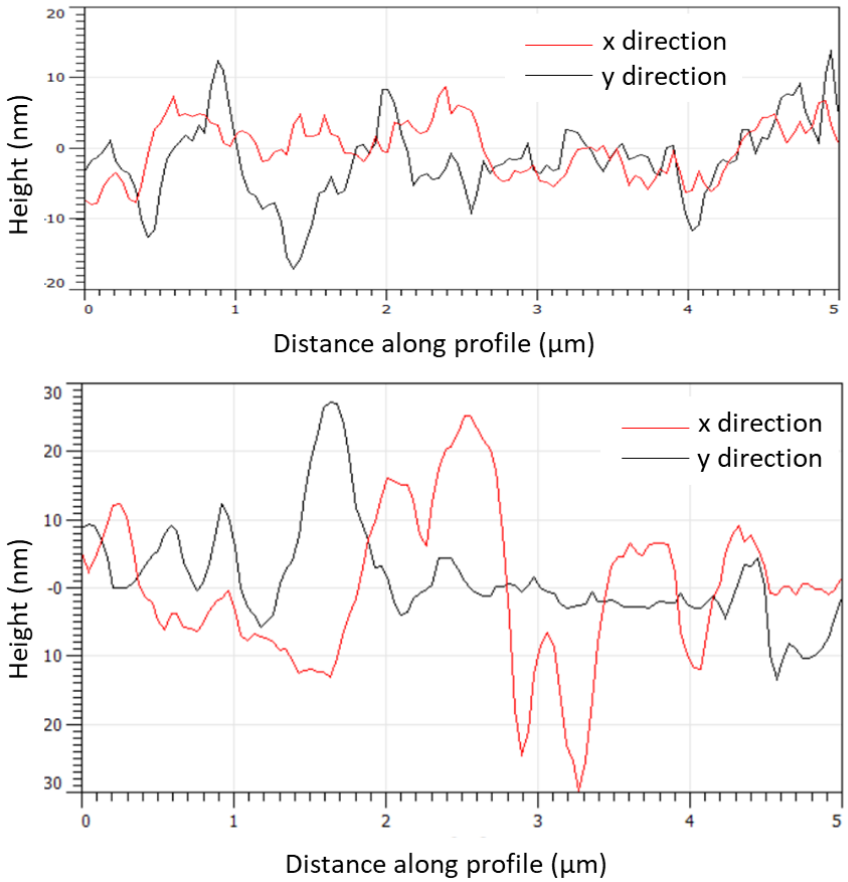

Figure 5.19 Profile of height along the horizontal (x) and vertical axis (y) from pristine (top) and weathered (bottom) polyester fibres, as measured using AFM

The Root Mean Square (RMS) of the surface measured peaks and valleys was calculated as described in Section 2.3 for three samples each from raw fibres and those treated with UVC/PDS, allowing quantification of the roughness (R_{RMS}) change due to weathering. Figure 5.20 shows the results graphically.

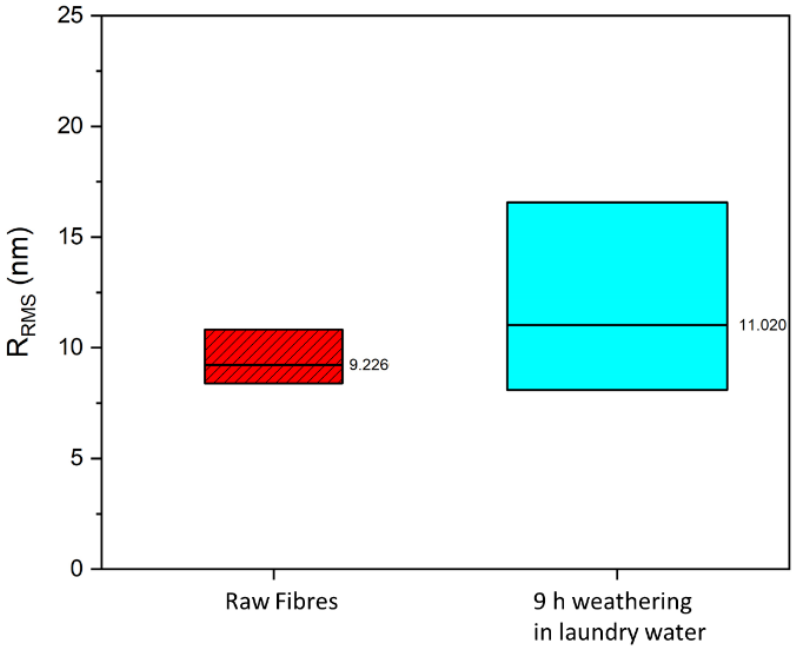

Figure 5.20 Root mean square of roughness (R_{RMS}) for pristine and weathered polyester fibres as calculated from AFM height images. Mean values are highlighted and 25, 75th percentile are marked on the box plot.

Weathering had limited effect on the roughness after 9 h in real laundry water, which matches well with the slow rate of mass loss (previously attributed to the high COD of the water competing with the MPs for reaction with oxidising radicals). The mean surface roughness R_{RMS} was 9.23 and 11.02 nm for the pristine and treated polyester fibres, respectively. This measurement of roughness should be interpreted carefully considering the presence of surface debris on the raw and weathered fibres, visible in the 3D surface image as sharp points of increased height. In addition to large scale surface texture change shown previously in the SEM images, on the nano-scale, roughness potentially affects the behaviour and fate of fibres in the environment. (332, 333) Roughness has been shown to correspond to a change in uptake of contaminants, rate of biofouling and behaviour in aquatic systems. (36, 334) Interaction of partially degraded fibres with persistent and hazardous co-contaminants within the wastewater, such as antibiotics, is a potential result of this and warrants further exploration. (301)

Results presented in this chapter shed light on the physical aspect of the mechanism of polyester fibre MP degradation. Surface changes are one of the major effects of MP

degradation as the roughness increases and holes, pits and fractures form as the plastic is degraded. These observations are in line with the transformation of polyester fibres exposed to UV weathering and UVC/H_2O_2 treatment. (196, 267) As degradation progresses, the release of smaller fragments and nanoplastics is observed, particularly in the ultrasound assisted treatment. This phenomenon has been observed for MP fibres during full-scale ozonation treatment. (335) Fibrils and nano-sized MP PET fragments pose a threat to aquatic environments and are known to be formed during textile washing. (336) Their formation during sulfate driven AOP treatment is an important insight into the fate and transformation of PET within WWTPs. Beyond physical fragmentation, the release of chain scission products has been observed by PET MPs exposed to UV light. (285) In their study, Gewert et al. reported the release of terephthalic acid among a series of carboxylic and dicarboxylic acids detected by LC-MS. The chemical changes on the PET surface were probed with FTIR spectroscopy. Nguyen-Tri et al. present evidence that UV degradation resulted in a decrease to the average molecular weight and tensile strength of PET, again supporting the belief that PET degradation proceeds via a chain scission mechanism. (196) Future work in this area should seek to confirm if the mechanism of degradation by sulfate driven systems results in a similar surface oxidation and release of organics in order to investigate the mechanism of chemical oxidation.

5.6 Conclusions

Polyester microplastic fibres exposed to persulfate based AOPs undergo physical and chemical transformation due to oxidative degradation. This work investigated the extent of this transformation which has implications for environmental fate of MP pollution. Activation of persulfate by UV irradiation, heat and ultrasound result in different rates of mass loss and observed degree of surface change were studied. It was observed that the rate of degradation in such systems is generally slow on the scale of hours to days meaning total removal from wastewater is challenging. However, during exposure to AOPs, transformation of the physical and chemical properties of MPs can occur, potentially increasing the environmental risk. These changes were studied using physical and chemical characterisation methods. UVC irradiation (31.8 mw cm^{-2}) combined with an optimised dose of 500 mg L^{-1} PDS results in an

18.5% mass loss from the MPs over 9 h. Cracking and pitting of the fibre surface was observed by SEM indicating a physical fragmentation process while chemical changes probed by FTIR showed a modest increase to the relative number of carbonyl groups on the polymer surface as a result of oxidation reaction. The roughness of the surface on the nano-scale was measured and imaged using AFM, which showed an increase due to weathering dependant on the time of treatment. In real laundry wastewater, a high background COD reduced the rate of mass loss but physical and chemical transformation of the surface was still evident after 9 h of the optimised treatment UVC/PDS. The transformation of the MP properties within this realistic matrix is highly likely to affect their environmental fate as well as interaction with organic contaminants present in the wastewater. Physical agitation of the solution during treatment by ultrasound-activated persulfate resulted in extensive fragmentation and fibrillation of fibres as observed by SEM as well as increased formation of carbonyl groups probed by FTIR as compared to heat and light activation. The formation of small micro and nano plastics as a result of such treatment should be carefully considered as it poses a potentially greater environmental risk than the bulk MP fibres. The results of this study shed light on how a range of sulfate driven AOPs affect polyester MPs in wastewater treatment systems and provide useful insight to the mechanism of degradation and environmental fate.

Of the research aims presented in Section 1.1, this chapter contributes to:

1) Determine the potential for sustainable advanced oxidation methods as a treatment option for MP polluted water.
2) Understand the transformation and degradation of MPs within these systems

The chemical and physical changes characterised within this chapter are expected to alter MPs interaction with chemical contaminants, such as pharmaceuticals in wastewater. Investigation of this interaction is the focus of Chapter 6 of this thesis.

6. Antibiotic adsorption by microplastics in water

This chapter explores the interaction of MPs with organic micro-pollutants present in wastewater. Within WWTPs, many pollutants are mixed, presenting the potential for adsorption and reaction between each to occur. The adsorption of one antibiotic is taken as an example of this interaction and investigated experimentally. Building on the previous chapters, the transformation of MPs via physical and chemical degradation was expected to affect their capacity for adsorption of organics. Therefore, the uptake of ceftazidime on MPs of varied type, shape, size and weathering degree is tested to explore this idea.

The highly complex mixture of polymer types, particle size and shapes found in wastewater presents a challenge in understanding the fate of persistent organic pollutants. This study aims to discover the effect of weathering, as well as the type, size and shape of MPs on the adsorption of ceftazidime. Five polymer types (polyethylene terephthalate, polyethylene, polystyrene, polyurethane, and tyre wear particles) in varying forms (fibers, beads, foam and fragments) and sizes (10–1000 µm) were studied. Weathering of MPs has the potential to drastically alter their environmental behavior. The MPs were subjected to various weathering methods simulating environmental conditions and characterized physical and chemical changes characterised through mass loss, carbonyl index, scanning electron and atomic force microscopy. Among the MPs studied, weathered polyethylene terephthalate fibers exhibited the highest adsorption reaching 1.432 mg g^{-1} after 48 h of contact time. This high sorption capacity was linked with the formation of holes, cracks and fragmentation of the MPs which increased the surface area and the number of adsorption sites. Findings of this study shed light on the interactions between MPs and antibiotics which occur in highly complex wastewater mixtures and aids in improving understanding of the risk MPs pose to the aquatic environment.

This chapter contributes to answering the research aim of understanding the implications of this transformation on MP interaction with organic pollutants present in domestic wastewater. Data presented in this chapter is included in the paper titled: Antibiotic adsorption by microplastics: Effect of weathering, polymer type, size and shape (*under review*).

6.1 Background and literature review

MPs are present in wastewater treatment systems where they interact with pollutants therefore amplifying their environmental and health risks due to increased ecotoxicity and disruption of aquatic ecosystems. (32) When combined with other pollutants, including pharmaceuticals and other emerging contaminants, via adsorption, the potential for transformation and altered environmental risk is increased. This interaction is important to consider in the framework of an effective risk evaluation of MPs. The large variety of MP types with different size and shape in wastewater presents a complex challenge for understanding such interactions. Different studies indicate that there is no clear pattern between the size distribution and shape of MPs found in WWTPs. For example, Murphy et al. reported that there are different shapes of MPs present in wastewater that include fragments (67.3%), fibres (18.5%), film (9.9%), beads (3.0%) and foam (1.3%). (4) While Le Tarte et al., 2019 found the MPs shapes in the order of foams (39%), fragments (22%), films (18%), fibers (11%) and pellets/beads (11%). (5) In addition to this, the composition varies throughout the stages in WWTPs, with significant differences across sampling sites.

Sources of MP fibres from domestic laundry wastewater are discussed in detail in previous chapters. Foams consisting of expanded polystyrene (PS) or polyurethane (PU) are commonly used in construction for insulation purposes or in the food industry. (70) Microbeads typically originate from personal care products that is also a primary source of MPs. (67) Tyre (rubber) wear particles (TWP) are also one of the main sources of MP pollution generated by the friction between tyres and roads and are transported into wastewater during rainfall. (72) Within municipal wastewater, antibiotics can interact with other substances and/or contaminants in water such as MPs. (36, 301, 337) Adsorption of contaminants to the plastic surface transports them through treatment systems into the environment, across much larger distances that would otherwise be impossible. (45) MP pollution not only presents an environmental risk in itself, but is coupled with a potential increase in the spread of harmful organic contaminants which carry with them the potential to increase environmental antibacterial resistance.

Ceftazidime (CAZ) is a 3rd generation beta lactam cephalosporin antibiotic and is listed by the World Health Organization as a critically important antimicrobial. (338) CAZ resistant bacteria have been identified in hospital and community wastewaters and are therefore likely to be in contact with large numbers of MPs, also shown to be in such wastewater. (330, 339) Some initial evidence supports this assumption as in the presence of MPs, larger numbers of CAZ resistant bacteria were identified in the intestinal communities of sea cucumbers. (340) Despite the importance of this drug to human health and the early evidence of bacteria resistance within wastewater, little information regarding the interaction with MPs is available in the literature. Due to the presence of CAZ alongside MPs in municipal wastewater, understanding their interaction is a key example of understanding how MPs can affect the fate of emerging pollutants within WWTPs via adsorption.

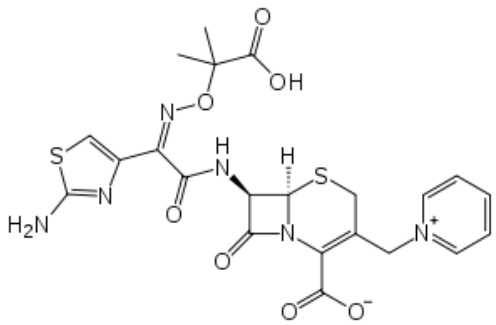

Figure 6.1 Chemical structure of ceftazidime (CAZ)

Although no study has reported CAZ uptake by MPs, data from the field of nanomaterials helps us to understand the adsorption behaviour of CAZ, mainly from a remediation perspective. Multi walled carbon nanotubes were tested as an adsorbent with a reported 70% removal in 10 minutes from a 30 mg L^{-1} solution of CAZ. (341) Removal reached a peak of 80% in 60 minutes and the authors observed pH dependence, linked to altered electrostatic interaction when CAZ is in the protonated state. Copper based metal organic frameworks, doped activated carbon and fly ash zeolites have also been tested as high capacity adsorbents for CAZ removal from water. (342-344) The physicochemical properties of MPs including surface area, crystallinity, and pore size are expected to influence the antibiotics adsorption capacity.

Pristine MPs present very different adsorption properties to weathered MPs due to physical degradation and roughening of the surface as well as chemical oxidation leading to changes in hydrophobicity. (191) As discussed in Chapter 5, when MPs travel through WWTPs, they may be partially degraded by oxidative conditions, therefore changing their adsorption potential. (301, 303, 308, 345, 346) Moreover, MP and antibiotic degradation can take place, particularly in WWTPs where oxidative tertiary treatment systems are deployed. There is limited evidence of how these complex systems, containing large number of distinct pollutants influence MP adsorption and transportation of organic contaminants. In previous studies pristine reference MPs of PE, PS, PVC and PP were tested for adsorption of organic contaminants, but the adsorption capacity of weathered MPs have not been widely tested yet. (51) CAZ has an octanol water partition coefficient of -1.60 (347) meaning that the antibiotic is hydrophilic and will have repulsive interaction with hydrophobic MPs. This repulsive interaction will be reduced by MP ageing as the formation of oxygen containing functional groups by oxidation decreases plastic hydrophobicity. (43)

This chapter presents the first study of CAZ adsorption by MPs with a focus on the changing behaviour of weathered MPs within WWTPs. Pristine and weathered samples of different polymer types with different size and shape are considered, to build an understanding of complex MP antibiotic interaction within these systems.

6.2 Materials and methods

The general materials and methods are described in detail in Chapter 2. The mass loss of plastic was used to track the weathering of PET and PE. Additionally, PE bead sizing was performed using images gathered by optical microscopy and particles (n= 50) were sized using ImageJ software. AFM and SEM were used to further probe the roughness of the PET fibre samples and to estimate particle size for PET, PU, PS and TWPs. FTIR was used to gather an IR spectra of each polymer surface to gain information on the presence of functional groups and chemical oxidation as a result of weathering. (180)

A robust method for quantification of CAZ in water and wastewater is required in order to study its adsorption by MPs. This section outlines the initial screening and selection of methods.

6.2.1 UV/visible spectrophotometry

In pure water it is possible to directly measure UV absorbance of CAZ in water. Routine testing of the drug in bulk and solid dose form has been reported in the literature. (348) CAZ has strong absorbance in the UV region and so appropriate dilution prior to analysis was required in these studies. As a starting point, the potential of direct UV absorbance as a quantitative measure of CAZ in water and wastewater was considered. The details of the methods are provided in Section 2.4.1.6 while Figure 2.8 shows the calibration curve. Direct measurement of the UV absorbance offers a linear range between 1-100 mg L^{-1} (and higher if solutions are further diluted) for a strong absorbance peak at 256 nm.

As CAZ is oxidised (For example by UVC irradiation), the colour of the solution changed from clear and colourless to pale yellow as shown in Figure 6.2. This is reflected in the UV-visible absorbance spectrum as shown in Figure 6.3.

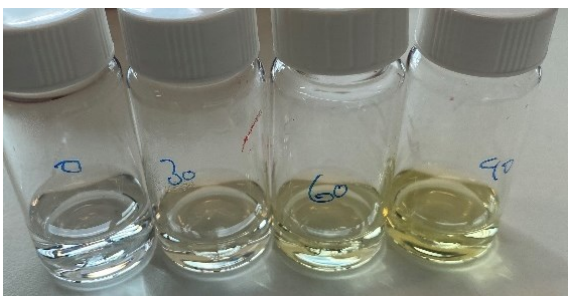

Figure 6.2 Ceftazidime in water upon exposure to UVC irradiation for (left to right) 0, 30, 60 and 90 minutes

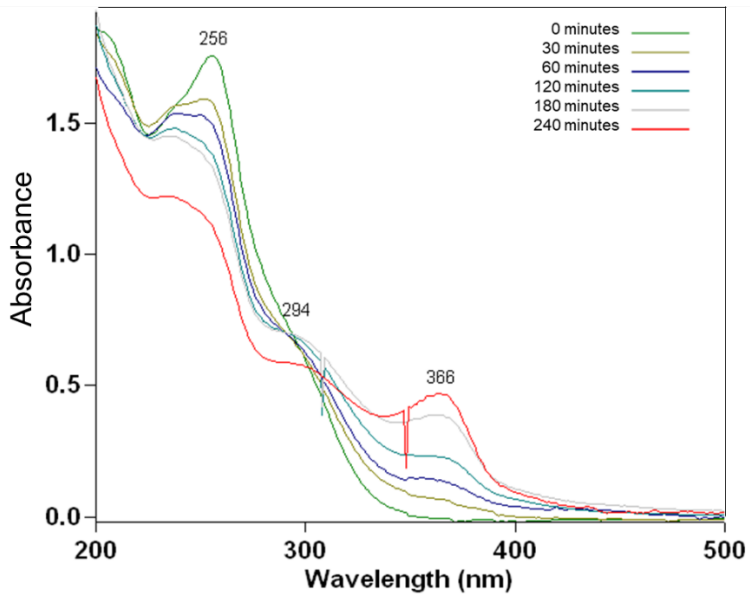

Figure 6.3 Ceftazidime UV-visible absorbance spectrum change over time with UVC irradiation (Initial CAZ concentration 0.5 g L^{-1}, UVC irradiation 31.8 mW cm^{-2})

Upon exposure to UVC irradiation, the characteristic CAZ peak at 256 nm decreases in absorbance intensity and a new peak emerges at 366 nm as well as a shoulder feature around 294 nm. The colour change and emergence of the peak at 366 nm indicates a UV active degradation product of CAZ photo-degradation. As degradation of CAZ was not the focus of this chapter, the identity of these degradation products was not further explored but provides an interesting avenue for future studies. Although this degradation product has not been identified in the current work, consideration of the degradation behaviour of similar cephalosporin antibiotics under oxidative conditions may be indicative of this case. Cephalexin, upon oxidative degradation, underwent transformation via opening of the beta-lactam ring. (348) The resulting partially degraded product displayed reduced toxicity towards S. cerevisiae as compared to the bulk antibiotic. The concentration of CAZ can be followed using the 256 nm absorbance value in reference to standard curve provided there are no interferances from co-contaminants. UV-visible spectrophotometry was considered as a high-throughput means to determine CAZ concentration in water but discarded due to poor sensitivity at low concentrations and potential interference from co-contaminants in real wastewater.

6.2.2 Derivitisation of ceftazidime for visible range spectrophotometry

The presence of organic contaminants in wastewater presents a challenge for the analytical determination of CAZ by simple UV absorbance as many of these chemicals also absorb in the UV range, causing interference. CAZ does not absorb in the visible light range but can be chemically modified to do so with the aim of allowing quantification in water when other UV active molecules are present.

In 2003, Nagajara et al. (349) reported a method for sulphonamide derivatives quantification within pharmaceutical formulations by coupling to 3-aminophenol. Although their method development did not test for CAZ. This poses a viable method for the drug class. More recently, Mohammed et al. (350) used a diazotised CAZ coupled with 4-tert-butanol to produce a coloured compound for simple UV-vis analysis. A general spectrophotometric method for cephalosporin antibiotic concentration determination (including CAZ) in bulk and within pharmaceutical formulations was reported by Roopa et al. (351) Diazotisation of CAZ followed by coupling to 3-aminophenol yields a red product which has a maximum absorbance at 500 nm. This method is applied here and the transformation shown schematically in Figure 6.4.

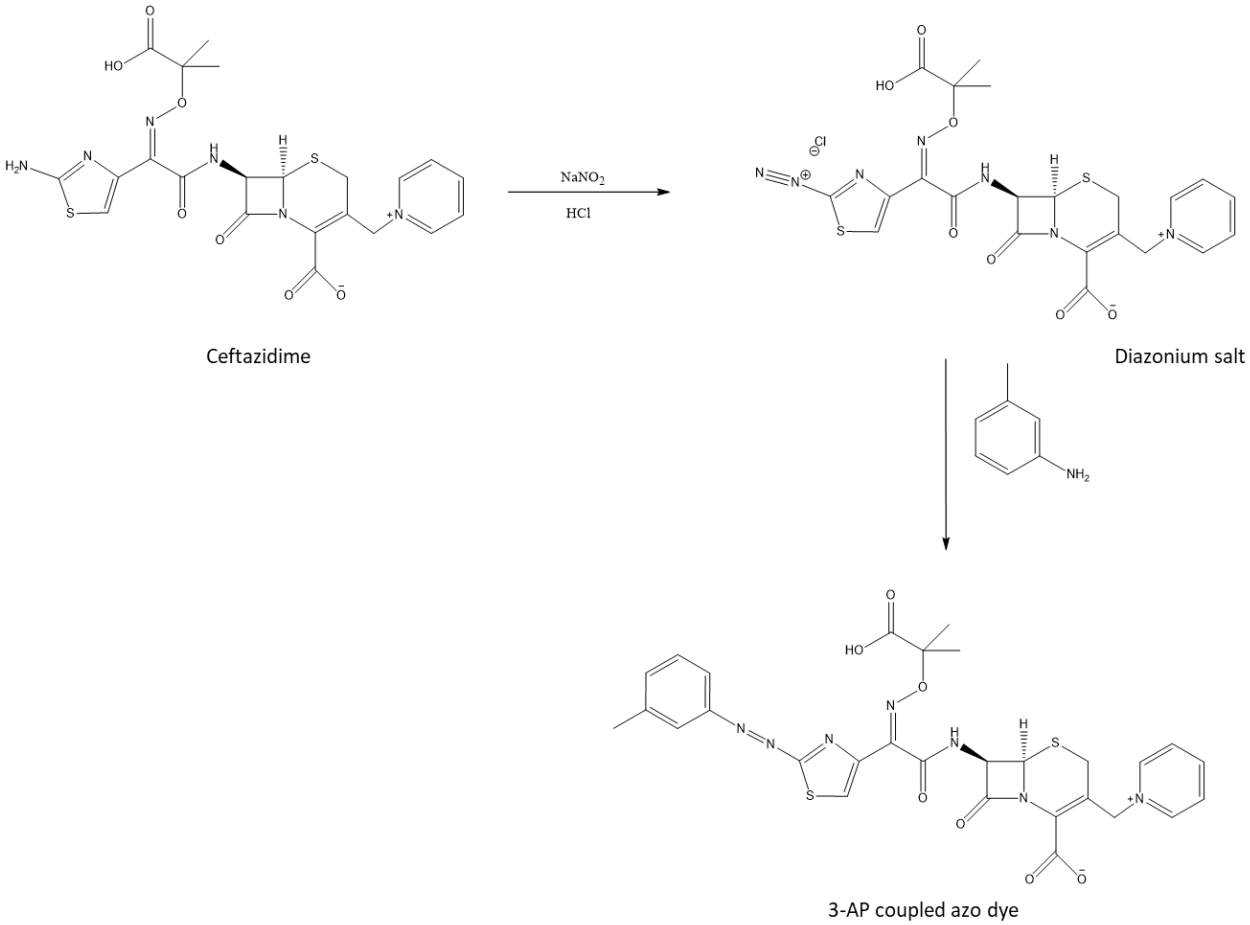

Figure 6.4 Reaction scheme for diazotisation of ceftazidime and coupling with 3-aminophenol

Preparation of the coupled azo-dye derivatised CAZ was achieved as follows. An aliquot (2.5 ml) of ceftazidime solution was transferred into a 10 mL calibrated flask. To the flask 2.5 mL of 0.1% sodium nitrite solution and 2.0 mL of 1 M hydrochloric acid was added. The flask was then allowed to cool in an ice bath at a temperature of -3 °C. The diazotisation was carried out with stirring for 20 minutes. After this 1.0 mL of 2% sulphamic acid was added to remove any excess nitrite in the solution followed by 1.0 mL of 0.3% aminophenol were added to couple with diazotised ceftazidime. The flask was then allowed to cool for 15 minutes in the ice bath and then removed to ambient temperature. After attaining room temperature, the flask was diluted to the 10mL mark with distilled water and mixed well. Then, after 10 minutes, the absorbance was measured at 500 nm. For high concentration solutions, a clear colour change from clear and colourless to deep orange/brown was observed (Figure 6.5).

Figure 6.5 Ceftazidime standard solutions after derivitisation (concentrations from left to right: 1000, 500, 200, 100, 50, 0 mg L^{-1})

A stock solution of Ceftazidime (1000 mg L^{-1}) was initially prepared. This standard stock solution was diluted with distilled water to obtain working standards of 1000, 500 200, 100, 50, 25, 10, 5, 2.5 and 1 mg L^{-1}. The calibration curve prepared from solutions in the range 100-1000 mg L^{-1} is shown in Figure 6.6. No calibration curve could be produced for lower concentrations due to no peak in the visible spectrum.

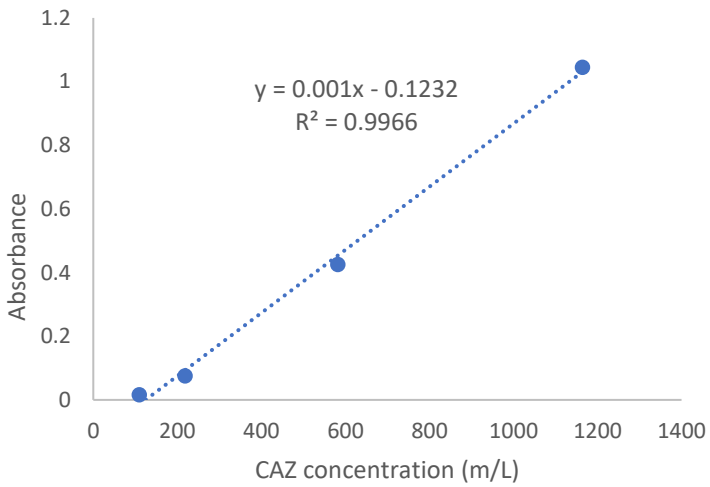

Figure 6.6 Calibration curve of derivatised ceftazidime in water measured at 500 nm

This method provides a linear calibration curve in the range of 100 – 1000 mg L^{-1}. However, no signal was detected for concentrations below 100 mg L^{-1}. For analysis at lower CAZ concentrations, it is not possible to produce a colour intense enough to observe in the visible spectrum, limiting the utility of this method for calculating absorbance of CAZ by MPs

presented in this chapter (as very low concentration changes are considered). Again, the change in the spectrum upon UVC irradiation was considered and is shown in Figure 6.7. In this case, azo-coupling reaction was performed on aliquots removed from the reactor after UV exposure for the designated time. As CAZ is degraded by UVC irradiation, the resulting peak at 500 nm is reduced in intensity. There is no clear emergence of a peak due to degradation product formation. In the absence of other reagents, the degradation of CAZ can therefore be followed using the derivitisation method (with the stipulation that high concentrations are required). However, in the presence of residual H_2O_2, the derivitisation process was unsuccessful without further quenching steps, limiting the use of the method for high-throughput testing where samples may contain residual AOP reagents.

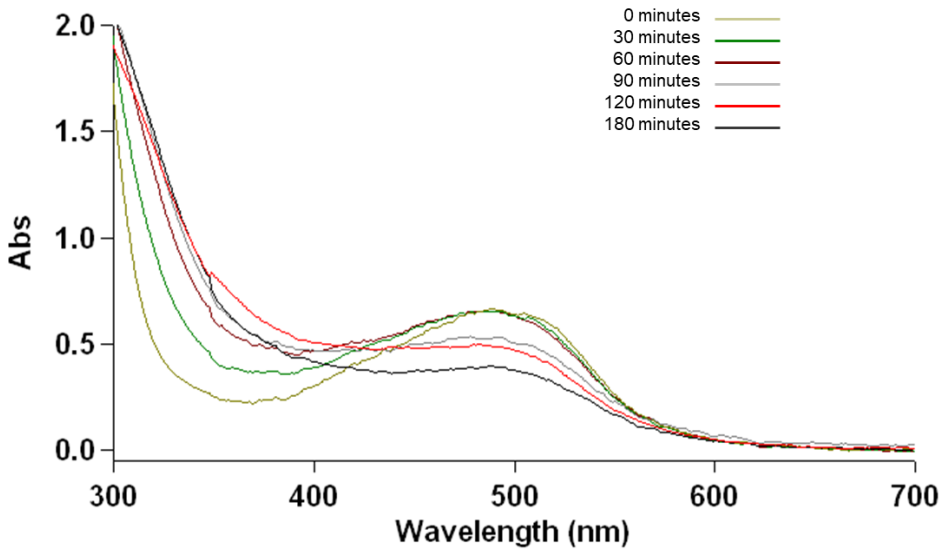

Figure 6.7 Azo-coupled ceftazidime UV-visible absorbance spectrum change over time with UVC irradiation (Initial CAZ concentration 0.5 g L^{-1}, UVC irradiation 31.8 mW cm^{-2})

To avoid the potential of interference and allow reliable quantification of CAZ at very low concentrations, HPLC was used for analysis in this chapter, as described in Section 2.4.1.7. HPLC peak area was compared to a standard curve to determine the concentration. (352) HPLC offers a highly sensitive means to determine CAZ concentration in water in the presence of degradation products and co-contaminants. For all experiments presented in the remainder of this chapter, HPLC data was used to calculate the adsorption by MPs.

Weathered PU adsorption could not be determined by HPLC due to interference from degradation products which could not be readily separated from CAZ. Future work should consider identification of these degradation products by mass spectrometry in order to develop a suitable separation method to allow quantification of CAZ adsorption by weathered PU.

6.3 Artificial weathering of MPs for adsorption testing

Various weathering processes were applied in order to prepare MPs with a degradation degree relevant to wastewater systems. To prepare PET fibres with a controlled degree of degradation, a standardised hydrolysis treatment was applied as described in Section 2.2.1. Fibres were weathered to three varying degrees of degradation by treating them for 1, 2 or 3 h. Figure 6.8 shows SEM images of the fibres after 1 and 2 h of treatment. Figure 6.9 shows the mass loss observed at each stage of degradation. Fibres treated for 3 h are shown in Figure 6.13.

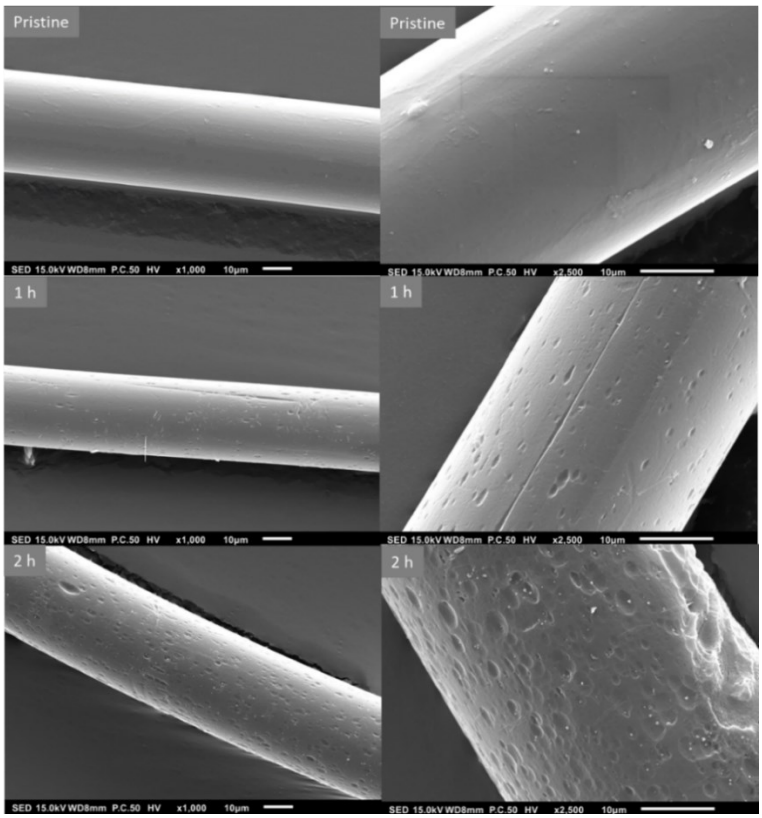

Figure 6.8 SEM images of polyester fibre surface at varying stages of degradation as result of hydrolysis accelerated degradation (0, 1, 2 h treatment)

The carbonyl index for raw PET fibres (6.7 ± 0.2) and those treated from 1 and 2 h (7.1 ± 0.4 and 6.8 ± 0.3) remain unchanged. The CI then decreases with treatment time of 3 h (5.5 ± 0.2), in contrast to samples aged by UV based weathering methods, where the CI increases with time during weathering. (267) This is due to the release of carbonyl groups in carboxylic acid degradation products released by the hydrolysis of ester bonds in the polymer. (165, 353) Fibres aged for 3 h were selected for use in adsorption studies as they represent heavily weathered fibres, providing a clear comparison to pristine fibres.

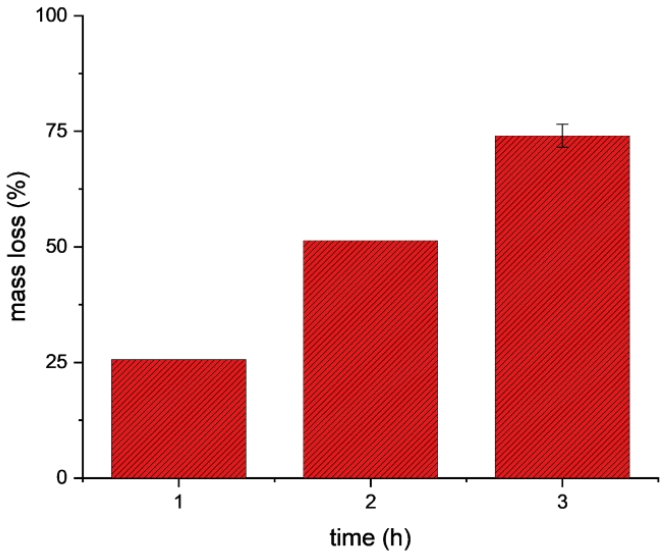

Figure 6.9 Mass loss of polyester fibres after hydrolysis accelerated weathering.

PE beads were weathered for 9 h using an ultraviolet activated hydrogen peroxide advanced oxidation method reported previously. (267) PS and PU foams were then weathered for 600 h in a Xenon test chamber, Q-SUN Xe-3 chamber, according to the ISO 4892-2:2013 standard to replicate environmental degradation. (168) During weathering, samples were exposed to 60 W m^{-2} of irradiation at 38 °C in the chamber with 50% relative humidity at a fan speed of 2000 rpm. TWPs were used as received from end-of-life commercial tyres and not subject to further artificial weathering. PS and PU foams and rubber TWPs were cryogenically ball milled in a Domel Tehtnica MillMix 20. Representative photographs of each MP type are included in Section 2.2.

6.4 Adsorption of ceftazidime by microplastics

In wastewater treatment systems, a broad range of MP shapes, types, and degradation degrees are present, impacting their interaction with co-contaminants. (49, 50) Ten MP of various polymer types and physical forms, described below in Table 6.1, were considered in experiments presented in this section. Adsorption of antibiotics by each MP will vary, therefore complicating attempts to quantify their spread in real systems. Figure 6.10 shows SEM images of representative MPs, commonly found in WWTPs, that were tested for CAZ adsorption. Additional SEM images to show hard and soft variants of PS and PU and all tyre brands are included in Section 6.5.1.

Table 6.1 Microplastic samples studied for CAZ adsorption

Microplastic type	Size range (µm)	Shape	Artificial weathering process
Polyester (PET)	40 (diameter) 70 - 2117 (length)	Fibre	Alkaline hydrolysis (NaOH. 3 h)
Polyethylene (PE)	250 – 850	Beads	UVC activated H_2O_2 (500 mg L^{-1}, 9 h)
Hard polystyrene (Hard PS)	50 - 80	Foam particle	Xenon lamp (600 h)
Soft polystyrene (Soft PS)	50 - 80	Foam particle	Xenon lamp (600 h)
Hard polyurethane (Hard PU)	10 – 80	Foam particle	Xenon lamp (600 h)
Soft polyurethane (Soft PU)	10 – 80	Foam particle	Xenon lamp (600 h)
Bridgestone Tyre	300 -1000	Rubber fragment	-
Kumho Tyre	300 -1000	Rubber fragment	-
Michelin Tyre	300 -1000	Rubber fragment	-
Goodyear Tyre	300 -1000	Rubber fragment	-

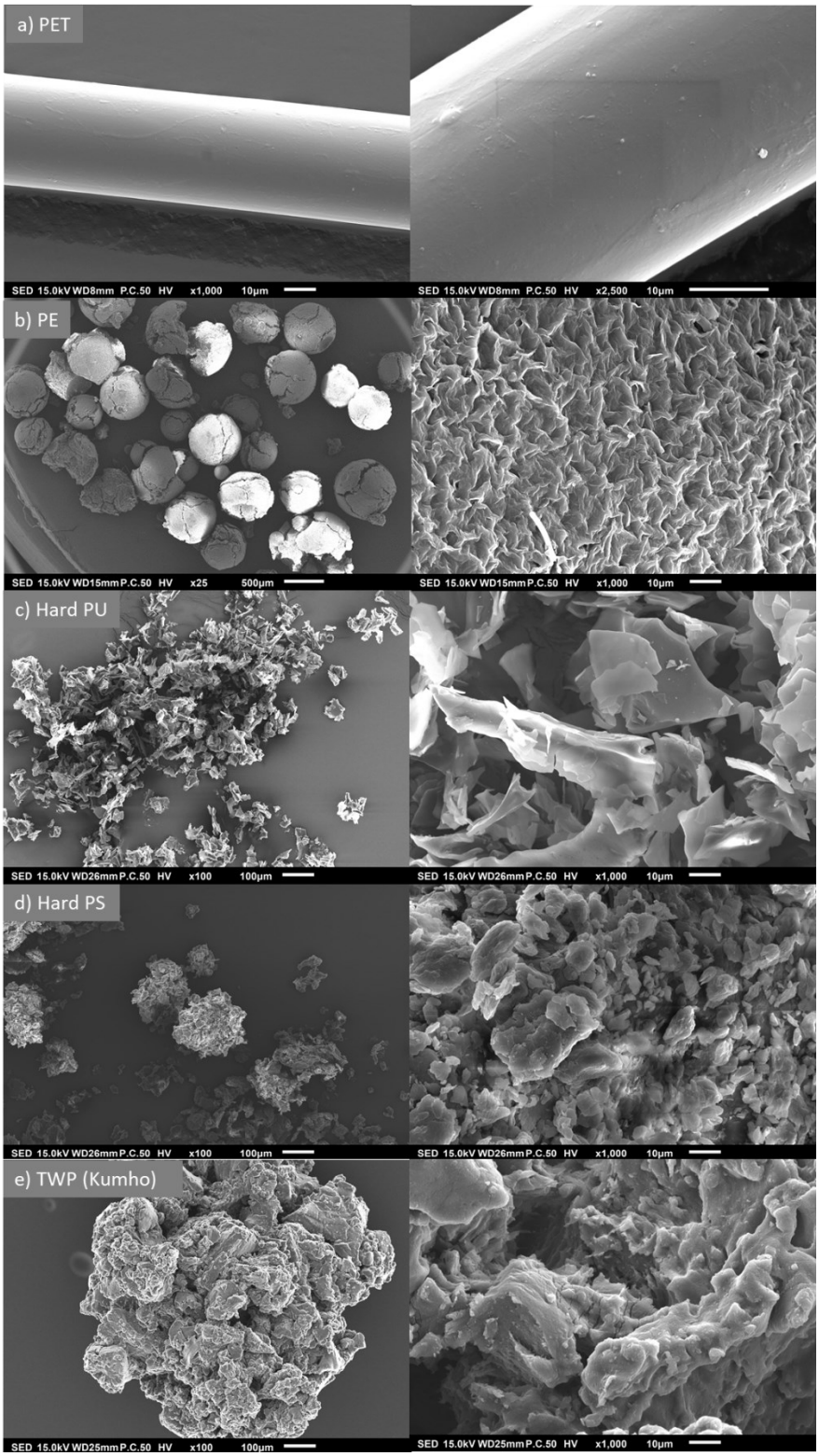

Figure 6.10 Representative SEM images of **a)** PET, **b)** PE, **c)** PU, **d)** PS and **e)** TWP MPs (left) and their magnified surface structure (right)

The MPs selected for this study show diverse particle size and surface morphology. PET (Figure 6.10 a) is semicrystalline and polar with aromatic groups and oxygen containing functionalities providing the potential for intermolecular interaction with CAZ molecules in water. Raw non-weathered PET fibres display a very smooth surface in SEM imaging with few features evident. In contrast, PE beads (Figure 6.10 b) extracted from facewash have a very rough surface due to their intended function as exfoliants. The extracted PE beads vary in size between 250 – 850 µm as shown in Figure 6.11.

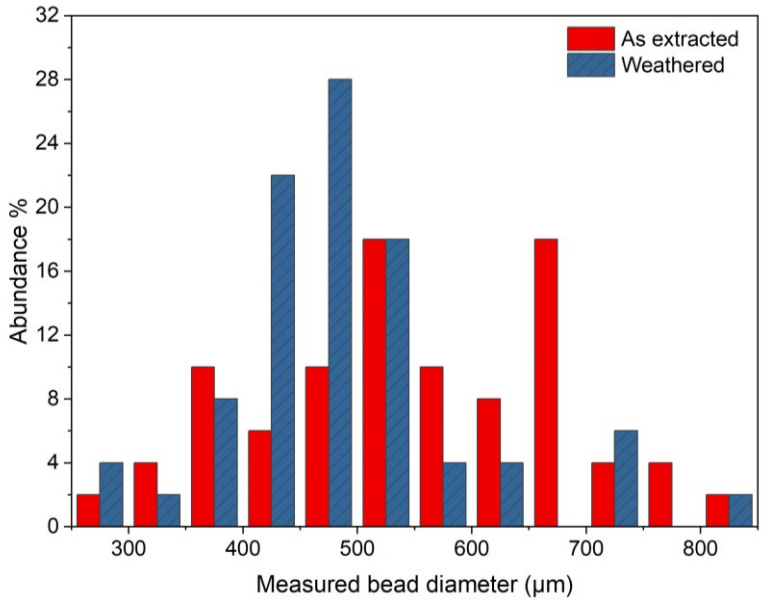

Figure 6.11 Size distribution of PE beads as extracted from facewash and weathered by advanced oxidation process (UVC/H_2O_2, 500 mg L^{-1}, 9 h)

Cracked and fragmented beads are commonly observed in all samples as well as whole spheres, matching the observations of MPs in facewash samples in the literature. (279) This textured surface promotes adsorption of organic contaminants as shown in related literature where a 5-fold increase in tetrabromobisphenol adsorption was recorded as compared to smooth reference PE spheres of the same size. (354) PU foam (Figure 6.10 c) is characterised by a flaked structure with a large number of small fragments collected in agglomerations. PS foam MPs (Figure 6.10 d) comprise of small (50-80 µm diameter) aggregations of many MPs with the individual fragments having a granular appearance. TWPs (Figure 6.10 e) are sized

within the range of 300 – 1000 µm and exhibit a rough, textured surface. The adsorption of CAZ by these MPs was studied over a 24 h period and the results are shown in Figure 6.12.

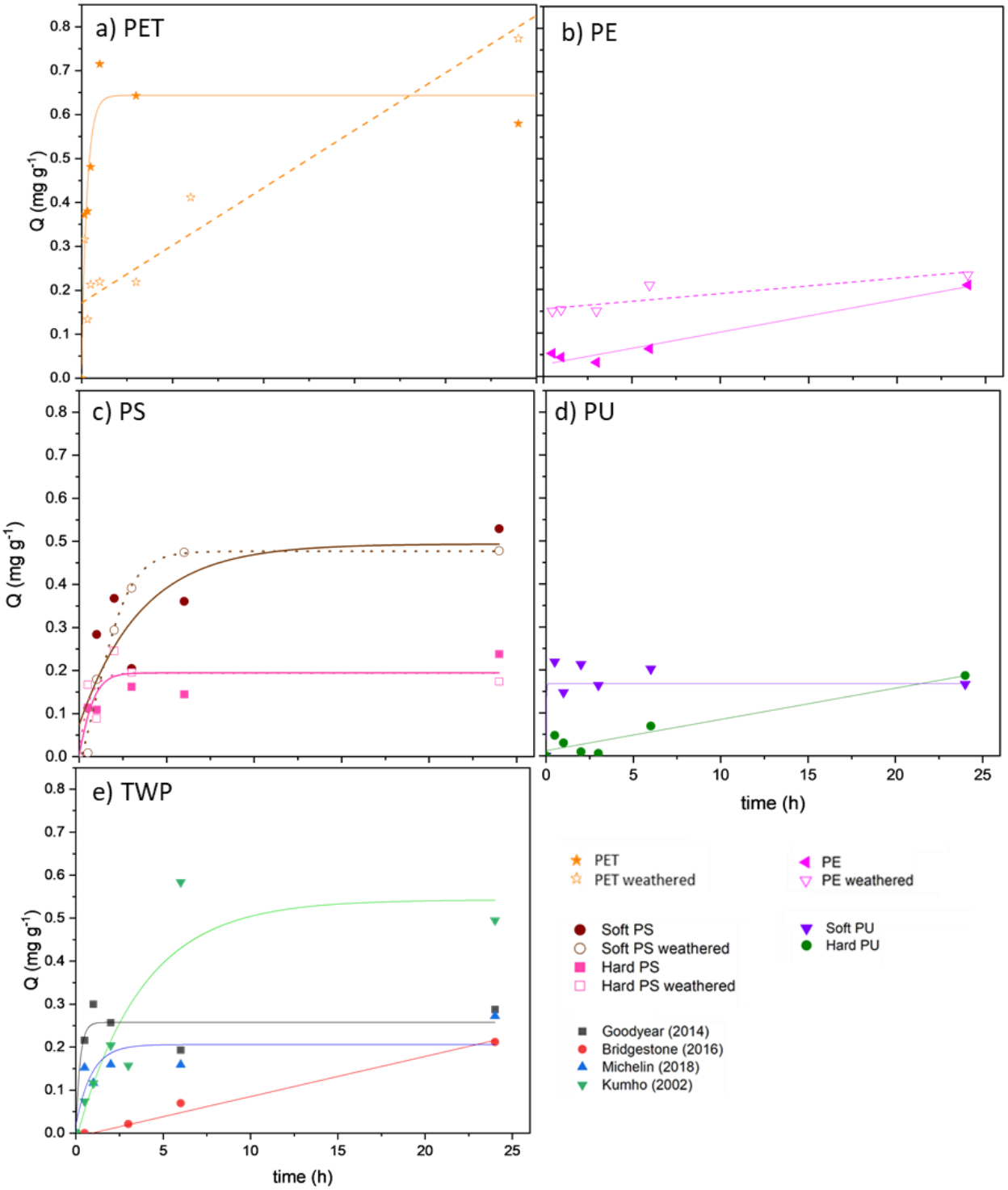

Figure 6.12 Adsorption capacity of CAZ over time by **(a)** PET fibers, **(b)** PE beads, **(c)** PS foams, **(d)** PU foams, and **(e)** TWP rubbers. (MPs concentration 2 g L^{-1}, CAZ concentration 10 mg L^{-1})

In Figure 6.12 a it was observed that pristine PET fibres reached a maximum adsorption of 0.664 mg g^{-1} within the first 3 h of contact which was then maintained almost unchanged throughout the rest of the contact time. However, the CAZ adsorption rate by the weathered PET fibres was initially slower than that of the pristine ones, but after 24 h the weathered fibres reached the highest adsorption of 0.773 mg g^{-1} compared to all the other MPs. Equilibrium was not reached in 24 h and CAZ adsorption capacity continued increasing, reaching 1.432 mg g^{-1} after 48 h of contact time. Figure 6.12 b shows that the adsorption of CAZ by PE microplastic beads increased linearly with time for both the raw extracted and weathered beads, reaching 0.210 and 0.234 mg g^{-1} in 24 h respectively. Adsorption capacity was higher for the weathered beads compared with the raw extracted ones. Regarding the soft PS foams displayed in Figure 6.12 c a substantially larger capacity for CAZ adsorption than the hard PS samples, reaching 0.53 mg g^{-1} and 0.48 mg g^{-1} in 24 h for pristine and weathered soft PS samples respectively, but CAZ adsorption for hard PS was only 0.24 mg g^{-1} (weathered) and 0.17 mg g^{-1} (pristine) after 24 h. Slower mass transfer at the plastic surface is expected in the high density polymer, a finding in agreement with a study measuring tetracycline adsorption, during which low-density polyethylene was found to have a greater adsorption capacity than high-density polyethylene due to mass transfer differences. (355) The difference in the adsorption capacity of soft and hard PS foams could also be influenced by the presence of additives. Weathered foams were tested for adsorption of CAZ and both hard and soft PS showed unchanged uptake over 24 h when compared to the pristine samples. This result is in line with results presented by Wu et al. where aged PS was shown to have a reduced capacity for adsorption of a polybrominated diphenyl ether due to a reduction in the number of available adsorption sites. Soft and hard PU foams had a low overall uptake, reaching 0.17 mg g^{-1} and 0.19 mg g^{-1} respectively after 24 h (Figure 6.12 d). It was also observed that the initial uptake increased more slowly for the hard PU compared to soft PU foam, again related to the rate of mass transfer related to the extent of chain branching and crosslinked polymer structure inhibiting movement of organics within the structure. (356)

Figure 6.12 e demonstrates that the Kumho TWP had the highest adsorption capacity of 0.495 mg g^{-1} after 24 h, followed by Goodyear (0.288 mg g^{-1}), Michelin (0.273 mg g^{-1}), and Bridgestone (0.212 mg g^{-1}). This difference in maximum value can be rationalised when the differences of each rubber are considered. Kumho TWPs are natural rubber whereas

Bridgestone, Michelin and Goodyear TWPs are artificial rubbers manufactured for passenger vehicle tyres made with styrene-butadiene rubber (SBR) which may influence the adsorption behavior due to their differing properties. (357) Also, the Kumho tyres essayed in this study were manufactured 12 years before the earliest passenger tyre sample (Goodyear 2014) indicating that during useful life there may be a higher degree of natural weathering, leading to changes in the adsorption properties. (301) Interestingly, Goodyear and Michelin show rapid increase in CAZ adsorption in the first 3 h, while Bridgestone increased at a slower linear rate reaching maximum adsorption after 24 h.

All in all, it was observed that CAZ adsorption, by different MPs followed the order, from higher to lower capacity: PET fibers (weathered) > PET fibers (pristine) > soft PS (pristine and weathered) > Kumho TWP > Goodyear TWP > Michelin TWP > hard PS (weathered) > PE weathered > Bridgestone TWP > PE (pristine) > hard PU > soft PU > hard PS (pristine). The chemistry and structure of the MPs were examined, and the results are discussed in the following sections, to further understand the differences in the adsorption capacity of the various MPs. The high adsorption observed for pristine PET as compared to other polymer types (weathered or pristine) indicates that the identity of polymer influences the interaction with antibiotics to a greater extent that the degree of weathering and therefore surface area. Intermolecular π-π interactions are possible in cases where the polymer chain contains an aromatic group which will contribute to the high adsorption of PS and PET, compared to PE. (358-360) Indeed, this observation is matched by Li et al. (361), who showed that PS had a greater adsorption capacity than PE for three different antibiotics due to this interaction. Functional groups within the polymer chain such as those in PU may also form hydrogen bonds with antibiotics (359), although low PU adsorption of CAZ observed in our study indicates that contribution of this interaction is not significant. Surface area is also likely to play a key role in maximum adsorption capacity as this is directly related to the number of adsorption sites. In general, weathering increases the adsorption of CAZ which can be explained by considering the increase in surface area by physical degradation of MPs during weathering. Due to their large surface area, TWPs were shown to have a greater adsorption capacity than PE MPs in a study by Fan et al. using chlortetracycline and amoxicillin. (72) In general the range of adsorption capacities identified in the current work are broadly similar

to those reported for other cephalosporin antibiotics.(362) These effects are explored further by studying the surface change of MPs induced by weathering.

6.5 The effect of weathering on microplastic surface structure

6.5.1 The effect of weathering on microplastic physical characteristics

SEM and AFM analyses of the weathered MPs were carried out to study the effect of ageing on the structure of the polymer surface. Representative SEM images are presented in Figure 6.13 shows weathered PET fibres, treated by hydrolysis for 3 h using the method outlined in Section 6.3. The weathered PET fibres, which showed the highest adsorption capacity among all MPs, showed clear changes on their surface imaged by SEM after the weathering process.

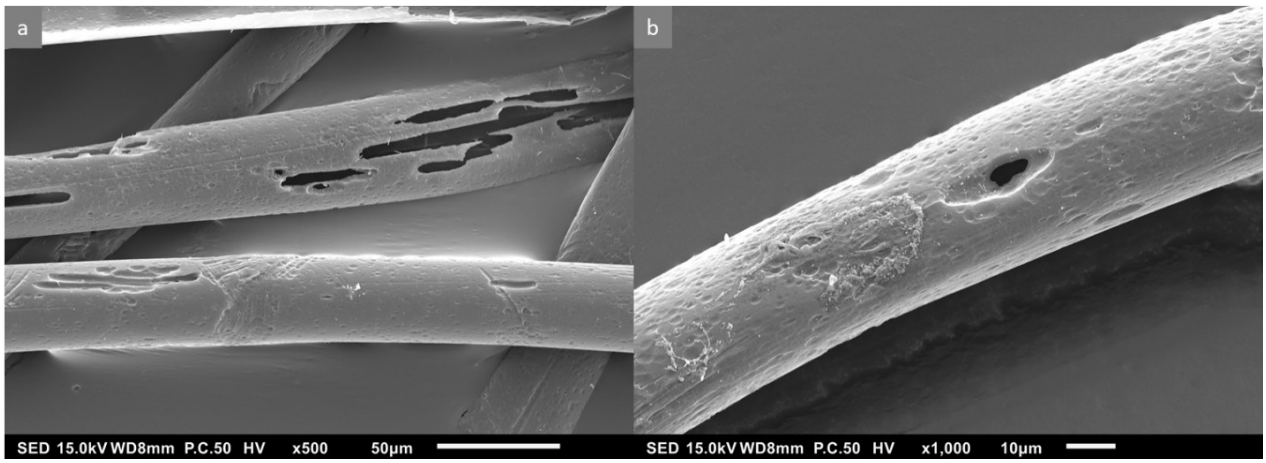

Figure 6.13 a, b) Representative SEM images of weathered PET fibres (NaOH alkaline hydrolysis, 3 h)

Cracking and fragmentation features are visible for the weathered fibres as well as surface hole and dimple formation. This weathering is consistent with previously observed accelerated fibre degradation under advanced oxidation treatment in wastewater and hydrolysis treatment. (165, 267) It should be also noted that the weathered fibres were greatly reduced in bulk mass by 74% compared the pristine fibres, indicating the aggressiveness of the hydrolysis weathering process that was applied and the high deterioration of the surface of the fibers.

The higher maximum adsorption capacity of weathered PET can be explained by a greatly increased surface area as shown by the increased surface cracking and pitting. The change in initial rate of CAZ adsorption may be influenced by the presence of MPs degradation products in the solution competing for adsorption sites or interaction with the antibiotic itself. Similarly, competition for adsorption sites was shown to reduce the rate of antibiotic adsorption as MP size was decreased to the nanoscale in a study of ciprofloxacin on PS particles. (363) During the weathering process of PET fibres, particles are fragmented into small micro and nano fragments which may also affect the rate of adsorption. (267)

As weathered PET fibres displayed the highest adsorption capacity of all MPs tested, the surface morphology was further investigated at the nano-scale. The surface roughness was measured by AFM and representative height plots and 3D surface maps for pristine and weathered fibre surfaces are shown in Figure 6.14 a and b. It can be seen that holes and ridges are visible in the images as dark and white areas of the 2D plot respectively. As compared to the untreated PET fibre, a large increase in surface roughness was observed with the mean value increasing from 9.23 nm (pristine fibers) to 31.38 nm after weathering (Figure 6.14 c). This increase of the roughness of the surface in both nano and micro (Figure 6.13) scale are both expected to positively influence to adsorption capacity of MPs.

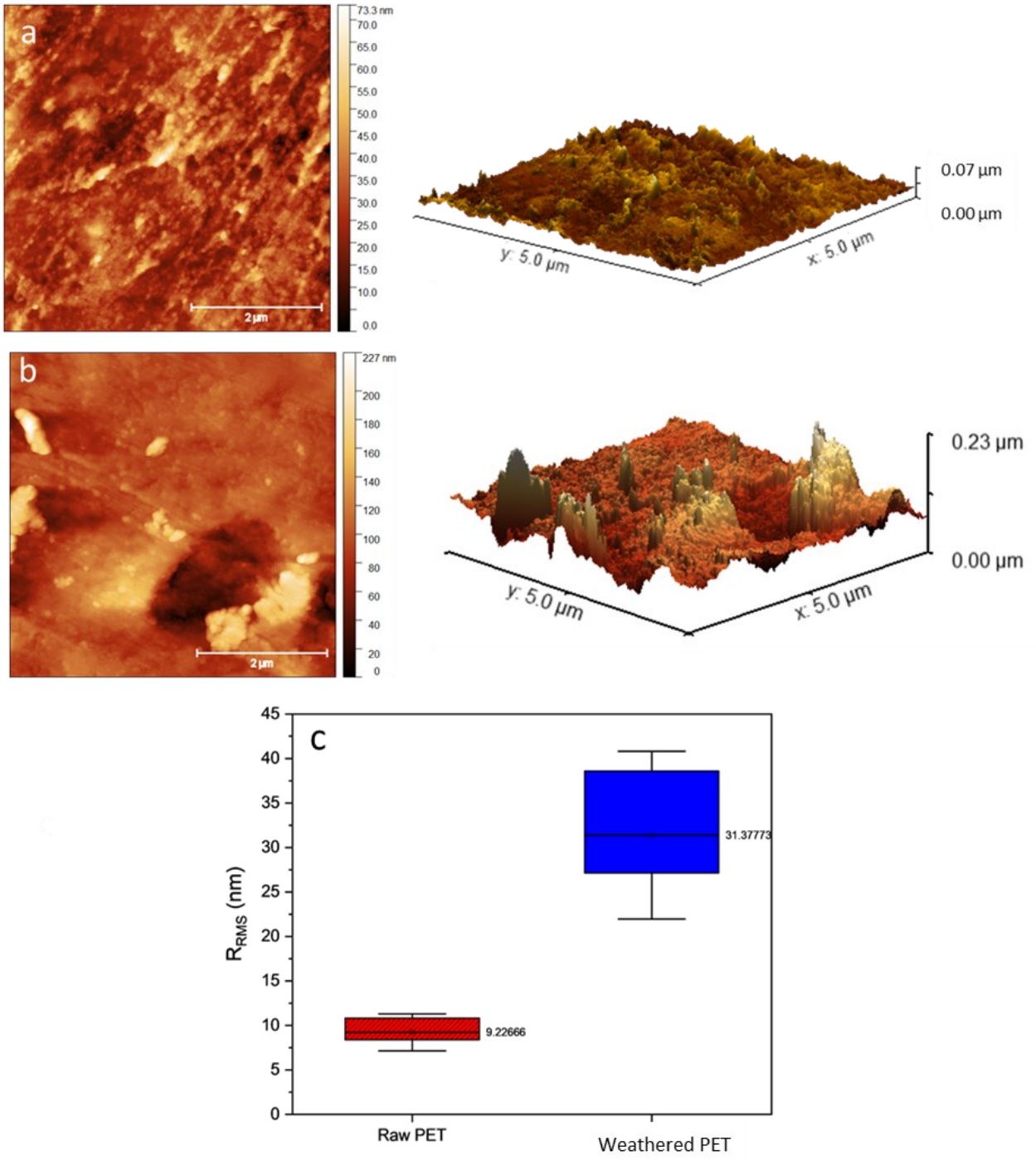

Figure 6.14 AFM height images and surface maps of **a)** pristine PET fibre, **b)** weathered PET fibre and **c)** Roughness (R_{RMS}) of pristine and weathered polyester fibres (mean values marked, 25/75th percentile and standard deviation represented in the box and whisker plot)

The surface of PE beads, PS/PU foams and TWPs were imaged by SEM and are presented in Figure 6.15, 6.16, 6.17 respectively.

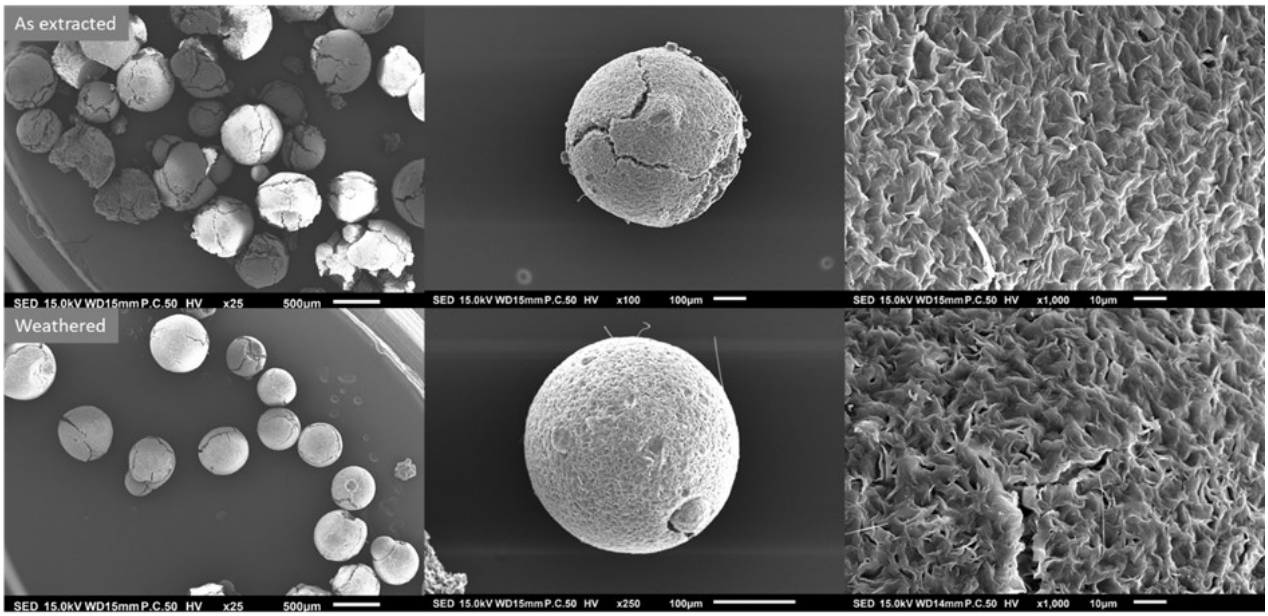

Figure 6.15 SEM images of PE beads extracted from facewash before (top) and after (bottom) weathering

Upon weathering of PE beads, little change is observed on the surface. However, a trend towards smaller diameter from a starting mean value of 552 µm to 485 µm was observed in the sizing data (Figure 6.11), although the overall range of bead size remained the same. Understanding their fragmentation during weathering sheds light on the potential change in toxicity. PE MPs have been shown to be size dependent due to an increased retention of small fragments in biota. (364, 365) This was accompanied by a bulk mass loss of 10.8% over 9 h of weathering. The trend in bead size towards smaller diameter MPs after weathering will affect the adsorption behavior. Smaller particle sizes are expected to accompany increased adsorption capacity due to surface area increases. However, competition at the surface was reported at a threshold size in the adsorption of ciprofloxacin onto PS micro and nanoplastics (363) indicating that very small particle sizes may impede the rate of antibiotic adsorption.

Significant changes to PS and PU foams were not observed in the SEM images upon weathering. This explains the limited change in maximum adsorption between pristine and weathered samples of each of these polymer types. Without a large change to the physical surface of these MPs and the associated surface area change, weathering did not significantly affect the adsorption of CAZ.

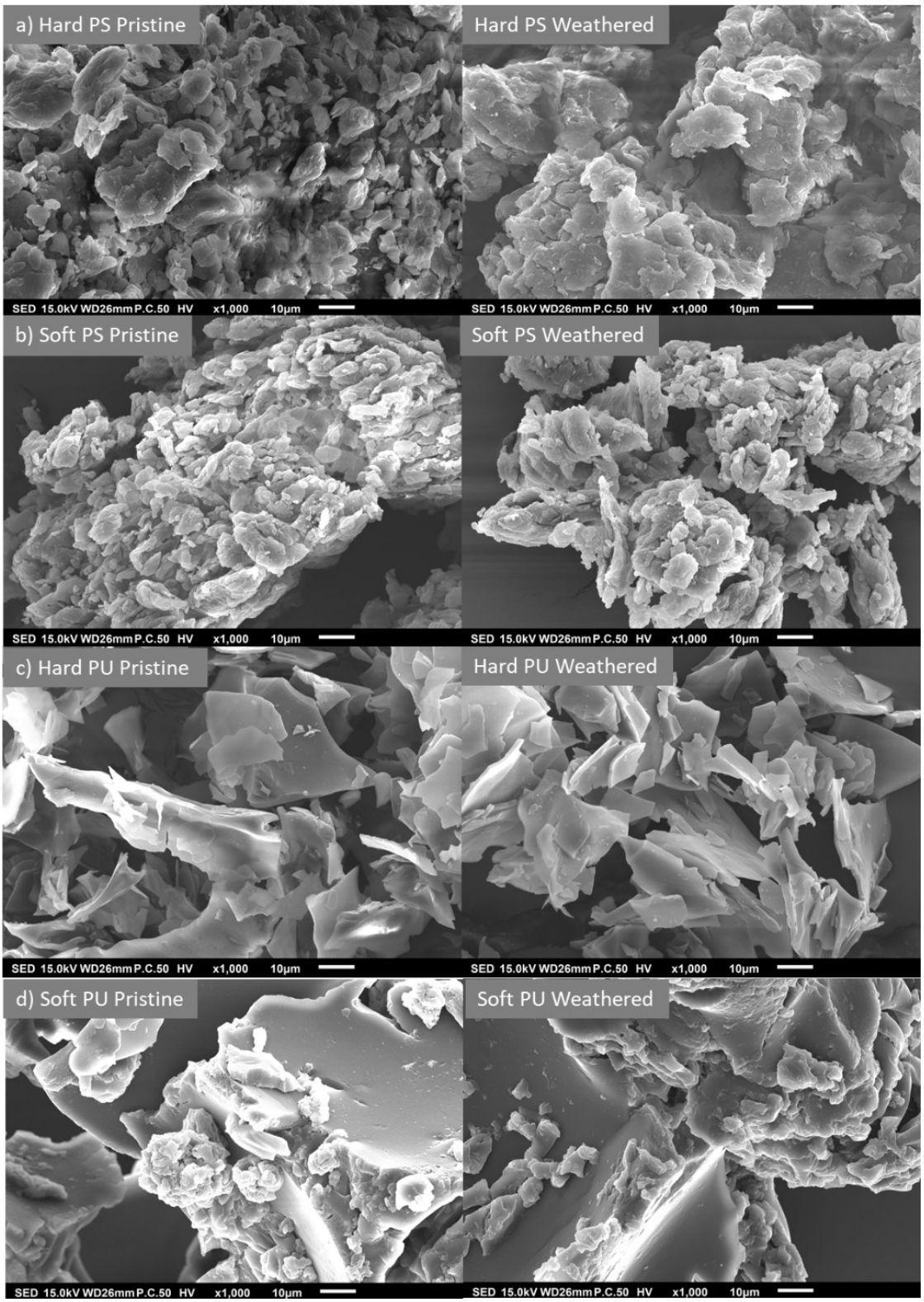

Figure 6.16 SEM images of a) Hard PS b) soft PS c) hard PU and d) soft PU before (left) and after (right) weathering

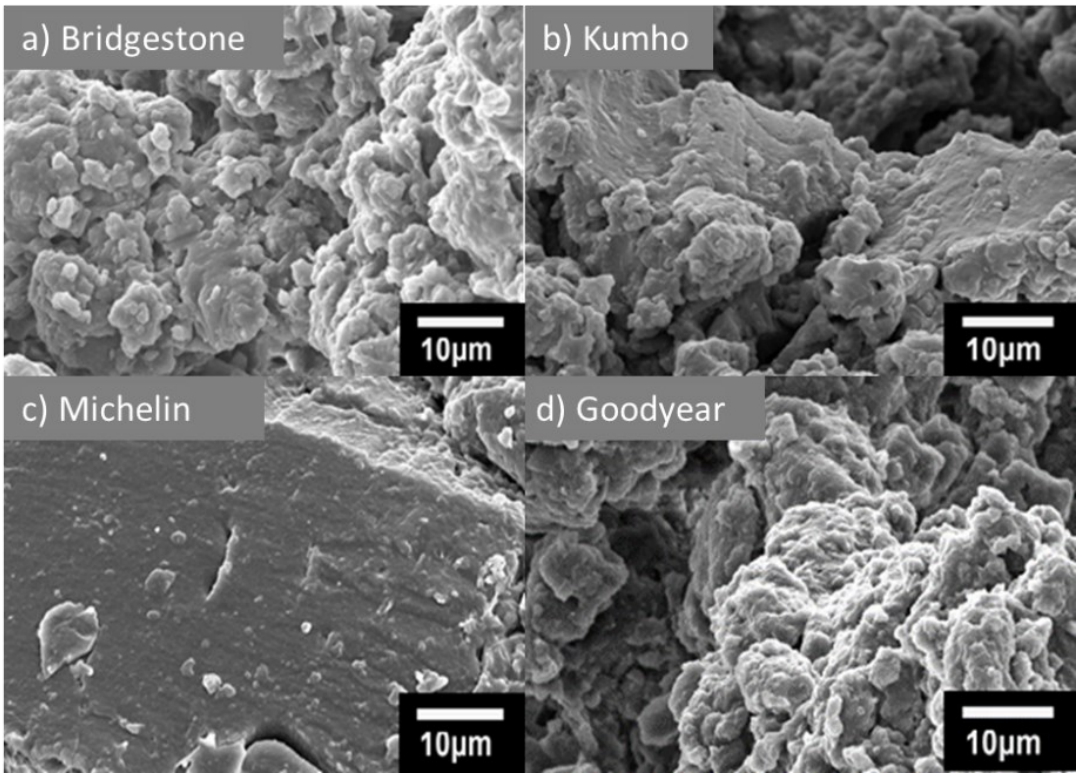

Figure 6.17 SEM images of a) Bridgestone, b) Kumho, c) Michelin, d) Goodyear TWPs

6.5.2 The effect of weathering on polymer surface chemistry

Weathering of polymer surfaces typically introduces oxygen containing functional groups which may be capable of stronger interaction with antibiotics, thus altering the adsorption behavior of MPs. (358, 362) FTIR spectra were gathered for PET, PE, PS, and PU samples before and after weathering with results summarized in Table 6.2. Where possible, the CI was calculated from the FTIR spectra.

Table 6.2 Calculated carbonyl index of PET, PE, PS and PU MP samples

	Carbonyl Index (CI)	
	Pristine	Weathered
PET	6.7	5.5
PE	-	-
Hard PS	0.31	2.35
Soft PS	0.37	3.51
Hard PU	2.26	2.39
Soft PU	0.74	1.70

PET fibres show a decrease in CI during hydrolysis weathering. This is in contrast to samples aged by UV based weathering methods, where the CI increases with time during weathering. (267) The release of carbonyl groups in carboxylic acid degradation products of by the hydrolysis of ester bonds in the polymer are responsible. (165, 353) PE beads have an averaged FTIR spectra unchanged by the weathering process, with no emergence of a clear carbonyl signal. Compared to a sample of PE film, the spectra of PE beads show typical identifying peaks for Linear low-density polyethylene. (184) Variable weathering of individual beads may not be captured in this data due to the FTIR spectra being measured as an average signal from a number of PE beads or insufficient weathering time to observe significant chemical changes. To investigate this, micro-FTIR analysis of individual PE beads displaying the physical characteristics of heavy weathering as observed in the SEM images may be a useful avenue for future work to show localised formation of oxygen containing groups. (366) For PS and PU foams, weathering of the MPs increased the CI.

6.6 PET fibre microplastic adsorption isotherms

The adsorption isotherms were calculated for pristine and weathered PET fibres, which presented the highest CAZ adsorption capacity. Figure 6.18 shows the adsorption capacity in relation to the CAZ concentration in water while the isotherm parameters are listed in Table 6.3. The plotted isotherm curves used in this calculation are included in Appendix A (Figure A.9).

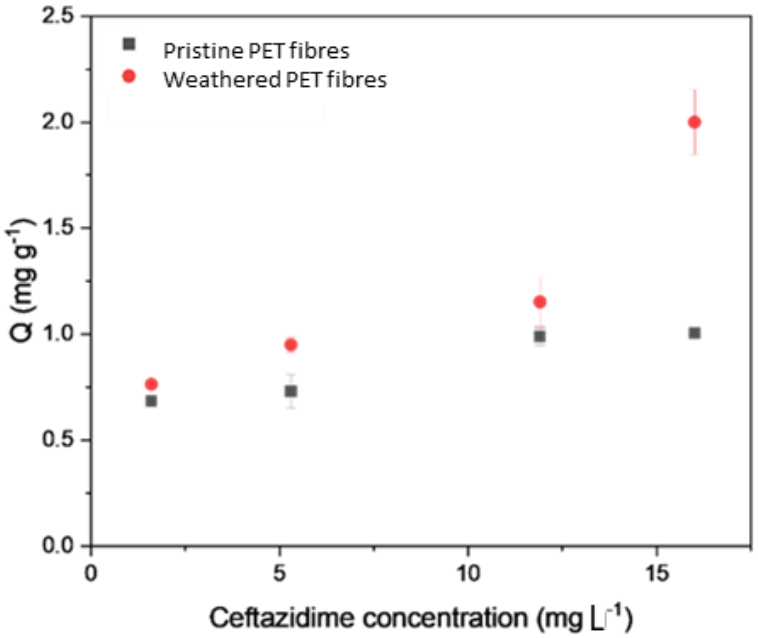

Figure 6.18 CAZ adsorption by PET fibre MPs (working volume 10 mL, MPs 2 g L^{-1})

The concentration of CAZ in solution and the concentration of adsorbent (MPs) were varied and the adsorption isotherms were plotted according to the linear and Langmuir models described in Section 2.4.3. These models were selected to enable comparison across other systems as they are commonly used in literature studies considering organic contaminant adsorption onto MPs. (72, 359, 360, 362)

Table 6.3 Linear and Langmuir isotherm fitting parameters for CAZ (1 – 12.5 mgL-1) adsorption by pristine and weathered PET fibers.

PET fibers	Linear		Langmuir		
	K_d (L g^{-1})	r^2	Q_{max} (mg g^{-1})	K_L (L mg^{-1})	r^2
Pristine	0.023 ± 0.002	0.983	1.10 ± 0.09	0.596	0.987
Weathered	0.045 ± 0.006	0.980	1.27 ± 0.09	0.753	0.995

The adsorption capacity of PET fibres for CAZ varied significantly between pristine and weathered samples. Both isotherm models show good fitting for data in the CAZ concentration range of 1-12.5 mg L^{-1}. Surface area, crystallinity and surface charge are all factors likely to contribute to the change between pristine and weathered samples. (367) No reported adsorption data for CAZ on MPs currently exists in the literature. The reported K_d

values from a linear model for sulfamethoxazole and sulfamethazine uptake by virgin PET were 0.0222 and 0.0226 L g^{-1} (360, 368), which are similar to the K_d obtained for CAZ adsorption in this study, while there were no literature values available for adsorption of antibiotics on weathered PET. (362)

6.7 Conclusions

The effect of MP type, size, shape and weathering on CAZ adsorption was studied via lab scale experiments. Varied rates of uptake and maximum adsorption capacity were linked to the polymer properties, highlighting the importance to consider the specific MPs present in wastewater when studying interactions with chemical co-contaminants. Five polymers (PET, PE, PS, PU, and TWPs) in different forms (fibers, beads, foam and fragments) and sizes (10–1000 µm) were compared. In some cases, weathering of MPs increased the surface roughness and altered the chemical properties as measured by SEM, AFM and FTIR. Weathered PET fibres exhibited the highest capacity for CAZ adsorption reaching 1.432 mg g^{-1} after 48 h contact, as compared to 0.664 mg g^{-1} for pristine PET fibers in the same timescale. The increased adsorption capacity, compared to the other MPs essayed, was linked to the higher surface area, created by the formation of cracks, holes and pitting formed during the weathering process. This trend was not extended across all MP samples with PE and PS showing negligible increase in adsorption upon weathering and the overall order following: PET fibers (weathered) > PET fibers (pristine) > soft PS (pristine and weathered) > Kumho TWP > Goodyear TWP > Michelin TWP > hard PS (weathered) > PE weathered > Bridgestone TWP > PE (pristine) > hard PU > soft PU > hard PS (pristine). Adsorption of antibiotics by MPs within wastewater increases the potential for transportation of pollution within the environment. The MP type, size, shape and ageing will heavily influence the rate and capacity of antibiotic adsorption and must be carefully considered in order to understand their impact on the aquatic environment.

7. Summary and conclusions

Plastic pollution is a global issue and currently holds the attention of the public and policymakers around the world. As a relatively new area of research within this field, the study of microplastics draws ever-increasing focus. An opportunity exists to capitalise on this awareness and implement sustainable solutions in wastewater treatment which can help tackle microplastic pollution in the aquatic environment.

At the outset of this research in 2020, only a few studies considered AOP treatment of MPs and even fewer considered how partial degradation in these systems may transform MPs and affect their interaction with micro-pollutants. The research presented within this thesis contributes to a rapidly expanding body of literature on this topic. The initial research questions outlined in Section 1.1 are addressed as follows:

1) Determine the potential for sustainable advanced oxidation methods as a treatment option for MP polluted water

Chapter 4 and 5 contribute to answering the first research question. These chapters focus on the effect of a number of AOPs on polyester MP fibres in water and real laundry wastewater. Based on a literature survey and a number of criteria for real-world applicability, heterogeneous photocatalysis and AOPs requiring complex equipment such as ozone generation were ruled out for experimental investigation. A number of photo-chemical AOPs were selected for screening alongside sulfate driven systems.

In Chapter 4, UV/H_2O_2 treatment was investigated. Variation of the wavelength of irradiation, amount of UV irradiance, total UV dose, H_2O_2 dose led to the development of a best-performing treatment with PET fibre half-life of 26.7 h (1200 mg L^{-1} H_2O_2 under UVC irradiance of 31.8 mW cm^{-2}). The mass loss was attributed to physical degradation of the fibres evident in SEM and AFM images. Upon irradiation with UVC light, the polyester surface becomes pock-marked with small holes and indentations. As the length of treatment increases, these features become more pronounced and numerous with micro-cracks forming across the width of the fibres. Mechanical weakening of the bulk fibre structure leads to fragmentation

into smaller MPs and nano-plastics. The mechanism of degradation was also probed chemically by tracking the emergence of oxygen-containing groups on the plastic surface. The carbonyl index, measured from FTIR spectra, allows quantitative comparison of these changes between treatment conditions. Up to a 10.6% increase in CI was observed for treated fibres, as compared to pristine samples. The potential of this method for application in real wastewater samples was tested using laundry wastewater from a hospital. In this complex and highly polluted matrix, UVC/ H_2O_2 was shown to reduce the MP mass, after an initial delay during which the background organic content of the wastewater was preferentially targeted by the oxidising radicals. These experiments indicate that with appropriate pre-treatment to reduce the COD, MPs within real wastewater can be targeted with this AOP. As the first study considering UVC/ H_2O_2 treatment of MP fibres, this chapter fills a research gap and provides a proof of concept for further optimisation.

Chapter 5 details experiments testing for the first time several sulfate driven AOPs for the removal of PET fibres from water and wastewater. Activation of persulfate by UV irradiation, heat and ultrasound result in varied rates of mass loss and observed degree of surface change. As in Chapter 4, these changes were probed in detail using physical and chemical characterisation methods. The rate of degradation in sulfate driven systems was slow with the best performing treatment (UVC/PDS, 500 mg L^{-1}, 31.8 mw cm^{-2}) resulting in only 18.5% mass loss after 9 h. In general, sulfate driven systems resulted in surface weathering without significant bulk loss of material. SEM imaging of the fibre surface revealed a similar progression of holes and cracks under light activated sulfate AOPs. Where ultrasound was applied, significant physical fragmentation of the fibres resulted due to the high energy of these systems, although to observe significant fragmentation high US power was required. The initiation method of persulfate was shown to be key in determining the mechanism of degradation and the eventual transformation of PET MP fibres in wastewater systems. Once again, as with the UVC/H_2O_2 AOP in real laundry wastewater, the rate of mass loss by the optimised UVC/PDS AOP was impeded by a high background COD.

The work in these sections provides information on the mechanism of MP degradation in water and wastewater by a number of selected AOPs. This information is key in enabling stakeholders and policy makers to make decisions on the direction of research in tackling the

MP pollution problem. In terms of developing a large-scale treatment solution for MP polluted wastewater, these lab-scale proof-of-concept studies are only the first step. Significant reductions in the concentration of H_2O_2 and total dose of UVC required for rapid mass loss are necessary to successfully treat large volumes of wastewater using UVC/ H_2O_2. The sulfate driven systems investigated are time-intensive and in some cases, energy intensive. For such systems to prove feasible at scale, testing of the most promising AOPs should be conducted in real WWTPs and their impact on MP loads in real wastewater determined. From the treatment types tested, UVC/H_2O_2 shows the most promising results for developing a treatment system capable of MP mineralisation.

2) Understand the transformation and degradation of MPs within these systems

Chapters 4, 5 and 6 contribute to answering the second research question. Within these chapters, a range of MP types, shapes and sized were exposed to varied oxidative weathering treatments. None of the tested AOPs achieved complete mineralisation of MPs within the timescale of the lab experiments. In all cases where degradation was observed (ie. mass loss was observed), the physical and chemical characteristics of MPs were altered.

Physical changes to the surface of PET fibres have been described in detail in terms of the topography change observed in SEM images. Additionally, AFM was used to quantify the changing roughness on the atomic scale throughout the thesis. In Chapter 4, the depth of surface holes formed during the optimised UVC/H_2O_2 treatment was estimated to range from 10 – 100 nm. In Chapter 5 and 6, the roughness of the pristine, UVC/PDS and hydrolysis weathered PET fibres was quantified, showing that the treatment type has a marked effect on the surface texture at the atomic scale. R_{RMS} was 9.23 and 11.02, 31.38 nm in each case, respectively. These insights indicate that the surface area of MPs after exposure to oxidizing AOPs is likely to be greatly increased due to the formation of micro/nano sized holes, cracks and texture. As a key parameter in how MPs interact with co-contaminants such as micro-pollutants, these insights are an important addition to our understanding of the transformation and fate of MPs within WWTPs.

Chemical information on the transformation of MPs in these systems was probed with FTIR spectroscopy. In the case of UVC/H_2O_2 treatment, the relative abundance of carbonyl groups on the polymer surface increased after treatment, proportional to the starting peroxide concentration of the system. Similar observations were made for UVC/PDS treated PET fibres, albeit to a lesser degree. The carbonyl group abundance on MP surfaces directly relates to their hydrophobicity and therefore their interaction with micro-pollutants in water.

Further work in this area should investigate in more detail the mechanism of polymer degradation by these systems. Application of detailed chemical characterisation techniques such as micro-FTIR, Raman and X-ray photoelectron spectroscopy would shed further light on the chemical changes MPs undergo during treatment. Of additional interest is the leaching of organics and polymer chain components to the water during the degradation process. Investigation into the formation of degradation products and their fate in these systems is essential to fully understand the fate of MPs under AOP degradation.

3) Understand the implications of this transformation on MP interaction with organic pollutants present in domestic wastewater

Chapter 6 answers the third research question by considering ceftazidime as an example micro-pollutant. A series of MPs of varied type, size, shape and weathering degree were tested in batch experiments in order to examine the influence of each parameter on antibiotic adsorption. Five polymers (PET, PE, PS, PU, and TWPs) in different forms (fibers, beads, foam and fragments) and sizes (10–1000 μm) were compared and certain samples weathered by various methods to produce MPs representative of those found in the environment or after AOP treatment.

The rate of ceftazidime uptake was shown to vary between all samples considered, with the highest adsorption capacity being hydrolysis weathered PET fibres at 1.432 mg g^{-1} after 48 h contact, as compared to 0.664 mg g^{-1} for pristine PET fibers. The changing rates of adsorption were linked to chemical and physical changes induced by the weathering process via SEM, AFM and FTIR characterisation. This trend was not uniform as PE and PS showed negligible increase in adsorption upon weathering. Maximum adsorption followed the order: PET fibers

(weathered) > PET fibers (pristine) > soft PS (pristine and weathered) > Kumho TWP > Goodyear TWP > Michelin TWP > hard PS (weathered) > PE weathered > Bridgestone TWP > PE (pristine) > hard PU > soft PU > hard PS (pristine).

The results show that interaction between MPs and micro-pollutants is possible within WWTPs and depends on the physical and chemical characteristics of the MPs. Further work should extend these experiments to consider many more examples of micro-pollutants with varied chemical characteristics in order to develop a relationship between MP type and its adsorption behaviour towards various micro-pollutant classes. In this way, a better understanding of the overall risk MPs pose (based on which organic contaminants they interact with) can be gained. This would allow MP pollution to be prioritized based on informed knowledge of its environmental and health risk.

4) Consider this work in the context of environmental and waste policy in Scotland

Chapter 3 offers a case study relevant to MP pollution in WWTPs and provides an illustration of the policy landscape any proposed change to waste treatment or management must consider. The MP and chemical pollution of sewage sludge is considered within the context of its use as an organic fertilizer material for agricultural land in Scotland. MP pollution in WWTPs is intertwined with this issue and the chapter seeks to show that environmental engineers seeking to solve this problem, must do so with a complex and diverse range of legislation and knock-on impacts in mind. These learnings are directly relevant to tackling pollution within wastewater which also presents a complex landscape of policy and stakeholders meaning that meaningful engineering intervention to solve environmental problems must be applied within this context. For example, engineering an AOP treatment capable of removing MPs from wastewater has direct knock-on effects to the quantity of MPs present in sludge and is therefore of relevance to all stakeholders considered in Chapter 3.

Future work and recommendations

The conclusions drawn from the results presented within this thesis offer a number of areas for future investigation. These are summarised within this section, alongside key recommendations for future experimental work, based on lessons learned during lab studies.

- The AOP treatments tested and optimised within this thesis should be considered pilot studies for the use of this technology to remove MP pollution from wastewater. In places, polyester MP fibres are selected as an important component of MP pollution and experiments are conducted in batch mode and at small scale. Future work should aim to extend the pilot studies to complex mixtures of MP type and shape in real wastewater, bringing the system closer to real conditions.

- Future work testing the degradation of complex mixtures of MPs is recommended. Firstly, this work should develop a robust analytical method for MP identification and quantification. This remains a challenge for MP researchers with no general consensus yet reached on best practice. Separation methods such as density separation and size filtration were reviewed within this thesis and could be employed to facilitate these experiments.

- Future work should seek to determine how scale affects the AOP treatment of MPs and their transformation. As mentioned, experiments presented here are batch mode and lab-scale, allowing comparison across varied treatment conditions and rapid recovery of MPs. In order to investigate how real systems may differ, large scale testing is required. In this case, a different method of determining MP degradation will be required as determination of MP mass when dispersed in a large volume and alongside additional contaminants will be greatly challenging. In this case, it is recommended to mass per volume or particle counting method to track the concentration of MPs.

- Experiments presented within this thesis show a slow rate of polyester MP removal by several AOPs, each requiring intense UV irradiation and chemical dosing when optimised for MP removal rate. It is recommended that further development of AOP systems for MP pollution treatment carefully consider the sustainability of the treatment in terms of energy and chemical use. A full Life cycle analysis is recommended if scale-up is considered.

- High-throughput continuous flow AOPs such as the UVC/H_2O_2 systems currently integrated in wastewater treatment plants have short residence times and are therefore unlikely to deliver sufficient UV dose to result in MP mineralisation. Separation of MPs into a concentrated phase would allow application of a larger total UV dose, potentially facilitating MP mineralisation. This hypothesis should be explored to determine the feasibility of scale-up of AOP treatment of MPs. Experiments which consider the combination of AOPs with subsequent biological treatment would give valuable insight into the real world potential of this technology.

- Ceftazidime is selected as an example micro-pollutant for study of adsorption by MPs. Future work should extend the investigation to test the interaction between MPs and a broad range of organic micropollutants to identify trends. An opportunity exists here to link the surface chemistry of partially degraded MPs with their interaction with organic micro-pollutants of different characteristics. More experimental data would allow a predictive model to be developed showing what chemical interaction is likely based on which MPs are present in wastewater. This model could then be used to predict the broad risk of MPs and their co-contaminants.

- The transformation of MPs during partial degradation within wastewater systems is a promising avenue for future work. This should further consider the formation of nanoplastics and organic degradation products during oxidative water treatment. Some evidence of these degradation products forming is presented within this thesis in the form of microscopy imaging and surface chemical change. Detailed chemical investigation using mass spectrometry would allow identification of degradation products in water, allowing a clear picture of the transformation mechanism of MPs.

Nano-filtration of the post-treatment liquid phase and microscopy imaging of any captured solids may allow identification and sizing of nano-sized fragments which were not considered in the experiments presented within this thesis.

Final thoughts

Plastic is an essential material in modern society and will continue to be used and mis-managed for the foreseeable future. Until an overhaul of our plastic-based lives is possible, waste management and treatment methods must be updated to tackle this waste before it causes irreversible harm to our environment. Wastewater treatment systems present an opportunity to capture high concentrations of plastic in water before it is dispersed into the world and becomes near-impossible to re-capture. This thesis has presented evidence that AOPs hold potential as a sustainable wastewater treatment method, capable of degrading MP pollution. With further development, such systems may prove able to completely mineralisation MPs, avoiding the formation of a solid waste entirely. Further research towards this goal must consider the practicality and sustainability of applying an energy and chemical intensive process at scale as well as the potential formation of degradation by-products where incomplete mineralisation of MPs occurs. It is vital that the solution to MP waste does not introduce a new problem of nano-plastic generation and chemical pollution. To this end, research into the mechanism of degradation and the interaction with co-contaminants such as the studies presented within this thesis is essential. By considering MP pollution in this holistic way, within the context of a complex and vast field of waste treatment and regulation, we can find our way to a truly sustainable solution.

References

1. Plastics - the Facts 2020. Plastics Europe; 2020.
2. OECD. Global Plastics Outlook Policy Scenarios to 2060: OECD Publishing; 2022.
3. Geyer R, Jambeck JR, Law KL. Production, use, and fate of all plastics ever made. Science advances. 2017;3(7):e1700782-e.
4. Horton AA, Walton A, Spurgeon DJ, Lahive E, Svendsen C. Microplastics in freshwater and terrestrial environments: Evaluating the current understanding to identify the knowledge gaps and future research priorities. Science of The Total Environment. 2017;586:127-41.
5. Iroegbu AOC, Ray SS, Mbarane V, Bordado JC, Sardinha JP. Plastic Pollution: A Perspective on Matters Arising: Challenges and Opportunities. ACS Omega. 2021;6(30):19343-55.
6. OECD. Global Plastics Outlook: Economic Drivers, Environmental Impacts and Policy Options: OECD publishing; 2022.
7. Meijer LJJ, van Emmerik T, van der Ent R, Schmidt C, Lebreton L. More than 1000 rivers account for 80% of global riverine plastic emissions into the ocean. Sci Adv. 2021;7(18).
8. Lau WWY, Shiran Y, Bailey RM, Cook E, Stuchtey MR, Koskella J, et al. Evaluating scenarios toward zero plastic pollution. Science. 2020;369(6510):1455.
9. Rochman CM, Browne MA, Halpern BS, Hentschel BT, Hoh E, Karapanagioti HK, et al. Classify plastic waste as hazardous. Nature. 2013;494(7436):169-71.
10. Campanale C, Massarelli C, Savino I, Locaputo V, Uricchio VF. A Detailed Review Study on Potential Effects of Microplastics and Additives of Concern on Human Health. Int J Environ Res Public Health. 2020;17(4):1212.
11. Arthur C, Sutton-Grier AE, Murphy P, Bamford H. Out of sight but not out of mind: Harmful effects of derelict traps in selected U.S. coastal waters. Marine Pollution Bulletin. 2014;86(1):19-28.
12. Raynaud J. Valuing Plastics: The Business Case for Measuring, Managing and Disclosing Plastic Use in the Consumer Goods Industry. United Nations Environment Programme; 2014.

13. Jenna Jambeck EMaBD. Leveraging Multi-Target Strategies to Address Plastic Pollution in the Context of an Already Stressed Ocean. Washington DC: World Resources Institute; 2020.
14. Buchanan JB. Pollution by synthetic fibres. Marine Pollution Bulletin. 1971;2(2):23.
15. Carpenter EJ, Smith Jr KL. Plastics on the Sargasso sea surface. Science. 1972;175(4027):1240-1.
16. Thompson RC, Olsen Y, Mitchell RP, Davis A, Rowland SJ, John AWG, et al. Lost at Sea: Where Is All the Plastic? Science. 2004;304(5672):838.
17. Eriksen M, Lebreton LC, Carson HS, Thiel M, Moore CJ, Borerro JC, et al. Plastic Pollution in the World's Oceans: More than 5 Trillion Plastic Pieces Weighing over 250,000 Tons Afloat at Sea. PLoS One. 2014;9(12):e111913.
18. Courtney Arthur JB, Holly Bamford, editor Proceedings of the International Research Workshop on the Occurrence, Effects and Fate of Microplastic Marine Debris.2008 September 9-11, 2008: National Oceanic and Atmospheric Administration.
19. Al-Azzawi MSM, Funck M, Kunaschk M, der Esch EV, Jacob O, Freier KP, et al. Microplastic sampling from wastewater treatment plant effluents: Best-practices and synergies between thermoanalytical and spectroscopic analysis. Water Research. 2022;219:118549.
20. Almuhtaram H, Andrews RC. Sampling Microplastics in Water Matrices: A Need for Standardization. ACS ES&T Water. 2022;2(8):1276-8.
21. Cerasa M, Teodori S, Pietrelli L. Searching Nanoplastics: From Sampling to Sample Processing. Polymers (Basel). 2021;13(21).
22. Hartl MGJ. Focus on nanomaterials and microplastics in the aquatic environment. CREW - Centre of Expertise for Waters; 2015.
23. Rozman U, Klun B, Kuljanin A, Skalar T, Kalčíková G. Insights into the shape-dependent effects of polyethylene microplastics on interactions with organisms, environmental aging, and adsorption properties. Scientific Reports. 2023;13(1):22147.
24. Tursi A, Baratta M, Easton T, Chatzisymeon E, Chidichimo F, De Biase M, et al. Microplastics in aquatic systems, a comprehensive review: origination, accumulation, impact, and removal technologies. RSC Advances. 2022;12(44):28318-40.

25. Mehinto AC, Coffin S, Koelmans AA, Brander SM, Wagner M, Thornton Hampton LM, et al. Risk-based management framework for microplastics in aquatic ecosystems. Microplastics and Nanoplastics. 2022;2(1):17.
26. Collicutt B, Juanes F, Dudas SE. Microplastics in juvenile Chinook salmon and their nearshore environments on the east coast of Vancouver Island. Environmental Pollution. 2019;244:135-42.
27. Wright SL, Kelly FJ. Plastic and Human Health: A Micro Issue? Environmental Science & Technology. 2017;51(12):6634-47.
28. Prata JC. Airborne microplastics: Consequences to human health? Environmental Pollution. 2018;234:115-26.
29. Dong C-D, Chen C-W, Chen Y-C, Chen H-H, Lee J-S, Lin C-H. Polystyrene microplastic particles: In vitro pulmonary toxicity assessment. Journal of Hazardous Materials. 2020;385:121575.
30. Bacchetta R, Winkler A, Santo N, Tremolada P. The Toxicity of Polyester Fibers in Xenopuslaevis. Water. 2021;13(23):3446.
31. Costigan E, Collins A, Hatinoglu MD, Bhagat K, MacRae J, Perreault F, et al. Adsorption of organic pollutants by microplastics: Overview of a dissonant literature. Journal of Hazardous Materials Advances. 2022;6:100091.
32. Miloloža M, Kučić Grgić D, Bolanča T, Ukić Š, Cvetnić M, Ocelić Bulatović V, et al. Ecotoxicological Assessment of Microplastics in Freshwater Sources—A Review. Water. 2021;13(1).
33. Gunaalan K, Fabbri E, Capolupo M. The hidden threat of plastic leachates: A critical review on their impacts on aquatic organisms. Water Research. 2020;184:116170.
34. Prata JC, da Costa JP, Lopes I, Duarte AC, Rocha-Santos T. Environmental exposure to microplastics: An overview on possible human health effects. Science of The Total Environment. 2020;702:134455.
35. Das A. The emerging role of microplastics in systemic toxicity: Involvement of reactive oxygen species (ROS). Sci Total Environ. 2023;895:165076.
36. Yu F, Yang C, Zhu Z, Bai X, Ma J. Adsorption behavior of organic pollutants and metals on micro/nanoplastics in the aquatic environment. Science of The Total Environment. 2019;694:133643.

37. Liu P, Shi Y, Wu X, Wang H, Huang H, Guo X, et al. Review of the artificially-accelerated aging technology and ecological risk of microplastics. Science of The Total Environment. 2021;768:144969.
38. Kallenbach EMF, Rødland ES, Buenaventura NT, Hurley R. Microplastics in Terrestrial and Freshwater Environments. In: Bank MS, editor. Microplastic in the Environment: Pattern and Process. Cham: Springer International Publishing; 2022. p. 87-130.
39. Sullivan GL, Delgado-Gallardo J, Watson TM, Sarp S. An investigation into the leaching of micro and nano particles and chemical pollutants from disposable face masks - linked to the COVID-19 pandemic. Water Research. 2021;196:117033.
40. Cole M, Lindeque P, Halsband C, Galloway TS. Microplastics as contaminants in the marine environment: A review. Marine Pollution Bulletin. 2011;62(12):2588-97.
41. Sun J, Zhu Z-R, Li W-H, Yan X, Wang L-K, Zhang L, et al. Revisiting Microplastics in Landfill Leachate: Unnoticed Tiny Microplastics and Their Fate in Treatment Works. Water Research. 2021;190:116784.
42. Pedrotti ML, Petit S, Eyheraguibel B, Kerros ME, Elineau A, Ghiglione JF, et al. Pollution by anthropogenic microfibers in North-West Mediterranean Sea and efficiency of microfiber removal by a wastewater treatment plant. Science of The Total Environment. 2021;758:144195.
43. Kumar M, Chen H, Sarsaiya S, Qin S, Liu H, Awasthi MK, et al. Current research trends on micro- and nano-plastics as an emerging threat to global environment: A review. Journal of Hazardous Materials. 2020:124967.
44. Dees JP, Ateia M, Sanchez DL. Microplastics and Their Degradation Products in Surface Waters: A Missing Piece of the Global Carbon Cycle Puzzle. ACS ES&T Water. 2020.
45. Du S, Zhu R, Cai Y, Xu N, Yap P-S, Zhang Y, et al. Environmental fate and impacts of microplastics in aquatic ecosystems: a review. RSC Advances. 2021;11(26):15762-84.
46. Lares M, Ncibi MC, Sillanpää M, Sillanpää M. Occurrence, identification and removal of microplastic particles and fibers in conventional activated sludge process and advanced MBR technology. Water Research. 2018;133:236-46.
47. Mason SA, Garneau D, Sutton R, Chu Y, Ehmann K, Barnes J, et al. Microplastic pollution is widely detected in US municipal wastewater treatment plant effluent. Environmental Pollution. 2016;218:1045-54.

48. Wu X, Zhao X, Chen R, Liu P, Liang W, Wang J, et al. Wastewater treatment plants act as essential sources of microplastic formation in aquatic environments: A critical review. Water Research. 2022;221:118825.
49. Liu W, Zhang J, Liu H, Guo X, Zhang X, Yao X, et al. A review of the removal of microplastics in global wastewater treatment plants: Characteristics and mechanisms. Environment International. 2021;146:106277.
50. Liu R, Tan Z, Wu X, Liu Y, Chen Y, Fu J, et al. Modifications of microplastics in urban environmental management systems: A review. Water Research. 2022;222:118843.
51. Okoffo ED, O'Brien S, O'Brien JW, Tscharke BJ, Thomas KV. Wastewater treatment plants as a source of plastics in the environment: a review of occurrence, methods for identification, quantification and fate. Environmental Science: Water Research & Technology. 2019;5(11):1908-31.
52. Murphy F, Ewins C, Carbonnier F, Quinn B. Wastewater Treatment Works (WwTW) as a Source of Microplastics in the Aquatic Environment. Environmental Science & Technology. 2016;50(11):5800-8.
53. Ziajahromi S, Neale PA, Rintoul L, Leusch FDL. Wastewater treatment plants as a pathway for microplastics: Development of a new approach to sample wastewater-based microplastics. Water Research. 2017;112:93-9.
54. Mintenig S GG, Löder M Abschlussbericht Mikroplastik in Trinkwasser: Untersuchung im Trinkwasserversorgungsgebiet des Oldenburgisch-Ostfriesischen Wasserverbandes (OOWV) in Niedersachsen Probenanalyse mittels Mikro-FTIR Spektroskopie. (German translation) 2014 [Available from: https://schlicktown.stadt-media.de/wp-content/uploads/Abschlussbericht_Mikroplastik_in_Klaeranlagen-3.pdf. .
55. Talvitie J, Mikola A, Koistinen A, Setala O. Solutions to microplastic pollution - Removal of microplastics from wastewater effluent with advanced wastewater treatment technologies. Water Research. 2017;123:401-7.
56. Lv XM, Dong Q, Zuo ZQ, Liu YC, Huang X, Wu WM. Microplastics in a municipal wastewater treatment plant: Fate, dynamic distribution, removal efficiencies, and control strategies. Journal of Cleaner Production. 2019;225:579-86.
57. Sun J, Dai XH, Wang QL, van Loosdrecht MCM, Ni BJ. Microplastics in wastewater treatment plants: Detection, occurrence and removal. Water Research. 2019;152:21-37.

58. Prajapati S, Beal M, Maley J, Brinkmann M. Qualitative and quantitative analysis of microplastics and microfiber contamination in effluents of the City of Saskatoon wastewater treatment plant. Environmental Science and Pollution Research. 2021;28(25):32545-53.
59. Browne MA, Crump P, Niven SJ, Teuten E, Tonkin A, Galloway T, et al. Accumulation of Microplastic on Shorelines Woldwide: Sources and Sinks. Environmental Science & Technology. 2011;45(21):9175-9.
60. De Falco F, Gullo MP, Gentile G, Di Pace E, Cocca M, Gelabert L, et al. Evaluation of microplastic release caused by textile washing processes of synthetic fabrics. Environmental Pollution. 2018;236:916-25.
61. Bond T, Ferrandiz-Mas V, Felipe-Sotelo M, van Sebille E. The occurrence and degradation of aquatic plastic litter based on polymer physicochemical properties: A review. Crit Rev Environ Sci Technol. 2018;48(7-9):685-722.
62. De Falco F, Di Pace E, Cocca M, Avella M. The contribution of washing processes of synthetic clothes to microplastic pollution. Scientific Reports. 2019;9(1):6633.
63. Lim SJ, Park Y-K, Kim H, Kwon J, Moon HM, Lee Y, et al. Selective solvent extraction and quantification of synthetic microfibers in textile laundry wastewater using pyrolysis-gas chromatography/mass spectrometry. Chemical Engineering Journal. 2022;434:134653.
64. Conley K, Clum A, Deepe J, Lane H, Beckingham B. Wastewater treatment plants as a source of microplastics to an urban estuary: Removal efficiencies and loading per capita over one year. Water Research X. 2019;3:100030.
65. Iyare PU, Ouki SK, Bond T. Microplastics removal in wastewater treatment plants: a critical review. Environmental Science: Water Research & Technology. 2020.
66. Belzagui F, Gutierrez-Bouzan C, Alvarez-Sanchez A, Vilaseca M. Textile microfibers reaching aquatic environments: A new estimation approach. Environmental Pollution. 2020;265:11.
67. Kutralam-Muniasamy G, Pérez-Guevara F, Elizalde-Martínez I, Shruti VC. An overview of recent advances in micro/nano beads and microfibers research: Critical assessment and promoting the less known. Science of The Total Environment. 2020;740:139991.
68. Government S. THE ENVIRONMENTAL PROTECTION (MICROBEADS) (SCOTLAND) REGULATIONS 2018. In: Directorate MS, editor. 2018.

69. Protecting environment and health: Commission adopts measures to restrict intentionally added microplastics [press release]. https://ec.europa.eu/commission/presscorner/detail/en/ip_23_45812023.
70. Faure F, Demars C, Wieser O, Kunz M, de Alencastro LF. Plastic pollution in Swiss surface waters: nature and concentrations, interaction with pollutants. Environmental Chemistry. 2015;12(5):582-91.
71. Kole PJ, Löhr AJ, Van Belleghem FGAJ, Ragas AMJ. Wear and Tear of Tyres: A Stealthy Source of Microplastics in the Environment. Int J Environ Res Public Health. 2017;14(10):1265.
72. Fan X, Gan R, Liu J, Xie Y, Xu D, Xiang Y, et al. Adsorption and desorption behaviors of antibiotics by tire wear particles and polyethylene microplastics with or without aging processes. Science of The Total Environment. 2021;771:145451.
73. Mattsson K, de Lima JA, Wilkinson T, Järlskog I, Ekstrand E, Sköld YA, et al. Tyre and road wear particles from source to sea. Microplastics and Nanoplastics. 2023;3(1):14.
74. Pivokonsky M, Cermakova L, Novotna K, Peer P, Cajthaml T, Janda V. Occurrence of microplastics in raw and treated drinking water. Science of the Total Environment. 2018;643:1644-51.
75. Magnusson KW, C. Screening of Microplastic Particles in and Down- Stream of a Wastewater Treatment Plant. Stockholm, Sweden: Swedish Environmental Research Institute; 2014.
76. Liu X, Yuan W, Di M, Li Z, Wang J. Transfer and fate of microplastics during the conventional activated sludge process in one wastewater treatment plant of China. Chemical Engineering Journal. 2019;362:176-82.
77. Michielssen MR, Michielssen ER, Ni J, Duhaime MB. Fate of microplastics and other small anthropogenic litter (SAL) in wastewater treatment plants depends on unit processes employed. Environmental Science: Water Research & Technology. 2016;2(6):1064-73.
78. Alavian Petroody SS, Hashemi SH, van Gestel CAM. Transport and accumulation of microplastics through wastewater treatment sludge processes. Chemosphere. 2021;278:130471.
79. Okoffo ED, Donner E, McGrath SP, Tscharke BJ, O'Brien JW, O'Brien S, et al. Plastics in biosolids from 1950 to 2016: A function of global plastic production and consumption. Water Research. 2021;201:117367.

80. Zilinskaite E, Futter M, Collentine D. Stakeholders' Perspectives on Microplastics in Sludge Applied to Agricultural Land. Frontiers in Sustainable Food Systems. 2022;6.
81. Hanvey JS, Lewis PJ, Lavers JL, Crosbie ND, Pozo K, Clarke BO. A review of analytical techniques for quantifying microplastics in sediments. Analytical Methods. 2017;9(9):1369-83.
82. Lares M, Ncibi MC, Sillanpää M, Sillanpää M. Intercomparison study on commonly used methods to determine microplastics in wastewater and sludge samples. Environmental Science and Pollution Research. 2019;26(12):12109-22.
83. Blair RM, Waldron S, Phoenix VR, Gauchotte-Lindsay C. Microscopy and elemental analysis characterisation of microplastics in sediment of a freshwater urban river in Scotland, UK. Environmental Science and Pollution Research. 2019;26(12):12491-504.
84. Wang Z, Lin T, Chen W. Occurrence and removal of microplastics in an advanced drinking water treatment plant (ADWTP). Science of The Total Environment. 2020;700:134520.
85. Ma B, Xue W, Ding Y, Hu C, Liu H, Qu J. Removal characteristics of microplastics by Fe-based coagulants during drinking water treatment. Journal of Environmental Sciences. 2019;78:267-75.
86. Ma B, Xue W, Hu C, Liu H, Qu J, Li L. Characteristics of microplastic removal via coagulation and ultrafiltration during drinking water treatment. Chemical Engineering Journal. 2019;359:159-67.
87. Skaf DW, Punzi VL, Rolle JT, Kleinberg KA. Removal of micron-sized microplastic particles from simulated drinking water via alum coagulation. Chemical Engineering Journal. 2020;386:123807.
88. Herbort AF, Sturm MT, Schuhen K. A new approach for the agglomeration and subsequent removal of polyethylene, polypropylene, and mixtures of both from freshwater systems - a case study. Environ Sci Pollut Res Int. 2018;25(15):15226-34.
89. Herbort AF, Schuhen K. A concept for the removal of microplastics from the marine environment with innovative host-guest relationships. Environ Sci Pollut Res Int. 2017;24(12):11061-5.
90. Perren W, Wojtasik A, Cai Q. Removal of Microbeads from Wastewater Using Electrocoagulation. ACS Omega. 2018;3(3):3357-64.

91. Wang Z, Sedighi M, Lea-Langton A. Filtration of microplastic spheres by biochar: removal efficiency and immobilisation mechanisms. Water Research. 2020;184:116165.
92. Siipola V, Pflugmacher S, Romar H, Wendling L, Koukkari P. Low-Cost Biochar Adsorbents for Water Purification Including Microplastics Removal. Applied Sciences. 2020;10(3):788.
93. Sun C, Wang Z, Chen L, Li F. Fabrication of robust and compressive chitin and graphene oxide sponges for removal of microplastics with different functional groups. Chemical Engineering Journal. 2020;393:124796.
94. Chen Y-J, Chen Y, Miao C, Wang Y-R, Gao G-K, Yang R-X, et al. Metal–organic framework-based foams for efficient microplastics removal. Journal of Materials Chemistry A. 2020;8(29):14644-52.
95. Malankowska M, Echaide-Gorriz C, Coronas J. Microplastics in marine environment: a review on sources, classification, and potential remediation by membrane technology. Environmental Science: Water Research & Technology. 2021;7(2):243-58.
96. Enfrin M, Lee J, Le-Clech P, Dumee LF. Kinetic and mechanistic aspects of ultrafiltration membrane fouling by nano- and microplastics. 2020;601.
97. Li J, Wang B, Chen Z, Ma B, Chen JP. Ultrafiltration membrane fouling by microplastics with raw water: Behaviors and alleviation methods. Chemical Engineering Journal. 2021;410:128174.
98. Ding H, Zhang J, He H, Zhu Y, Dionysiou DD, Liu Z, et al. Do membrane filtration systems in drinking water treatment plants release nano/microplastics? Science of The Total Environment. 2021;755:142658.
99. Makropoulou T, Kortidis I, Davididou K, Motaung DE, Chatzisymeon E. Photocatalytic facile ZnO nanostructures for the elimination of the antibiotic sulfamethoxazole in water. Journal of Water Process Engineering. 2020;36:101299.
100. Kanakaraju D, Glass BD, Oelgemöller M. Advanced oxidation process-mediated removal of pharmaceuticals from water: A review. Journal of Environmental Management. 2018;219:189-207.
101. Deng Y, Zhao R. Advanced Oxidation Processes (AOPs) in Wastewater Treatment. Current Pollution Reports. 2015;1(3):167-76.

102. Kim S, Sin A, Nam H, Park Y, Lee H, Han C. Advanced oxidation processes for microplastics degradation: A recent trend. Chemical Engineering Journal Advances. 2022;9:100213.
103. Stefan MI. Advanced oxidation processes for water treatment : fundamentals and applications. 2018:52-60.
104. Ariza-Tarazona MC, Villarreal-Chiu JF, Hernández-López JM, Rosa JRDl, Barbieri V, Siligardi C, et al. Microplastic pollution reduction by a carbon and nitrogen-doped TiO2: Effect of pH and temperature in the photocatalytic degradation process. Journal of Hazardous Materials. 2020;395
105. Llorente-García BE, Hernández-López JM, Zaldívar-Cadena AA, Siligardi C, Cedillo-González EI. First Insights into Photocatalytic Degradation of HDPE and LDPE Microplastics by a Mesoporous N–TiO2 Coating: Effect of Size and Shape of Microplastics. Coatings. 2020;10(7):658.
106. Nabi I, Bacha A-U-R, Li K, Cheng H, Wang T, Liu Y, et al. Complete Photocatalytic Mineralization of Microplastic on TiO₂ Nanoparticle Film. iScience. 2020;23(7).
107. Tofa TS, Ye F, Kunjali KL, Dutta J. Enhanced Visible Light Photodegradation of Microplastic Fragments with Plasmonic Platinum/Zinc Oxide Nanorod Photocatalysts. Catalysts. 2019;9(10):819.
108. Ariza-Tarazona MC, Villarreal-Chiu JF, Barbieri V, Siligardi C, Cedillo-González EI. New strategy for microplastic degradation: Green photocatalysis using a protein-based porous N-TiO2 semiconductor. Ceramics International. 2019;45(7, Part B):9618-24.
109. Tofa TS, Kunjali KL, Paul S, Dutta J. Visible light photocatalytic degradation of microplastic residues with zinc oxide nanorods. Environmental Chemistry Letters. 2019;17(3):1341-6.
110. Uheida A, Mejía HG, Abdel-Rehim M, Hamd W, Dutta J. Visible light photocatalytic degradation of polypropylene microplastics in a continuous water flow system. Journal of Hazardous Materials. 2020:124299.
111. Jae-Mee L, Rosa B, In-Cheol C, Sung-Ho L, Jong-Kyu K, Luiza CC. Photocatalytic Degradation of Polyamide 66: Evaluating the Feasibility of Photocatalysis as a Microfibre-Targeting Technology. Water (Basel). 2020;12(3551):3551.
112. Kang J, Zhou L, Duan X, Sun H, Ao Z, Wang S. Degradation of Cosmetic Microplastics via Functionalized Carbon Nanosprings. Matter. 2019;1(3):745-58.

113. Jiang R, Lu G, Yan Z, Liu J, Wu D, Wang Y. Microplastic degradation by hydroxy-rich bismuth oxychloride. Journal of Hazardous Materials. 2021;405:124247.
114. Allé PH, Garcia-Muñoz P, Adouby K, Keller N, Robert D. Efficient photocatalytic mineralization of polymethylmethacrylate and polystyrene nanoplastics by TiO2/β-SiC alveolar foams. Environmental Chemistry Letters. 2021;19(2):1803-8.
115. de Souza ZSB, Silva MP, Fraga TJM, Motta Sobrinho MA. A comparative study of photo-Fenton process assisted by natural sunlight, UV-A, or visible LED light irradiation for degradation of real textile wastewater: factorial designs, kinetics, cost assessment, and phytotoxicity studies. Environmental Science and Pollution Research. 2021;28(19):23912-28.
116. Liu P, Lu K, Li J, Wu X, Qian L, Wang M, et al. Effect of aging on adsorption behavior of polystyrene microplastics for pharmaceuticals: Adsorption mechanism and role of aging intermediates. Journal of Hazardous Materials. 2020;384:121193.
117. Liu P, Qian L, Wang H, Zhan X, Lu K, Gu C, et al. New Insights into the Aging Behavior of Microplastics Accelerated by Advanced Oxidation Processes. Environmental Science & Technology. 2019;53(7):3579-88.
118. Tagg AS, Harrison JP, Ju-Nam Y, Sapp M, Bradley EL, Sinclair CJ, et al. Fenton's reagent for the rapid and efficient isolation of microplastics from wastewater. Chemical Communications. 2017;53(2):372-5.
119. Hu K, Zhou P, Yang Y, Hall T, Nie G, Yao Y, et al. Degradation of Microplastics by a Thermal Fenton Reaction. ACS ES&T Engineering. 2022;2(1):110-20.
120. Piazza V, Uheida A, Gambardella C, Garaventa F, Faimali M, Dutta J. Ecosafety Screening of Photo-Fenton Process for the Degradation of Microplastics in Water. Frontiers in Marine Science. 2022;8.
121. Zafar R, Park SY, Kim CG. Surface modification of polyethylene microplastic particles during the aqueous-phase ozonation process. Environmental Engineering Research. 2021;26(5):200412-0.
122. Hidayaturrahman H, Lee T-G. A study on characteristics of microplastic in wastewater of South Korea: Identification, quantification, and fate of microplastics during treatment process. Marine Pollution Bulletin. 2019;146:696-702.
123. Gomes de Aragão Belé T, F. Neves T, Cristale J, Prediger P, Constapel M, F. Dantas R. Oxidation of microplastics by O3 and O3/H2O2: Surface modification and adsorption capacity. Journal of Water Process Engineering. 2021;41:102072.

124. Ebrahimbabaie P, Yousefi K, Pichtel J. Photocatalytic and biological technologies for elimination of microplastics in water: Current status. Science of The Total Environment. 2022;806:150603.
125. Ahmed T, Shahid M, Azeem F, Rasul I, Shah AA, Noman M, et al. Biodegradation of plastics: current scenario and future prospects for environmental safety. Environmental Science and Pollution Research. 2018;25(8):7287-98.
126. Enyoh CE, Fadare OO, Paredes M, Wang Q, Verla AW, Shafea L, et al. An Overview of Physical, Chemical and Biological Methods for Removal of Microplastics. In: Sillanpää M, Khadir A, Muthu SS, editors. Microplastics Pollution in Aquatic Media: Occurrence, Detection, and Removal. Singapore: Springer Singapore; 2022. p. 273-89.
127. Campo P, Holmes A, Coulon F. A method for the characterisation of microplastics in sludge. MethodsX. 2019;6:2776-81.
128. Wei W, Chen X, Peng L, Liu Y, Bao T, Ni B-J. The entering of polyethylene terephthalate microplastics into biological wastewater treatment system affects aerobic sludge digestion differently from their direct entering into sludge treatment system. Water Research. 2021;190:116731.
129. Wei W, Huang Q-S, Sun J, Wang J-Y, Wu S-L, Ni B-J. Polyvinyl Chloride Microplastics Affect Methane Production from the Anaerobic Digestion of Waste Activated Sludge through Leaching Toxic Bisphenol-A. Environmental Science & Technology. 2019;53(5):2509-17.
130. Li L, Liu D, Song K, Zhou Y. Performance evaluation of MBR in treating microplastics polyvinylchloride contaminated polluted surface water. Marine Pollution Bulletin. 2020;150:110724.
131. Auta HS, Emenike CU, Jayanthi B, Fauziah SH. Growth kinetics and biodeterioration of polypropylene microplastics by Bacillus sp. and Rhodococcus sp. isolated from mangrove sediment. Marine Pollution Bulletin. 2018;127:15-21.
132. Yang J, Yang Y, Wu W-M, Zhao J, Jiang L. Evidence of Polyethylene Biodegradation by Bacterial Strains from the Guts of Plastic-Eating Waxworms. Environmental Science & Technology. 2014;48(23):13776-84.
133. Jeon HJ, Kim MN. Isolation of a thermophilic bacterium capable of low-molecular-weight polyethylene degradation. Biodegradation. 2013;24(1):89-98.

134. Park SY, Kim CG. Biodegradation of micro-polyethylene particles by bacterial colonization of a mixed microbial consortium isolated from a landfill site. Chemosphere. 2019;222:527-33.
135. Paço A, Duarte K, da Costa JP, Santos PSM, Pereira R, Pereira ME, et al. Biodegradation of polyethylene microplastics by the marine fungus Zalerion maritimum. Science of The Total Environment. 2017;586:10-5.
136. Sangeetha Devi R, Rajesh Kannan V, Nivas D, Kannan K, Chandru S, Robert Antony A. Biodegradation of HDPE by Aspergillus spp. from marine ecosystem of Gulf of Mannar, India. Marine Pollution Bulletin. 2015;96(1):32-40.
137. Gong J, Kong T, Li Y, Li Q, Li Z, Zhang J. Biodegradation of Microplastic Derived from Poly(ethylene terephthalate) with Bacterial Whole-Cell Biocatalysts. Polymers. 2018;10(12):1326.
138. Li X, Wu H, Gong J, Li Q, Li Z, Zhang J. Improvement of biodegradation of PET microplastics with whole-cell biocatalyst by interface activation reinforcement. Environmental Technology. 2022:1-10.
139. Miri S, Saini R, Davoodi SM, Pulicharla R, Brar SK, Magdouli S. Biodegradation of microplastics: Better late than never. Chemosphere. 2022;286:131670.
140. Ru J, Huo Y, Yang Y. Microbial Degradation and Valorization of Plastic Wastes. Frontiers in Microbiology. 2020;11.
141. Jansen J. PLASTIC FAILURE THROUGH MOLECULAR DEGRADATION. Plastics Engineering. 2015.
142. Anderson ZT, Cundy AB, Croudace IW, Warwick PE, Celis-Hernandez O, Stead JL. A rapid method for assessing the accumulation of microplastics in the sea surface microlayer (SML) of estuarine systems. Scientific Reports. 2018;8(1):9428.
143. Chamas A, Moon H, Zheng J, Qiu Y, Tabassum T, Jang JH, et al. Degradation Rates of Plastics in the Environment. ACS Sustainable Chemistry & Engineering. 2020;8(9):3494-511.
144. Wiesinger H, Wang Z, Hellweg S. Deep Dive into Plastic Monomers, Additives, and Processing Aids. Environmental Science & Technology. 2021;55(13):9339-51.
145. Yousif E, Haddad R. Photodegradation and photostabilization of polymers, especially polystyrene: review. Springerplus. 2013;2:398.

146. Gewert B, Plassmann MM, MacLeod M. Pathways for degradation of plastic polymers floating in the marine environment. Environmental Science: Processes & Impacts. 2015;17(9):1513-21.
147. Gardette M, Perthue A, Gardette J-L, Janecska T, Földes E, Pukánszky B, et al. Photo- and thermal-oxidation of polyethylene: Comparison of mechanisms and influence of unsaturation content. Polymer Degradation and Stability. 2013;98(11):2383-90.
148. Polymer Properties Database [21st September 2020]. Available from: https://polymerdatabase.com/polymer%20chemistry/Photo%20Oxidation.html.
149. Martínez-Romo A, González-Mota R, Soto-Bernal JJ, Rosales-Candelas I. Investigating the Degradability of HDPE, LDPE, PE-BIO, and PE-OXO Films under UV-B Radiation. Journal of Spectroscopy. 2015;2015:586514.
150. Day M, Wiles DM. Photochemical degradation of poly(ethylene terephthalate). II. Effect of wavelength and environment on the decomposition process. Journal of Applied Polymer Science. 1972;16(1):191-202.
151. Day M, Wiles DM. Photochemical degradation of poly(ethylene terephthalate). III. Determination of decomposition products and reaction mechanism. Journal of Applied Polymer Science. 1972;16(1):203-15.
152. Osborn KR. The photolysis of polyethylene terephthalate. Journal of Polymer Science. 1959;38(134):357-67.
153. Sang T, Wallis CJ, Hill G, Britovsek GJP. Polyethylene terephthalate degradation under natural and accelerated weathering conditions. Eur Polym J. 2020;136:13.
154. Venkatachalam S, Shilpa GN, Jayprakash VL, Prashant RG, Krishna R, Anil KK. Degradation and Recyclability of Poly (Ethylene Terephthalate). In: Hosam El-Din MS, editor. Polyester. Rijeka: IntechOpen; 2012. p. Ch. 4.
155. Amelia D, Fathul Karamah E, Mahardika M, Syafri E, Mavinkere Rangappa S, Siengchin S, et al. Effect of advanced oxidation process for chemical structure changes of polyethylene microplastics. Materials Today: Proceedings. 2022;52:2501-4.
156. Nolte TM, Nauser T, Gubler L. Attack of hydroxyl radicals to α-methyl-styrene sulfonate polymers and cerium-mediated repair via radical cations. Physical Chemistry Chemical Physics. 2020;22(8):4516-25.

157. Yang Y, Banerjee G, Brudvig GW, Kim J-H, Pignatello JJ. Oxidation of Organic Compounds in Water by Unactivated Peroxymonosulfate. Environmental Science & Technology. 2018;52(10):5911-9.
158. Guerra-Rodríguez S, Rodríguez E, Singh DN, Rodríguez-Chueca J. Assessment of Sulfate Radical-Based Advanced Oxidation Processes for Water and Wastewater Treatment: A Review. Water. 2018;10(12):1828.
159. Guerra-Rodríguez S, Ribeiro ARL, Ribeiro RS, Rodríguez E, Silva AMT, Rodríguez-Chueca J. UV-A activation of peroxymonosulfate for the removal of micropollutants from secondary treated wastewater. Science of The Total Environment. 2021;770:145299.
160. Sharma J, Mishra IM, Dionysiou DD, Kumar V. Oxidative removal of Bisphenol A by UV-C/peroxymonosulfate (PMS): Kinetics, influence of co-existing chemicals and degradation pathway. Chemical Engineering Journal. 2015;276:193-204.
161. Lee J, von Gunten U, Kim J-H. Persulfate-Based Advanced Oxidation: Critical Assessment of Opportunities and Roadblocks. Environmental Science & Technology. 2020;54(6):3064-81.
162. Government S. Ban on wet wipes containing plastic moves closer. In: Directorate M, editor. https://www.gov.scot/publications/strategic-environmental-assessment-proposed-ban-manufacture-supply-sale-wet-wipes-containing-plastic-environmental-report/2024.
163. Government S. Microplastic Filters (Washing Machines) Bill. https://publications.parliament.uk/pa/bills/cbill/58-02/0205/210205.pdf2023.
164. Alexy P, Anklam E, Emans T, Furfari A, Galgani F, Hanke G, et al. Managing the analytical challenges related to micro- and nanoplastics in the environment and food: filling the knowledge gaps. Food Additives & Contaminants: Part A. 2020;37(1):1-10.
165. Sarno A, Olafsen K, Kubowicz S, Karimov F, Sait STL, Sørensen L, et al. Accelerated Hydrolysis Method for Producing Partially Degraded Polyester Microplastic Fiber Reference Materials. Environmental Science & Technology Letters. 2021;8(3):250-5.
166. Sørensen L, Groven AS, Hovsbakken IA, Del Puerto O, Krause DF, Sarno A, et al. UV degradation of natural and synthetic microfibers causes fragmentation and release of polymer degradation products and chemical additives. Science of The Total Environment. 2020:143170.
167. Cheung PK, Fok L. Characterisation of plastic microbeads in facial scrubs and their estimated emissions in Mainland China. Water Research. 2017;122:53-61.

168. Budhiraja V, Urh A, Horvat P, Krzan A. Synergistic Adsorption of Organic Pollutants on Weathered Polyethylene Microplastics. Polymers (Basel). 2022;14(13).
169. Li J, Liu H, Paul Chen J. Microplastics in freshwater systems: A review on occurrence, environmental effects, and methods for microplastics detection. Water Research. 2018;137:362-74.
170. Zarfl C. Promising techniques and open challenges for microplastic identification and quantification in environmental matrices. Anal Bioanal Chem. 2019;411:3743+.
171. Bordós G, Gergely S, Háhn J, Palotai Z, Szabó É, Besenyő G, et al. Validation of pressurized fractionated filtration microplastic sampling in controlled test environment. Water Research. 2021;189:116572.
172. Hale RC. Analytical challenges associated with the determination of microplastics in the environment. Analytical Methods. 2017;9(9):1326-7.
173. Shim WJ, Hong SH, Eo SE. Identification methods in microplastic analysis: a review. Analytical Methods. 2017;9(9):1384-91.
174. Blair RM, Waldron S, Phoenix V, Gauchotte-Lindsay C. Micro- and Nanoplastic Pollution of Freshwater and Wastewater Treatment Systems. Springer Science Reviews. 2017;5(1):19-30.
175. Fu W, Min J, Jiang W, Li Y, Zhang W. Separation, characterization and identification of microplastics and nanoplastics in the environment. Science of The Total Environment. 2020;721:137561.
176. Löder MGJ, Kuczera M, Mintenig S, Lorenz C, Gerdts G. Focal plane array detector-based micro-Fourier-transform infrared imaging for the analysis of microplastics in environmental samples. Environmental Chemistry. 2015;12(5):563-81.
177. Primpke S, A. Dias P, Gerdts G. Automated identification and quantification of microfibres and microplastics. Analytical Methods. 2019;11(16):2138-47.
178. Song YK, Hong SH, Jang M, Han GM, Rani M, Lee J, et al. A comparison of microscopic and spectroscopic identification methods for analysis of microplastics in environmental samples. Marine Pollution Bulletin. 2015;93(1):202-9.
179. Lenz R, Enders K, Stedmon CA, Mackenzie DMA, Nielsen TG. A critical assessment of visual identification of marine microplastic using Raman spectroscopy for analysis improvement. Marine Pollution Bulletin. 2015;100(1):82-91.

180. Almond J, Sugumaar P, Wenzel MN, Hill G, Wallis C. Determination of the carbonyl index of polyethylene and polypropylene using specified area under band methodology with ATR-FTIR spectroscopy. e-Polymers. 2020;20(1):369-81.
181. Donelli I, Freddi G, Nierstrasz VA, Taddei P. Surface structure and properties of poly-(ethylene terephthalate) hydrolyzed by alkali and cutinase. Polymer Degradation and Stability. 2010;95(9):1542-50.
182. Hobbs JP, Sung CSP, Krishnan K, Hill S. Characterization of surface structure and orientation in polypropylene and poly(ethylene terephthalate) films by modified attenuated total reflection IR dichroism studies. Macromolecules. 1983;16(2):193-9.
183. Hemen Dave LL, Nisha Chandwani, Purvi Kikani, Bhakti Desai. Surface Modification of Polyester Fabric by Non-Thermal Plasma Treatment and Its Effect on Coloration Using Natural Dye. Journal of Polymer Materials. 2013;30(3):291-303.
184. Smith BC. The Infrared Spectra of Polymers II: Polyethylene. Spectroscopy. 2021;36(9):24-9.
185. Thinh PX, Basavaraja C, Kim DG, Huh DS. Characterization and electrochemical behaviors of honeycomb-patterned poly(N-vinylcarbazole)/polystyrene composite films. Polymer Bulletin. 2012;69(1):81-94.
186. Smith BC. Infrared Spectroscopy of Polymers XIII: Polyurethanes. Spectroscopy. 2023;38(7):14-6.
187. Groele J, Foster J. Hydrogen Peroxide Interference in Chemical Oxygen Demand Assessments of Plasma Treated Waters. Plasma. 2019;2(3):294-302.
188. Talinli I, Anderson GK. Interference of hydrogen peroxide on the standard cod test. Water Research. 1992;26(1):107-10.
189. Kang YW, Cho M-J, Hwang K-Y. Correction of hydrogen peroxide interference on standard chemical oxygen demand test. Water Research. 1999;33(5):1247-51.
190. Kaur R, Saini S, Patel A, Sharma T, Kaur R, Katare OP, et al. Developing a Validated HPLC Method for Quantification of Ceftazidime Employing Analytical Quality by Design and Monte Carlo Simulations. J AOAC Int. 2021;104(3):620-32.
191. Ricardo IA, Alberto EA, Silva Júnior AH, Macuvele DLP, Padoin N, Soares C, et al. A critical review on microplastics, interaction with organic and inorganic pollutants, impacts and effectiveness of advanced oxidation processes applied for their removal from aqueous matrices. Chemical Engineering Journal. 2021:130282.

192. Wagner J, Wang Z-M, Ghosal S, Rochman C, Gassel M, Wall S. Novel method for the extraction and identification of microplastics in ocean trawl and fish gut matrices. Analytical Methods. 2017;9(9):1479-90.

193. Wang Z-M, Wagner J, Ghosal S, Bedi G, Wall S. SEM/EDS and optical microscopy analyses of microplastics in ocean trawl and fish guts. Science of The Total Environment. 2017;603-604:616-26.

194. Gniadek M, Dąbrowska A. The marine nano- and microplastics characterisation by SEM-EDX: The potential of the method in comparison with various physical and chemical approaches. Marine Pollution Bulletin. 2019;148:210-6.

195. Nguyen-Tri P, Ghassemi P, Carriere P, Nanda S, Assadi AA, Nguyen DD. Recent Applications of Advanced Atomic Force Microscopy in Polymer Science: A Review. Polymers. 2020;12(5):1142.

196. Nguyen-Tri P, Prud'homme RE. Nanoscale analysis of the photodegradation of polyester fibers by AFM-IR. Journal of Photochemistry and Photobiology A: Chemistry. 2019;371:196-204.

197. Nečas D, Klapetek P. Gwyddion: an open-source software for SPM data analysis. Open Physics. 2012;10(1):181-8.

198. Rupert Hough DT, Fiona Nicholson, Steve Pierson, John Williams, Dan, Munro DD. Spreading of sewage sludge to land. The James Hutton Institute; 2016.

199. Fidra. Steps Towards Protecting Scotland's Soil Health 2023 [Available from: https://www.fidra.org.uk/news/sewage_sludge_and_soil_health/.

200. Hussain A. Digestion and Disposal of Primary and Secondary Sludge. Advanced Design of Wastewater Treatment Plants: Emerging Research and Opportunities. Hershey, PA, USA: IGI Global; 2019. p. 255-92.

201. Towers W. Towards a strategic approach to sewage sludge utilization on agricultural land in Scotland. Journal of Environmental Planning and Management. 1994;37(4):447-60.

202. Water S. 2021/22 ANNUAL REPORT AND ACCOUNTS. Scottish Water; 2022.

203. PUBLIC HEALTH S. The Sludge (Use in Agriculture) Regulations 1989. 1989.

204. Jumoke Oladejo KS, Xiang Luo, Gang Yang and Tao Wu. Sludge-to-energy recovery methods – a review Sludge Processing2020 [Available from: https://www.sludgeprocessing.com/features/sludge-to-energy-recovery-methods-an-overview/.

205. Sichler TC, Adam C, Montag D, Barjenbruch M. Future nutrient recovery from sewage sludge regarding three different scenarios - German case study. Journal of Cleaner Production. 2022;333:130130.
206. UK W. The Safe Sludge Matrix Guidelines for the Application of Sewage Sludge to Agricultural Land. 2001.
207. Biosolids A. The BAS Standard. 2020.
208. Agency E. Environment Agency strategy for safe and sustainable sludge use. 2020.
209. Gardner MJ, Comber SDW, Ellor B. Summary of data from the UKWIR chemical investigations programme and a comparison of data from the past ten years' monitoring of effluent quality. Science of The Total Environment. 2022;832:155041.
210. 91/271/EEC concerning urban waste water treatment. 1991.
211. WORKING DOCUMENT SLUDGE AND BIOWASTE. In: Industry D-GEDC-, editor. Brussels2010.
212. Ex-post evaluation of certain waste stream Directives Final Report. In: Environment ECD, editor. 2014.
213. Government S. SP Bill 31 Circular Economy (Scotland) Bill. 2023.
214. Bringhurst TA, Brosnan J. Chapter 6 - Scotch whisky: raw material selection and processing. In: Russell I, Stewart G, editors. Whisky (Second Edition). San Diego: Academic Press; 2014. p. 49-122.
215. Tytła M. Assessment of Heavy Metal Pollution and Potential Ecological Risk in Sewage Sludge from Municipal Wastewater Treatment Plant Located in the Most Industrialized Region in Poland-Case Study. Int J Environ Res Public Health. 2019;16(13).
216. Inglezakis V, Zorpas A, Karagiannidis A, Samaras P, Voukkali I, Sklari S. European Union legislation on sewage sludge management. Fresenius Environmental Bulletin. 2014;23:635-9.
217. (JRC) EC-JRC. EU Wide Monitoring Survey on Waste Water Treatment Plant Effluents. 2012.
218. Charlton A, Sakrabani R, McGrath SP, Campbell CD. Long-term Impact of Sewage Sludge Application on biovar : An Evaluation Using Meta-Analysis. J Environ Qual. 2016;45(5):1572-87.

219. Yang G-h, Zhu G-y, Li H-l, Han X-m, Li J-m, Ma Y-b. Accumulation and bioavailability of heavy metals in a soil-wheat/maize system with long-term sewage sludge amendments. Journal of Integrative Agriculture. 2018;17(8):1861-70.
220. Jamali MK, Kazi TG, Arain MB, Afridi HI, Jalbani N, Kandhro GA, et al. Heavy metal accumulation in different varieties of wheat (Triticum aestivum L.) grown in soil amended with domestic sewage sludge. Journal of Hazardous Materials. 2009;164(2):1386-91.
221. Eid EM, Shaltout KH. Bioaccumulation and translocation of heavy metals by nine native plant species grown at a sewage sludge dump site. International Journal of Phytoremediation. 2016;18(11):1075-85.
222. Zaragüeta A, Enrique A, Virto I, Antón R, Urmeneta H, Orcaray L. Effect of the Long-Term Application of Sewage Sludge to A Calcareous Soil on Its Total and Bioavailable Content in Trace Elements, and Their Transfer to the Crop. Minerals. 2021;11(4):356.
223. Nascimento AL, Souza AJ, Andrade PAM, Andreote FD, Coscione AR, Oliveira FC, et al. Sewage Sludge Microbial Structures and Relations to Their Sources, Treatments, and Chemical Attributes. Frontiers in Microbiology. 2018;9.
224. Gholipour S, Ghalhari MR, Nikaeen M, Rabbani D, Pakzad P, Miranzadeh MB. Occurrence of viruses in sewage sludge: A systematic review. Science of The Total Environment. 2022;824:153886.
225. Bibby K, Peccia J. Identification of Viral Pathogen Diversity in Sewage Sludge by Metagenome Analysis. Environmental Science & Technology. 2013;47(4):1945-51.
226. Madoni P. Protozoa in wastewater treatment processes: A minireview. Italian Journal of Zoology. 2011;78(1):3-11.
227. Hinckley GT, Johnson CJ, Jacobson KH, Bartholomay C, McMahon KD, McKenzie D, et al. Persistence of pathogenic prion protein during simulated wastewater treatment processes. Environ Sci Technol. 2008;42(14):5254-9.
228. EVALUATION OF SLUDGE TREATMENTS FOR PATHOGEN REDUCTION – FINAL REPORT. In: ENVIRONMENT ECD-G, editor. 2001.
229. Bondarczuk K, Markowicz A, Piotrowska-Seget Z. The urgent need for risk assessment on the antibiotic resistance spread via sewage sludge land application. Environment International. 2016;87:49-55.

230. Jauregi L, Epelde L, Alkorta I, Garbisu C. Agricultural Soils Amended With Thermally-Dried Anaerobically-Digested Sewage Sludge Showed Increased Risk of Antibiotic Resistance Dissemination. Frontiers in Microbiology. 2021;12.
231. Su JQ, Wei B, Ou-Yang WY, Huang FY, Zhao Y, Xu HJ, et al. Antibiotic resistome and its association with bacterial communities during sewage sludge composting. Environ Sci Technol. 2015;49(12):7356-63.
232. Riber L, Poulsen PH, Al-Soud WA, Skov Hansen LB, Bergmark L, Brejnrod A, et al. Exploring the immediate and long-term impact on bacterial communities in soil amended with animal and urban organic waste fertilizers using pyrosequencing and screening for horizontal transfer of antibiotic resistance. FEMS Microbiol Ecol. 2014;90(1):206-24.
233. Rahube TO, Marti R, Scott A, Tien YC, Murray R, Sabourin L, et al. Impact of fertilizing with raw or anaerobically digested sewage sludge on the abundance of antibiotic-resistant coliforms, antibiotic resistance genes, and pathogenic bacteria in soil and on vegetables at harvest. Appl Environ Microbiol. 2014;80(22):6898-907.
234. Hölzel CS, Schwaiger K, Harms K, Küchenhoff H, Kunz A, Meyer K, et al. Sewage sludge and liquid pig manure as possible sources of antibiotic resistant bacteria. Environ Res. 2010;110(4):318-26.
235. Chen Q, An X, Li H, Su J, Ma Y, Zhu YG. Long-term field application of sewage sludge increases the abundance of antibiotic resistance genes in soil. Environ Int. 2016;92-93:1-10.
236. Mejías C, Martín J, Santos JL, Aparicio I, Alonso E. Occurrence of pharmaceuticals and their metabolites in sewage sludge and soil: A review on their distribution and environmental risk assessment. Trends in Environmental Analytical Chemistry. 2021;30:e00125.
237. Verlicchi P, Zambello E. Pharmaceuticals and personal care products in untreated and treated sewage sludge: Occurrence and environmental risk in the case of application on soil - A critical review. Sci Total Environ. 2015;538:750-67.
238. Biale G, La Nasa J, Mattonai M, Corti A, Castelvetro V, Modugno F. Seeping plastics: Potentially harmful molecular fragments leaching out from microplastics during accelerated ageing in seawater. Water Research. 2022;219:118521.
239. Rodríguez-Narvaez OM, Goonetilleke A, Perez L, Bandala ER. Engineered technologies for the separation and degradation of microplastics in water: A review. Chemical Engineering Journal. 2021;414:128692.

240. Horton AA, Cross RK, Read DS, Jürgens MD, Ball HL, Svendsen C, et al. Semi-automated analysis of microplastics in complex wastewater samples. Environmental Pollution. 2021;268:115841.
241. Corradini F, Meza P, Eguiluz R, Casado F, Huerta-Lwanga E, Geissen V. Evidence of microplastic accumulation in agricultural soils from sewage sludge disposal. Science of The Total Environment. 2019;671:411-20.
242. Zeng Y, Tang X, Fan C, Tang L, Zhou M, Zhang B, et al. Evaluating the Effects of Different Pretreatments on Anaerobic Digestion of Waste Activated Sludge Containing Polystyrene Microplastics. ACS ES&T Water. 2022;2(1):117-27.
243. Margot J, Rossi L, Barry DA, Holliger C. A review of the fate of micropollutants in wastewater treatment plants. WIREs Water. 2015;2(5):457-87.
244. D'Alessio M, Yoneyama B, Kirs M, Kisand V, Ray C. Pharmaceutically active compounds: Their removal during slow sand filtration and their impact on slow sand filtration bacterial removal. Sci Total Environ. 2015;524-525:124-35.
245. Blair B, Nikolaus A, Hedman C, Klaper R, Grundl T. Evaluating the degradation, sorption, and negative mass balances of pharmaceuticals and personal care products during wastewater treatment. Chemosphere. 2015;134:395-401.
246. Armstrong DL, Rice CP, Ramirez M, Torrents A. Influence of thermal hydrolysis-anaerobic digestion treatment of wastewater solids on concentrations of triclosan, triclocarban, and their transformation products in biosolids. Chemosphere. 2017;171:609-16.
247. Shin M, Duncan B, Seto P, Falletta P, Lee D-Y. Dynamics of selected pre-existing polybrominated diphenylethers (PBDEs) in municipal wastewater sludge under anaerobic conditions. Chemosphere. 2010;78(10):1220-4.
248. Mailler R, Gasperi J, Chebbo G, Rocher V. Priority and emerging pollutants in sewage sludge and fate during sludge treatment. Waste Manag. 2014;34(7):1217-26.
249. Patureau D, Trably E. Impact of anaerobic and aerobic processes on polychlorobiphenyl removal in contaminated sewage sludge. Biodegradation. 2006;17(1):9-17.
250. Siebielska I, Sidełko R. Polychlorinated biphenyl concentration changes in sewage sludge and organic municipal waste mixtures during composting and anaerobic digestion. Chemosphere. 2015;126:88-95.

251. GarcIa M, Rico D. Presence of Siloxanes in the Biogas of a Wastewater Treatment Plant Separation in Condensates and Influence of the Dose of Iron Chloride on its Elimination. International Journal of Waste Resources. 2016;06.
252. Appels L, Baeyens J, Dewil R. Siloxane removal from biosolids by peroxidation. Energy Conversion and Management. 2008;49(10):2859-64.
253. Paterakis N, Chiu TY, Koh YKK, Lester JN, McAdam EJ, Scrimshaw MD, et al. The effectiveness of anaerobic digestion in removing estrogens and nonylphenol ethoxylates. Journal of Hazardous Materials. 2012;199-200:88-95.
254. Hernandez-Raquet G, Soef A, Delgenès N, Balaguer P. Removal of the endocrine disrupter nonylphenol and its estrogenic activity in sludge treatment processes. Water Res. 2007;41(12):2643-51.
255. Fließbach A, Martens R, Reber HH. Soil microbial biomass and microbial activity in soils treated with heavy metal contaminated sewage sludge. Soil Biology and Biochemistry. 1994;26(9):1201-5.
256. Picariello E, Pucci L, Carotenuto M, Libralato G, Lofrano G, Baldantoni D. Compost and Sewage Sludge for the Improvement of Soil Chemical and Biological Quality of Mediterranean Agroecosystems. Sustainability. 2021;13(1):26.
257. Eid EM, Alrumman SA, El-Bebany AF, Fawy KF, Taher MA, Hesham AE-L, et al. The evaluation of sewage sludge application as a fertilizer for broad bean (Faba sativa Bernh.) crops. Food and Energy Security. 2018;7(3):e00142.
258. Optimising the application of bulky organic fertilisers. Edinburgh: Scotland's Rural College; 2013.
259. Kim KR, Owens G. 6.21 - Potential for Enhanced Phytoremediation of Landfills Using Biosolids – A Review. In: Moo-Young M, editor. Comprehensive Biotechnology (Second Edition). Burlington: Academic Press; 2011. p. 239-47.
260. Spicer S. Fertilizers, manure; or biosolids? Water Environment and Technology. 2002;14(7):32-5.
261. Nanzer S, Oberson A, Berger L, Berset E, Hermann L, Frossard E. The plant availability of phosphorus from thermo-chemically treated sewage sludge ashes as studied by 33P labeling techniques. Plant and Soil. 2014;377(1):439-56.
262. Petersen SO, Petersen J, Rubæk GH. Dynamics and plant uptake of nitrogen and phosphorus in soil amended with sewage sludge. Applied Soil Ecology. 2003;24(2):187-95.

263. SRUC. Optimising the application of bulky organic fertilisers. 2013.

264. Andriamananjara A, Rabeharisoa L, Prud'homme L, Morel C. Drivers of Plant-Availability of Phosphorus from Thermally Conditioned Sewage Sludge as Assessed by Isotopic Labeling. Frontiers in Nutrition. 2016;3.

265. Wood S, Cowie A. A Review of Greenhouse Gas Emission Factors for Fertiliser Production2004. 20 p.

266. Grylls B. Government must appreciate importance of fertiliser in food security: Food Manufacture; 2022 [Available from: https://www.foodmanufacture.co.uk/Article/2022/12/22/fertiliser-is-important-for-food-security-nfu-scotland-say.

267. Easton T, Koutsos V, Chatzisymeon E. Removal of polyester fibre microplastics from wastewater using a UV/H2O2 oxidation process. Journal of Environmental Chemical Engineering. 2023;11(1):109057.

268. Kelly MR, Lant NJ, Kurr M, Burgess JG. Importance of Water-Volume on the Release of Microplastic Fibers from Laundry. Environmental Science & Technology. 2019;53(20):11735-44.

269. Hernandez E, Nowack B, Mitrano DM. Polyester Textiles as a Source of Microplastics from Households: A Mechanistic Study to Understand Microfiber Release During Washing. Environmental Science & Technology. 2017;51(12):7036-46.

270. Frehland S, Kaegi R, Hufenus R, Mitrano DM. Long-term assessment of nanoplastic particle and microplastic fiber flux through a pilot wastewater treatment plant using metal-doped plastics. Water Research. 2020;182:115860.

271. Cai Y, Yang T, Mitrano DM, Heuberger M, Hufenus R, Nowack B. Systematic Study of Microplastic Fiber Release from 12 Different Polyester Textiles during Washing. Environmental Science & Technology. 2020;54(8):4847-55.

272. Graham ER, Thompson JT. Deposit- and suspension-feeding sea cucumbers (Echinodermata) ingest plastic fragments. Journal of Experimental Marine Biology and Ecology. 2009;368(1):22-9.

273. Au SY, Bruce TF, Bridges WC, Klaine SJ. Responses of Hyalella azteca to acute and chronic microplastic exposures. Environmental Toxicology and Chemistry. 2015;34(11):2564-72.

274. Hämer J, Gutow L, Köhler A, Saborowski R. Fate of Microplastics in the Marine Isopod Idotea emarginata. Environmental Science & Technology. 2014;48(22):13451-8.
275. Watts AJR, Urbina MA, Corr S, Lewis C, Galloway TS. Ingestion of Plastic Microfibers by the Crab Carcinus maenas and Its Effect on Food Consumption and Energy Balance. Environmental Science & Technology. 2015;49(24):14597-604.
276. Cole M. A novel method for preparing microplastic fibers. Scientific Reports. 2016;6(1):34519.
277. Eitzen L, Paul S, Braun U, Altmann K, Jekel M, Ruhl AS. The challenge in preparing particle suspensions for aquatic microplastic research. Environmental Research. 2019;168:490-5.
278. von der Esch E, Lanzinger M, Kohles AJ, Schwaferts C, Weisser J, Hofmann T, et al. Simple Generation of Suspensible Secondary Microplastic Reference Particles via Ultrasound Treatment. Frontiers in Chemistry. 2020;8(169).
279. Napper IE, Bakir A, Rowland SJ, Thompson RC. Characterisation, quantity and sorptive properties of microplastics extracted from cosmetics. Marine Pollution Bulletin. 2015;99(1):178-85.
280. Sait STL, Sørensen L, Kubowicz S, Vike-Jonas K, Gonzalez SV, Asimakopoulos AG, et al. Microplastic fibres from synthetic textiles: Environmental degradation and additive chemical content. Environmental Pollution. 2021;268:115745.
281. Priyadarshini M, Das I, Ghangrekar MM, Blaney L. Advanced oxidation processes: Performance, advantages, and scale-up of emerging technologies. Journal of Environmental Management. 2022;316:115295.
282. Advanced Oxidation Processes for Water Treatment: Fundamentals and Applications: IWA Publishing; 2017. Available from: https://doi.org/10.2166/9781780407197.
283. Lutterbeck CA, Colares GS, Dell'Osbel N, da Silva FP, Kist LT, Machado ÊL. Hospital laundry wastewaters: A review on treatment alternatives, life cycle assessment and prognosis scenarios. Journal of Cleaner Production. 2020;273:122851.
284. Zotesso JP, Cossich ES, Janeiro V, Tavares CRG. Treatment of hospital laundry wastewater by UV/H(2)O(2) process. Environ Sci Pollut Res Int. 2017;24(7):6278-87.

285. Gewert B, Plassmann M, Sandblom O, MacLeod M. Identification of Chain Scission Products Released to Water by Plastic Exposed to Ultraviolet Light. Environmental Science & Technology Letters. 2018;5(5):272-6.
286. Arrieta JS, Richaud E, Fayolle B, Nizeyimana F. Thermal oxidation of vinyl ester and unsaturated polyester resins. Polymer Degradation and Stability. 2016;129:142-55.
287. Thiruvenkatachari R, Kwon TO, Jun JC, Balaji S, Matheswaran M, Moon IS. Application of several advanced oxidation processes for the destruction of terephthalic acid (TPA). Journal of Hazardous Materials. 2007;142(1-2):308-14.
288. Michael SG, Michael-Kordatou I, Nahim-Granados S, Polo-López MI, Rocha J, Martínez-Piernas AB, et al. Investigating the impact of UV-C/H2O2 and sunlight/H2O2 on the removal of antibiotics, antibiotic resistance determinants and toxicity present in urban wastewater. Chemical Engineering Journal. 2020;388:124383.
289. Lin J, Yan D, Fu J, Chen Y, Ou H. Ultraviolet-C and vacuum ultraviolet inducing surface degradation of microplastics. Water Research. 2020;186:116360.
290. Walker NL, Williams AP, Styles D. Pitfalls in international benchmarking of energy intensity across wastewater treatment utilities. Journal of Environmental Management. 2021;300:113613.
291. Lambert S, Wagner M. Formation of microscopic particles during the degradation of different polymers. Chemosphere. 2016;161:510-7.
292. Schwaferts C, Niessner R, Elsner M, Ivleva NP. Methods for the analysis of submicrometer- and nanoplastic particles in the environment. TrAC Trends in Analytical Chemistry. 2019;112:52-65.
293. Chang M-W, Chung C-C, Chern J-M, Chen T-S. Dye decomposition kinetics by UV/H2O2: Initial rate analysis by effective kinetic modelling methodology. Chemical Engineering Science. 2010;65(1):135-40.
294. Rubio-Clemente A, Chica E, Peñuela GA. Kinetic Modeling of the UV/H2O2 Process: Determining the Effective Hydroxyl Radical Concentration. In: Ahmad RFaZ, editor. Physico-Chemical Wastewater Treatment and Resource Recovery: IntechOpen; 2017.
295. Goldstein S, Aschengrau D, Diamant Y, Rabani J. Photolysis of Aqueous H2O2: Quantum Yield and Applications for Polychromatic UV Actinometry in Photoreactors. Environmental Science & Technology. 2007;41(21):7486-90.

296. Beltrán-Sanahuja A, Casado-Coy N, Simó-Cabrera L, Sanz-Lázaro C. Monitoring polymer degradation under different conditions in the marine environment. Environmental Pollution. 2020;259:113836.
297. Hurley CR, Leggett GJ. Quantitative Investigation of the Photodegradation of Polyethylene Terephthalate Film by Friction Force Microscopy, Contact-Angle Goniometry, and X-ray Photoelectron Spectroscopy. ACS Applied Materials & Interfaces. 2009;1(8):1688-97.
298. Braga J, Varesche M. Commercial Laundry Water Characterisation. American Journal of Analytical Chemistry. 2014;5(1):8-16.
299. Wu N, Cao W, Qu R, Zhou D, Sun C, Wang Z. Photochemical transformation of decachlorobiphenyl (PCB-209) on the surface of microplastics in aqueous solution. Chemical Engineering Journal. 2021;420:129813.
300. Easton T, Maksymiuk K, Charlton L, Koutsos V, Chatzisymeon E. Transformation of polyester fibre microplastics by sulfate based advanced oxidation processes. Journal of Environmental Chemical Engineering. 2024:112988.
301. Bhagat K, Barrios AC, Rajwade K, Kumar A, Oswald J, Apul O, et al. Aging of microplastics increases their adsorption affinity towards organic contaminants. Chemosphere. 2022;298:134238.
302. Ouyang Z, Li S, Zhao M, Wangmu Q, Ding R, Xiao C, et al. The aging behavior of polyvinyl chloride microplastics promoted by UV-activated persulfate process. Journal of Hazardous Materials. 2022;424:127461.
303. Liu X, Deng Q, Zheng Y, Wang D, Ni B-J. Microplastics aging in wastewater treatment plants: Focusing on physicochemical characteristics changes and corresponding environmental risks. Water Research. 2022;221:118780.
304. Wang Q, Rao P, Li G, Dong L, Zhang X, Shao Y, et al. Degradation of imidacloprid by UV-activated persulfate and peroxymonosulfate processes: Kinetics, impact of key factors and degradation pathway. Ecotoxicology and Environmental Safety. 2020;187:109779.
305. Gabet A, Métivier H, de Brauer C, Mailhot G, Brigante M. Hydrogen peroxide and persulfate activation using UVA-UVB radiation: Degradation of estrogenic compounds and application in sewage treatment plant waters. Journal of Hazardous Materials. 2021;405:124693.

306. Zhong Y, Zhang B, Zhu Z, Wang G, Mei X, Fang Y, et al. Photocatalytic-Driven Self-Degradation of Polyester Microplastics Under Solar Light. Journal of Polymers and the Environment. 2023;31(6):2415-23.
307. Jeong Y, Gong G, Lee H-J, Seong J, Hong SW, Lee C. Transformation of microplastics by oxidative water and wastewater treatment processes: A critical review. Journal of Hazardous Materials. 2023;443:130313.
308. Zhang Y, Luo Y, Yu X, Huang D, Guo X, Zhu L. Aging significantly increases the interaction between polystyrene nanoplastic and minerals. Water Research. 2022;219:118544.
309. Gujar SK, Divyapriya G, Gogate PR, Nidheesh PV. Environmental applications of ultrasound activated persulfate/peroxymonosulfate oxidation process in combination with other activating agents. Crit Rev Environ Sci Technol. 2023;53(6):780-802.
310. Cai Y, Mitrano DM, Hufenus R, Nowack B. Formation of Fiber Fragments during Abrasion of Polyester Textiles. Environmental Science & Technology. 2021;55(12):8001-9.
311. Ahn Y-Y, Choi J, Kim M, Kim MS, Lee D, Bang WH, et al. Chloride-Mediated Enhancement in Heat-Induced Activation of Peroxymonosulfate: New Reaction Pathways for Oxidizing Radical Production. Environmental Science & Technology. 2021;55(8):5382-92.
312. Ji Y, Shi Y, Dong W, Wen X, Jiang M, Lu J. Thermo-activated persulfate oxidation system for tetracycline antibiotics degradation in aqueous solution. Chemical Engineering Journal. 2016;298:225-33.
313. Kolthoff IM, Miller IK. The Chemistry of Persulfate. I. The Kinetics and Mechanism of the Decomposition of the Persulfate Ion in Aqueous Medium1. Journal of the American Chemical Society. 1951;73:3055-9.
314. Yang Q, Ma Y, Chen F, Yao F, Sun J, Wang S, et al. Recent advances in photo-activated sulfate radical-advanced oxidation process (SR-AOP) for refractory organic pollutants removal in water. Chemical Engineering Journal. 2019;378:122149.
315. Sonawane S, Rayaroth MP, Landge VK, Fedorov K, Boczkaj G. Thermally activated persulfate-based Advanced Oxidation Processes — recent progress and challenges in mineralization of persistent organic chemicals: a review. Current Opinion in Chemical Engineering. 2022;37:100839.

316. Zhou T, Du J, Wang Z, Xiao G, Luo L, Faheem M, et al. Degradation of sulfamethoxazole by MnO2/heat-activated persulfate: Kinetics, synergistic effect and reaction mechanism. Chemical Engineering Journal Advances. 2022;9:100200.
317. Shuchi SB, Suhan MBK, Humayun SB, Haque ME, Islam MS. Heat-activated potassium persulfate treatment of Sudan Black B dye: Degradation kinetic and thermodynamic studies. Journal of Water Process Engineering. 2021;39:101690.
318. Liu Y, Wang S, Wu Y, Chen H, Shi Y, Liu M, et al. Degradation of ibuprofen by thermally activated persulfate in soil systems. Chemical Engineering Journal. 2019;356:799-810.
319. Behnami A, Aghayani E, Benis KZ, Sattari M, Pourakbar M. Comparing the efficacy of various methods for sulfate radical generation for antibiotics degradation in synthetic wastewater: degradation mechanism, kinetics study, and toxicity assessment. RSC Advances. 2022;12(23):14945-56.
320. Guan Y-H, Ma J, Li X-C, Fang J-Y, Chen L-W. Influence of pH on the Formation of Sulfate and Hydroxyl Radicals in the UV/Peroxymonosulfate System. Environmental Science & Technology. 2011;45(21):9308-14.
321. Mahdi-Ahmed M, Chiron S. Ciprofloxacin oxidation by UV-C activated peroxymonosulfate in wastewater. Journal of Hazardous Materials. 2014;265:41-6.
322. Yang S, Wang P, Yang X, Shan L, Zhang W, Shao X, et al. Degradation efficiencies of azo dye Acid Orange 7 by the interaction of heat, UV and anions with common oxidants: Persulfate, peroxymonosulfate and hydrogen peroxide. Journal of Hazardous Materials. 2010;179(1):552-8.
323. Mouamfon MV, Li W, Lu S, Qiu Z, Chen N, Lin K. Photodegradation of sulphamethoxazole under UV-light irradiation at 254 nm. Environ Technol. 2010;31(5):489-94.
324. Wang J, Wang S. Activation of persulfate (PS) and peroxymonosulfate (PMS) and application for the degradation of emerging contaminants. Chemical Engineering Journal. 2018;334:1502-17.
325. Matzek LW, Carter KE. Activated persulfate for organic chemical degradation: A review. Chemosphere. 2016;151:178-88.

326. Wacławek S, Lutze HV, Grübel K, Padil VVT, Černík M, Dionysiou DD. Chemistry of persulfates in water and wastewater treatment: A review. Chemical Engineering Journal. 2017;330:44-62.
327. Xia X, Zhu F, Li J, Yang H, Wei L, Li Q, et al. A Review Study on Sulfate-Radical-Based Advanced Oxidation Processes for Domestic/Industrial Wastewater Treatment: Degradation, Efficiency, and Mechanism. Frontiers in Chemistry. 2020;8.
328. Zhao D, Liao X, Yan X, Huling SG, Chai T, Tao H. Effect and mechanism of persulfate activated by different methods for PAHs removal in soil. J Hazard Mater. 2013;254-255:228-35.
329. Wacławek S, Lutze HV, Sharma VK, Xiao R, Dionysiou DD. Revisit the alkaline activation of peroxydisulfate and peroxymonosulfate. Current Opinion in Chemical Engineering. 2022;37:100854.
330. Ajala OJ, Tijani JO, Salau RB, Abdulkareem AS, Aremu OS. A review of emerging micro-pollutants in hospital wastewater: Environmental fate and remediation options. Results in Engineering. 2022;16:100671.
331. Rayaroth MP, Aravindakumar CT, Shah NS, Boczkaj G. Advanced oxidation processes (AOPs) based wastewater treatment - unexpected nitration side reactions - a serious environmental issue: A review. Chemical Engineering Journal. 2022;430:133002.
332. Duan J, Bolan N, Li Y, Ding S, Atugoda T, Vithanage M, et al. Weathering of microplastics and interaction with other coexisting constituents in terrestrial and aquatic environments. Water Research. 2021;196:117011.
333. Asamoah BO, Roussey M, Peiponen K-E. On optical sensing of surface roughness of flat and curved microplastics in water. Chemosphere. 2020;254:126789.
334. Hossain MR, Jiang M, Wei Q, Leff LG. Microplastic surface properties affect bacterial colonization in freshwater. J Basic Microbiol. 2019;59(1):54-61.
335. Dos Santos NdO, Busquets R, Campos LC. Insights into the removal of microplastics and microfibres by Advanced Oxidation Processes. Science of The Total Environment. 2023;861:160665.
336. Yang T, Luo J, Nowack B. Characterization of Nanoplastics, Fibrils, and Microplastics Released during Washing and Abrasion of Polyester Textiles. Environ Sci Technol. 2021;55(23):15873-81.

337. Galafassi S, Sabatino R, Sathicq MB, Eckert EM, Fontaneto D, Dalla Fontana G, et al. Contribution of microplastic particles to the spread of resistances and pathogenic bacteria in treated wastewaters. Water Research. 2021;201:117368.
338. Organisation WH. Critically Important Antimicrobials for Human Medicine. 2018.
339. Gaşpar C-M, Cziszter LT, Lăzărescu CF, Ţibru I, Pentea M, Butnariu M. Antibiotic Resistance among Escherichia coli Isolates from Hospital Wastewater Compared to Community Wastewater. Water. 2021;13(23):3449.
340. Tejedor-Junco MT, Díaz VC, González-Martín M, Tuya F. Presence of microplastics and antimicrobial-resistant bacteria in sea cucumbers under different anthropogenic influences in Gran Canaria (Canary Islands, Spain). Marine Biology Research. 2021;17(7-8):537-44.
341. Zhang H, HU X. Adsorption of Ceftazidime from Aqueous Solution by Multi-Walled Carbon Nanotubes. Polish Journal of Environmental Studies. 2015;24(5):2285-93.
342. Wang G, Sun T, Sun Z, Hu X. Preparation of copper based metal organic framework materials and its effective adsorptive removal of ceftazidime from aqueous solutions. Applied Surface Science. 2020;532:147411.
343. Hu X, Zhang H, Sun Z. Adsorption of low concentration ceftazidime from aqueous solutions using impregnated activated carbon promoted by Iron, Copper and Aluminum. Applied Surface Science. 2017;392:332-41.
344. Tumrani SH, Soomro RA, Zhang X, Bhutto DA, Bux N, Ji X. Coal fly ash driven zeolites for the adsorptive removal of the ceftazidime drug. RSC Advances. 2021;11(42):26110-9.
345. Shi K, Zhang H, Xu H, Liu Z, Kan G, Yu K, et al. Adsorption behaviors of triclosan by non-biodegradable and biodegradable microplastics: Kinetics and mechanism. Science of The Total Environment. 2022;842:156832.
346. Song Y, Zhao J, Zheng L, Zhu W, Xue X, Yu Y, et al. Adsorption behaviors and mechanisms of humic acid on virgin and aging microplastics. Journal of Molecular Liquids. 2022;363:119819.
347. Tables for Organic Chemistry. In: Stenutz, editor. 2023.
348. Arun K, Chidambaram S, Balachandar R, Kumuthavalli MV, Jayakar B. UV-Spectrophoto -metric determination of Ceftazidime in pure and pharmaceutical formulation. J Chem Pharm Res. 2010;2:424-31.

349. Nagaraja P, Yathirajan HS, Raju CR, Vasantha RA, Nagendra P, Hemantha Kumar MS. 3-Aminophenol as a novel coupling agent for the spectrophotometric determination of sulfonamide derivatives. Farmaco. 2003;58(12):1295-300.
350. Mohammed NS, M. Hassan MJ, Mahdi AS. New Spectrophotometric Method for Estimation of Ceftazidime in pure and pharmaceutical dosage. Al-Mustansiriyah Journal of Science. 2019;30(3):47-52.
351. Roopa KP, Jayanna BK. Spectrophotometric Determination of Some Cephalosporins in Bulk and in Pharmaceutical Formulations. Analytical Chemistry Letters. 2016;6(2):143-52.
352. Wu J, Xu P, Chen Q, Ma D, Ge W, Jiang T, et al. Effects of polymer aging on sorption of 2,2',4,4'-tetrabromodiphenyl ether by polystyrene microplastics. Chemosphere. 2020;253:126706.
353. Conradie W, Dorfling C, Chimphango A, Booth AM, Sørensen L, Akdogan G. Investigating the Physicochemical Property Changes of Plastic Packaging Exposed to UV Irradiation and Different Aqueous Environments. Microplastics. 2022;1(3):456-76.
354. Yu Y, Ma R, Qu H, Zuo Y, Yu Z, Hu G, et al. Enhanced adsorption of tetrabromobisphenol a (TBBPA) on cosmetic-derived plastic microbeads and combined effects on zebrafish. Chemosphere. 2020;248:126067.
355. Hu E, Yuan H, Du Y, Chen X. LDPE and HDPE Microplastics Differently Affect the Transport of Tetracycline in Saturated Porous Media. Materials (Basel). 2021;14(7).
356. Fu L, Li J, Wang G, Luan Y, Dai W. Adsorption behavior of organic pollutants on microplastics. Ecotoxicology and Environmental Safety. 2021;217:112207.
357. Baensch-Baltruschat B, Kocher B, Stock F, Reifferscheid G. Tyre and road wear particles (TRWP) - A review of generation, properties, emissions, human health risk, ecotoxicity, and fate in the environment. Science of The Total Environment. 2020;733:137823.
358. Changfu Y, Jiani G, Yidi Y, Yijin L, Yiyao L, Yu F. Interface behavior changes of weathered polystyrene with ciprofloxacin in seawater environment. Environmental Research. 2022;212:113132.
359. Sun M, Yang Y, Huang M, Fu S, Hao Y, Hu S, et al. Adsorption behaviors and mechanisms of antibiotic norfloxacin on degradable and nondegradable microplastics. Science of The Total Environment. 2022;807:151042.

360. Guo X, Chen C, Wang J. Sorption of sulfamethoxazole onto six types of microplastics. Chemosphere. 2019;228:300-8.
361. Li J, Zhang K, Zhang H. Adsorption of antibiotics on microplastics. Environmental Pollution. 2018;237:460-7.
362. Zhuang S, Wang J. Interaction between antibiotics and microplastics: Recent advances and perspective. Science of The Total Environment. 2023;897:165414.
363. Xiong Y, Zhao J, Li L, Wang Y, Dai X, Yu F, et al. Interfacial interaction between micro/nanoplastics and typical PPCPs and nanoplastics removal via electrosorption from an aqueous solution. Water Research. 2020;184:116100.
364. An D, Na J, Song J, Jung J. Size-dependent chronic toxicity of fragmented polyethylene microplastics to Daphnia magna. Chemosphere. 2021;271:129591.
365. Bråte ILN, Blázquez M, Brooks SJ, Thomas KV. Weathering impacts the uptake of polyethylene microparticles from toothpaste in Mediterranean mussels (M. galloprovincialis). Science of The Total Environment. 2018;626:1310-8.
366. Rathore C, Saha M, Gupta P, Kumar M, Naik A, de Boer J. Standardization of micro-FTIR methods and applicability for the detection and identification of microplastics in environmental matrices. Science of The Total Environment. 2023;888:164157.
367. Wang F, Shih KM, Li XY. The partition behavior of perfluorooctanesulfonate (PFOS) and perfluorooctanesulfonamide (FOSA) on microplastics. Chemosphere. 2015;119:841-7.
368. Guo X, Liu Y, Wang J. Sorption of sulfamethazine onto different types of microplastics: A combined experimental and molecular dynamics simulation study. Marine Pollution Bulletin. 2019;145:547-54.

Appendix A: Supplementary data

Table A.1 Spiked recovery of MP fibres from ultrapure water

Spiked mass (g)	Recovered mass (g)	Recovery (%)	Group average (%)	Standard deviation
0.0646	0.0637	98.6	**98.9**	**0.29**
0.0571	0.0567	99.3		
0.0627	0.0620	98.9		
0.0684	0.0677	99.0		
0.0102	0.0101	99.0	**99.6**	**1.04**
0.0096	0.0095	99.0		
0.0127	0.0128	100.8		
0.0038	0.0037	97.4	**98.2**	**3.41**
0.0043	0.0041	95.3		
0.0050	0.0051	102.0		
0.0016	0.0015	93.8	**93.4**	**1.57**
0.0019	0.0018	94.7		
0.0024	0.0022	91.7		
0.0014	0.0011	78.6	**92.9**	**12.37**
0.0011	0.0011	100.0		
0.0014	0.0014	100.0		
0.0005	0.0004	80.0	**88.6**	**10.30**
0.0006	0.0006	100.0		
0.0007	0.0006	85.7		

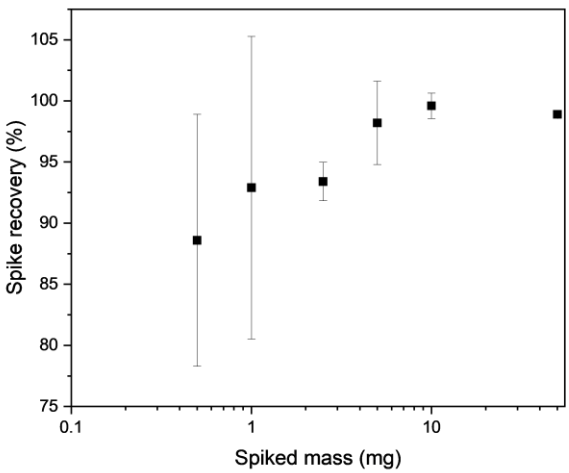

Figure A.1 Spiked mass recovery of cut polyester fibres in ultrapure wastewater

Table A.2 Spiked recovery of MP fibres from real laundry wastewater

Spiked mass (g)	Recovered mass (g)	Recovery (%)	Group average (%)	Standard deviation
0.0574	0.05699	99.3%	**98.3**	**0.6**
0.0544	0.05311	97.6%		
0.0519	0.05104	98.3%		
0.0588	0.0575	97.8%		
0.0109	0.0105	96.3%	**97.8**	**1.1**
0.0104	0.0102	98.1%		
0.0103	0.0102	99.0%		
0.0053	0.0051	96.2%	**92.7**	**3.5**
0.005	0.0044	88.0%		
0.0049	0.0046	93.9%		
0.0024	0.0015	62.5%	**84.8**	**19.5**
0.0022	0.0018	81.8%		
0.002	0.0022	110.0%		
0.0011	0.0009	81.8%	**83.2**	**5.8**
0.0011	0.001	90.9%		
0.0013	0.001	76.9%		
0.0005	0.0003	60.0%	**74.4**	**10.3**
0.0006	0.0005	83.3%		
0.0005	0.0004	80.0%		

Table A.3 Spiked recovery of uncut polyester fibres from ultrapure water

Spiked mass (g)	Recovered mass (g)	Recovery (%)	Average (%)
0.0627	0.0624	99.5	99.6
0.0684	0.0682	99.7	
0.0096	0.0095	99.0	98.3
0.0127	0.0124	97.6	
0.0038	0.0037	97.4	98.7
0.005	0.005	100.0	
0.0024	0.0023	95.8	97.9
0.0016	0.0016	100.0	
0.0014	0.0014	100.0	96.5
0.0014	0.0013	92.9	
0.0006	0.0006	100.0	92.9
0.0007	0.0006	85.7	

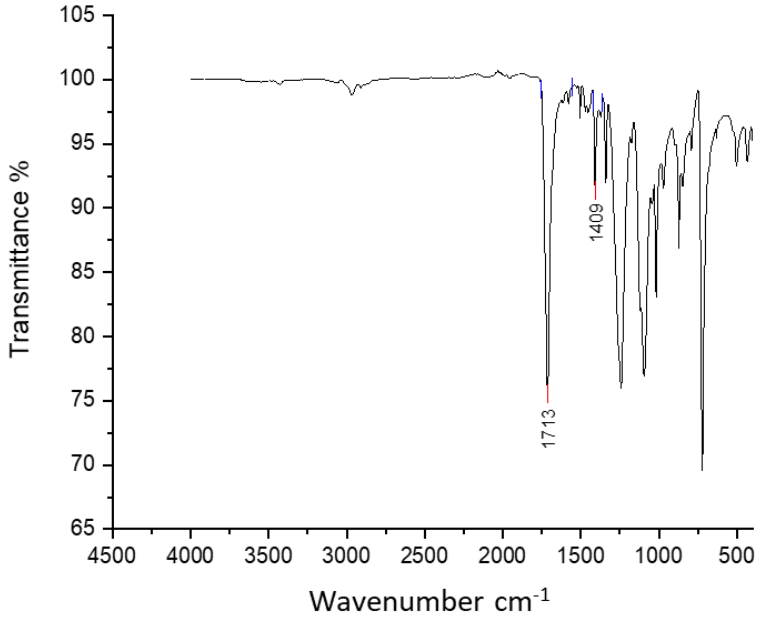

Figure A.2 FTIR spectra of polyester fibres - Control Experiment

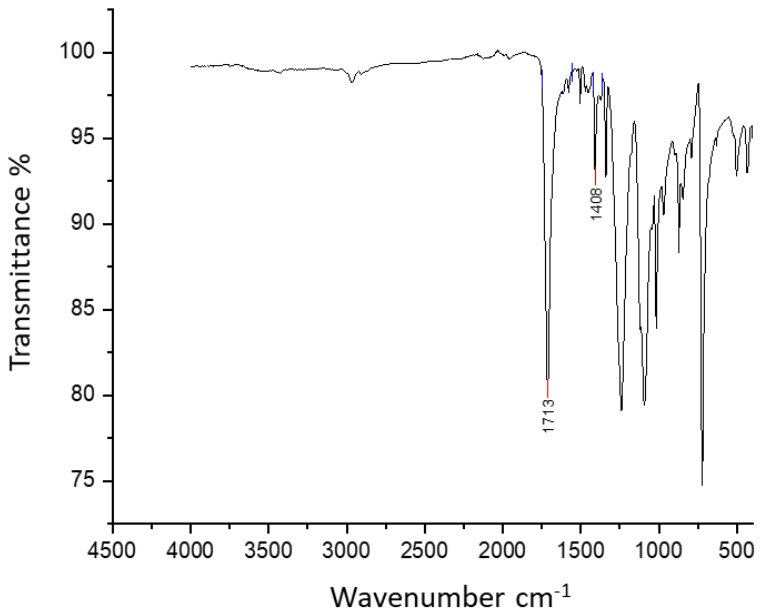

Figure A.3 FTIR spectra of polyester fibres – treated with H_2O_2/dark (500 mg L^{-1} H_2O_2)

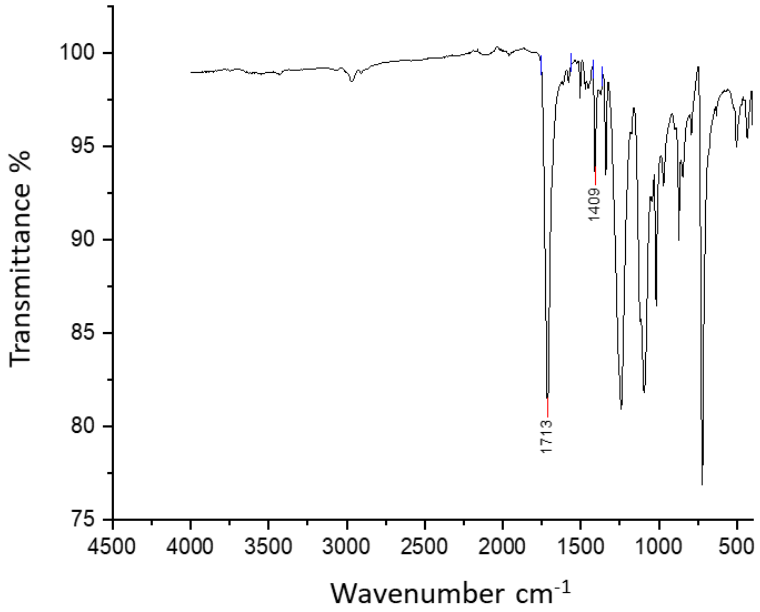

Figure A.4 FTIR spectra of polyester fibres - treated with UVC

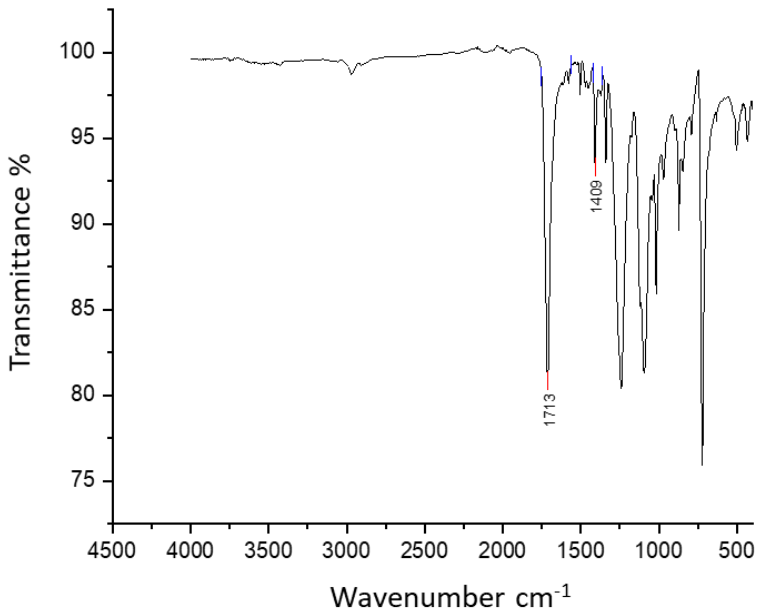

Figure A.5 FTIR spectra of polyester fibres - treated with UVC/ H_2O_2 (500 mg L^{-1} H_2O_2)

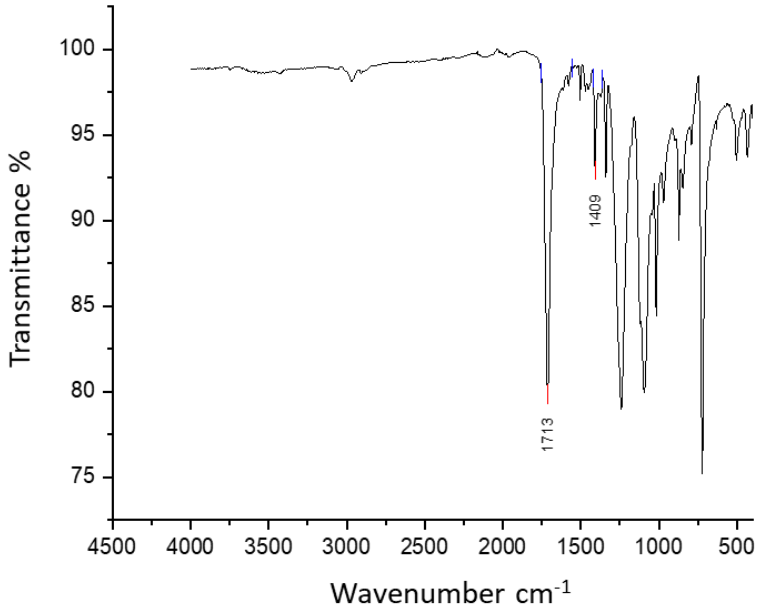

Figure A.6 FTIR spectra of polyester fibres - treated with UVC/ H_2O_2 (800 mg L^{-1} H_2O_2)

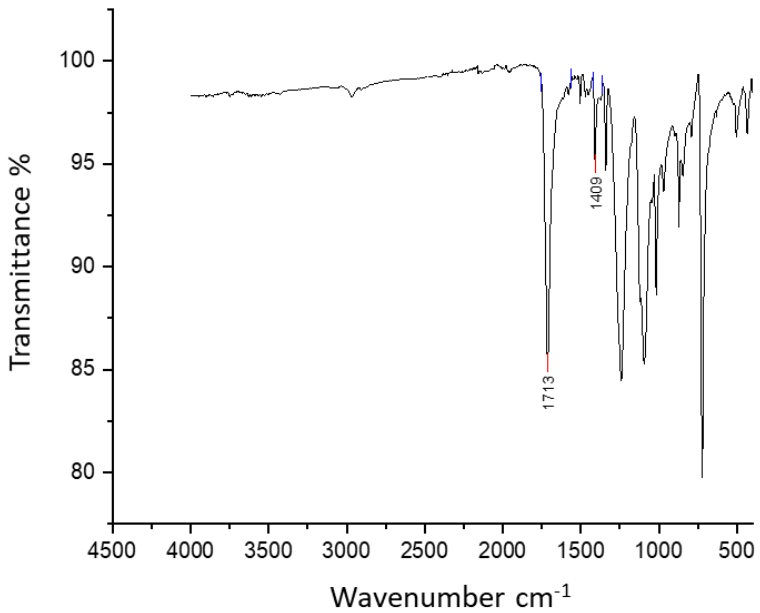

Figure A.7 FTIR spectra of polyester fibres - treated with UVC/ H_2O_2 (1200 mg L^{-1} H_2O_2)

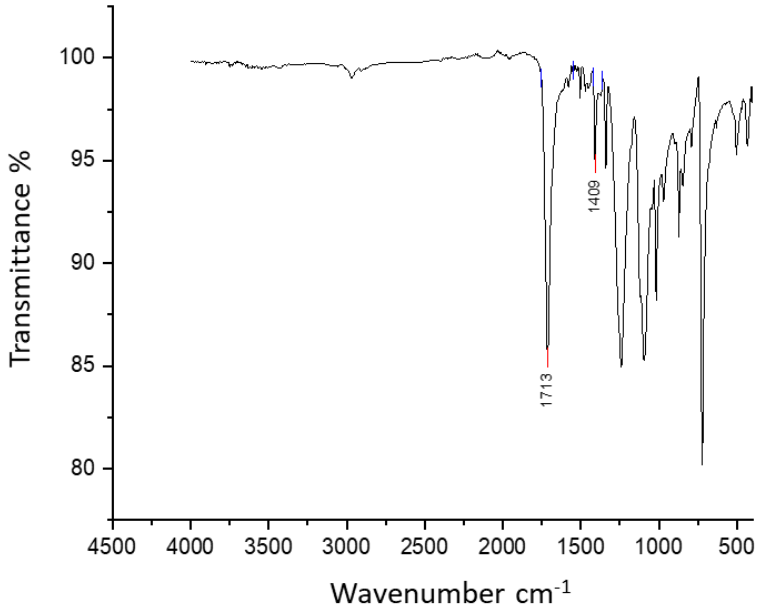

Figure A.8 FTIR spectra of polyester fibres - treated with UVC/ H_2O_2 (2000 mg L^{-1} H_2O_2)

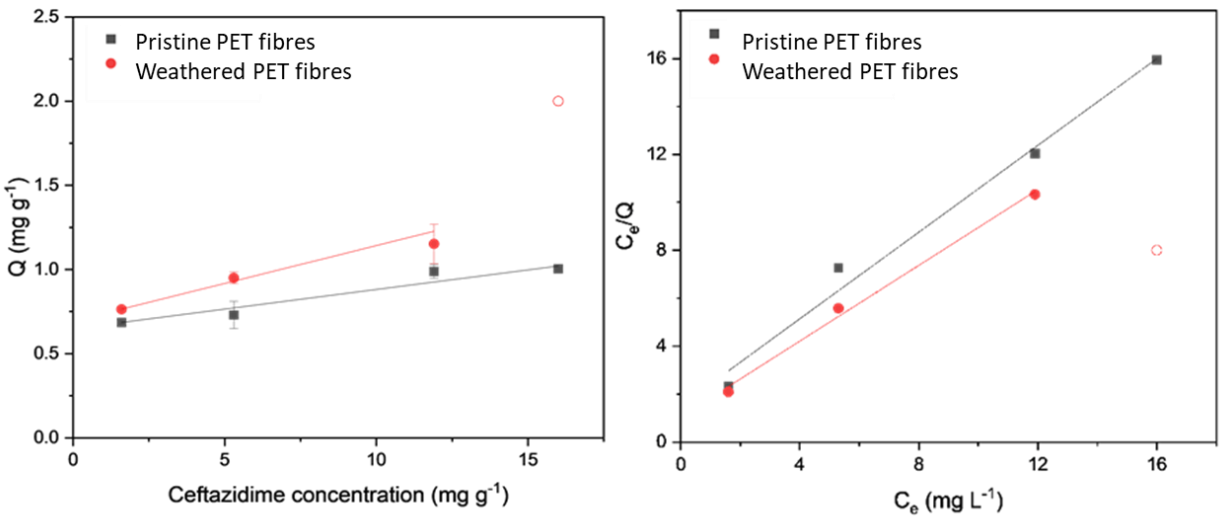

Figure A.9 Isotherm fitting plots for linear (left) and Langmuir (right) models

Table A.4 Isotherm fitting data for ceftazidime adsorption by PET fibres

	Pristine (a)	Weathered (b)
Linear model		
Intercept	0.648 ± 0.012	0.693 ± 0.014
Slope	0.023 ± 0.002	0.045 ± 0.006
R-Square (COD)	0.983	0.980
Langmuir model		
Intercept	1.519 ± 0.763	1.049 ± 0.435
Slope	0.904 ± 0.073	0.790 ± 0.057
R-Square (COD)	0.986	0.994

Table A.5 Chemical Oxygen Demand (COD) of treated polyester fibres by UVC/H_2O_2 AOP

Treatment	Final COD (mg L^{-1})
No treatment	1.4 ± 1.2 mg L^{-1}
UVC/H_2O_2 (4.0 mW cm^{-2})	6. 0 ± 1.4 mg L^{-1}
UVC/H_2O_2 (31.8 mW cm^{-2})	11.3 ± 1.6 mg L^{-1}
UVC (4.0 mW cm^{-2})	7.0 ± 3.6 mg L^{-1}
UVC (31.8 mW cm^{-2})	1.9 ± 1.8 mg L^{-1}

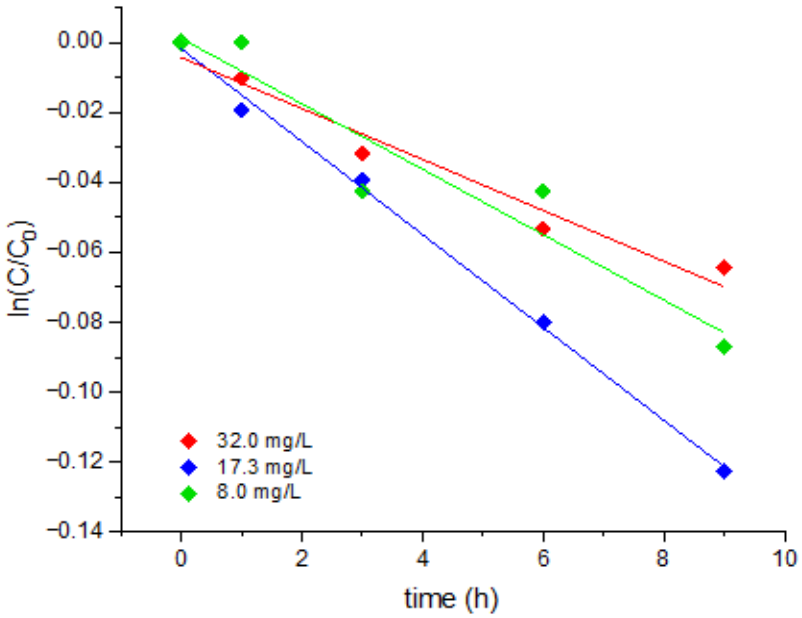

Figure A.10 Kinetic fitting of polyester fibre concentration decrease over time with varied starting concentrations (UVC/H_2O_2 treatment parameters: 31.8 mW cm^{-2} UVC, 500 mg L^{-1} H_2O_2 treatment over 9 h).

Table A.6 Kinetic fitting parameters used to calculate rate of polyester removal by UVC/H_2O_2 under varied H_2O_2 concentrations

	H_2O_2 concentration (mg/L)					
	0	50	100	200	400	500
Time (h)	Mass of polyester in reactor (g)					
0	0.010167	0.010167	0.0096	0.010733	0.0111	0.010267
1	0.009967	0.0101	0.009567	0.010533	0.010933	0.010133
3	0.009867	0.010067	0.009533	0.0104	0.0109	0.009867
6	0.009767	0.009667	0.009233	0.010167	0.0106	0.009833
9	0.009633	0.009433	0.008833	0.009433	0.009733	0.0096
	Concentration of polyester (g/L)					
0	0.203333	0.203333	0.192	0.214667	0.222	0.205333
1	0.199333	0.202	0.191333	0.210667	0.218667	0.202667
3	0.197333	0.201333	0.190667	0.208	0.218	0.197333
6	0.195333	0.193333	0.184667	0.203333	0.212	0.196667
9	0.192667	0.188667	0.176667	0.188667	0.194667	0.192
	Ln(C/C_0)					
0	0	0	0	0	0	0
1	-0.00863	-0.00286	-0.00151	-0.00817	-0.00657	-0.00568
3	-0.01301	-0.00429	-0.00303	-0.0137	-0.0079	-0.01726
6	-0.01743	-0.0219	-0.01691	-0.02356	-0.02002	-0.01873
9	-0.0234	-0.03251	-0.03615	-0.05607	-0.05706	-0.02916

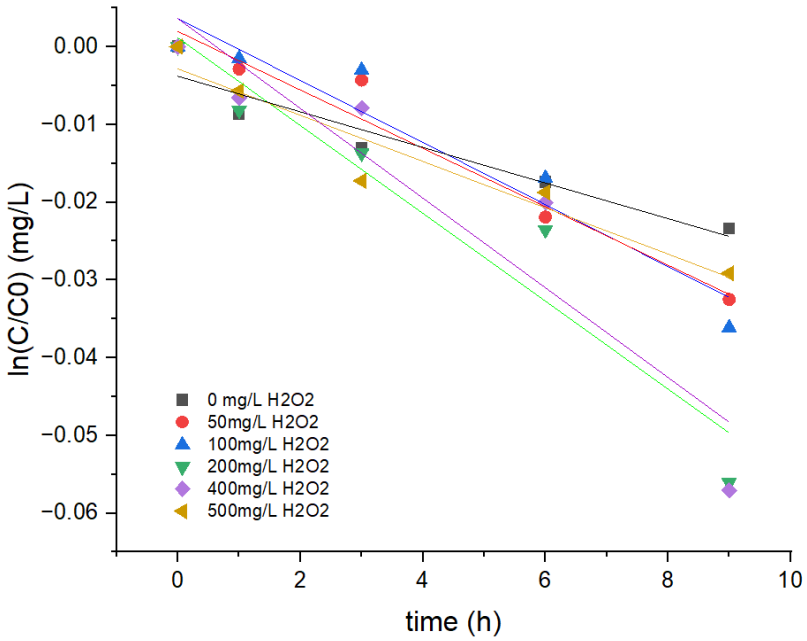

Figure A.11 Kinetic fitting of polyester fibre concentration decrease over time with varied starting concentrations of H_2O_2 (UVC/H_2O_2 treatment parameters: 31.8 mW cm^{-2} UVC, H_2O_2 treatment over 9 h)

Appendix B: Contaminants of concern present in sewage sludge

As listed in the James Hutton Institute Report:

Benzo(a)anthracene
Benzo(a)pyrene
Benzo(b)fluoranthene
Benzo(k)fluoranthene
Chrysene
Indeno(1,2,3-cd)pyrene
Naphthalene
PCB 28 (2,4-dichloro-1-(4- chlorophenyl)benzene)
PCB 52 (1,4-dichloro-2-(2,5- dichlorophenyl)benzene)
PCB 95 (1,2,4-trichloro-3-(2,5- dichlorophenyl)benzene)
PCB 101 (1,2,4-trichloro-5-(2,5- dichlorophenyl)benzene)
PCB 118 (1,2,4-trichloro-5-(3,4- dichlorophenyl)benzene)
PCB 132 (1,2,3-trichloro-4-(2,3,6- trichlorophenyl)benzene)
PCB 138 (1,2,3-trichloro-4-(2,4,5- trichlorophenyl)benzene)
PCB 149 (1,2,4-trichloro-3-(2,4,5- trichlorophenyl)benzene)
PCB 153 (1,2,4-trichloro-5-(2,4,5- trichlorophenyl)benzene)
PCB 174 (1,2,3,4-tetrachloro-5-(2,3,6- trichlorophenyl)benzene)
PCB 180 (1,2,3,4-tetrachloro-5-(2,4,5- trichlorophenyl)benzene)
2,3,7,8-TeCDD (2,3,7,8-tetrachlorodibenzo-pdioxin)
1,2,3,7,8-PeCDD (1,2,3,7,8-pentachlorodibenzop-dioxin)
1,2,3,4,6,7,8-HpCDD (1,2,3,4,6,7,8- heptachlorodibenzo-p-dioxin)
2,3,4,7,8-PeCDF (2,3,4,7,8- pentachlorodibenzofuran)
1,2,3,4,7,8-HxCDF (1,2,3,4,7,8- hexachlorodibenzofuran)
1,2,3,6,7,8-HxCDF (1,2,3,6,7,8- hexachlorodibenzofuran)
2,3,4,6,7,8-HxCDF (2,3,4,6,7,8- hexachlorodibenzofuran)
Nonylphenol (4-nonylphenol)
Nonylphenol diethoxylate (2-[2-(4- nonylphenoxy)ethoxy]ethanol)
PBDE 99 (1,2,4-tribromo-5-(2,4- dibromophenoxy)benzene)
PBDE 209 (1,2,3,4,5-pentabromo-6- (2,3,4,5,6- pentabromophenoxy)benzene)
PFOA (2,2,3,3,4,4,5,5,6,6,7,7,8,8,8- pentadecafluorooctanoic acid)
PFOS (1,1,2,2,3,3,4,4,5,5,6,6,7,7,8,8,8- heptadecafluorooctane-1- sulfonic acid)
TDCP (tris(1,3-dichloropropan-2-yl) phosphate)
DEHP (bis(2-ethylhexyl) benzene-1,2- dicarboxylate)
BBP (2-O-benzyl 1-O-butyl benzene1,2-dicarboxylate)

Appendix C: Statistical t-test outputs

Table A.7 Outputs of statistical t-test of fibre length distribution assuming equal variance

UVC/H2O2	***Variable 1***	***Variable 2***
Mean	0.849278986	0.627668
Variance	0.309448938	0.286427
Observations	552	551
Pooled Variance	0.297948599	
Hypothesized Mean Difference	0	
df	1101	
t Stat	6.741839905	
P(T<=t) one-tail	1.25944E-11	
t Critical one-tail	1.646238786	
P(T<=t) two-tail	2.51888E-11	
t Critical two-tail	1.962120966	
UVC/H2O2 (200ppm)	*Variable 1*	*Variable 2*
Mean	0.849278986	0.695184
Variance	0.309448938	0.2882
Observations	552	532
Pooled Variance	0.299020901	
Hypothesized Mean Difference	0	
df	1082	
t Stat	4.638182724	
P(T<=t) one-tail	1.97203E-06	
t Critical one-tail	1.64626313	
P(T<=t) two-tail	3.94406E-06	
t Critical two-tail	1.962158885	
UVC	*Variable 1*	*Variable 2*
Mean	0.849278986	0.852585
Variance	0.309448938	0.354345
Observations	552	542
Pooled Variance	0.33169149	
Hypothesized Mean Difference	0	
df	1092	
t Stat	-0.094925118	
P(T<=t) one-tail	0.46219586	
t Critical one-tail	1.646250212	
P(T<=t) two-tail	0.924391721	
t Critical two-tail	1.962138763	

Appendix D: Conference participation & Invited talks

i. School of Engineering, Research conference, 8 April 2022, Edinburgh, UK, poster presentation.

ii. 11th European Conference on Solar Chemistry and Photocatalysis for Environmental Applications (SPEA11), 6-10 July 2022, Turin, Italy, poster presentation.

iii. Stuart's Melville College, 8 December 2022, Edinburgh, UK, invited talk.

iv. Sustainable Plastics Live, Global Research & Innovation in Plastics (GRIPS), 10-11 May 2023, online workshop.

v. Re-Fashioning Scotland's Textile Industry, 27 April 2023, Scottish Parliament Building, Edinburgh, UK, workshop.

vi. Environmental Standards Scotland, 22 June 2023, Thistle House, Edinburgh, UK, invited talk.

vii. Early Career Researcher Microplastics Workshop, 12-17 November 2023, Ascona, Switzerland, poster presentation, oral presentation, workshop.

viii. 12th European Conference on Solar Chemistry and Photocatalysis for Environmental Applications (SPEA12), 17-21 June 2024, Belfast, UK, oral presentation.